



University
of Glasgow

Mohan, Gokula (2012) *Chromatin-binding HMGN proteins and the neuronal differentiation of embryonal carcinoma cells in vitro.*

PhD thesis

<http://theses.gla.ac.uk/3316/>

Copyright and moral rights for this thesis are retained by the author

A copy can be downloaded for personal non-commercial research or study, without prior permission or charge

This thesis cannot be reproduced or quoted extensively from without first obtaining permission in writing from the Author

The content must not be changed in any way or sold commercially in any format or medium without the formal permission of the Author

When referring to this work, full bibliographic details including the author, title, awarding institution and date of the thesis must be given

**Chromatin-binding HMGN proteins and the
neuronal differentiation of embryonal
carcinoma cells *in vitro***

Thesis submitted for the degree of Doctor of Philosophy

By

Gokula Mohan

Institute of Cancer Sciences
College of Medical, Veterinary and Life Sciences
University of Glasgow
G11 6NT

April 2012

Abstract

Embryonic stem (ES) cells are able to differentiate *in vitro* into endodermal, mesodermal and ectodermal cell types. ES cells and their close counterparts, embryonic carcinoma (EC) cells, are a useful model system for studying the mechanisms governing neuronal differentiation. Since High Mobility Group-nucleosome binding (HMGN) genes are regulated in a developmental-stage specific manner during mouse embryogenesis and cellular differentiation, their roles in undifferentiated and neural differentiating P19 EC cells were examined. Work presented in this thesis firstly optimises the Retinoic Acid (RA) -induced neural differentiation protocol of P19 EC cells based on key neuronal and glia markers. Two crucial steps of RA concentration and cell plating density were shown to increase the efficiency of neuronal differentiation. Analysis of HMGN proteins showed they were ubiquitously expressed in undifferentiated and neural differentiating P19 cells. HMGN2 and HMGN3 were up-regulated while HMGN1 remained unchanged upon neural commitment. Unusually, HMGN3 protein was localised in the cytoplasm of P19 cells. To study the possible role of HMGN proteins, HMGN1 and HMGN2 were knocked down using siRNAs. HMGN1 and HMGN2 knockdown in undifferentiated P19 EC cells dramatically down-regulated the key pluripotency regulator genes Oct4, Nanog and Sox2. Furthermore, HMGN1 and HMGN2 knockdown in neural differentiating cells affected seven neuron-specific genes. These data suggest that HMGN proteins may play roles in regulating genes that are involved in maintaining pluripotency and regulating neural differentiation in P19 cells.

Table of contents

Abstract.....	2
Table of contents.....	3
List of tables	7
List of figures	8
Acknowledgement	11
Author’s declaration	12
List of abbreviation/definition.....	13
Chapter 1 Introduction	14
1.1 Mouse embryo development and stem cells.....	14
1.2 Embryonal carcinoma cells	15
1.3 Embryonic Stem cells and Pluripotency.....	16
1.3.1 Extracellular signalling in pluripotency and self-renewal.....	16
1.3.2 Transcriptional network to maintain pluripotency.....	17
1.3.2.1 Oct4	19
1.3.2.2 Sox2	20
1.3.2.3 Nanog	20
1.4 ES/EC cells and neuronal differentiation <i>in vitro</i>	21
1.4.1 Neural development	21
1.4.1.1 Retinoic acid signalling	22
1.4.2 In vitro neuronal differentiation of ES/EC cells	22
1.4.3 Embryoid Body formation in generating neuroectoderm and neuronal differentiation in vitro.....	24
1.4.3.1 Retinoic acid protocol to produce neurons from ES/EC cells	25
1.4.3.2 Conditioned medium in inducing neural differentiation.....	26
1.4.4 Default mechanism in directing neuronal differentiation from ES cells	26
1.4.4.1 Serum free medium in promoting neural differentiation from ES cells.....	27
1.4.4.2 Low density culture in directed neural differentiation.....	27
1.4.4.3 Feeder-independent ES cells cultured as monolayer at moderate densities promotes neural induction.....	28
1.4.4.4 Stromal cell co-culture of ES cells in neuronal differentiation	28
1.5 Identification and characterisation of neuronal derivatives from ES/EC cells	29
1.6 P19 EC cells as a model system for <i>in vitro</i> neuronal differentiation ..	30
1.7 Chromatin and gene transcription	32
1.7.1 Histone modification	33
1.7.1.1 Histone acetylation	33
1.7.1.2 Histone Methylation.....	35
1.7.2 DNA methylation	37
1.7.3 ATP-dependent chromatin remodelling.....	38
1.7.4 The role of REST/NRSF complex in ES cells and neuronal differentiation.....	39
1.7.5 The use of P19 EC cells to study epigenetic mechanisms	40

1.8	Overview of HMG chromosomal proteins	41
1.9	HMGN proteins; structure and their interaction with nucleosomes.....	41
1.10	Dynamic binding of HMGNs to chromatin	43
1.11	HMGN proteins in chromatin structure	44
1.11.1	HMGN antagonises the chromatin condensing activity of linker histone H1	44
1.11.2	HMGN alter the activity of ATP-dependent chromatin remodelling complexes.....	45
1.11.3	HMGN regulate the levels of post-translational modification in core histones.....	45
1.12	Transcription regulation by HMGN proteins	46
1.13	HMGN knockout mice and their functional analysis	48
1.14	HMGN expression and possible function in development and cellular differentiation	48
1.14.1	HMGN1 and HMGN2 expression and functional role in development and differentiation.....	49
1.14.2	HMGN3 expression in development and differentiation.....	51
1.14.3	HMGN5 expression in development and differentiation.....	51
1.15	Aims and objective of this thesis	52
Chapter 2 Materials and Methods.....		53
2.1	Cell line and cells	53
2.1.1	P19 EC cells	53
2.1.2	Hippocampal neuron from adult brain	53
2.2	Reagents.....	53
2.2.1	Antibodies.....	53
2.2.2	Oligonucleotide primers.....	54
2.2.3	Other reagents	54
2.3	Formulation of buffer solution	55
2.4	Tissue culture	56
2.4.1	Culturing and passaging of undifferentiated P19 EC cells.....	56
2.4.2	Cell cryopreservation.....	57
2.4.3	Retinoic acid-induced neural differentiation from P19 EC cells ..	57
2.4.4	Generating HMGN1 and HMGN2 knockdowns.....	59
2.5	Protein isolation and analysis by western blotting	61
2.5.1	Preparation of whole cell lysates.....	61
2.5.2	Protein concentration quantification	61
2.5.3	Polyacrylamide Gel Electrophoresis (SDS-PAGE)	62
2.6	Real-time PCR for gene expression analysis.....	66
2.6.1	RNA extraction	66
2.6.2	Synthesis of cDNA	67
2.6.3	Real-time PCR amplification	69
2.6.4	Real-time PCR analysis	71
2.7	Immunofluorescence.....	73
2.7.1	Immunofluorescence staining	73
2.7.2	Immunofluorescence image analysis	75

Chapter 3 Optimisation and characterisation of Retinoic acid-induced P19 neuronal differentiation.....	76
3.1 Introduction	76
3.2 Objectives	77
3.3 Analysis of Nanog expression to determined pluripotency in subcultured P19 undifferentiated cells.....	79
3.4 Retinoic acid dosage determines the rate of neuronal differentiation in P19 EC cells.	82
3.5 Mash1 and Mash2 reciprocal RNA expression determines optimal seeding density of programmed EBs for achieving increased capacity of neuronal differentiation	86
3.6 Characterisation of retinoic acid induced P19 neuronal differentiation... ..	90
3.6.1 Pluripotent markers Oct4, Nanog and Sox2 are down-regulated upon retinoic acid induction	90
3.6.2 RA- induced P19 EC expressed markers specific to neurons and glia	94
3.6.2.1 Map2 RNA and protein is expressed in P19 neuronal differentiation	95
3.6.2.2 NF-160 kDa and Nestin are expressed in P19 neuronal differentiation	98
3.6.2.3 RA-induced P19 cells expressed neuron specific markers NSE and NMDA receptor	102
3.6.2.4 Glia cell marker is expressed in the later stage of RA- induced P19 differentiation	104
3.7 Discussion.....	106
3.8 Conclusion.....	108
 Chapter 4 Characterisation of HMGN expression in neural differentiation of P19 EC cells and hippocampal neurons from adult mouse brain	109
4.1 Introduction	109
4.2 Objectives.....	110
4.3 Expression of HMGN in RA-induced EBs derived from P19 EC undifferentiated cells.....	111
4.4 Expression of HMGN in P19 neuronal differentiation.....	114
4.4.1 Expression of HMGN1 in the neuronal differentiation of P19 EC cells	115
4.4.2 Expression of HMGN2 in the neuronal differentiation of P19 EC cells	117
4.4.3 Expression of HMGN3 in the neuronal differentiation of P19 EC cells	119
4.5 Cellular localisation of HMGN in undifferentiated P19 EC cells.	121
4.6 Cellular localisation of HMGN proteins in neural differentiated cultures of P19 EC cells.	126
4.7 HMGN expression in hippocampal neurons	128
4.8 Discussion.....	130

Chapter 5 HMGN1 and HMGN2 knockdown affect the expression of key genes in undifferentiated P19 EC cells and RA-induced neural differentiation.....	132
5.1 Introduction	132
5.2 Objectives	133
5.3 Establishing an siRNA-based protocol for HMGN1 and HMGN2 knockdown	133
5.4 Validating HMGN1 and HMGN2 knockdowns in P19 EC cells.....	139
5.4.1 HMGN1 and HMGN2 knockdowns in undifferentiated P19 EC cells	139
5.4.2 HMGN1 and HMGN2 double knockdown in undifferentiated P19 EC cells	142
5.5 HMGN knockdowns in undifferentiated cells down-regulate the expression of key pluripotent genes	144
5.6 HMGN2 knockdown in undifferentiated cells down-regulates GlyT1a gene but does not affect the expression of GlyT2.....	146
5.7 Expression of Rest and various neural lineage-specific genes remained unchanged following HMGN knockdowns in undifferentiated cells	149
5.8 HMGN1/2 depletion in undifferentiated cells does not have a long term effect on neural commitment.	151
5.9 HMGN1 and HMGN2 knockdown during neural differentiation of P19 EC cells	153
5.10 HMGN2 knockdown during neural differentiation down-regulates Rest expression	155
5.11 HMGN knockdown during neural differentiation affects the expression of early neural induced genes	157
5.12 HMGN knockdowns during neural differentiation affect the expression of neural specific genes	159
5.13 Discussion.....	163
5.13.1 HMGN knockdowns in undifferentiated and neuronal differentiating P19 cells	163
5.13.2 HMGN knockdowns affect the expression of pluripotency-related genes in undifferentiated cells	163
5.13.3 HMGN knockdowns affected the expression of neural-related genes in day 3 cells.....	164
5.13.4 Cell-type specific effects of HMGN1 and HMGN2.....	166
5.14 Summary.....	166
Chapter 6 Summary and future work.....	167
6.1 Summary	167
6.1.1 Characterisation of RA-induced neuronal differentiation of P19 cells (Chapter 3)	167
6.1.2 HMGN expression during neuronal differentiation (chapter 4) ..	168
6.1.3 HMGN1 and HMGN2 knockdowns in undifferentiated and neural differentiating P19 cells	169
6.2 Future work	169
6.3 Concluding remarks	171
Appendix.....	172
List of references.....	172

List of Tables

Table 2.1: List of commercially available antibodies used in this project.....	54
Table 2.2: List of siRNA, target sequence and final concentration used in knockdown experiments. * siRNAs used for all downstream functional experiments.	59
Table 2.3: List of oligonucleotide primers used for real-time (qRT-PCR) analysis and primer efficiencies	70
Table 3.1: List of neuronal markers used in the characterisation of RA-induced P19 neuronal differentiation.	94
Table 5.1: siRNA library and their designated names for HMGN1 and HMGN2 knockdown.	136
Table 5.2: Summary of the knockdown conditions for HMGN1 and HMGN2 in P19 EC cells.	136

List of Figures

Figure 1.1: Organisation of chromatin.	32
Figure 1.2: HMGN protein structure consist of three distinct domains, namely a bipartite nuclear localisation signal (NLS), a conserved 30-amino acid long nucleosome-binding domain (NBD) and C-terminal chromatin regulatory domain (RD).	43
Figure 3.1: An outline of the RA-induced P19 neuronal differentiation model system.	78
Figure 3.2: Expression of the pluripotency marker Nanog decreases with passage number for undifferentiated P19 EC cells.	80
Figure 3.3: Retinoic acid concentration affects the efficacy of neuronal differentiation.	83
Figure 3.4: Plating density affects the efficacy of neuronal differentiation as assayed by Mash1 and Mash2 expression.	87
Figure 3.5: Oct4 RNA and protein are highly expressed in undifferentiated cells and are loss upon RA-induced neuronal differentiation.	91
Figure 3.6: Nanog and Sox2 expressions are down-regulated upon RA-induced neuronal differentiation.	92
Figure 3.7: Map2 expression is induced to high levels upon neural commitment from undifferentiated P19 EC cells.	96
Figure 3.8: NF-160 kDa is highly expressed in day 3 and 6 neural differentiation from undifferentiated P19 EC cell.	99
Figure 3.9: Nestin neural progenitor marker is induced upon RA-induced neural differentiation from P19 EC cells	100
Figure 3.10: Nse and Nmda receptor are expressed in the later stages of neural differentiation derived from P19 EC cells.	103
Figure 3.11: Gfap RNA levels are induced to high levels from day 6 whereas the proteins are detected on day 9 of P19 neural differentiation.	105

Figure 4.1: HMGN1 expression shows discrepancies between RNA and proteins levels whilst HMGN2 expression is up-regulated in RA-programmed EBs.....	111
Figure 4.2: The RNA expression of HMGN3a and HMGN3b are up-regulated whilst the protein levels are slightly down-regulated in RA-programmed EBs.	113
Figure 4.3: HMGN1 RNA and protein expression during neural differentiation of P19 EC cells.	116
Figure 4.4: Expression of HMGN2 is up-regulated upon neural differentiation of P19 EC cells.	118
Figure 4.5: Expression of HMGN3a and HMGN3b are up-regulated upon neural differentiation of P19 EC cells.	120
Figure 4.6: Expression of HMGN1 protein is ubiquitous and localises within the nuclei of undifferentiated P19 EC cells.	122
Figure 4.7: Expression of HMGN2 protein is ubiquitous and localises within the nuclei of undifferentiated P19 EC cells.	123
Figure 4.8: HMGN3a and HMGN3b proteins are ubiquitously expressed but predominantly localise with the cytoplasm.	124
Figure 4.9: Expressions of HMGN proteins in RA-induced neural differentiation of P19 EC cells.	127
Figure 4.10: Expressions of HMGN proteins are not ubiquitous in day 18 hippocampal neuronal cultures.	129
Figure 5.1: siRNA knockdowns reduce levels of HMGN1 protein to approximately 90% after 72 hours post transfection in undifferentiated P19 EC cells.	137
Figure 5.2: HMGN2 knockdown is achieved using siRNA at 40nM final concentration of after 72 hours post-transfection in undifferentiated P19 EC cells.	138
Figure 5.3: HMGN1 protein levels are knockdown by more than 90% in undifferentiated P19 EC cells.	140

Figure 5.4: HMGN2 protein levels are knockdown by more than 90% in undifferentiated P19 EC cells.	141
Figure 5.5: HMGN1 and HMGN2 proteins are lost following double knockdown in undifferentiated P19 EC cells	143
Figure 5.7: HMGN knockdowns in undifferentiated P19 EC cells dramatically down-regulate pluripotency genes Oct4, Nanog and Sox2.....	145
Figure 5.8: GlyT1a and GlyT2 expression during RA-induced P19 EC cell differentiation.	147
Figure 5.9: GlyT1a is down-regulated whereas GlyT2 is unchanged upon HMGN knockdowns in undifferentiated P19 EC cells.	148
Figure 5.10: Rest expression in undifferentiated P19 EC cells remained unchanged after HMGN knockdowns.	150
Figure 5.11: HMGN1/2 depletion in undifferentiated cells does not have a long term effect on neural commitment.	152
Figure 5.12: HMGN1, HMGN2 and HMGN1/2 knockdowns in day 3 neural differentiation	154
Figure 5.13: HMGN2 knockdown in day 3 neural differentiation cells down-regulates Rest expression.	156
Figure 5.14: HMGN knockdowns in neural differentiating cells affect the expression of Nestin and Zfp521.	158
Figure 5.15: Map2 expression remained unchanged but NF-160 kDa is up-regulated following HMGN knockdowns.....	160
Figure 5.16: Nse and Nmda-receptor subunit 2 demonstrate complimentary expression pattern in HMGN knockdown cells.	161
Figure 5.17: GlyT2 expression is significantly down-regulated in HMGN2 knockdown cells.	162
Figure A.1: Cell images showing RA-induced neuronal differentiation from P19 EC cells at day 2 from different EB plating densities.....	171

Acknowledgement

I owe my deepest gratitude to my supervisor, Dr. Katherine West, who has supported me throughout my thesis and PhD research. Katherine has allowed me to work on my own way and it has made my PhD time very enjoyable. I especially thank her for being so patient and very importantly not giving up on being my supervisor. One cannot ask for a better supervisor and this thesis would have not been possible without Katherine.

Secondly, I thank my co-supervisor, Dr. Tomoko Iwata and advisor, Dr. David Gillespie for all their ideas and support. I am grateful to Dr. Adam West for all his valuable advice and ideas.

I am indebted to all present and past members of the WEST lab. I am especially grateful to Dr. Grainne Barkess who supported me throughout my time in Glasgow. Grainne is a mentor, colleague, and a good friend. I wish to thank Carolyn Low and Elaine Gourlay for being the nicest lab mates and supporting me especially during my thesis writing period. The nights (well, days too) in OTTO will always be remembered, except for the shots.

Dr. Chrisanne Dias Campos and Andre Campos have stand by me and took care of me like family. No words can express my gratitude for all that they have done.

It is difficult to overstate my gratitude to my friend Koorosh Korfi. Koorosh has made days in Glasgow very “interesting” and “exciting” (note the code language). Thank you so much my friend. I could not ask for a better colleague and friend.

I would like to thank all my friends in Malaysia. I especially thank Kavitha Kolandai for instilling the belief that I can someday be a PhD graduate. I also thank Geral, Jayan and Mahen for all their support.

I want to express my deeply-felt thanks to Aliya. Aliya has supported me in every way possible and I am very grateful to have a friend like her. I thank her for being very patient and helping me during my thesis writing.

Lastly, and most importantly, I thank my parents, Ruby Devi and Paul Dushi for all their support, advice and guidance. I dedicate this thesis to them. I would like to also thank my siblings Morgan, Sanjeet and Preetha for their continuous support.

Author's Declaration

I declare that, except where explicit reference is made to the contribution of others, that this dissertation is the result of my own work and has not been submitted for any other degree at the University of Glasgow or any other institution.

Gokula Mohan

List of abbreviation/definition

APS= ammonium persulphate	PBS= phosphate buffered saline
ATRA=All- <i>trans</i> retinoic acid	PCR=Polymerase chain reaction
BSA=Bovine Serum Albumin	RA=Retinoic Acid
ChIP=Chromatin Immunoprecipitation	RARE=RA-response elements
EB=Embryoid Body	RARs=retinoic acid receptors
EC=Embryonic Carcinoma	RD=regulatory domain
EDTA= Ethylenediaminetetraacetic acid	RT=Room temperature
EG=Embryonic Germ	SDS= sodium dodecyl sulfate
ES=Embryonic Stem	siRNA=short interfering RNA
GOI= Gene of Interest	TE=trophectoderm
HMGN=High Mobility Group Nucleosome	TEMED= Tetramethylethylenediamine
HRP= horseradish peroxidase	TF=Transcription factor
IF= Immunofluorescence	TRIS= tris(hydroxymethyl)aminomethane
MEF=Mouse embryonic fibroblast	TS=trophoblast stem
NBD=nucleosome binding domain	TSS=Transcription start sites
NPC=neural progenitor cells	WT=wild type
NSC=neural stem cell	XEN=extraembryonic endoderm stem

Chapter 1

Introduction

1.1 Mouse embryo development and stem cells

The development of a mouse embryo starts with the fertilization of an ovum, resulting in the formation of a zygote. The zygote reaches the morula stage (4-16 cells) and goes on to form the blastocyst (40-150 cells) before implantation. The first definitive differentiation decisions are made at the blastocyst stage, which is composed of three distinct cell types: trophectoderm (TE), primitive endoderm, and epiblast (primitive ectoderm). All three cell lineages, the TE, primitive endoderm, and epiblast give rise to stem cell populations. TE potentially gives rise to trophoblast stem (TS) cells, primitive endoderm gives rise to extraembryonic endoderm stem (XEN) cells, while epiblast forms embryonic stem (ES) cells. The next stage is called gastrulation and involves the differentiation of pluripotent epiblast cells into three embryonic germ layers known as endoderm, mesoderm and ectoderm. Primordial germ cells (PGCs) originate from a small population of mesodermal cells from the epiblast and give rise to embryonic germ (EG) cells.

Mouse ES cell lines were first described in the early 1980s and were derived from the Inner cell mass (ICM) of the pre-implantation embryo (Evans and Kaufman, 1981; Martin, 1981). Similar to the ICM of the early epiblast stage, ES cells are pluripotent cells that have the capabilities both *in vivo* and *in vitro* to differentiate into all cell types of the adult organism. ES cells have been shown to differentiate into neurogenic, hematopoietic, cardiogenic, myogenic, epithelial, endothelial and vascular smooth cells (Wobus et al., 2001; Wobus and Boheler 1999; Wobus and Guan 1998).

EG cell lines were previously established from PGCs embryonic day 8.5 (E8.5) and E11 (Matsui et al., 1992). EG cells are pluripotent cells and can contribute to all three embryonic germ layers (Labosky et al., 1994). EG cells are shown to have similar morphology as ES cells in culture (Mclaren and Durcova-Hillis, 2001).

TS cells are isolated from the TE of pre-implantation embryos. However, TS cells show limited ability to differentiate compared to ES cells. TS cells can form giant cells *in vitro* (Yan et al., 2001; Tanaka et al., 1998) and contribute to the differentiation of trophodermal cell lineages *in vivo*. Although ES cells can be induced to become TS cells, the induced TS cells do not retain the differentiation potential of ES cells (Niwa et al., 2000).

1.2 Embryonal carcinoma cells

Embryonal carcinoma (EC) cells are known as the malignant counterpart of ES cells. EC cells are derived from teratocarcinomas, a subset of germline tumours. These malignant tumours arise in the testes of mice and human, and contain a variety of differentiated tissue and a population of undifferentiated stem cells. These undifferentiated stem cells are pluripotent and are known as EC cells. EC cells from teratocarcinomas are responsible for the malignant component as opposed to the differentiated tissue present in the tumor (Kleinsmith and Pierce, 1964). This was shown through a study where transplantation of a single EC cell into a new host mouse was adequate to regenerate a new tumour (Kleinsmith and Pierce, 1964). In a separate study, the grafting of mouse egg cylinders into the kidney capsules also formed teratomas containing both undifferentiated and differentiated cells (Solter et al., 1970).

Mouse EC cells was first derived and cultured *in vitro* without losing their pluripotency in 1967 (Finch and Ephrussi, 1967). Like mouse ES cells, EC cells express pluripotent markers Oct4 and surface antigen SSEA-1 (Niwa et al., 2000; Andrew et al., 1996). Two mouse EC cell lines that have been used in stem cell research are F9 EC cells (Verheijen et al., 1999a; Verheijen et al., 1999b; Lehtonen et al., 1998; Alonso et al., 1991) and P19 EC cells (McBurney, 1993).

1.3 Embryonic Stem cells and Pluripotency

Pluripotency is defined by the capability of a cell to differentiate into all types of cell that make up an organism (Solter, 2006). ES cells possess the ability to replicate indefinitely in culture and differentiate into a host of functionally distinct cell types. Because of this, ES cells have become a unique tool to study the early molecular and cellular processes that regulate normal development. The mechanisms by which ES cells choose between pluripotency and differentiation are thought to be orchestrated by several factors. The progression of pluripotent or undifferentiated ES cells to a differentiated phenotype is regulated by changes in gene expression, in which, genes that are responsible for self-renewal are down-regulated while lineage-specific genes are up-regulated.

The regulatory mechanisms that control the pluripotency and self-renewal in ES cells are not yet fully understood. Nonetheless several factors have been identified as crucial in maintaining the pluripotency of ES cells: among them are extracellular signalling, transcription factor networks and epigenetic factors.

1.3.1 Extracellular signalling in pluripotency and self-renewal

Several key extracellular signalling pathways have been identified to be crucial in maintenance of pluripotency and self-renewal of ES cells. Leukemia inhibitory factor (LIF), a member of the IL6 family, binds to leukemia inhibitory factor receptor (LIFR) and acts via gp130 receptor resulting in the activation of Jak kinases and Stat3 (Burdon et al., 2002). Activated STAT3 protein is then translocated into the nucleus and activates the transcription of several key genes that are involved in pluripotency such c-Myc and Klf4 (Niwa et al., 2009; Cartwright et al., 2005). When Stat3 is inhibited, ES cells start to differentiate, whereas the over-expression of Stat3 maintains ES cell pluripotency in the absence of LIF (Matsuda et al., 1999; Niwa et al., 1998). Binding of LIFR to gp130 also activates the PI(3)K/AKT pathway through which T-box3 (Tbx3) is activated. Over expression of Tbx3 inhibits differentiation in the absence of Lif by maintaining Nanog expression, whereas the knockdown

of Tbx results in differentiation (Niwa et al., 2009; Ivanova et al., 2006; Paling et al., 2004). The LIFR- gp130 signalling also leads to the activation of Ras/mitogen-activated protein kinase (MAPK)/extracellular signal-regulated kinase (ERK) pathway. Activated forms of ERKs translocate their targets into the nucleus which then regulates the activities of key transcription factors such as Myc and Elk. The inhibition of ERK signalling in ES cells has shown to facilitate self-renewal rather than activate differentiation (Burdon et al., 1999).

Wnt signalling is also known to play a role in ES cell maintenance through glycogen synthase kinase 3 (GSK3) and adenomatous polyposis coli (Apc), inducing the translocation of β -catenin into the nucleus forming β -catenin /Tcf3 (Transcription factor 3) (Wray et al., 2011; Willert et al., 2006). β -catenin/Tcf activates the transcription of downstream targets that are responsible for pluripotency maintenance. Over-expression of Wnt protein members contributes to the maintenance of pluripotency (Hao et al., 2006; Ogawa et al., 2006; Kielman et al., 2002).

There are other signalling cascades involved in ES cells that are not discussed above such as Fibroblast growth factor 4 (Fgf4) signalling (Kunath et al., 2007), Bone morphogenic protein (BMP) signalling (Ying et al., 2003), ACTH/SAF activation (Ogawa et al., 2004), GABA and BNP signalling (Abdelalim and Tooyama, 2009). The extracellular signalling cascades are known to regulate ES cell pluripotency via two different mechanisms: targeting core pluripotency transcription factors and targeting cell cycle progression - related genes. Lif-Stat, Lif- PI(3) Kinase, TGF- β , Wnt and Fgf4 signalling all target core transcription factors that are responsible for pluripotency, while ACTH/SAF activation, GABA and BNP signalling target genes that are involved in cell cycle progression.

1.3.2 Transcriptional network to maintain pluripotency

A network of inter-related transcription factors (TF) is central to the maintenance of ES cell pluripotency (Ema et al., 2008; Chambers et al., 2007; Masui et al., 2007; Niwa et al., 2005; Chambers et al., 2003; Niwa et al.,

2000). Indeed, a large scale RNAi mediated knockdown study identified 8 genes that are crucial for maintaining the undifferentiated state of ES cells, of which 7 are transcription factors or chromatin associated proteins: Oct4, Nanog, Sox2, Tbx3, Esrrb, Tcl1 and Dppa4 (Ivanova et al., 2006). Among the core members of this pluripotency associated TF network are Oct4, Sox2 and Nanog (Chambers et al., 2007; Masui et al., 2007; Niwa et al., 2000). During mouse development, the pluripotent state requires the expression of Oct4 (Nichols et al., 1998) and Nanog (Mitsui et al., 2003) but not Sox2 (Avilion et al., 2003), and it has been proposed that this is due to the presence of long-lived maternal Sox2 protein (Avilion et al., 2003).

Genome wide studies using chromatin immunoprecipitation (ChIP) - based techniques have revealed co-binding of Oct4, Nanog and Sox2 in ES cells, suggesting a probable TF circuit that might direct ES cell identity (Loh et al., 2006; Boyer et al., 2005). Studies conducted by Loh et al and Boyer et al mapped the transcriptional regulatory network and demonstrate that Oct4 and Nanog co-occupy and share a cohort of their target genes. In mouse ES cells, Nanog co-occupies 44.5% (345) of Oct4-bound genes, while 353 target genes are co-bound by Oct4, Nanog and Sox2 in human ES cells (Loh et al., 2006; Boyer et al., 2005). These studies revealed that Oct4, Nanog and Sox2 maintain pluripotency by promoting the expression of downstream self-renewal genes while simultaneously repressing the transcription of differentiation linked-genes.

Subsequent genome-wide ChIP based studies mapped the binding sites of additional TF and their co-regulators in mouse ES cells (Chen et al., 2008; Kim et al., 2008). These studies grouped the pluripotent associated TF into “Oct4-related” and “Myc-related” modules. The Oct4-related module includes Oct4, Sox2, Nanog, Smad1, Stat3 and Tcf3 (Chen et al., 2008; Cole et al., 2008). Smad, Stat3 and Tcf3 are known downstream effectors for signalling pathways regulated by BMP, LIF and Wnt, providing a mechanistic basis for the role of these signals in maintaining ES cell pluripotency. Other TFs involved in the Oct4-related module are Dax1, Nac1, Zfp281, Esrrb, Nr5a2 and Klf4 (Heng et al., 2010; Dejosez et al., 2010; Feng et al., 2009; Kim et al., 2008). The depletion of Oct4 markedly reduces the co-binding of Smad1, Stat3, Dax1 and

Esrrb analysed using ChIPs, providing evidence that Oct4 acts a mediator in the assembly and maintenance of these multi-protein complexes on DNA (van den Berg et al., 2010; Chen et al., 2008).

The Myc-related TF module includes the transcription factors c-Myc, n-Myc, E2f1, Zfx, Rex1 and Ronin (Dejosez et al., 2010; Chen et al., 2008; Kim et al., 2008). The key difference between the Oct4-related and c-Myc-related modules is that the latter involves TFs that occupy sites close to transcription start sites (TSS) in the genome, while the former involves TFs that bind further away from TSS. The TFs in Oct4-related module have been proposed to act as enhancers (Dejosez et al., 2010; Kim et al., 2008). The c-Myc-related module mostly targets genes associated with protein metabolism and cancer related genes (Kim et al., 2010).

Another vital dimension to the pluripotency-associated TF network is the ability of many of these TFs to self-regulate their own expression, including Oct4, Sox2, Nanog, Esrrb, Sall4, Dax1, Klf2, Klf4, Klf5, Stat3 and Tcf3 expression (Feng et al., 2009; Chen et al., 2008; Kim et al., 2008; Cole et al., 2008; Lim et al., 2008; Jiang et al., 2008; Boyer et al., 2005; Loh et al., 2006; Chew et al., 2005). The accurate regulation of these TFs is crucial, as their over and/or under-expression would affect ES cell identity and differentiation state (Mitsui et al., 2003; Niwa et al., 2000).

Amongst all pluripotent associated TFs, Oct4, Sox2 and Nanog appear to be involved in a feed- forward self activating gene regulation circuit that plays a key role in maintaining the core pluripotency TF network, maintaining ES cell self-renewal and determining cell fate.

1.3.2.1 Oct4

Oct3/4, also known as Pou5f1, was first described as either Oct3 or Oct4 in three different studies (Rosner et al., 1990; Scholer et al., 1990; Okamoto et al., 1990). Throughout this thesis, Oct3/4 will simply be referred as Oct4. Oct4 consists of a DNA binding domain called the POU domain and two flanking C/N-terminal trans-activating domains. Oct4 expression is found in

pluripotent cell lineages such as the ICM and germ cells *in vivo* and undifferentiated ES cells *in vitro* (Rosner et al., 1990; Scholer et al., 1990; Okamoto et al., 1990; Nichols et al., 1998; Palmieri et al., 1994). Oct4 is known to regulate a broad spectrum of target genes, and from an embryonic developmental perspective, the main target of Oct4 is Cdx2. Depletion of Oct4 in ES cells leads to differentiation into trophectoderm via the up-regulation of Cdx2 (Niwa et al., 2005).

1.3.2.2 Sox2

The protein structure of Sox2 consists of a DNA-binding HMG domain and a transactivation domain that can be divided into three subdomains (Ambrosetti et al., 2000). Sox2 was initially identified as an Oct-Sox enhancer element binding protein on the regulatory region of the Fgf4 gene (Yuan et al., 1995). Later, Sox2 was shown to occupy the regulatory regions of genes that are specifically expressed in pluripotent stem cells (Rodda et al., 2005; Kuroda et al., 2005; Tokuzawa et al., 2003; Tomioka et al., 2002; Nishimoto et al., 1999). The loss of Sox2 *in vivo* is embryonic lethal due to the improper ICM growth, indicating that Sox2 is essential for pluripotent stem cell maintenance (Avilion et al., 2003).

1.3.2.3 Nanog

The Nanog protein structure consists of three domains: a DNA-binding homeodomain and two C/N terminal flanking transactivating domains (Wang et al., 2008; Pan et al., 2003). Nanog was identified from a functional screen based on the capability to maintain ES cell pluripotency in the absence of Lif (Chambers et al., 2003). The repression of Nanog *in vivo* results in early embryonic lethality (Mitsui et al., 2003). However, ES cells depleted of Nanog still maintain pluripotency, although with increasing inclination to differentiate, suggesting that Nanog is not a critical factor in the pluripotent transcriptional network of ES cells (Chambers et al., 2007). In contrast, over-expression of Nanog in ES cells under differentiation conditions increased the tendency towards the undifferentiated state, suggesting that Nanog may play a role in stabilising pluripotency related factors (Chambers et al., 2007).

1.4 ES/EC cells and neuronal differentiation *in vitro*

1.4.1 Neural development

Neuronal differentiation is a process that involves the generation of various neuronal subtypes from progenitor cells. The development of the CNS begins during prenatal development, following the induction of neuroectoderm. The neuroectoderm forms a thickened region on the dorsal side of the early embryo called neural plate. The neural plate is then converted to the neural tube that will later form the brain and spinal cord.

The molecular mechanisms that trigger the neuroectoderm induction were elucidated mainly from studies conducted using *Xenopus*, chick and other lower vertebrates. These studies identified multiple pathways that include the activation of Fibroblast growth factor (Fgf) and Notch, inhibition of bone morphogenetic protein (BMP) and inactivation of Wnt signalling in orchestrating the induction of neuroectoderm (Stern, 2006; Stern, 2005; Wilson and Edlund, 2001). Likewise, mouse ES cell models show the involvement of FGF, BMP antagonists and Wnt inactivation in neuron differentiation, mimicking early neuroectoderm development *in vivo* (Ying et al., 2003; Aubert et al., 2002; Tropepe et al., 2001).

FGF signalling is one of the initial known mechanisms implicated in neural induction and specification. It is activated prior to and also synergistically with BMP inhibition and Notch activation (Stern, 2006; Lowell et al., 2006). The FGF signalling acts through the activation of extracellular signal-regulated kinase (ERK1/2) pathway promoting transcription of target genes. In the mouse ES system, inhibition of FGF signalling eliminates the neuroectodermal induction from undifferentiated cells (Ying et al., 2003). In embryogenesis, BMP signalling blocks neuroectoderm formation and favours the activation of other lineage choices. BMP acts through a SMAD-dependent pathway resulting in the transcriptional activation of genes involved in other lineages. For the induction of neuroectoderm, BMP antagonists Noggin, Chordin and Follistatin are produced by mesodermal cells to inhibit BMP signalling. The role of Wnt signalling in neuroectoderm development is complex. In a study conducted

using *Xenopus* model, neuroectoderm induction requires the activation of Wnt (β -Catenin) as this pathway represses BMP expression (Baker et al., 1999). However, the Wnt signalling must be antagonised in the later stages to allow neural specification (Stern, 2006). Studies conducted in the chick model show that Wnt inactivation together with FGF signalling is required for neuroectoderm induction (Wilson and Edlund, 2001; Wilson et al., 2001). Finally, the evidence that neuroectoderm induction requires Notch signalling was shown in chick and *Drosophila* models, and later corroborated in mouse and human ES cells (Lowell et al., 2006; Akai et al., 2005; Gaiano and Fishell 2002). In chick and fly, it has been shown that Notch ligand Delta 1 signalling together with FGF activation induced neural specification (Akai et al., 2005; Gaiano and Fishell 2002).

1.4.1.1 Retinoic acid signalling and neural development

Retinoic acid (RA) plays crucial roles in the nervous system including regulating neural differentiation, axon outgrowth and neural patterning (Maden, 2007; Li et al., 2005). The concentration of RA is found to be higher in the posterior hindbrain and spinal cord compared to the anterior region in a developing embryo. The lack of RA signalling leads to the abnormal formation of the posterior hindbrain and spinal cord suggesting the crucial role of RA during neural development (Maden, 2007). During neuronal and glial differentiation, RA promotes the activation of several genes that include TFs and cell signalling molecules (the role of RA in neuronal differentiation is further discussed in section 1.4.3.1). Additionally, studies from Jacobs et al uncovered the effect of RA deficiency on granule cell differentiation, suggesting that RA is required for neuronal differentiation of isolated adult brain NSCs (Jacobs et al., 2006).

1.4.2 *In vitro* neuronal differentiation of ES/EC cells

ES/EC cells are pluripotent because they can self-renew and have the ability to differentiate into cell types of all three germ layers (Labosky et al., 1994; McBurney 1993). Specifically, they have the ability to differentiate into neurons and glia, and can maintain a population of neural stem cells *in vitro*

(Schmidt et al., 2001; Strübing et al., 1995; McBurney 1993; Evans and Kaufman, 1981; Martin, 1981).

The specification of neurons and glia arising from neuroectoderm is a crucial process in early CNS development, as the time and position where each neuron is born determines the ultimate location and role that the cell will perform. Each neuron expresses a distinct set of neurotransmitters and receptors, enabling it to perform a highly specialised function. Accordingly, *in vitro* ES/EC neuronal differentiation involves the induction of neuroectoderm or neural stem cells (NSC) (also sometimes referred as neural progenitor cells, NPC or often used interchangeably), which give rise to various neuron subtypes depending on the morphogens used in the differentiation culture (Zhang, 2006). The same morphogen added into ES/EC cultures at different times or different concentrations can give rise to different populations of neuron subtypes (Guan et al., 2001). Hence, achieving directed neuronal differentiation from ES/EC cells is a major challenge.

Multiple protocols have been established for neuroectodermal induction and the generation of NSC from ES cells. These protocols are based on the mechanisms underlying both neural induction during embryogenesis and neurogenesis in the adult CNS. NSCs of the embryonic CNS are known as radial glial cells, whereas adult brain NSCs are astrocyte-like stem cells (Doetsch, 2003). ES cell-derived NSCs are shown to have similar properties to embryonic radial glial cells, and have the ability to self-renew and differentiate into neurons, astrocytes and oligodendrocytes (Nat et al., 2007; Liour et al., 2006; Plachta et al., 2004; Liour and Yu, 2003). Some studies have compared ES cell-derived NSCs to NSC from adult brain and found that the former proliferate readily and prefer adherent cultures compared to brain NSC that proliferate better as clusters of cells floating freely in the medium (Colombo et al., 2006). Transcriptional profiling demonstrated close similarities between NSCs from both origins, although ES cell-derived NSC showed a wider range of neuronal subtype markers such as rostral spinal cord-specific markers (Colombo et al., 2006).

Meanwhile, studies conducted by several groups show ES cell-derived neurogenesis mimics embryonic neurogenesis through the expression of lineage-specific TF such as Sox2, Sox3, Otx2 and Pax6 (Barberi et al., 2003; Wilson and Edlund 2001). These results suggest that ES cell-derived neuronal differentiation mimics neural development during embryogenesis and in the adult brain, establishing it as a good model system for studying the molecular events governing neural differentiation.

Protocols established for directed neuronal differentiation *in vitro* from ES cells are based on two approaches. The first protocol uses embryoid body (EB) formation to mimic the environment that leads to neuroectoderm induction in the embryo, thus providing appropriate cell-to-cell interactions and adding a morphogen such as retinoic acid to imitate signalling molecules. The second protocol involves growing ES cells in serum free media, in a feeder cell-free culture, or at a low cell density, thus removing the signalling molecules that inhibit neural commitment and evoking a default mechanism for generating NSC. Although current protocols are based around these two approaches, the individual steps can vary between research laboratories. Furthermore, the end product is heterogeneous in terms of the neuronal subtypes generated. Consequently, *in vitro* neuronal differentiation from ES/EC cells requires optimisation of culture conditions to achieve directed differentiation, and extensive characterisation of the neurons produced.

1.4.3 Embryoid Body formation in generating neuroectoderm and neuronal differentiation in vitro

Early studies on neuronal differentiation from mouse EC cells were based upon neuroectoderm induction through the formation of EBs (Martin et al., 1981; Pierce and Dixon, 1959; Stevens, 1959). EC cell-derived EBs show a similar pattern of neuronal differentiation when compared to isolated inner cell mass cells cultured *in vitro* (Martin et al., 1977). Similarly, mouse ES cells grown in suspension without LIF form aggregates within 2-4 days and have the ability to generate cells from all three germ layers (Maye et al., 2004; Rathjen et al., 2002). From day 6 onwards, EBs form an inner epithelial layer which consists of cells committed to definitive ectoderm, characterised by the expression of

Fgf5, Otx2, Sox1 and Six3 (Maye et al., 2004; Rathjen et al., 2002; Coucouvanis and Martin, 1995). Two protocols for the generation of neurons and glia through EBs from mouse ES/EC cells using RA and conditioned media have been established, and are discussed below.

1.4.3.1 Retinoic acid protocol to produce neurons from ES/EC cells

The outcome of neuronal differentiation from ES cells through the formation of EBs can be significantly increased by the addition of retinoic acid (RA), (Gotlieb et al., 2002; Guan et al., 2001). RA promotes the induction of neuroectoderm through the formation of EBs and neuronal differentiation from EC (Bain and Gotlieb, 1994; Jones-Villeneuve et al., 1983).

Mouse ES cells are treated with RA in a protocol known as the RA (4-/4+), where the cells are allowed to form aggregates in suspension for 4 days and treated with RA for another 4 days, before transferring single cells from the EBs to adherent culture to generate neurons and glia. The extent of differentiation was then determined based upon cell morphology, expression of cell-type specific markers and electrophysiological measurement (Bain et al., 1995). For EC cells, the protocol utilises RA (2+/2-), where the cells are allowed to form aggregates in suspension for 2 days in the presence of RA and then for 2 additional days without RA, before transferring single cells to adherent cultures to form neurons and glia cells (McBurney 1993; Jones-Villeneuve et al., 1983).

The addition of RA was shown to significantly induce neuronal differentiation from ES/EC cells as shown by the production of neuroectodermal cells (Strübing et al., 1995; Fraichard et al., 1995; Bain et al., 1995; Wobus et al., 1994). RA-induced neuronal cells at the initial stages of differentiation expressed neuron-specific markers such as Neurofilament (NFL) protein 68 kDa, NFL 160 kDa and the synaptic vesicle protein synaptophysin (Strübing et al., 1995; Fraichard et al., 1995; Bain et al., 1995; Rohwedel et al., 1998). Further differentiation leads to the expression of markers such Microtubule-associated proteins MAP2, MAP5, B-III Tubulin, NF 200 kDa and NCAM (Finley et al., 1996; Strübing et al., 1995; Fraichard et al., 1995; Bain et al., 1995).

The mechanism of RA in inducing neural commitment from stem cells *in vitro* was investigated by Berg and McBurney, where they revealed RA can be present for as short as 2-4 hours and still be effective in inducing the irreversible neuronal differentiation of P19 EC cells (Berg and McBurney, 1990). However, the mechanisms whereby RA induces neural differentiation of ES/EC cells are not fully understood. The possible mechanism of RA action involves a group of nuclear retinoic acid receptors (RARs) that are known ligand-dependent TFs (Umesono et al., 1988). It is hypothesised that RA-responsive genes may play a role in activating a cascade of reaction leading to transcriptional activation of genes involved in neural specification. RARs interact with RA-response elements (RARE) and activate the transcription of genes involved in developmental regulation such as Pax6, Mash1, sonic hedgehog, NeuroD in neuronal differentiating mouse ES cells (Guan et al., 2001).

1.4.3.2 Conditioned medium in inducing neural differentiation

Neural induction using conditioned medium during EB formation from ES cells was introduced by Rathjen and co-workers. They demonstrated that conditioned medium from the human hepatocellular carcinoma cell line, Hep-G2, promotes homogeneous differentiation of primitive ectoderm-like cells from mouse ES cells (Rathjen et al., 1999). Cells from EBs formed through this method express specific NSC markers such Sox1 and Nestin (Rathjen, 2002; Rathjen et al., 1999). These NSCs can go on to generate functional neurons and glia when exposed to appropriate signalling molecules (Rathjen et al., 2002). However, the molecules in Hep-G2 that trigger neuronal differentiation have not been identified and this protocol has not been applied to human ES cells.

1.4.4 Default mechanism in directing neuronal differentiation from ES cells

The default mechanism protocols are based on studies conducted using *Xenopus* and chick, which proposed that in the absence of specific signalling molecules, pluripotent cells become committed to neural specification (Hemmati-Brivalou and Melton, 1997). The model suggests that the inhibition

of BMP signalling could promote neural specification (Fainsod et al., 1997; Piccolo et al., 1996; Sasai et al., 1995; Smith et al., 1992; Hemmati-Brivalou and Melton, 1994). Recent work, however, has demonstrated that the mechanism of inducing neural commitment not only requires the inhibition of certain signalling molecules but also requires positive factors for the survival of these committed cells (Stern, 2005). Based on the evidence for a default pathway in triggering neural induction, several protocols were derived for obtaining neurons and glia from ES cells. These included the use of serum-free medium, culturing cells at low density, feeder-independent culture and stromal cell co-culture, discussed below.

1.4.4.1 Serum free medium in promoting neural differentiation from ES cells

Culturing ES cells in serum-free medium or nutrient-poor neurobasal medium successfully promotes the commitment and enrichment of NSCs (Okabe et al., 1996). These media conditions were originally used for culturing NSCs derived from embryonic or adult brain regions (Reynolds and Weiss, 1996). The principle of culturing in serum-free media is based on the observation that serum contains a neural differentiation inhibitor, most likely to be BMP derivatives (Sasai et al., 1995). Current protocols involve culturing ES cells in serum-free medium coupled with other conditions such as feeder-independence or low cell density to obtain neural induction.

1.4.4.2 Low density culture in directed neural differentiation

Several studies have shown that ES cells can be induced to form NSC in low clonal densities (1-20 cells/well) under feeder-free and serum free conditions (Tropepe et al., 2001). It was shown that a single neural stem cell isolated from the neural tube when cultured with EGF or FGF2 could proliferate forming floating clonal spheres of undifferentiated neural precursor cells (Reynolds and Weiss, 1996). This low density culture protocol generates NSCs, neurons, astrocytes and oligodendrocytes albeit at lower success rate (Tropepe et al., 2001). The production of NSCs from ES cells using this method is low, as only a reported 0.2% go on to form neurosphere colonies in the

defined medium. This result suggests that this method is not an efficient system for generating neuronal differentiation from ES cells.

1.4.4.3 Feeder-independent ES cells cultured as monolayer at moderate densities promotes neural induction

Neural commitment from ES cells can be achieved under serum-free conditions at moderate densities, but is most effective when cells are cultured in adherent monolayer cultures under feeder-independent conditions (Ying et al., 2003). This protocol was established using mouse ES cells that express green fluorescent protein (GFP) driven by the Sox1 promoter. Sox1 is a NSC marker, so the GFP provides an accurate readout for NSC in live cultures. These mouse ES cells cultured using this protocol produced 75% GFP positive cells by 5 days and could be selected to further differentiate into neurons, astrocytes and oligodendrocytes. The advantages of this protocol include the ability to generate NSC culture from ES cells within a short induction time (4-6 days) and the ability to isolate NSCs using Fluorescence Activated Cell Sorting (FACS) method.

1.4.4.4 Stromal cell co-culture of ES cells in neuronal differentiation

This protocol is based on the successful survival, proliferation and differentiation of hematopoietic stem cells with bone marrow stromal cells (Kaushansky, 2006). ES cells plated with a variety of stromal cell lines in serum free medium (or serum replacement) have the ability to direct neural induction (Barberi et al., 2003; Kawasaki et al., 2000). This protocol generates NSCs from mouse ES cells characterised by markers such as Nestin and neural cell adhesion molecule (NCAM) by day 6 before further differentiating into neuron and glia (Barberi et al., 2003; Kawasaki et al., 2000).

Advantages of this protocol include the generation of a homogeneous population of neural cells and short NSCs induction time. The neuronal differentiation from this protocol generates high percentage of NSC although this has not been quantified (Barberi et al., 2003; Kawasaki et al., 2000).

1.5 Identification and characterisation of neuronal derivatives from ES/EC cells

One important aspect of ES/EC/EG derived neurons, regardless of the protocol applied, is the identification and characterisation of the cell type(s) in the differentiated population. Not only does *in vitro* differentiation produce different subtypes of neurons, it also generates astrocytes and oligodendrocytes. Besides that, in most protocols, some differentiation down the mesodermal lineage is often unavoidable. The typical approach is to assay for the expression of genes that are specific for particular cell types. Such genes are often referred to as molecular markers and have been a useful tool for gauging differentiation efficiency.

Markers are chosen because they are known to be expressed in particular subtypes of cells. These can include markers that should be silenced in the differentiated population. For example, pluripotent factors such as Oct4, Nanog and Sox2 should be absent in neurons derived from ES/EG/EC cells, while the expression of these factors indicates the presence of pluripotent cells. Most commonly, markers of *in vitro* neural differentiation are selected to represent both early neural differentiation (including NSCs), and intermediate and/or terminal differentiation (i.e. mature neurons and glia cells). The application of this method has its caveats, however, as markers can often span several differentiation stages or more than one cell type. Therefore, a cohort of several markers is usually required to interrogate the differentiated population at various times during the differentiation period.

Among the key markers used for detecting neuronal differentiation from ES/EC cells at the early stage (EB formation stage-day1 neural differentiation) are Nestin, Mash1, Otx1, Otx2, Pax2, Pax5 and Wnt-1 genes (Okabe et al., 1996; Johnson et al., 1992). Among these markers, Nestin expressed both RNA and protein whereas other markers expressed the RNA but not the proteins (Rolletschek et al., 2001). The markers used to characterise cells in intermediate and terminal differentiation vary among studies. However the most used markers are Neurofilament proteins (NF-160/NF-200), β -III Tubulin, Synaptophysin and the production of neurotransmitter such as dopamine,

serotonin, GABA and glutamate. Additionally, GFAP is used to identify glia/astrocyte cell in neuronal differentiation cultures.

1.6 P19 EC cells as a model system for *in vitro* neuronal differentiation

P19 murine EC cells were first introduced as an *in vitro* neuronal differentiation model system by McBurney and Jones-Villeneuve in the year 1982 (Rossant and McBurney, 1982; Jones-Villeneuve, 1982). In these studies, RA was used to induce neuronal differentiation through the formation of EBs. The expression of neural related genes occurs in stages dependent on the time of differentiation in culture, which closely resemble early neuroectodermal development *in vivo* (Bain et al., 1995; Wobus et al., 1994; Staines et al., 1994). P19 EC cells transplanted into adult rat striatum survived and differentiated into functional neurons and glia (Morassuti et al., 1994). This evidence suggests that P19 EC cells are a suitable model system to study events underlying neuronal differentiation.

Undifferentiated P19 EC cells were shown to be pluripotent as they give rise to cells of all three germ layers when injected into mouse blastocysts (Rossant and McBurney, 1982). Undifferentiated EC cells *in vitro* have the ability to self-renew and proliferate at high rates, besides expressing gene profiles similar to embryonic stem cells (Andrews et al., 2005; Niwa et al., 2000). Similar to ES cells, P19 EC cells lose the expression of Oct4 and SSEA-1 upon differentiation *in vitro* (Andrews et al., 2005; Niwa et al., 2000). P19 EC cells can be grown indefinitely in the undifferentiated state, making it a good resource for the generation of neurons.

The RA (All *trans* RA) protocol for inducing neuronal differentiation from P19 EC cells can be divided into two stages. Stage one, EB formation, occurs in suspension, whereas stage two involves differentiation of neurons and generation of glia cells in adherent culture (Zhongqiu et al., 2010; Zhigang Jin et al., 2008; McBurney, 1993; Johnson et al., 1992; Rossant and McBurney, 1982; Jones-Villeneuve, 1982). In stage one, undifferentiated cells are

cultured in suspension with the addition of RA for 2 days and further 2 days without RA. By day 4, the cells formed EBs consisting of neuroectodermal cells that express the markers Nestin and β -III Tubulin, together with the loss of the pluripotent marker Oct4 (Teets et al., 2011; Soprano et al., 2007; Bain et al., 1995).

In stage two, neuroectoderm-containing EBs are disaggregated and plated as single cells in adherent culture to allow neuronal differentiation. Cells project neurite outgrow and first form mature neurons followed by glia cells. A study by Staines et al concluded that the morphology of neurons derived from P19 EC cells mimics those from the rostrum region of the mammalian nervous system (Staines et al., 1994). The P19-derived neurons express specific markers such as Nestin, MAP2, Tau, Neuron specific enolase, Synaptophysin, NF-160, NF-200, Mash1 and β -III Tubulin (Zhigang Jin et al., 2008; Yi Wei et al., 2002; Guan et al., 2001; Rohwedel et al., 1998; Strübing et al., 1995; Bain et al., 1995; Johnson et al., 1992). Glial cells appear later in the differentiation culture (Day 10 onwards), assayed through the expression of Gfap (Hadinger et al., 2009; Santiago et al., 2005).

Evidence for the functionality of RA-induced neurons from P19 EC cells has been presented by various groups. McBurney and co-workers showed that these neurons establish axonal-dendritic polarity and form functional excitatory and inhibitory synapses (Finley et al., 1996; MacPherson et al., 1997). The neurons are capable of producing GABA, glutamate, neuropeptide Y, somatostatin and other neurotransmitters (Macpherson et al., 1997; Lin et al., 1996; Parnas and Linial, 1995). These studies support the use of P19 neuronal differentiation as a suitable model for studying the mechanisms underlying neural differentiation.

The vast majority of studies using the RA-induced neuronal differentiation from P19 EC cells, besides characterisation of the system, are centred on elucidating regulatory factors that govern the neuronal differentiation process. These factors include TFs (modulating pluripotency, differentiation, and cell cycle), signalling molecules and pathways, epigenetic factors and

microRNAs. Other studies have investigated neurotransmitter receptor signalling, the metabolite transport system and electrophysiology.

1.7 Chromatin and gene transcription

In eukaryotes, DNA is organised into DNA-protein complexes known as chromatin, allowing the efficient “packaging” of genomic DNA (Figure 1.1). The fundamental unit of the chromatin is the nucleosome, which is made up of four core histone proteins called H2A, H2B, H3 and H4 with 147 bp of DNA wound around its surface (Horn and Peterson, 2006; Felsenfeld and Groudine, 2003). Adjacent nucleosome units are connected by DNA linker histone (10-100 bp long) resembling a “beads on the string” - like structure. The next level of organisation is called the 30 nm meter fibre, which is then folded into higher order structures.

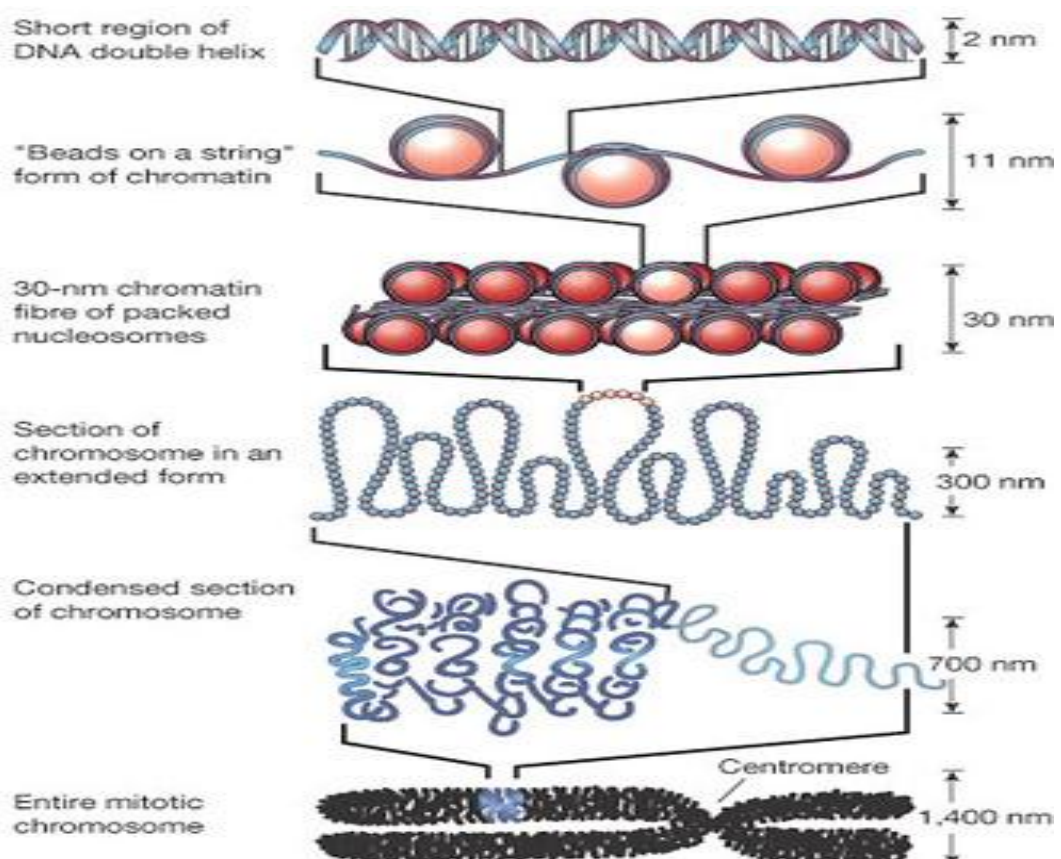


Figure 1.1: Organisation of chromatin.

The fundamental unit of chromatin is the nucleosome, in which DNA is wound around a core histone octamer resembling a “beads on the string” - like structure. Reproduced from (Felsenfeld and Groudine, 2003).

Higher order chromatin structure is characterised by condensed heterochromatin and euchromatin regions within the genome. Heterochromatin regions are highly condensed and transcriptionally silent, while euchromatin regions are less compact and more transcriptionally active (Horn and Peterson, 2006). Two types of heterochromatin structures have been described: constitutive heterochromatin, which is found at centromeres and telomeres, and facultative heterochromatin, which upon certain stimuli can become euchromatin, examples include the inactive X chromosome and autosomal imprinted genes (Trojer and Reinberg, 2007). Besides the role of efficiently packing genomic DNA, chromatin also functions as platform for the regulation of gene transcription. Gene expression can be regulated by interrelated processes such as nucleosome remodelling, histone modification and DNA methylation. These processes along with their cognate regulatory proteins are classified under the general term “epigenetic mechanisms”.

Studies of gene regulation in pluripotency and self-renewal initially focused on TF network regulation, until several recent papers highlighted the importance of epigenetic mechanisms in ES cell pluripotency, differentiation and early development (Reik et al., 2007). Epigenetic factors that have been shown to play a role in the regulation of ES cell pluripotency and neuronal differentiation include covalent modifications of histones, DNA methylation and ATP-dependent chromatin remodelling. These various mechanisms are discussed below with some examples from ES cells and neuronal differentiation.

1.7.1 Histone modification

Specific residues within the core histone tails, which protrude out from the nucleosome surface, are subjected to various reversible post-translational modifications including acetylation, methylation and phosphorylation (Kouzarides, 2007).

1.7.1.1 Histone acetylation

Histone acetylation occurs on lysine residues (K) on N-terminal tails of all four core histones. Some of the most studied acetylation marks are those on

histones H3 (H3K9ac, H3K14ac) and H4 (H4K5ac, H4K8ac, H3K12ac, H3K16ac). Histone acetylation is mediated by histone acetyl transferases (HATs), which are divided into three main families: the p300/CBP family, MYST family and Gcn5/PCAF family (Sterner and Berger, 2000). Histone acetylation is strongly linked to activation of transcription (Reid et al., 2000). There is evidence that multiple histone acetylation marks can lead to chromatin unfolding *in vitro* (Tse et al., 1998). However, it is also known that histone acetylation facilitates transcription by acting as a docking or binding site for co-activators that contain bromodomains (Hassan et al., 2002; Agalioti et al., 2002). In contrast, HAT activity is counteracted by histone deacetylase enzymes (HDAC). In metazoans, HDACs are classified into 3 groups based on sequence similarity; Class 1, Class 2 and class 3. As an example, class 1 HDACs include HDAC1, HDAC2 and HDAC3 and are found in four different multiprotein complexes, the Sin3a, NuRD, Co-Rest and NCoR/SMRT complexes.

In ES cells, the histone acetyltransferase p300 functions as transcriptional co-activator and regulates the expression of pluripotency-related TFs (Zhong and Jin, 2009; Chen et al., 2008). Another HAT, Tip60, was also shown to regulate the pluripotency transcription network by targeting genes similar to Nanog (Fazio et al., 2008). The Tip60-p400 complex appears to activate genes responsible for repressing key developmental regulators (Fazio et al., 2008). Meanwhile, HDACs are also essential for the pluripotency of ES cells. The HDAC Mbd3, a core subunit of the Nucleosome remodelling deacetylase (NURD) complex, is vital for pluripotency (Denslow et al., 2007; Kaji et al., 2006). Mbd3 depletion in ES cells results in defects in growth and differentiation (Kaji et al., 2006). Similarly, another HDAC known as NODE interacts with Nanog and Oct4, resulting in the inhibition of developmental regulators in ES cells (Liang et al., 2008). In addition, WUS-interacting proteins such as WSIP1 and WSIP2 recruit HDACs to repress the transcription of genes that are involved in regulating differentiation (Kieffer et al., 2006).

The regulation of histone acetylation is also important for the progression of ES cells to NSCs and neurons. ES cells appear to have higher global levels of histone acetylation than lineage-restricted stem cells and differentiated cells (Efroni et al., 2008). As NSCs commit to the neuronal lineage, expression of

HDAC2 is up-regulated while HDAC1 is down-regulated (MacDonald and Roskams, 2008). Conversely, HDAC1 expression is sustained in glia lineage cells (astrocytes and oligodendrocytes), in which HDAC2 is not detected (MacDonald and Roskams, 2008). Consistent with this data, the use of different HDAC mutants showed that HDAC2 inhibits astrocyte differentiation (Humprey et al., 2008). The importance of HDACs in neuronal differentiation has also been demonstrated using the HDAC inhibitor valproic acid, which induces neuronal differentiation of NSCs but inhibits glia cell differentiation (Hsieh et al., 2004). In this study, valproic acid promotes the up-regulation of neuron-specific genes, including the neurogenic basic helix-loop-helix transcription factor, NeuroD, resulting in the induction of neuronal differentiation.

1.7.1.2 Histone Methylation

Histone methylation can occur on lysine (K) or arginine (R) residues of the core histones (Kouzarides, 2007). Each lysine residue can be mono-, di- or trimethylated whereas arginine can be either mono- or dimethylated (Kouzarides, 2007). Methylation of histone residues can mediate both active and repressive signals, which regulate gene transcription through recruitment of specific downstream effector proteins. Histone methylation is catalysed by a range of multiprotein complexes containing histone methyltransferases (HMTs). Among the protein complexes that are involved in depositing and removing these histone marks are the trithorax (TrxG) and polycomb (PcG) complexes (Muller and Verrijzer, 2009; Kerppola, 2009; Schuettengruber et al., 2007). TrxG and PcG have reciprocal functions: TrxG proteins work together to activate transcription while PcG proteins repress transcription.

TrxG proteins are multi-subunit complexes that can be generally classified into two categories; the histone modifiers and nucleosome remodelers (Strahl and Allis, 2000). The histone modifiers include HMTs that establish histone modifications that promote transcription. Among the examples of HMTs in this category are TRX and ASH1 that methylate histone H3 lysine 4 (H3K4) active mark.

PcG complexes are made up of Polycomb repressive complex 2 (PRC2) and Polycomb repressive complex 1 (PRC1). PRC2 complex establishes the histone code while PRC1 interprets this code (Levine et al., 2004). The mammalian PRC2 complex consists of enhancer of zeste homologue 2 (EZH2), embryonic ectoderm development (EED), suppressor of zeste homologue 12 (SUZ12) and retinoblastoma-binding protein 4 (RBBP4) (Sparmann and van Lohuizen, 2006). EZH2 contains a SET domain that deposits the H3K27me3 inactive chromatin mark, whereas EED and SUZ12 do not contribute to HMT activity but are essential for supporting EZH2 catalytic activity (Cao and Zhang, 2004). The inactive chromatin mark established by PRC2 is recognised by PRC1. The PRC1 complex can take multiple forms that contain a chromobox protein (CBX2, CBX4, CBX8) and a polyhomeotic homologue 1 family member (PHC1-3, BMI1 Ring finger protein 1 (RING1), Ring finger protein 2 (RNF2)). In general, CBX proteins contain a chromodomain that is responsible for recognising and binding H3K27me3 mark established by PRC2. BMI1, RING1 and RNF2 have RING finger motifs that are E3 ligases that are essential for ubiquitination (Whitcomb and Taylor, 2009). The regulatory effects of PcG and TrxG are broad and are mediated through various histone modifications and nucleosome remodelling. Some of the specific examples in ES cells are discussed below.

Two key histone modifications that are heavily involved in ES cell gene regulation are H3K4me3 and H3K27me3, which are typically associated with active and repressive chromatin regions, respectively (Ku et al., 2008; Mikkelsen et al., 2007; Bernstein et al., 2006). A major discovery in ES cell biology is the co-occupancy of both H3K4me3 and H3K27me3 on large number of promoter sequences (Mikkelsen et al., 2007; Bernstein et al., 2006). These regions of chromatin are named “bivalent” domains and are thought to hold genes in a poised state, ready to be either transcribed or repressed. This bivalent chromatin signature occupies the promoters of genes that are involved in development and lineage commitment (Mikkelsen et al., 2007; Bernstein et al., 2006). Initial studies suggested a model where this bivalent chromatin signature was crucial to the pluripotent status of ES cells (Bernstein et al., 2006). However, more recent ChIP-seq data revealed the existence of

bivalent chromatin domains on the promoters of developmentally regulated genes in differentiated cell types (Barski et al., 2007; Mikkelsen et al., 2007; Azuara et al., 2006).

The PRC2 complex targets a number of developmentally vital genes and rather interestingly these genes are co-occupied by Oct4, Nanog and Sox2 in ES cells (Lee et al., 2006). Bernstein et al confirm this model by showing that Oct4, Nanog and Sox2 are marked by both H3K27me3 (inactive) and H3K4 (active) modification (Bernstein et al., 2006). Most of the bivalent patterns of histone modification were erased upon ES cell differentiation into neural progenitor cells (Bernstein et al., 2006). The neural genes retained the H3K4 active mark and lost the H3K27me3 repressive mark. Additionally, a subset of genes that function in terminally differentiated neurons gain H3K27me3 during the transition from ES cell to NSCs (Mohn et al., 2008). These genes eventually lose H3K27me3 and hence become expressed upon terminal differentiation of neurons.

1.7.2 DNA methylation

Like histone methylation, DNA methylation also plays a role in regulating gene expression in ES cells. DNA methylation occurs on the cytosine base of the DNA within CpG dinucleotides and correlated to gene silencing. DNA methylation at promoter regions is inversely correlated with gene activity, although this association is dependent on CpG density within the promoter region. Methylated CpG dinucleotides are recognised by methyl-CpG binding domain (MBD)-containing protein family member such as MeCP2 and MBD1 and consequently suppress the gene expression (Cross et al., 1997; Nan et al., 1997).

DNA methylation is carried out by DNA methyl transferase (DNMT) family of enzymes. The de novo establishment of DNA methylation is performed by DNMT3a and DNMT3b, whereas the maintenance of DNA methylation depends on DNMT1. The role of DNMTs in ES cells has been established using homozygous mutants. DNMT1^{-/-} ES cells divide and maintain pluripotency in culture but failed to survive after being induced to differentiate, possibly due

to the lack of repression of pluripotent genes such as Oct4 and Nanog through methylation (Jackson et al., 2004). DNMT3b mutant embryos appear to develop normally before embryonic day 9.5 but consequently demonstrate developmental defects (Okano et al., 1999).

Similar to somatic cells, ES cells show high global levels of DNA methylation with approximately 60-80% methylation in CpG dinucleotides (Meissner et al., 2008). Extensive mapping shows that DNA methylation profiles in ES cells and somatic cells have a bimodal distribution, with most of the genomic regions 'largely methylated' or 'largely unmethylated' (Meissner et al., 2008). Almost all high density CpG promoter regions enriched for H3K4me3 in ES cells are devoid of DNA methylation (Meissner et al., 2008; Mikkelsen et al., 2007). Low density CpG promoters, which are generally linked to tissue-specific genes, are mostly methylated except for a small subset that is enriched for H3K4me3/me2 active marks. Pluripotency genes are generally enriched for H3K4 methylation and show DNA hypomethylation (Mikkelsen et al., 2007).

An example of how DNA methylation regulates gene expression during differentiation is provided by the GFAP gene. GFAP expression is induced as NSCs differentiate into astrocytes in foetal brain. The Stat3-binding site within the GFAP promoter in NSCs was found to be highly methylated in NSCs (Takizawa et al., 2001). As NSCs differentiated, the Stat3-binding site is demethylated allowing the binding of STAT3 and inducing the expression of GFAP. DNA methylation is also shown to regulate the progression of undifferentiated ES cells to NSCs through RE1 silencing transcription factor (REST)/neuron restrictive silencing factor (NRSF) (section 1.7.4).

1.7.3 ATP-dependent chromatin remodelling

ATP-dependent chromatin remodelling involves changes in chromatin structure through the destabilisation of DNA and histone interactions, and can be associated with both transcriptional activation and repression. Depending on which remodelling complex is involved, this can enable a nucleosome to 'slide' along the DNA, thus facilitating the access of TFs to the DNA, or it can allow histones to be swapped for other variants. ATP-dependent chromatin

remodelling complexes consist of four main families: Switching/Sucrose non-fermenting (SWI/SNF), Imitation of SWI (ISWI), Chromodomain and helicase-like domain containing (CHD) and Inositol requiring (INO80) (Bao and Shen, 2007). Mammalian SWI/SNF can contain either Brahma (BRM) or Brahma related gene 1 (BRG1) as its core ATPase subunit, and other members of the complex are termed Brahma/Brg associated factors (BAFs).

In ES cells, BRG1 binds to the regulatory regions of Oct4, Nanog and Sox2 and is involved in the maintenance of pluripotency and initiation of differentiation (Keenen and de la Serna, 2009). The loss of BRG1 leads to the loss of self-renewal ability in ES cells (Ho et al., 2009; Keenen and de la Serna, 2009). In a separate study, BRG1 was shown to be recruited to RE1 sites of REST target genes (Ooi et al., 2006). Inhibition of BRG1 activity increased the expression of REST target genes, and it was suggested that BRG1 facilitates the interaction of REST with chromatin, thus facilitating transcriptional repression.

The role of BAF complexes was also elucidated in neural development (Lessard et al., 2007). This study demonstrates the 'switching' of BAF member expression between NSCs and post-mitotic neurons derived from newly born (P0) mouse brain. In NSCs, BAF45a and BAF53a are expressed and are assembled into the BAF complex, while in post-mitotic neurons, the place of BAF45a and BAF53a are taken over by BAF45b and BAF53b. Inhibiting BAF45a and BAF53a lead to a reduction in NSC proliferation. Similarly, BAF60c was also assembled into the NSC specific BAF complex consisting of BAF45a and BAF53a in retina cells (Lamba et al., 2008). BAF60c was shown to promote Notch signalling, which inhibits neuronal differentiation but maintains the proliferation of NSC through the transcriptional activation of basic helix-loop-helix genes Hes1 and Hes2.

1.7.4 The role of REST/NRSF complex in ES cells and neuronal differentiation

In ES cells and non-neuronal cells, neuronal genes containing the 21 bp response element 1 (RE1) are repressed by the binding of RE1 silencing

transcription factor (REST) (also known as neuron restricted silencing factor, NRSF) (Lunyak and Rosenfel, 2005; Lunyak et al., 2002). Rest-null mice develop normally till E9 but dies soon after from unidentified causes (Chen et al., 1998). Genome-wide ChIP studies have shown that REST binds close to many genes that are expressed in mature neurons (Otto et al., 2007).

REST represses neuron-specific genes through the recruitment of HDAC1/2, Sin3a and CoRest (Ballas et al., 2001; Andres et al., 1999). During neuronal differentiation, REST protein levels are reduced, possibly through protein degradation, resulting in the removal of REST-associating transcriptional repressors from neuronal genes (Ballas et al., 2005). In terminally differentiated non-neuronal cells, long term repression of neuronal genes is achieved through the recruitment of DNMT1 to RE1 sites followed by DNA methylation and MeCP2 binding (Ballas et al., 2005). Another mechanism by which REST may control neuron-specific gene expression is through a neuron specific microRNA, mir-9 (Packer et al., 2008). Mir-9 has been shown to target Rest mRNA and the over-expression of mir-9 promotes neuronal differentiation.

1.7.5 The use of P19 EC cells to study epigenetic mechanisms

Among the examples of epigenetic-related studies in P19 neuronal differentiation are those conducted by Hwang et al showing evidence of chromatin remodelling and TF regulation on the mu-opioid receptor gene (MOR) (Hwang et al., 2010; Hwang et al., 2009; Hwang et al., 2007). Hwang et al showed that in undifferentiated P19 cells, the MOR gene promoter is methylated and transcription is repressed by MeCP2. During neuronal differentiation, the promoter becomes de-methylated and active histone modifications are deposited. This allows binding of the chromatin remodeller Brg1, which remodels the nucleosome upstream of the transcription start site, thus allowing the transcription factor Sp1 to bind and induce MOR expression (Hwang et al., 2007, 2010). This model for MOR regulation was supported by similar experiments in micro dissected mouse brain regions (Hwang et al 2009).

In a separate study, Wu et al presented evidence for the role of histone marks and chromatin remodellers in the regulation of the neurogenin1 gene, which is a basic-helix-loop-helix protein crucial for neurogenesis (Wu et al., 2009). Upon RA induction, the repressive histone mark H3K27me3 is replaced by active marks H3K9ac, H3K14ac and H3K4me3. The remodeller Brm is then recruited, which coincides with the expression of neurogenin1, (Wu et al., 2009). Taken together, these studies not only show the role of epigenetic mechanisms in regulating neural-specific genes, but also demonstrate the suitability of the P19 neuronal differentiation model system for studying the epigenetic events that govern the transition from pluripotency to neural commitment.

1.8 Overview of HMG chromosomal proteins

High Mobility Group (HMG) proteins are a family of nuclear proteins that bind DNA and nucleosomes and induce changes in chromatin dynamics. HMG proteins play important roles in modulating chromatin structure, which affects various DNA-dependent activities such as transcription, replication and DNA repair (Bustin and Reeves, 1996; Bustin, 1999). HMG proteins are grouped into three distinct families based on their unique functional motifs, HMG-AT-hook (HMGA), HMG-box (HMGB) and HMG-nucleosome binding (HMGN).

1.9 HMGN proteins; structure and their interaction with nucleosomes

The HMGN family of proteins contains a functional motif that specifically binds the 147 base pair nucleosome core particle. The HMGN family consists of 5 members encoded by different genes; HMGN1, HMGN2, HMGN3a/b, HMGN4 and HMGN5 (previously known as NBP-45 and NSBP1). These proteins are characterised by three distinct domains, namely a bipartite nuclear localisation signal (NLS), a conserved 30-amino acid long nucleosome-binding domain (NBD) and a negatively charged C-terminal chromatin regulatory domain (RD), previous called the chromatin unfolding domain (Figure 1.2). HMGN1 to 4 are about -100 amino acids long (HMGN1=96 amino acids; HMGN2=90 amino acids; HMGN3a=99 amino acids; HMGN3b=77 amino acids;

HMGN4= 92 amino acids) while the recently discovered HMGN5 is composed of 406 amino acids (Rochman et al., 2010). HMGN3 consists of two splice variants called HMGN3a and HMGN3b, with the latter missing most of the RD (West et al., 2001).

The NBD of all HMGN proteins consists of a unique conserved octapeptide motif, RRSARLSA, which is encoded by exon 3. This NBD motif is the core region that is shown to anchor the HMGN proteins to nucleosome particles. Deletion and point mutation analyses of HMGN proteins revealed that while other domains of the protein affect the nucleosome binding affinity, mutation in the conserved NBD motif abolishes the interaction with nucleosomes (Ueda et al., 2008).

HMGN proteins contain a high number of charged amino acids and a disordered secondary structure that allows the formation of multiple protein-protein complexes (Singh et al., 2009). Indeed HMGN1 and HMGN2 form multiple metastable protein complexes *in vivo* (Lim et al., 2004).

HMGN proteins do not bind to specific DNA sequences within chromatin. With the exception of HMGN5, they appear to interact with all nucleosomes throughout the genome. Conversely, mouse HMGN5 binds preferentially to nucleosomes in euchromatin regions and is excluded from the heterochromatin due its highly acidic RD (Rochman et al., 2009). One of the major questions in HMGN biology is whether these proteins are enriched at particular chromatin regions, and if so, how are they recruited there?



Figure 1.2: HMGN protein structure consist of three distinct domains, namely a bipartite nuclear localisation signal (NLS), a conserved 30-amino acid long nucleosome-binding domain (NBD) and C-terminal chromatin regulatory domain (RD).

1.10 Dynamic binding of HMGNs to chromatin

The interaction of HMGN proteins with the chromatin is clearly illustrated by Catez et al using fluorescence recovery after photobleaching (FRAP) experiments (Catez et al., 2006; Bustin et al., 2005). This study revealed that the interactions of HMGN proteins and histone H1 with chromatin in living cells are dynamic and transient. HMGN proteins constantly move throughout the nucleus in a “stop and go” fashion in which each protein associates with a specific nucleosome for a limited time and then dissociates and binds to a different nucleosome.

The dynamic interaction of HMGN proteins with chromatin is thought to be fundamental to their role in chromatin regulation (Postnikov and Bustin, 2010). The amount of HMGN protein present in the nucleus is sufficient to bind only about 1% of the nucleosomes. Nevertheless, FRAP analysis showing that HMGN proteins can rapidly associate and dissociate from chromatin indicates that they can cover the entire genome in less than one minute (Catez et al., 2006). Thus, the dynamic nature of their binding interaction ensures that all nucleosomes will be contacted by HMGN proteins on a regular basis (Postnikov and Bustin, 2010).

1.11 HMGN proteins in chromatin structure

HMGN proteins bind nucleosome core particles and modulate chromatin structure, thus regulating DNA-dependent processes. Initial studies showed that HMGN proteins increased the DNase I hypersensitivity of transcriptionally active genes, suggesting that the proteins decompact the chromatin fibres (Weisbrod and Weintraub 1981; Weisbrod et al., 1980). Successive studies using nuclease restriction digestion and sedimentation analysis provided evidence that HMGN proteins reduce the compaction of chromatin assembled *in vitro* (Rochman et al., 2009; Ding et al., 1997; Crippa et al., 1993).

Several studies to date are aimed at addressing the mechanism by which HMGN proteins might affect chromatin structure and regulate transcription. There is evidence for three general mechanisms: competition between HMGN and linker histone proteins, inhibition of ATP-dependent chromatin remodelling by HMGNs, and the effect of HMGN activity on the levels of post-translational modification in core histones.

1.11.1 HMGN antagonises the chromatin condensing activity of linker histone H1

Linker histone H1 plays a key role in chromatin compaction and various studies suggest that HMGN proteins compete with histone H1 for chromatin binding sites (Catez et al, 2006; Ding et al., 1997). The binding footprint of HMGN1 and HMGN2 partially overlaps that of histone H1 (Alfonso et al., 1994). A recent study conducted by Rochman using immunofluorescence analysis in mouse cells expressing exogenous HMGN5 indicates that the protein reduces the compaction of chromatin fibres and modulates the cellular transcription profile (Rochman et al., 2009). *In vitro* sedimentation and cross-linking experiments further support the model that HMGN5 counteracts the linker histone-mediated condensation of the chromatin fibres (Rochman et al., 2009). However, the evidence that HMGN1 could counteract linker histone-mediated compaction was less clear in this study (Rochman et al., 2009). Thus, while there is evidence that HMGN1-4 may compete with linker histones for binding to nucleosomes *in vivo*, it is not clear whether this affects the

level of chromatin compaction *in vivo*, or whether this has a direct impact on gene transcription.

1.11.2 HMGN alter the activity of ATP-dependent chromatin remodelling complexes

ATP-dependent chromatin remodelling complexes play a crucial role in regulating the dynamics of chromatin organisation (Horn and Peterson, 2002; Smith and Peterson, 2005). One study conducted by Rattner et al showed that HMGN1 and HMGN2 suppress ATP-dependent nucleosome remodelling by ACF and BRG1 (Rattner et al., 2009). This report is contrary to a previously published study claiming that HMGN1 does not affect the dynamics of SWI/SNF-dependent nucleosome remodelling (Hill et al., 2005). Thus it is possible that HMGN proteins play a role in gene regulation by inhibiting ATP-dependent chromatin remodelers, but more research is required to investigate this further.

1.11.3 HMGN regulate the levels of post-translational modification in core histones

Histone modifications have been shown to play key roles in most biological processes including development and cellular differentiation (Berger et al., 2002; Rice and Allis, 2001; Cheung et al., 2000). There are more than 100 different post-translational modification associated with nucleosomal core histones (Kouzarides, 2007). Given that HMGN proteins bind specifically to nucleosomes, it is possible that they could influence the levels of histone modification and hence the organisation of chromatin and cellular processes.

Analysis of fibroblast cells derived from *Hmgn1*^{-/-} mice compared to their wild type littermates revealed the loss of HMGN1 corresponded to changes to the global levels of H3K14ac, H3K9ac, H3S10p, H3S28p, H4S1p and H2AS1p (Postnikov et al., 2006; Lim et al., 2005; Lim et al., 2004). HMGN1 is thought to increase H3K14ac by enhancing the activity of HATs rather than inhibiting HDACs (Lim et al., 2005). In this study, *HMGN1*^{-/-} and *HMGN1*^{+/+} mouse embryonic fibroblast cells (MEFs) treated with trichostatin A (TSA), a HDAC inhibitor showed that *HMGN1*^{+/+} cells had increased levels of H3K14ac was due

to increased activity of HATs rather than inhibiting HDACs. In the similar study, HMGN1 were shown to affect the expression of a subset of immediate early (IE) genes by reducing phosphorylation of histone 3 serine 10 (H3S10p) while promoting H3K4ac.

1.12 Transcription regulation by HMGN proteins

The interaction of HMGN proteins with chromatin leads to changes in transcriptional processes (Rochman et al., 2010; Bustin, 2001; Ding et al., 1994; Paranjape et al. 1995). The link between HMGN proteins and transcription was first demonstrated by Weisbrod and Weintraub in their work using chromatin purified from chicken erythrocytes, which showed that HMGN1/2 were associated with DNase I hypersensitive regions of the β -globin gene (Weisbrod and Weintraub, 1979). Subsequent studies also suggested that HMGN1/2 bind preferentially to active genes (Postnikov et al., 1991; Weisbrod, 1982; Gazit et al., 1980; Goodwin et al., 1979).

Further evidence of the ability of HMGN proteins to act as activators of transcription came from studies conducted using SV40 minichromosomes isolated from CV-1 cells and minichromosomes assembled in *Drosophila* embryo or *Xenopus* egg extracts (Weigmann et al., 1997; Ding et al., 1997; Tremethick et al., 1996; Trieschmann et al., 1995; Ding et al., 1994). In each system, HMGN1/2 enhanced the rate of transcription only from chromatin but not in naked DNA templates, suggesting that HMGN1/2 are chromatin-specific transcriptional activators.

The studies above indicate that HMGN proteins can act as general transcriptional facilitators, but their ability to act as specific transcriptional modulators was shown by gene expression profiling in cells lacking a particular HMGN variant. The loss of HMGN1 in MEFs altered the expression of 3% of active genes (Rubinstein et al., 2005). Similarly, stable over-expression of HMGN3 in Hepa cells affected the levels of 0.8% of expressed genes (West et al., 2004). These studies indicate that HMGN proteins affect only subset of genes and may play a role as specific modulators of gene expression.

Studies using Chromatin Immunoprecipitation (ChIP) have revealed binding of HMGN proteins at specific gene targets in specific cell types. For example, HMGN3 was shown to bind and activate the genes *Glyt1* and *Glut2* in Hepa cells and MIN6 cells, respectively (Ueda et al., 2009; West et al., 2004). HMGN1 increases the rate of heat-shock-induced Hsp70 activation by binding to the Hsp70 promoter in MEFs (Belova et al., 2008). In contrast, HMGN1 binds and represses the *Sox9* gene in mouse limb bud micromass cultures (Furusawa et al., 2006). Additionally, HMGN1 binds to and inhibits the induction of certain estrogen-induced genes in MCF7 cells and various anisomycin-induced immediately early genes in MEFs (Zhu and Hansen, 2007; Lim et al., 2004). More recently, a study using ChIP-sequencing and genome-wide analysis has revealed that HMGN1 in CD4⁺ T cells binds specific genomic regions corresponding to DNaseI hypersensitive sites, promoters, functional enhancers and transcription factor binding sites (Cuddapah et al., 2011). These studies suggest that, in addition to transiently interacting with all nucleosomes, HMGN1 may be enriched at certain regulatory sites where it may play specific roles in gene regulation (Cuddapah et al., 2011).

HMGN1-4 have similar protein structures and share functional properties in how they interact with chromatin and affect histone modifications. These features lead to the suggestion that HMGN proteins may be functionally redundant. However, the studies described above using mice and/or cells with altered HMGN content show that the HMGN variants are not fully redundant. Furthermore, direct comparison of transcription profiles of MEFs in which HMGN1, HMGN3 or HMGN5 are knocked out or overexpressed revealed limited redundancy between the variants (Rochman et al., 2011).

Although there are studies demonstrating the role of HMGN proteins in cellular transcription, the mechanisms of how they affect particular subsets of genes and whether they play variant-specific roles in transcription regulation remain unclear. Given that HMGN1 and HMGN2 are ubiquitously expressed in most adult cells, while HMGN3 and HMGN5 show distinct developmental and tissue-specific expression, it is possible that HMGN proteins play key roles in orchestrating specific cellular transcription profiles.

1.13 HMGN knockout mice and their functional analysis

Knockout mice for HMGN1 and HMGN3 have been developed while Hmgn2^{-/-} has proven to be embryonic lethal (Bustin Lab communication, although this work has never been published and it is not possible to mention at what embryonic stage the embryos die). Hmgn1^{-/-} mice appear to develop normally but are present at a reduced frequency in HMGN1^{+/-} crosses (Birger et al., 2005; Birger et al., 2003). HMGN1^{-/-} mice demonstrate differences in the cellular processes when subjected to stress (Birger et al., 2005; Birger et al., 2003). When exposed to UV and ionizing radiation, Hmgn1^{-/-} mice and cells derived from these mice show unusual hypersensitivity compared to wild type littermates (Birger et al., 2005; Birger et al., 2003). This is thought to be due to less efficient nucleotide excision repair of DNA damage in Hmgn1^{-/-} cells (Birger et al 2003, Fousteri et al 2006; Subramanian et al 2009). Meanwhile, Hmgn1^{-/-} mice and cells exposed to ionizing radiation reveal increased tumorigenicity due to impaired ability to activate G2-M checkpoint (Birger et al., 2005). Hmgn1^{-/-} mice also show defects in the development of corneal epithelium, which is linked to the altered expression of cell adhesion molecules and p63 (Birger et al., 2006).

Hmgn3^{-/-} mice appear to develop normally but show mild defects in insulin secretion (Ueda et al., 2009). Functional analysis elucidated that HMGN3 affects the transcription regulation of key genes involved in pancreatic B islet cells including Glut2 and Kir6 (Ueda et al., 2009).

1.14 HMGN expression and possible function in development and cellular differentiation

Proper embryonic development and cellular differentiation requires multiple changes in gene expression and a pre-programmed pattern of transcription activities. It has been shown that precise control of chromatin structure plays a crucial role in regulating the outcome of development and differentiation processes. The chromatin structure of specific genes is crucial for the maintenance of the pluripotency of the inner cell mass (Boyer et al., 2006).

Remodelling of chromatin is also important for the commitment of pluripotent cells to specific lineages (Kondo, 2006) and terminal differentiation (Palacios and Puri, 2006; Wilson et al., 2005; Hsieh and Gage, 2004). Given that chromatin plays an extensive role in determining and carrying out specific pre-programmed gene expression in development and differentiation, it can be expected that the HMGN family of chromatin binding proteins would affect the outcome of these processes.

Studies on the role of HMGNs in development and cellular differentiation are mainly based on *in vitro* model systems of mouse, chicken or human cells and *in vivo* functional analysis of knockout mice. The expression patterns of Hmgn family members in embryonic development and cellular differentiation are unique, and suggest a specialised role for each variant. Most of the expression data regarding HMGNs are for HMGN1 and HMGN2 only, because they are the founding members and have been studied for over 4 decades. For the purposes of this discussion, the expression patterns of HMGN1 and HMGN2 are considered together, followed by those of HMGN3 and HMGN5. HMGN4 expression has not been studied in the context of development.

1.14.1 HMGN1 and HMGN2 expression and functional role in development and differentiation

HMGN1 and HMGN2 are ubiquitously expressed in all adult tissues, although the highest expression is detected during embryogenesis (Furusawa et al., 2006; Lehtonen et al., 2001). The expression of HMGN1 and HMGN2 is regulated in a developmental-specific manner, in which the proteins are progressively down-regulated throughout the entire embryo except in cells that are committed and continuously undergoing differentiation (Furusawa et al., 2006; Lehtonen et al., 2001). In early stage embryogenesis, HMGN1 and HMGN2 proteins are detected throughout oogenesis while Hmgn1 and Hmgn2 transcripts are present beyond the two-cell stage. When antisense oligonucleotides of HMGN1 and HMGN2 were injected into mouse oocytes, the transient loss of HMGN1 and HMGN2 delayed cell cleavage and the onset of the blastocyst stage (Mohamed et al., 2001).

In early stage bovine embryo development, HMGN1 and HMGN2 are expressed in oocytes but are steadily down-regulated upon fertilization and almost lost by the eight-cell stage (Vigneault et al., 2004). Sustained HMGN2 expression in an *in vitro* fertilization study of bovine embryos showed that enhanced levels of HMGN2 resulted in the embryos failing to develop into a blastocyst due to H3K14ac mediated chromatin remodelling (Bastos et al., 2008).

In *Xenopus* development, the Hmgn1 and Hmgn2 genes are expressed in the three germinal layers. However the proteins are only detected after the mid-blastula transition and continue during neurula and tadpole embryo development (Korner et al., 2003). Both over-expression and depletion of HMGN1 and HMGN2 after the mid-blastula transition resulted in clear developmental defects, suggesting that mis-regulation of these proteins leads to abnormal development (Korner et al., 2003).

In vitro cellular differentiation model systems revealed that HMGN1 and HMGN2 are linked to differentiation processes such as erythropoiesis, myogenesis and chondrogenesis (Furusawa et al., 2006; Lehtonen et al., 2001; Crippa et al., 1991; Pash et al., 1990). During chondrocyte differentiation, HMGN1 and HMGN2 have been shown to bind and repress Sox9, which is a transactivator and master regulator of chondrogenic fate (Furusawa et al., 2006). HMGN1 is down-regulated during chondrocyte differentiation, with concomitant induction of Sox9 expression (Furusawa et al., 2006). HMGN1 expression is also down-regulated during myogenesis, and over-expression of HMGN1 in myoblasts inhibited their differentiation to myotubes (Crippa et al., 1991; Pash et al., 1990). Taken together, this evidence suggests that HMGN1 and HMGN2 expression is down-regulated during cellular differentiation and over-expression of these proteins inhibits *in vitro* differentiation.

In a more recent study, developmentally regulated expression of HMGN1 and HMGN2 expression was observed in hair follicles (Furusawa et al., 2009). HMGN1 and HMGN2 are expressed some stem cells (undifferentiated bulge cell) of the mature hair follicle (Furusawa et al., 2009). Both HMGN1 and HMGN2 expression are found in relatively less-differentiated cells (outer root sheath and basal layer cells) compared to terminally-differentiated cells

(inner root sheath cells, hair shaft and supra-basal layer) (Furusawa et al., 2009).

1.14.2 HMGN3 expression in development and differentiation

HMGN3 consist of 2 splice variants, HMGN3a and HMGN3b, with the latter lacking most of the RD domain. HMGN3 protein, unlike HMGN1/2, shows tissue-specific expression. In mouse and human tissue, HMGN3 is highly expressed in eye and brain (Ito and Bustin, 2002; West et al., 2001). In embryonic eye development, HMGN3 protein is detected in the presumptive corneal epithelium and lens fibre, whereas in the adult eye, HMGN3 is specifically expressed in the lens fibre and inner nuclear layer of the retina (Lucey et al., 2008). HMGN3 expression is also highly expressed in adult pancreatic islet cells (Ueda et al., 2009).

1.14.3 HMGN5 expression in development and differentiation

HMGN5 is four times longer than other HMGN family members, due to a 300 amino acids C-terminal domain. In mouse day 7.5 embryos, HMGN5 is expressed in the ectoplacental cone (Shirakawa et al., 2009). HMGN5 is also highly expressed in trophoblast giant cells, spongiotrophoblast and trophoblast cells in the placental labyrinth while the expression in other parts of the embryo remains relatively weak (Shirakawa et al., 2009). These expression patterns suggest that HMGN5 may play role in trophoblast development in embryogenesis (Shirakawa et al., 2009). During Rcho-1 differentiation, an *in vitro* model system for trophoblast differentiation, HMGN5 was shown to be up-regulated (Shirakawa et al., 2009). The depletion and over-expression of HMGN5 in this system affected the differentiation-linked expression of several prolactin-related genes (Shirakawa et al., 2009). In the same study, HMGN5 was shown to bind prolactin-related genes in Rcho1 cells but not in H4IIE, a non-trophoblastic cell line. These observations indicate that HMGN5 modulates expression of specific genes in trophoblast differentiation through chromatin (Shirakawa et al., 2009). These results also show that unlike HMGN1 and HMGN2, HMGN5 expression is up-regulated during differentiation.

1.15 Aims and objective of this thesis

This project was commenced with an aim to study the role of HMGN1-3 in stem cells and neural differentiation. P19 EC cells were used as model system as they resemble ES cells in their neuronal differentiation ability. The general aims of this work are summarised below:

1. To characterise the RA-induced neuronal differentiation system of P19 EC cells.
2. To study the expression of HMGN1-3 in undifferentiated and neuronal differentiation of P19 EC cells.
3. To establish siRNA knockdowns of HMGN1-3 in undifferentiated cells and during neural differentiation.
4. To study the changes of key pluripotency and neural-specific genes upon HMGN knockdown.

Chapter 2

Materials and Methods

Materials

2.1 Cell line and cells

2.1.1 P19 EC cells

Undifferentiated P19 EC cell line was provided by Dr. Andrew Hamilton, Institute of Cancer Sciences, University of Glasgow. The P19 EC cells provided were at passage 14. For ease of labelling and recording, the passage number was reset to 0 (P14 = P0).

2.1.2 Hippocampal neuron from adult brain

Hippocampal neurons from adult brain at day 18 culture were provided by Paul Turko from Dr. Sturt Cobbs's group from the Section of Neuroscience, University of Glasgow. These cells were only used for immunofluorescence staining experiments.

2.2 Reagents

2.2.1 Antibodies

Custom antibodies generated by the West lab used in this project are anti-mmHMGN1, anti-hsHMGN2, and anti-mmHMGN3a. They were raised against the C-terminal 15 amino acids of each protein:

- mm HMGN1: NQSPASEEEEKEAKSD
- hs HMGN2: KTDQAQKAEGAGDAK (detects both mouse and human HMGN2)
- mouse HMGN3a: VEEAQRTEsIEKEGE (detects HMGN3a but not HMGN3b)

Custom antibodies were raised in rabbit by Eurogentec and affinity purified. Affinity purified anti-HMGN3-2752 was a gift from Dr. Michael Bustin (West et al, 2001), and was raised against an internal peptide of human HMGN3: KTSAKKEPGAKISRGA. It detects mouse HMGN3a and HMGN3b.

Commercially available antibodies used in this project are listed below:

Table 2.1: List of commercially available antibodies used in this project.

Antibody	Species raised	Supplier	Catalogue number
OCT4	Goat	Abcam	Ab21603
MAP2	Mouse	Abcam	Ab24640
NF-160 kDA	Rabbit	Abcam	Ab9034
GFAP	Mouse	Abcam	Ab4648
Alexa Fluor 488	Goat anti-mouse	Invitrogen	A11055
Alexa Fluor 488	Donkey anti-goat	Invitrogen	A21121
Alexa Fluor 596	Goat anti-rabbit	Invitrogen	A11012
β -Actin	Goat	Santa Cruz	Sc-1615
HRP	Goat anti-rabbit	Pierce	HJ108849
HRP	Rabbit anti-goat	Pierce	31402

2.2.2 Oligonucleotide primers

Custom oligonucleotide primers were purchased from MWG Eurofin. Sequences of primers are listed in table 2.3.

2.2.3 Other reagents

- All-*trans* Retinoic Acid (ATRA) (Invitrogen)
- Ethanol (Fisher)
- Methanol (Fisher)
- Freezing Media (Gibco)

2.3 Formulation of buffer solution

All buffers are prepared using sterile deionised H₂O and where mentioned buffers were prepared in 1X PBS (Gibco).

2 X Sample loading buffer

- 62 mM Tris-HCl, pH 6.8
- 2% SDS
- 10 mM DTT (dithiothreitol)
- 10% Glycerol
- 0.01% Bromophenol blue

4 X Gel separating buffer

- 1.5 M Tris-HCl, pH 8.8
- 0.4% SDS

4 X Gel Stacking buffer

- 0.5 M Tris-HCl, pH 6.8
- 0.4% SDS

10 X SDS PAGE Running buffer

- 1.92 M Glycine
- 250 mM Tris, pH 8.8
- 1% SDS

1 X Western Transfer buffer

- 0.192 M Glycine
- 25 mM Tris, pH 8.8
- 10% SDS

10 X PBS solution for washing

- 1.37 M NaCl
- 27 mM KCl
- 43 mM Na₂HPO₄
- 14.7 mM KH₂PO₄

Blocking buffer for western blotting

Following were dissolved in 90 ml of water:

- 10 ml 10xPBS
- 1g/5 g Non-fat milk powder(Marvel) OR Bovine Serum Albumin (BSA)
- 100 µl Tween-20

Cell lysis buffer (CLB)

- 45 mM Tris-HCl pH7.5 or 8
- 1 mM EDTA
- 1% SDS
- 10% Glycerol
- 0.01% approx bromophenol blue
- 50 ml Water
- Protease inhibitors
(50 nM okadaic acid, 100 μ M sodium orthovanadate, 10 mM sodium butyrate, 0.5 μ g/ml TSA, protease inhibitor tablets from Roche)

Paraformaldehyde

- 4% paraformaldehyde
- 1 X PBS

Blocking buffer for immunofluorescence

- 2.5% BSA
- 0.03% Triton
- 1 X PBS

Methods

2.4 Tissue culture

2.4.1 Culturing and passaging of undifferentiated P19 EC cells

Undifferentiated mouse P19 EC cells were cultured on untreated tissue culture plasticware in the absence of feeder cells in Minimum Essential Medium (MEM)-alpha containing deoxyribonucleotides, ribonucleosides and ultraglutamine 1 (Lonza, BE02-002F) supplemented with 7.5% new born calf serum (heat inactivated, Source Bioscience, 7.03Hi) and 2.5% fetal bovine serum (heat inactivated, Sigma, F9665) (undifferentiated media) in standard conditions of 5% CO₂ at 37°C. Undifferentiated cells were passaged every second day when approximately 80-90% confluent. For passaging the following protocol was followed:

1. Media from confluent cell cultures are aspirated and the cell layer was briefly rinsed with PBS solution.
2. The cell layer was trypsinised by applying Trypsin-0.5 mM EDTA (w.v) 0.25% (Gibco) solution and incubated at 37°C for 1-2 minutes.

3. Trypsin was deactivated by adding 5 volumes of fresh media and cells were transferred to a 15 ml falcon tube using a pipette.
4. The cells were collected by centrifugation at 300g for 5 minutes. The supernatant was discarded and the cell pellet was resuspended in fresh media.
5. Cells were seeded into new tissue culture plasticware at a dilution factor of 1:5.

2.4.2 Cell cryopreservation

For preparation of frozen cell stocks, cells were collected following the method described in section 2.4.1. The cell pellets were resuspended in 4 ml of freezing media (Gibco) solution drop wise. The cells in freezing media were distributed into 1 ml aliquots in polypropylene cryotubes. The cryotubes were cooled in isopropanol freezing container at -80°C for 72 hours and then transferred into liquid nitrogen vapour phase for long term storage. For recovery, cell were rapidly thawed at 37°C, resuspended in 9 ml fresh media and centrifuged at 300g for 4 minutes. The cell pellets was resuspended in 10 ml fresh media and cultured in a 25 cm² vented flask (Nunc).

2.4.3 Retinoic acid-induced neural differentiation from P19 EC cells

The protocol for RA-induced neural differentiation from undifferentiated P19 EC cells was carried out as described by McBurney and Jones-Villeneuve with several optimised steps discussed in chapter 3 (Runnicki and McBurney, 1987; Jones-Villeneuve et al., 1982). This protocol utilises a '+2 -2' procedure that involves two stages. The first stage is called the suspension stage to formed neuroectodermal EBs followed by an adherent stage where the cells are further differentiated to formed functional neurons and glia (Chapter 3).

Induction of neural differentiation

For neural induction, 1 X 10⁶ undifferentiated P19 EC cells were seeded in 10 cm bacteriological petri dishes (Sterilin) in GIBCO™ Minimum Essential Medium (MEM)-alpha supplemented with 5% fetal bovine serum (differentiation media)

under standard conditions of 5% CO₂ at 37°C. All-*trans* retinoic acid (ATRA) was added to a final concentration of 1.0 µM (for optimisation experiment, a concentration range of 0.5-2.5 µM was used) and cells were allowed to form EBs for 2 days. ATRA stock (1 mM in water) was distributed into 1 ml aliquots and stored in the dark at -80°C and discarded after 3 months. After 2 days, cultures were aspirated into 15 ml falcon tubes and left in tissue culture hood for 5 minutes to allow the cells to settle at the bottom of the tube. The media was removed without dislodging the cells at the bottom of the tube and immediately resuspended slowly with 10 ml fresh media without ATRA. Cells were then cultured under conditions mentioned above for another 2 days.

Plating cells from EBs

At this stage, the cells have been in suspension for 4 days (2 days with ATRA and 2 days without ATRA). Visible formation of aggregates was observed. The aggregates were transferred into 15 ml falcon tubes and left in tissue culture hood for 5 minutes to allow the aggregates to settle down at the bottom of the tube. The media was aspirated out and aggregates were washed with MEM-alpha media without serum and left in the tissue culture hood for 5 minutes to allow the aggregates to settle down at the bottom of the tube. The media was aspirated and 2 ml Trypsin-0.5 mM EDTA (w.v) 0.25% (Gibco) solution was added. The resulting mixture of cell in trypsin solution was very gently pipetted up-and-down using a 5 ml pipette to dislodge the aggregates and incubated at 37°C for 30 seconds. This step is repeated 4 times. After that, 4 ml of fresh media (differentiation media) was added to deactivate the trypsin. The cells were centrifuged at 300g for 5 mins and the supernatant discarded. The cell pellets were resuspended into fresh media (differentiation media) and counted. For plating, cells were seeded at 3.5×10^6 cells (for optimisation, a range of $1.5-7.5 \times 10^6$ cells were used) into 10 cm tissue culture grade (Nunc) plasticware and grown under standard conditions of 5% CO₂ at 37°C. After 3 days, the media in the culture was removed and replaced with fresh media (differentiation media) very gently. Culture was allowed to grow up to the required length of time with total RNA and whole cell lysates harvested. For immunofluorescence experiments, cells were plated in 4-well

or 8-well LabTek™ Chamber II (Nalge Nunc) slides and cultured as described above.

2.4.4 Generating HMGN1 and HMGN2 knockdowns

HMGN1 and HMGN2 knockdowns were generated using siRNA technology. The siRNAs were obtained from Qiagen's Flexitube GeneSolution system. The transfection reagent, INTERFERin™ and protocol used for these experiments were provided by Polyplus. Detailed siRNA screening and optimising experiments are discussed in chapter 5. The list of siRNA used in this project is presented in table 2.2. For HMGN1 targeted knockdown, siRNAs N1₀₂ and N1₀₃ were used, while for HMGN2 knockdown, siRNAs N2₀₁ and N2₀₄ were used. For double knockdown of both HMGN1 and HMGN2, siRNAs N1₀₂ and N2₀₁ were used. Allstars negative control siRNA (Qiagen) was used as a negative control that should not have any effect on mammalian cells. siRNA knockdown was carried out on undifferentiated P19 EC cells and during neural differentiation.

Table 2.2: List of siRNA, target sequence and final concentration used in knockdown experiments. * siRNAs used for all downstream functional experiments.

Target & siRNA		Target Sequence	Final concentration (nM) (after optimisation)
HMGN1	N1 ₀₁	CCCGTGTTTCTAGTAGAACCA	20
*HMGN1	N1 ₀₂	CACTGGAACAAGTTCAAAGA	20
*HMGN1	N1 ₀₃	TTGTGATAATGTGCTGTGAAA	20
HMGN1	N1 ₀₄	CACAATGTGACTTCAGAGTTT	20
*HMGN2	N2 ₀₁	CAGATTGATAATTCTGCCTAA	40
HMGN2	N2 ₀₂	ATCCTTAATGTGAAATGTCAA	40
HMGN2	N2 ₀₃	AACATAGACTTAATTCCTTA	40
*HMGN2	N2 ₀₄	AAGGATCATGTGTCAGTAACA	40

siRNA knockdown protocol

Day 1

1. For knockdown in undifferentiated cells, 1×10^5 cells were seeded in 1 ml undifferentiated media into 12-well plates. For knockdown in neural differentiating cells, the culturing conditions are similar to neural differentiation protocol.
2. Incubate cells under standard growth conditions of 5% CO₂ at 37°C for 24 hours for 24 hours. For knockdown in neural differentiating, undifferentiated P19 EC cells were transfected with siRNAs specific to HMGN1 and HMGN2. 72 hours post transfection, the cells were induced with RA and allowed to form EBs using the similar system explained in chapter 3. At day -3 (2nd day of EBs in suspension) and precisely 12 hours after seeding, cells were transfected with siRNAs at the similar final concentration mentioned above. Cells transfected any time before 12 hours did not survive. At day 2 (post seeding), media was carefully replaced without damaging the cells. Single siRNA transfection on day 1 neural differentiation was also conducted. At this point, morphology of the cells was similar to wild type cells. At day 3, total RNA and whole cell lysates were harvested for qRT-PCR analysis and western blotting.

Day 2

3. The culture was 50-60% confluent at this stage for undifferentiated cell and approximately 30-40% confluent for neural differentiating cells. siRNAs at the final concentration shown in table 2.2 using MEM-alpha media without serum with addition of 6 µl and 10 µl INTERFERin™ transfection reagent for single and double siRNA knockdown experiments (in a total volume of 100 µl) was prepared.
*For optimisation of siRNA concentration, a range of 5-20 nM siRNA specific to HMGN1 and a range of 5-40nM siRNA specific to HMGN2 was tested were tested (Chapter 3).
4. The siRNA complex was vortexed and left to incubate for 10-12 minutes at room temperature.

5. The siRNA complex was added drop wise to each well for knockdown in undifferentiated cells. For knockdown in neural differentiating cells, the siRNA complex was added drop wise into neural differentiating culture 12 hours after seeding.
6. The cells were then incubated under standard growth conditions for the required length of time before sampling to assess the siRNA-induced target gene knockdown.

2.5 Protein isolation and analysis by western blotting

2.5.1 Preparation of whole cell lysates

1. Approximately 3.5×10^6 cells (undifferentiated or neural differentiation) were harvested for western blotting experiments using methods described for undifferentiated and neural differentiation cultures (section 2.4).
2. Cells were washed with PBS and collected by scraping. The cell pellet in PBS was centrifuged at 300g for 5 minutes, washed in PBS, counted and centrifuge as before.
3. The cell pellet was resuspended in 300 μ l of ice-cold cell lysis buffer and transferred to a 1.5 ml microcentrifuge tube. The samples were homogenised using a P1000 pipette and incubated on ice for 5 minutes.
4. The samples (whole cell lysates) was either stored in -20 C for short term usage or frozen using isopropanol bath to be stored at -80 C for long term usage.

2.5.2 Protein concentration quantification

The protein concentration in the isolated whole cell lysates was estimated by measuring the absorbance at 280 nm using a spectrophotometer. Before SDS-PAGE, protein samples were mixed with an equal volume of 2x Sample

Loading Buffer and incubated at 70° C for 10 minutes. Equal concentrations of samples were then subjected to denaturing Polyacrylamide Gel Electrophoresis (SDS-PAGE), and the gel was stained with colloidal coomassie brilliant blue (Fisher) using the methods described below (section 2.5.3). Equal concentrations of samples based on the coomassie blue staining were then loaded on subsequent gels for protein expression analysis.

2.5.3 Polyacrylamide Gel Electrophoresis (SDS-PAGE)

Equipment used

1. X-Cell Sure Lock™ Mini-cell electrophoresis tank (Invitrogen).
2. X-Cell II blot apparatus module (Invitrogen).
3. NuPage™ 1mm gel casting cassettes (Invitrogen).
4. 10/15-well 1mm gel combs (Invitrogen).

Gel Casting

1. The formulation for a 15% final acrylamide concentration of resolving gel was prepared using the solution listed below. The solutions were mixed in a 50 ml falcon tube and pipetted into gel casting cassettes. The solution was overlaid with dH₂O and left to polymerise for 1 hour at RT.
 - 3.75 ml Resolving Buffer
 - 2.81 ml of 40% Acrylamide (37.5 acrylamide: 1 bis-acrylamide)
 - 0.83 ml dH₂O
 - 0.75 ml of 10% SDS
 - 0.50 ml of 10% APS
 - 0.12 ml TEMED
2. The dH₂O layer was removed from the gel cassette was removed, washed and dried by blotting with filter paper. The solutions for stacking gel listed below were mixed together and pipetted on top of the polymerised resolving gel. A 10/15-well comb was inserted. The stacking gel was left to polymerise for 30 minutes at RT.

- 1.5 ml Stacking Buffer
- 0.375 ml of 40% Acrylamide (37.5 acrylamide/ 1 bis-acrylamide)
- 1.05 ml dH₂O
- 0.30 ml of 10% SDS
- 0.30 ml of 10% APS
- 0.10 ml TEMED

Electrophoresis of protein samples

3. The plastic comb and white tap at the bottom of the polymerised gel cassette were removed and the wells were washed using excess of dH₂O.
4. The gel cassette was placed and clamped into the electrophoresis tank. The electrophoresis tank was filled with 1 X SDS-PAGE Running Buffer enough to cover the wells (500-600 ml).
5. The proteins samples, prepared earlier as described above, were loaded into each well alongside 5 µl of SeeBlue[®] Plus 2 (Invitrogen) pre-stained markers.
6. The gel was run at 130 V constant voltage for 90-110 minutes.

Protein transfer onto PVDF membrane

7. The gel cassette was forced open, and the stacking gel and the foot of the gel were removed. The remaining gel was transferred to a container filled with 1 X Western Transfer Buffer and left on an orbital shaker for 10 minutes to wash off excess SDS.
8. During the incubation of the gel, the blotting pads and filter paper (Whatman, cut to a size of 7.5 X 8 cm) were soaked in 1 X Western Transfer Buffer.

9. PVDF transfer membrane (Millipore, 0.45 μm pore size, cut to a size 7.5 X 8 cm) was soaked in 100% methanol for 1 minute and then in 1 X Western Transfer Buffer.
10. The transfer stack was directly assembled into the X-Cell Blot transfer apparatus. The arrangement was as follows:
 - i. Top plate of the blot module (cathode)
 - ii. 2 X blotting pads
 - iii. Filter paper
 - iv. PVDF transfer membrane
 - v. Gel
 - vi. Filter paper
 - vii. 2 X blotting
 - viii. Bottom plate of the blot module (anode)
11. The transfer blot apparatus was then held together and placed in the gel tank.
12. The gel tank was filled with 1 X Western Transfer Buffer until the gel/membrane stack was fully immersed in the buffer.
13. The transfer was carried out at a constant voltage of 25 V for 90 minutes.

Detection of specific proteins

Procedures for detection of specific proteins including membrane blocking, incubation with primary and secondary antibodies raised are specific to the individual antibodies used. Western blotting using antibodies against HMGN1, HMGN2, HMGN3 and β -Actin were performed using the conditions described below:

14. The PVDF transfer membranes were blocked for 1 hour at RT (except stated) on an orbital shaker in the following blocking solution:
 - HMGN1: PBS + Tween 20 (0.05%) + Marvel (Non-fat dairy milk) (5%).

- HMGN2: PBS + Tween 20 (0.05%) + Marvel (Non-fat dairy milk) (5%).
- mHMGN3: PBS + Tween 20 (0.05%) + Marvel (Non-fat dairy milk) (5%).
- HMGN3-2752: PBS + Tween 20 (0.0001%) + Marvel (Non-fat dairy milk) (1%) incubated overnight at 4° C.
- β -Actin: PBS + Tween 20 (0.05%) + Marvel (Non-fat dairy milk) (5%).

15. The membranes were then incubated with the primary antibody diluted in the corresponding blocking solution and incubated for 90 minutes on an orbital shaker. The dilution ratios for all primary antibodies were 1:2000

16. The membranes were washed three times, 10 minutes each on an orbital shaker in PBS + Tween 20 (0.05%) solution.

17. The membranes were incubated with an appropriate secondary antibody (HRP conjugated goat anti-rabbit or mouse anti-goat) diluted 1:2000 in PBS + Tween 20 (0.05%) + Marvel (Non-fat dairy milk) (5%) for 90 minutes.

18. The membranes were washed three times, 10 minutes each on an orbital shaker in PBS + Tween 20 (0.05%) solution.

19. SuperSignal™ West Dura Extended Duration Substrate (Pierce) ECL detection kit was used to visualise the proteins bands. SuperSignal™ luminal enhancer and stable peroxide solutions were mixed in equal proportion and applied onto the membranes.

20. The reactions were in the dark for 6 minutes and the resulting chemiluminescence was detected using a CCD camera imaging system (LAS3000, Fuji). Typical exposure time was 2 minutes for all HMGNs and 1 minute for β -Actin to visualise the protein bands.

2.6 Real-time PCR for gene expression analysis

2.6.1 RNA extraction

Total RNA extractions from cultured cells were conducted using RNeasy[®] Mini kit from Qiagen following the manufacture's protocol:

1. Cultured cells were washed in PBS, trypsinised and centrifuged at 300G for 5 minutes. Cell pellet was counted using haemocytometer and approximately 10^6 - 10^7 cells were used for each RNA preparation.
2. Cells were disrupted by adding 600 μ l of buffer RLT.
3. Cell lysate in RLT buffer was homogenised using 0.9 mm diameter needle fitted to an RNase-free syringe. The lysate was passed through the needle for approximately 5-9 times.
4. One volume (600 μ l) of 70% methanol was added to the cell lysate and mixed well by pipetting.
5. Up to 700 μ l of the sample was transferred to an RNeasy spin column placed in a 2 ml collection tube. The tube was centrifuged at 10,000 rpm using a benchtop centrifuge for 15 seconds. The flow-through was discarded. The remaining aliquot of the sample was loaded into the sample spin column and centrifuged as above. The flow-through was discarded.
6. Buffer RW1 at a volume of 700 μ l was added to the spin column and centrifuge using the same condition described above. The flow-through was discarded.
7. At this point, on column DNase digestion using RNase-free DNase enzyme step was carried out. DNase mix (10 μ l DNase stock + 70 μ l RDD buffer) was added to the sample and left to incubate for 15 minutes at RT.

8. Buffer RPE at a volume of 500 μ l was added to the spin column and centrifuged using the conditions above. The flow-through was discarded.
9. Step 8 was repeated but centrifuged at 10,000 rpm for 2 minutes using benchtop centrifuge. The flow-through was discarded.
10. The RNeasy spin column was placed into a new 2 ml collection tube. The tube was centrifuged at 10,000 rpm for 1 minute using a benchtop centrifuge. Any remaining flow-through was discarded.
11. The RNeasy spin column was placed into a new 1.5 ml collection tube. 50 μ l of RNase-free dH₂O was added and centrifuged at 10,000 rpm for 1 minute to elute the RNA.
12. To increase the concentration of the RNA, the RNA suspension from step 11 was pipetted into same spin column and centrifuged as above.
13. The final RNA suspension was then transferred into new 1.5 ml RNase-free microcentrifuge tubes.
14. RNA concentration was quantified using spectrophotometer nanodrop.
15. RNA samples if to be used immediately for cDNA synthesis was stored in -20°C or stored in -80°C for long term storage.

2.6.2 Synthesis of cDNA

Total RNA was extracted using methods described in section 2.6.1. The RNA was used in a first strand cDNA synthesis reactions using SuperScript™ III kit (Invitrogen). cDNA synthesis was carried out using oligo(dT)₂₀ primer in order to reverse transcribed polyadenylated transcripts only. The following steps were employed:

Denaturation/ Annealing steps

1. The following reaction was set up and incubated at 65°C for 5 minutes and then rapidly cooled on ice for 5 minutes.

Reagents	Final volume (µl)
RNA (300 ng in 10 µl dH ₂ O)	10
oligo(dT) ₂₀ (100 µM)	0.5
dNTPs (50 µM)	0.5
Total	11

Reverse transcription

2. cDNA synthesis master mix was prepared as below and added to the RNA/primer/dNTPs mix. The mix was incubated first at 25°C for 10 minutes and then at 50°C for 50 minutes. The reaction was heat inactivated at 85°C for 5 minutes.

Reagents	Final volume (µl)
5 X RT buffer	3
DTT (0.1 M)	1
RNaseOUT™	0.5
SuperScript™ III	0.5
Total	5

RNA digestion

3. The RT reaction was cooled on ice for 30 seconds. The RNA component was degraded by adding 1 µl of RNase H. The reaction were incubated at 37°C for 20 minutes and then either used for Real-time PCR amplification or stored at -20°C.

2.6.3 Real-time PCR amplification

The gene expression profiles studies shown in this project were conducted using SYBR[®]-green assays. This assay is based on detection of double stranded PCR products formed in the reaction using oligonucleotide primers. The primers for specific genes were design using either Primer Express or Primer 3 software. The basic criteria for primer design included designing primers over exon-intron-junctions, melting temperatures of 55-60° and an amplicon of 100-150 bp were applied. The primer pair sequences were compared against the entire mouse genome using BLAST alignment tool. The concentration of each primer was optimised, using dissociation curves to detect primer dimer formation and standard curves to check PCR efficiency. The list of primer sets used and primer efficiency are shown in table 2.3.

The PCR reaction efficiency achieved for each primer set was calculated using standard curve by plotting Ct values vs. five serial dilutions of cDNA encompassing a range of 10 fold. The primer efficiency was calculated using the formula $10^{-1/\text{slope}}$ where the slope is obtained from the standard curve and the theoretical maximum is 2.0, E = 2. This means that during the logarithmic phase of the reaction, the PCR product of interest is doubling with each cycle.

The cDNA used in real-time PCR amplification was diluted 1:5, and 5 µl of this used in all PCR reactions. The PCR reactions was set up using transparent 96-well PCR plates (Abgene) in 25 µl reactions, typically in triplicates for each sample, by mixing all the reagents shown below. Fast start universal SYBR green master mix (Rox) from Roche was used (cat. no. 04 913 914 001).

SYBR [®] -green assay	Final volume (µl)
SYBR PCR mix	12.5
Forward primer (2.5-7.5 µM)	3
Reverse primer (2.5-7.5 µM)	3
dH ₂ O	1.5
Template DNA	5

PCR was performed on an MxPro 3000P (4 filter set plate) (Stratagene) using the thermal cycling conditions shown below. All SYBR green readings were normalised to Rox dye fluorescence. A dissociation curve (double stranded PCR product melting curve) was carried out to allow screening for non-specific products amplified.

Segment	Number of cycles	Thermal cycling condition	
1	1	10 minutes	95°C
2	40	15 seconds	95°C
		1 minute	60°C
3	1	1 minute	95°C
		30 seconds	55°C
		30 seconds	95°C

Table 2.3: List of oligonucleotide primers used for real-time (qRT-PCR) analysis.

Gene	Primer	Sequence	Primer Efficiency
Hmgn1	Forward	AGAGACGGAAAACCAGAGTCCAG	1.98
	Reverse	CGTGATGGATGCTTAGTCGGA	
Hmgn2	Forward	AAAAGGCCCTGCGAAGAA	1.96
	Reverse	TGCCTGGTCTGTTTTGGCA	
Hmgn3a	Forward	GAAGAAGGAAGAAAAGCAGGAAGC	1.93
	Reverse	CATTTGCAGATGGTGCAGTACC	
Hmgn3b	Forward	TGGAGAGGAAGGCACAGAGAAC	1.98
	Reverse	TCCACGACAATTCACTCTCCCT	
GlyT1a	Forward	TGAACGCAAGAGTCTGCAAGT	1.95
	Reverse	GGCACAGCACCATTCAACATC	
GlyT1b	Forward	ACCCCTTCCCCAGAACAGAAT	1.92
	Reverse	CCCACGCTCGTCAGTACAAACT	
GlyT2	Forward	ATGCCACGGTATGGAAGGATG	2.0
	Reverse	CAGTTGTTGTGGAATTTGTT	
Nestin	Forward	AAAGTTCAGCTGGCTGT	1.95
	Reverse	CACTTCCAGACTAAGGGACAT	
Map2	Forward	TCTGCCTTAGCAGCCGAAG	1.96
	Reverse	CACTGTGGCTGTTTGTCTG	
Nse	Forward	CTCATCCTGCCTGTGCCGGCCTT	1.97
	Reverse	TGAGGGTGTGGTACACCTCTGC	
Nf-160 kDa	Forward	CTCAGCAGCTACCAGGACAC	1.94
	Reverse	CGATCTCGATGTCCAGGGCC	
Nmda-receptor subunit 2	Forward	GGCTTCTACAGAATCCCCGT	1.93
	Reverse	TTCTGCGCTGCCCGGCCCTCGT	
Gfap	Forward	CAACCTGGCTGCGTATAACCAG	1.95
	Reverse	TTAAGAAGTGGATCTCCTCC	

Oct4	Forward Reverse	CGTTCTCTTTGGAAAGGTGTTCA GGTTCTCATTGTTGTCGGCTTC	1.98
Nanog	Forward Reverse	ACCTGAGCTATAAGCAGGTTAAG TCAGACCATTGCTAGTCTTC	2.0
Sox2	Forward Reverse	GGAACAGCATGGCGAGCGG CGTTCATGTGCGCGTAGCTG	1.96
Rest	Forward Reverse	GTGCGAACTCACACAGGAGAACG AGTCCGCATGTGTCGCGTTAGA	1.94
Zfp521	Forward Reverse	GAGCGAAGAGGAGTTTTTGG AGTTCCAAGGTGGAGGTCAC	1.95
Gapdh	Forward Reverse	GATGCCCCCATGTTTGTGAT GGTCATGAGCCCTTCCACAAT	2.0
α -tubulin	Forward Reverse	ACCCACGGTCATCGATGAAGTT TCCTTGCCAATGGTGTAGTGGC	1.98
β -Actin	Forward Reverse	GTGAAAAGATGACCCAGATC GTGTGGGTGACCCCGTCTCC	1.97
Mash1	Forward Reverse	CCAAGTGGTTCTGAGGACCTG CTGCCATCCTGCTTCCAAA	1.93
Mash2	Forward Reverse	TTTTTCGAGGACGCAATAAGC ACCAGTCAAGGTGTGCTTCCA	1.95

2.6.4 Real-time PCR analysis

Acquisition of Ct values

Real-time PCR amplification curves were analysed using MxPro v4.10 software as follows:

1. Baseline fluorescence levels were calculated based on the readings obtained for cycles between 5 and 10 (at least 5 cycles before the log phase of amplification).
2. Threshold fluorescence was set at the level of mid-log phase on the amplification curves for individual primer sets.
3. Threshold crossing point (Ct) values for individual PCR reactions were extracted and further analysed using Microsoft Excel.
4. Gene expression data were analysed using the comparative Ct method (discussed below).

Selection of housekeeping gene

For the selection of best housekeeping gene (HKG), the expression of Gapdh, α -tubulin and β -actin was analysed using geNORM algorithm (Vandesompele et

al., 2002). The geNORM software calculates geometric averages from Ct values obtained from different samples and ranks the best HKG that should be used as a normalising factor. The best HKGs listed in sequence are Gapdh, α -tubulin and β -actin. The margin of difference between the HKGs tested was small and gene expression profiles analysed using any of the HKGs showed similar results. Detailed description and formulas used to calculate the best HKG are given in geNorm manual available from

http://medgen.ugent.be/~jydesomp/genorm/geNorm_manual.pdf

Comparative Ct quantification method and statistical analysis

1. A fold change in gene expression is calculated using delta-delta Ct values.

Delta (Δ) Ct values were calculated as followed:

$\Delta\text{Ct} = \text{Ct}(\text{HKG}) - \text{Ct}(\text{GOI})$, where

HKG-housekeeping gene

GOI-Gene of interest, whose expression is to be quantified

2. Delta-delta ($\Delta\Delta\text{Ct}$) values were calculated as followed:

$\Delta\Delta\text{Ct} = \text{Ct}(\text{internal control or reference}) - \Delta\text{Ct}(\text{sample})$, where

Internal control or reference is the arbitrary selected sample (most of the time undifferentiated or wild type) to which GOI expression levels are compared.

3. A fold change in gene expression levels relative to reference sample was calculated as followed:

Fold Change = $N^{(\Delta\Delta\text{Ct})}$, where N is set as 2.

The data analysed using $N = 2$ rather than the calculated primer efficiency (table 2.3) did not alter the results presented in results chapters. Error bars are calculated using standard deviation from PCR triplicates reflecting well to well efficiency of PCR reaction.

4. For statistical analysis to compare undifferentiated cells with differentiated cells, or wild-type with knockdown cells, a two sample equal variance Student's T-test using two-tailed distribution was

applied using Microsoft Excel. P-values below 0.001, $P < 0.001$ were marked in the results as * while P-values above 0.001, $P > 0.001$, were marked as N.S (not significant). P-values were calculated for results in chapter 4 and chapter 5. Bonferroni correction was applied for undifferentiated wild-type with knockdown data (n=6 genes, total number of 6 genes in 2 biological replicates). The alpha value (α) was set as 0.01 (a 1 in 100 likelihood of the observed change being due to chance), and the value of 0.0016 was obtained after Bonferroni correction, α/n . For significance analysis, $P < 0.001$ was selected for higher stringency. However, it can be argued that using the Bonferroni correction to lower the alpha value in this context is irrelevant as to the number of genes (n) tested is small.

2.7 Immunofluorescence

2.7.1 Immunofluorescence staining

Immunofluorescence (IF) analysis in this project was carried out to study the distribution of HMGN proteins and the expression of neural and glia markers. The general protocol involving all antibodies is as follows.

1. Undifferentiated P19 EC cells were seeded on a 4-well Lab-Tek™ II chamber slide at 4.5×10^5 cells per slide, one day before fixing the cells for IF analysis. For IF analysis in neural differentiation, single cells from EBs were plated at $4.5\text{-}4.8 \times 10^6$ cells and later fixed at the sampling time-points (days 3, 6, 9). For hippocampal neuron staining, cells were provided at day 18 culture grown on cover slips in 6-well plates.
2. Cells from all the conditions were washed twice with 1 X PBS solution and fixed with 4% paraformaldehyde for 30 minutes at RT.
3. Cells were then washed very gently to remove any excess paraformaldehyde using 1 X PBS. This step is repeated 5 times.

4. To quench any excess aldehyde components in the fixed cells, 50 mM ammonium chloride solution for 10 minutes at RT.
5. This first quenching step is followed by the second quenching step by using 20 mM fresh glycine solution for 10 minutes at RT.
6. The fixed cells were washed with 1 X PBS and incubated in blocking buffer (2.5% BSA, 0.3% Triton in 1 X PBS) for 1 hour at RT.
7. The samples were then incubated with individual primary antibodies diluted in blocking solution for 1 hour at RT. The table below shows the dilution for the primary antibodies used.

Primary Antibodies	Dilution
HMGN1	1:1000
HMGN2	1:1000
mHMGN3a (detects HMGN3a)	1:5000
2752 (detects both HMGN3a and HMGN3b)	1:10,000
OCT4	1:500
MAP2	1:200
NF-160 kDA	1:500
GFAP	1:200

8. The samples were then washed 5 times using 1 X PBS + 0.1% Triton.
9. The samples were then incubated with corresponding Alexa Fluor (Invitrogen) secondary antibodies that were prepared at a dilution of 1:1000 in blocking solution.
10. The samples were then washed 5 times using 1 X PBS + 0.1% Triton.
11. One final wash was done in dH₂O and the slides were mounted with cover slips using Prolong® Gold (Invitrogen) containing the blue-fluorescent nuclear counter stain DAPI. Slides were left to dry in the dark at RT.

12. Slides were then stored either in 4°C for short term or -20°C for up to 4 weeks before analysing images.

2.7.2 Immunofluorescence image analysis

IF images were taken using Olympus (IX51) microscope at 40 X objective using filters corresponding to the wavelength of the Alexafluor-tagged secondary antibodies. The exposure time was manually set and at least 10-30 field of images were taken for one sample. The images were then analysed using ImageJ software.

Chapter 3

Optimisation and characterisation of Retinoic acid-induced P19 neuronal differentiation

3.1 Introduction

The mammalian central nervous system consists of many subtypes of neurons and glia cells. Neurogenesis is a differentiation program defined by the successive development of neural progenitor cells, which then give rise to neurons, glia/astrocytes and oligodendrocytes. Elucidating the mechanism involved in neurogenesis is essential to understanding the development of the central nervous system. Various model systems are used to study neuronal differentiation especially those derived from pluripotent ES/EC/EG cells. Pluripotent ES/EC/EG cells are undifferentiated cells that possess the capacity to differentiate into endoderm, ectoderm and mesoderm *in vitro* under appropriate culture conditions or specific chemical inducers. RA is a known chemical inducer that triggers the ectoderm lineage commitment of pluripotent ES/EC/EG cell *in vitro*.

P19 EC cells induced with RA generate specific type of neurons and glia (Runnicki and McBurney, 1987; Jones-Villeneuve et al., 1982). Upon RA induction, undifferentiated P19 EC cells through the formation of EBs give rise to neuronal and glia cells that mimic the developmental process occurring *in vivo* (Bain et al., 1995; Wobus et al., 1994; Staines et al., 1994; Morassuti et al., 1994; Runnicki and McBurney, 1987; Jones-Villeneuve et al., 1982). The *in vitro* differentiation capacity of P19 EC cells have been previously characterised using neuron and glia specific markers by several groups (Zhongqiu Xie et al., 2010; Zhigang Jin et al., 2009; Yi Wey et al., 2002; McBurney, 1993; Johnson et al., 1992; McBurney and Rodgers, 1982; Jones-Villeneuve et al., 1982).

One of the protocols that are often used in inducing neural commitment in P19 EC cells is the RA-induce formation of EBs in suspension. The RA-induced

EB formation protocol for neuronal differentiation is particularly good for producing neurons since it takes a shorter time to generate neuronal cultures compared to other methods that do not utilise EB formation. This protocol normally utilises a '+2 -2' procedure that involves two stages (Figure 3.1). The first stage is called the suspension stage to form neuroectodermal EBs followed by an adherent stage where the cells are further differentiated to form functional neurons and glia. At this point the cells form committed neuroectodermal EBs that are then seeded in adherent culture to further differentiate (stage 2).

The characterisation of RA-induced P19 neuronal differentiation is often carried out using gene markers specific to neuronal and glia cell types. Although this model system has been previously described, there are variations in the protocol that may alter the outcome of neuronal differentiation.

The aims of this chapter are to address crucial factors and steps in the RA protocol in generating a more robust system in producing neuronal differentiation from P19 EC cells.

3.2 Objectives

1. To optimise key steps of RA-induced P19 neuronal differentiation:
 - (a) Analyse the pluripotent state of 'early and late' undifferentiated cells in culture using molecular marker Nanog.
 - (b) Study the optimal RA concentration required for increased neuronal differentiation capacity based on Nanog and Map2 markers.
 - (c) Study the optimal seeding density for EBs required for increased neuronal differentiation capacity based on Mash1 and Mash2 markers.

2. To characterise the P19 neuronal differentiation model system using a cohort of markers specific to undifferentiated cells, neural progenitors, neuronal and glia cells.

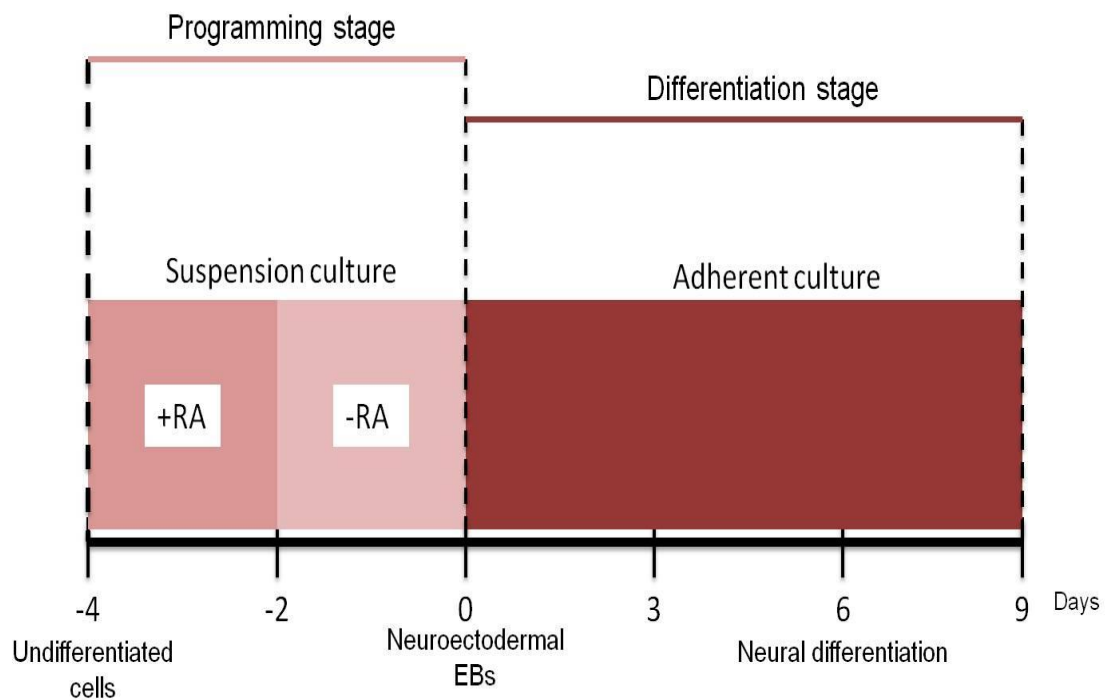


Figure 3.1: An outline of the RA-induced P19 neuronal differentiation model system.

Undifferentiated cells were treated with RA for 2 days in suspension before removing the RA by changing the media and left for another 2 days in suspension to form neuroectodermal EBs. EBs were then plated in adherent cultures for neuronal differentiation.

3.3 Analysis of Nanog expression to determine pluripotency in subcultured P19 undifferentiated cells

P19 EC cells can be maintained in their undifferentiated state *in vitro* and induced to achieve directed differentiation of all three germ layers (Martin, 1980). Due to the innate ability of EC/ES/EG cells to differentiate, the maintenance of their pluripotent state in culture is critical. Undifferentiated mouse ES cells grow in rounded colonies with well defined edges as opposed to their differentiated counterparts that appear as individual cells with a flattened morphology (Brook and Gardner, 1997). In order to maintain the undifferentiated state, mouse ES cells are grown in sub-confluent density and routinely passaged every 2-3 days (Matise et al., 2000; Tompers and Labosky, 2004). Undifferentiated P19 EC cells grow in a monolayer and are cultured at higher densities compared to mouse ES cells. At low densities, P19 EC cells differentiate spontaneously and therefore are always cultured approximately at a cell confluency of 70-80% (Rudnicki and McBurney, 1987). In order to assess the pluripotency state of mouse ES/EC/EG cells, several features including morphological conditions, expression of surface markers such as stage-specific embryonic antigen SSEA-3, and expression of several pluripotency associated transcription factors such as Oct4, Nanog and Sox2 have been employed (Andrews et al., 1996; Niwa et al., 2000; Lebkowski et al., 2001).

P19 EC cell line (passage 14) used in this research were obtained from Dr Andrew Hamilton (University of Glasgow). The passage number was re-set to passage 0 (passage 14 = passage 0). The relative RNA expression of stem cell marker Nanog was analysed using RT-PCR to determine the pluripotent state of P19 EC cells. Nanog, a homeodomain protein, is a transcription factor that regulates the expression of a set of target genes involved in ES cell pluripotency and is drastically down-regulated upon differentiation (Mitsui et al., 2003). Nanog expression in undifferentiated P19 EC cells was monitored between passages 2 (early) to 10 (late) (Figure 3.2). The cells in the different passages were seeded at similar densities and had near similar cell confluency of 70-80% on sampling time-points.

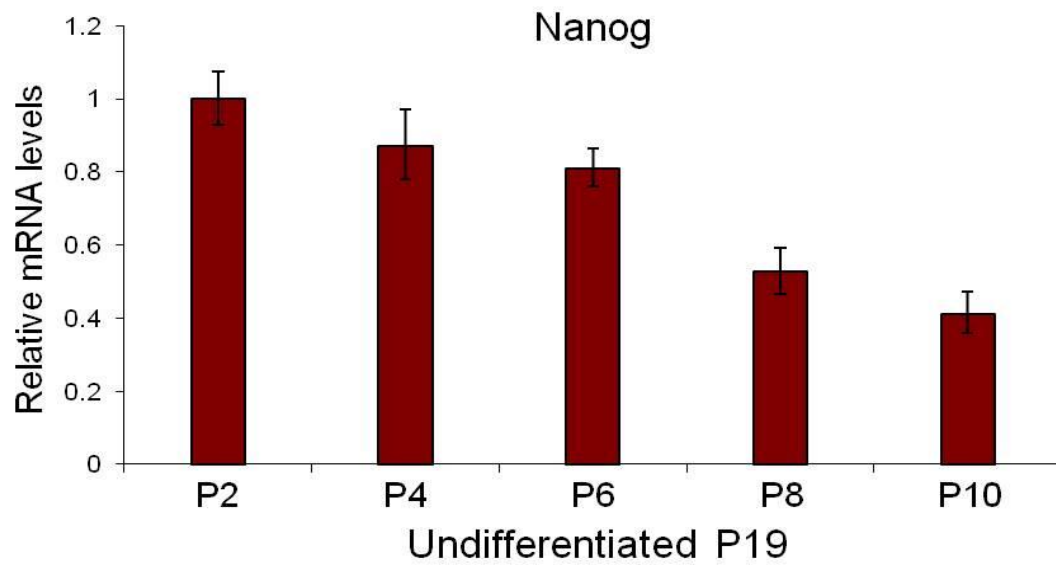


Figure 3.2: Expression of the pluripotency marker Nanog decreases with passage number for undifferentiated P19 EC cells.

RNA levels are normalised using Gapdh as the control housekeeping gene and shown relative to P2 levels. Error bars reflect standard deviation from three RT-PCR reaction replicates.

A gradual decline in Nanog expression was observed, and that by passage 8, the expression was reduced by 50%. This suggests a gradual decrease in pluripotency state of undifferentiated P19 EC cells with time in culture.

However, the cells in passage 8 and 10 showed morphology similar to undifferentiated EC cells and in passage 2- 6. Besides that, there was no evidence of the cells in passage 8 and 10 showing commitment to the ectodermal lineage when they were subjected to qRT-PCR with oligonucleotide primers specific to the ectodermal marker gene Nestin (data not shown). Taken together, although the cells in the later stage of the culture (P8-P10) showed a drop in Nanog RNA levels, they did not display the morphology or lineage- specific gene expression that represents ectodermal commitment. Nevertheless, to avoid variation that could be caused by the drop in Nanog RNA levels, differentiation experiments using undifferentiated P19 EC cells were conducted between passage 4 and 6. Further confirmation of the pluripotency state between “early and late” stage of undifferentiated P19 EC cell could be investigated by RNA expression profiling of other stem cell specific genes such as Oct3/4, Sox2, and Rex1. Besides that, cells from passage 10 could be subjected to directed differentiation in vitro to analyse the lineage specific reprogramming capacity compared to cells from passage 2.

3.4 Retinoic acid dosage determines the rate of neuronal differentiation in P19 EC cells.

Retinoic acid (RA) signalling and regulation is essential for embryonic development and cellular differentiation (Clagett-Dame and De Luca, 2002; Ross et al. 2000). In the developing nervous system, RA has shown to play crucial roles in patterning of the neural plate and neuronal differentiation (Liu et al., 2001; Glover et al., 2006 Jones-Villeneuve et al., 1982). Mouse EC/ES/EG cells can be induced with RA to differentiate into neurons *in vitro* (Rohwedel et al., 1999; Jones-Villeneuve et al., 1982). RA-induced neuronal differentiation protocols mostly rely on the formation of floating aggregates called embryoid bodies (EBs) which gives rise to neuroectodermal cells (Mansergh et al., 2009; Okabe et al., 1996; Bain et al., 1995). These programmed EBs are then plated in adherent culture to further differentiate into specific neuronal cells that include Glutamatergic, GABAergic, motoneurons, interneurons and dividing glial cells (Sanalkumar et al., 2010; Kaomei Guan et al., 2001). EC/ES/EG derived neuronal cells expressed neuron specific genes in a developmentally controlled manner (Jung et al., 2010; Kaome Guan et al., 2001). Genes such as Neurofilament 68 kDa (NFL), Neurofilament 160 kDa (NFM) and Microtubule-associated protein 2 (Map2) are expressed early in the EBs as compared to genes involved in the formation of neural specific receptors such N-methyl-D-Aspartate (NMDA) and Gamma-aminobutyric acid (Sanalkumar et al., 2010; Rohwedel et al., 1999; Strübing et al., 1995). Undifferentiated P19 EC cells induced with RA differentiate into neurons and emulate the expression profile of neuronal cells derived from ES/EG cells (Teets et al., 2011, Zhongqiu Xie et al., 2010, Jones-Villeneuve et al., 1982).

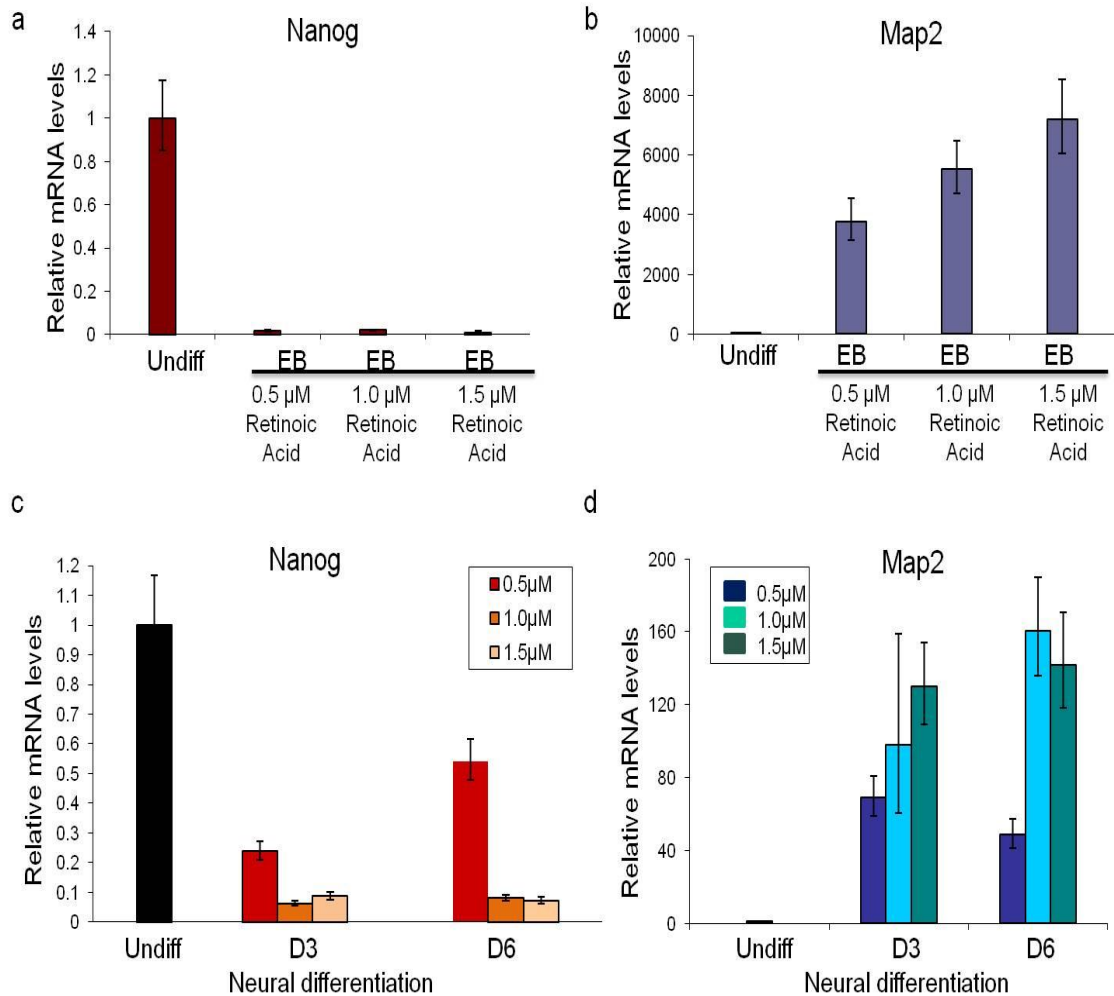


Figure 3.3: Retinoic acid concentration affects the efficacy of neuronal differentiation

RNA expression is normalised to Gapdh and shown relative to undifferentiated cells. (a) & (b) Nanog and Map2 RNA expression of EBs treated with 0.5 μ M, 1.0 μ M and 1.5 μ M RA. (c) & (d) Expression of Nanog and Map2 RNA in day 3 and day 6 neuronal differentiation from EBs treated with 0.5 μ M, 1.0 μ M and 1.5 μ M RA. Error bars reflect standard deviation from three RT-PCR reaction replicates. Neuronal differentiation was conducted using the same batch of undifferentiated P19 EC cells.

The rate of neuronal differentiation in P19 EC cells is RA dosage- dependent (Edwards and McBurney, 1983). P19 aggregates exposed to doses of RA in the range of 0.1 μM - 1.0 μM were capable of generating neuron and glia cells. The concentration of RA used in P19 neuronal differentiation studies mostly vary between 0.1 μM and 0.5 μM . To determine the optimal concentration of RA required for efficient programming of undifferentiated P19 EC cells to neurons and glia, P19 aggregates were treated with increasing amount of RA (0.5 to 1.5 μM) and subjected to qRT- PCR to analyse expression of Nanog pluripotent marker and Map2 neuronal marker. Optimal RA concentration is selected based on aggregates that demonstrate increased expression of Map2 in parallel to the loss of Nanog signalling relative to undifferentiated cells.

P19 EC cells were differentiated into neurons using the protocol described in section 2.4.3. Briefly, a single batch of undifferentiated cells were grown in suspension and separately treated with increasing concentrations of RA from 0.5 μM to 1.5 μM . The EBs formed were trypsinised and plated at 3.5×10^6 cells in adherent culture for 3 or 6 days. RNA was isolated from EBs, D3, D6 and undifferentiated cells. For qRT-PCR, cDNA prepared from isolated RNA was amplified using oligonucleotide primers specific to Nanog, Map2 and Gapdh (housekeeping gene). Normalised Nanog and Map2 RNA levels in EBs, day 3 and day 6 of neuronal differentiation were calculated relative to undifferentiated cells (Figure 3.3). Nanog RNA levels were dramatically down-regulated in EBs treated with 0.5, 0.1 and 1.5 μM RA, relative to undifferentiated cells (Figure 3.3a). The loss of Nanog expression in EBs treated with three different dosages was similar suggesting that a minimum 0.5 μM RA to be sufficient in inducing the silencing of Nanog transcription in EBs. Conversely, the rate of neuronal differentiation based on Map2 expression showed a RA dose-dependent fold increase in EBs relative to undifferentiated cells (Figure 3.3b). EBs treated with 1.5 μM RA showed the highest fold increase of 7000 compared to 5000 and 4000 for EBs treated with 1.0 μM and 0.5 μM respectively.

In attempt to determine neuronal differentiation capacity of the EBs treated with 0.5-1.5 μM RA, EBs were plated and allowed to differentiate for 6 days. Map2 neuronal marker expression was analysed to determine the rate of

differentiation. For the purpose of discussion, the different samples in this experiment are defined using the time-point and the RA concentration used, for an example, day 3 cells derived from 0.5 μM RA will be denominated as D3 (0.5RA). Rather surprisingly, D3 (0.5RA) and D6 (0.5RA) showed re-emergence of Nanog pluripotent marker (Figure 3.3c). The RNA levels of Nanog at D3 (0.5RA) and D6 (0.5RA) were 4 and 1.8 folds lower compared to undifferentiated cells. The expression of Nanog in D3 (1.0RA & 1.5RA) and D6 (1.0 & 1.5RA) had decreased to levels below 10 folds compared to undifferentiated cells.

Map2 neuronal marker analysed in day 3 and day 6 cultures provide evidence that EBs treated with 1.0 μM and 1.5 μM RA had higher neuronal differentiation capacity compared to EBs treated with 0.5 μM RA (Figure 3.2d). Map2 RNA levels in D3 (0.5RA) demonstrated a fold increase of 70, compared to the 130 fold increase achieved in D3 (1.5RA). Similarly, D6 (1.0RA) showed approximately 160 fold induction in Map2 RNA levels compared to 50 fold induction in D6 (0.5RA). D3 (1.0RA) showed higher expression of Map2 compared to D3 (1.5RA) suggesting that the latter dosage had increase the capacity of neuronal differentiation.

These findings demonstrate a correlation between the RA concentrations required for programming of neuronal differentiation. Efficient neuronal differentiation based on the loss of Nanog expression and up-regulation of Map2 was achieved with 1.0 μM and 1.5 μM RA. Undifferentiated cells treated with 0.5 μM RA had characteristics of neural-lineage commitment in EBs, but express Nanog when further differentiated in culture. In this experiment, cells treated with 2.0 μM and 2.5 μM RA had proved to be toxic and induced enormous cell death. EBs programmed with RA concentration of 2.0 μM and 2.5 μM when plated had failed to further differentiate let alone survive in culture.

Both RA dosages of 1.0 μM and 1.5 μM demonstrated higher efficacy in inducing neuronal differentiation compared to 0.5 μM . The RA dosage of 1.5 μM had slightly higher efficiency in inducing neuronal differentiation based on Map2 expression. However, the RA concentration of 1.0 μM was used in all

subsequent neuronal differentiation experiments for few reasons. Firstly, the RA concentration of 1.0 μM was selected so that the results obtain here could be compared to the studies in the literature that utilise the similar RA dosage in inducing neuronal differentiation. Secondly, the results obtained here are conducted only using one neuronal marker (Map2) and this may not signify the overall rate of neuronal differentiation.

3.5 Mash1 and Mash2 reciprocal expression analysis used in determining optimal seeding density for neuronal differentiation

Since the introduction of P19 in vitro model system, various studies were conducted in characterizing RA-induced neuronal differentiation and could be assume as a well established and widely used protocol. However, one key area of the protocol that is unclear is the density of cells from RA programmed EBs that needed to be plated in adherent culture for the differentiation and maturation of neurons. In RA-induced P19 EC neuronal differentiation protocol, EBs are formed in suspension for 4 days to derived neuroectodermal committed cells. These EBs are then trypsinised and plated as single cell in adherent culture, a step often referred to as “plating of EBs or aggregates”. The plating density in previous reports varies between groups or is most often left unstated. To study whether the cell density at plating is crucial in RA-induced neuronal differentiation protocol and also to determine the optimal cell density, single cells derived from EBs were seeded at varying densities and examined for morphological differences and analysed for Mash1 and Mash2 RNA expression.

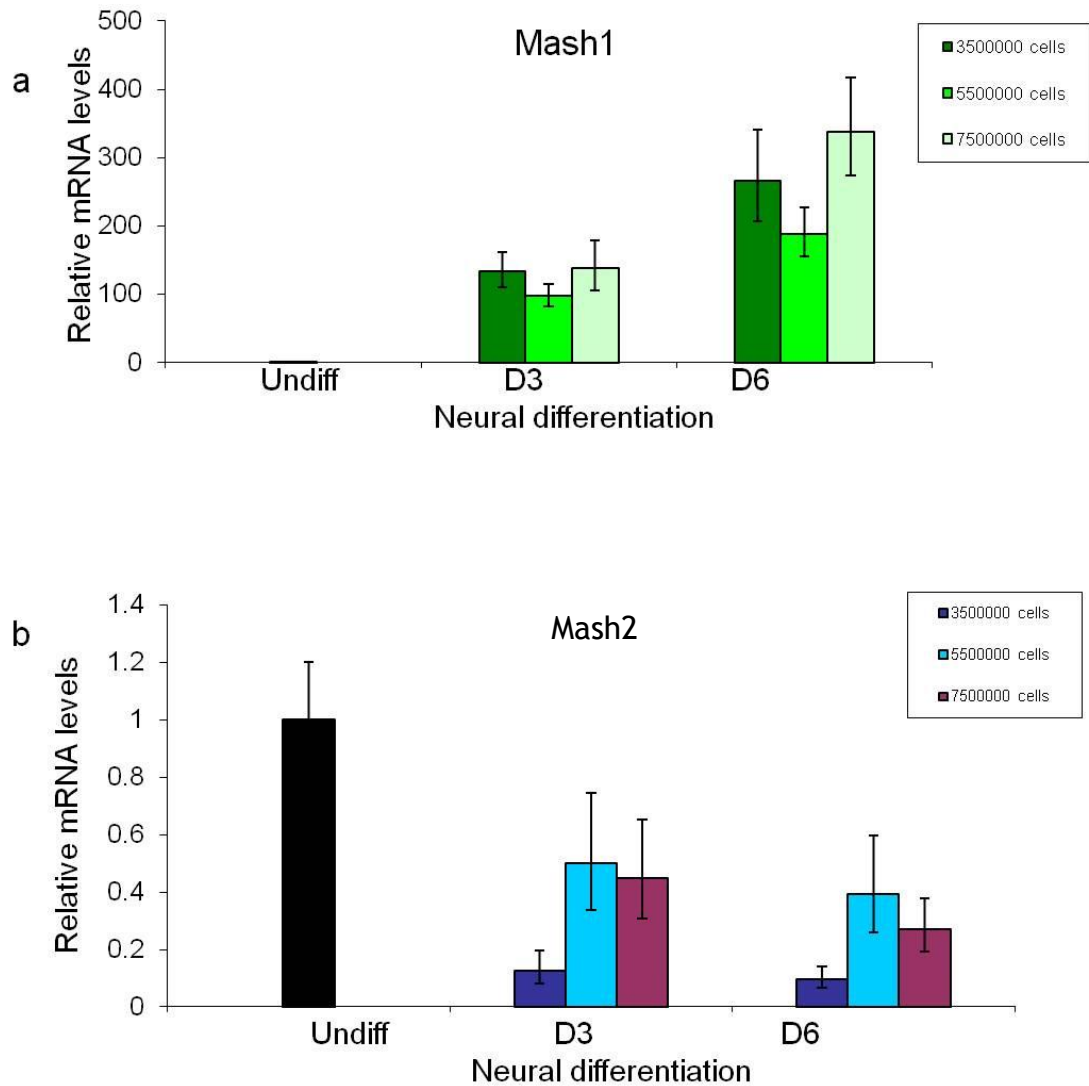


Figure 3.4: Plating density affects the efficacy of neuronal differentiation as assayed by Mash1 and Mash2 expression.

RNA expression is normalised to Gapdh and showed relative to undifferentiated cells. (a) & (b) Mash1 and Mash2 RNA expression in day 3 and day 6 neural differentiation derived from EBs seeded using 3.5×10^6 , 5.5×10^6 and 7.5×10^6 cells. Error bars reflect standard deviation from triplicates of RT-PCR reaction.

P19 EC cells were differentiated into neurons using the protocol described in section 2.4.3. Briefly, cells were treated with 1.0 μM RA in suspension for 4 days to form EBs. EBs were then trypsinised and seeded in adherent culture at densities ranging from 1.5×10^6 to 9.5×10^6 per 10 cm tissue culture dish. Five different cell densities were tested; 1.5×10^6 , 3.5×10^6 , 5.5×10^6 , 7.5×10^6 and 9.5×10^6 . Neuronal cultures from cells seeded at 1.5×10^6 failed to survive and by day 2 had severe cell death (data not shown). On the contrary, cultures seeded at 9.5×10^6 cells, although they showed neuronal morphology as early as 16 hours after plating had become confluent by the beginning of day 2. If not passaged at this point, the cells failed to survive and demonstrated enormous cell death. Neuronal cultures derived from EBs plated at 3.5×10^6 , 5.5×10^6 and 7.5×10^6 showed proper differentiation into neuronal cell types (data discuss below).

Two key morphological cues including average axon length and time-scale of non-neuronal dividing cell appearing in culture was carefully observed to discriminate between cultures seeded at 3.5×10^6 , 5.5×10^6 and 7.5×10^6 . In general, axon length is a characteristic of culture differentiating into neuronal cell types. Whereas the time-scale in which dividing cells appear in culture can be explained by previous studies that show RA-induced P19 EC cells differentiate into neurons in a developmentally dependent manner (Bain and Gottlieb, 1994; Runnicki and McBurney, 1987; Jones-Villeneuve et al., 1982). Neuronal differentiation of P19 EC cells develop in two stages. First is the post-mitotic cell stage which includes predominantly neuronal cells in culture followed by dividing cell stage which consist of non-neuronal cell such as glia and possibly neural progenitor cells. The average axon length between cultures seeded at 3.5×10^6 , 5.5×10^6 and 7.5×10^6 is almost similar to each other in both day 3 (Figure Appendix 1). However, the time-scale in which dividing cells appear in culture vary significant between the different plating densities. Neuronal culture seeded at 3.5×10^6 had dividing cells appearing from day 4-5 onwards. Whereas dividing cells in both cultures seeded at 5.5×10^6 and 7.5×10^6 became visible as early as day 3 (data estimated by eye). These disparities in the neuronal differentiation suggested that the seeding density of EBs could be crucial in determining directed neurogenesis in vitro.

Mash1 and Mash2 are mammalian homologues of the *Drosophila* achaete-scute genes that encodes for the basic helix-loop-helix family of transcription factors (Johnson et al., 1990). In *Drosophila*, these proteins are required for the development of neurons in the central and peripheral nervous system (Ghysen and Dambly-Chaudiere, 1988). MASH1 is expressed in a subset of cells in the central and peripheral nervous system during rat embryonic development (Lo et al., 1991). In P19 EC cells, Mash1 mRNA is undetectable in undifferentiated cells but is expressed to high levels upon RA induction coinciding with neuronal differentiation (Bain et al., 1994; Johnson et al., 1992). In contrast, Mash2 mRNA is expressed in undifferentiated cells and is dramatically down-regulated upon RA treatment (Johnson et al., 1992). Thus, the reciprocal expressions of Mash1 and Mash2 in P19 system are relevant molecular markers when studying RA-induced neuronal differentiation.

To determine optimal seeding densities, RNA levels of Mash1 and Mash2 were analysed. cDNA was generated from RNA obtained from day 3 and day 6 cultures and cDNAs were subjected to qRT-PCR for primers specific to Mash1 and Mash2. Normalised Mash1 and Mash2 RNA levels in day 3 and day 6 of neuronal differentiation are shown relative to undifferentiated cells (Figure 3.4). Mash1 RNA was induced by approximately 100 fold at day 3 neural differentiation from cultures seeded at 3.5×10^6 , 5.5×10^6 and 7.5×10^6 (Figure 3.4a). Mash1 RNA levels in day 6 were induced to up to approximately 250 fold from the three different seeding densities. Similar levels of Mash1 induction suggest that the three different seeding densities support neuronal differentiation to similar extent.

However, the analysis of Mash2 RNA demonstrated increased expression in neuronal cultures seeded at higher density (5.5×10^6 and 7.5×10^6) compared to the lower density of 3.5×10^6 (Figure 3.4b). These results suggest that the seeding density of 3.5×10^6 produces a neuronal culture that is more highly committed to neural differentiation due to its low expression of Mash2. In contrast neuronal cultures seeded using 5.5×10^6 and 7.5×10^6 contains a sub-population of cells that are still expressing Mash2 albeit at lower levels than undifferentiated cells. These results not only established an optimal EBs seeding density that is required for a controlled and directed differentiation

but also highlighted the crucial step in RA-induced neuronal differentiation protocol.

3.6 Characterisation of retinoic acid induced P19 neuronal differentiation

3.6.1 Pluripotent markers Oct4, Nanog and Sox2 are down-regulated upon retinoic acid induction

Several markers including surface markers, intracellular markers and transcription factors have been used to characterise mouse EC/ES/EG cells. The analysis of these markers is used to identify the “state” of EC/ES/EG cells, thus allowing accurate categorisation of the cells into the undifferentiated state or committed lineages such as endoderm, mesoderm and ectoderm. Among the commonly used markers are transcription factors that have been shown to regulate the state of EC/ES/EG cells. OCT4, NANOG and SOX2 are transcription factors that are crucial for the maintenance of the pluripotent state (Chambers et al., 2007; Masui et al., 2007; Niwa et al., 2000). The inactivation of this transcription factor network has been linked to the loss of the pluripotent state and aberrant differentiation of EC/ES/EG cells (Avilion et al., 2003; Mitsui et al., 2003; Nichols et al., 1998).

OCT4 (Pou5f1) is grouped into the Octamer class of TF that regulate target genes that are involved in pluripotency (Boyer et al., 2005). SOX2 is a member of the High mobility group (HMG) box DNA binding protein family, and acts as co-activator for Oct4 in targeting pluripotency related genes (Niwa, 2001; Ambrosetti et al., 1997). NANOG is a homeobox domain TF that is closely regulated by the binding of OCT4/SOX2 to its promoter sequence and plays a role in BMP dependent signalling in regulating pluripotency (Suzuki et al., 2006).

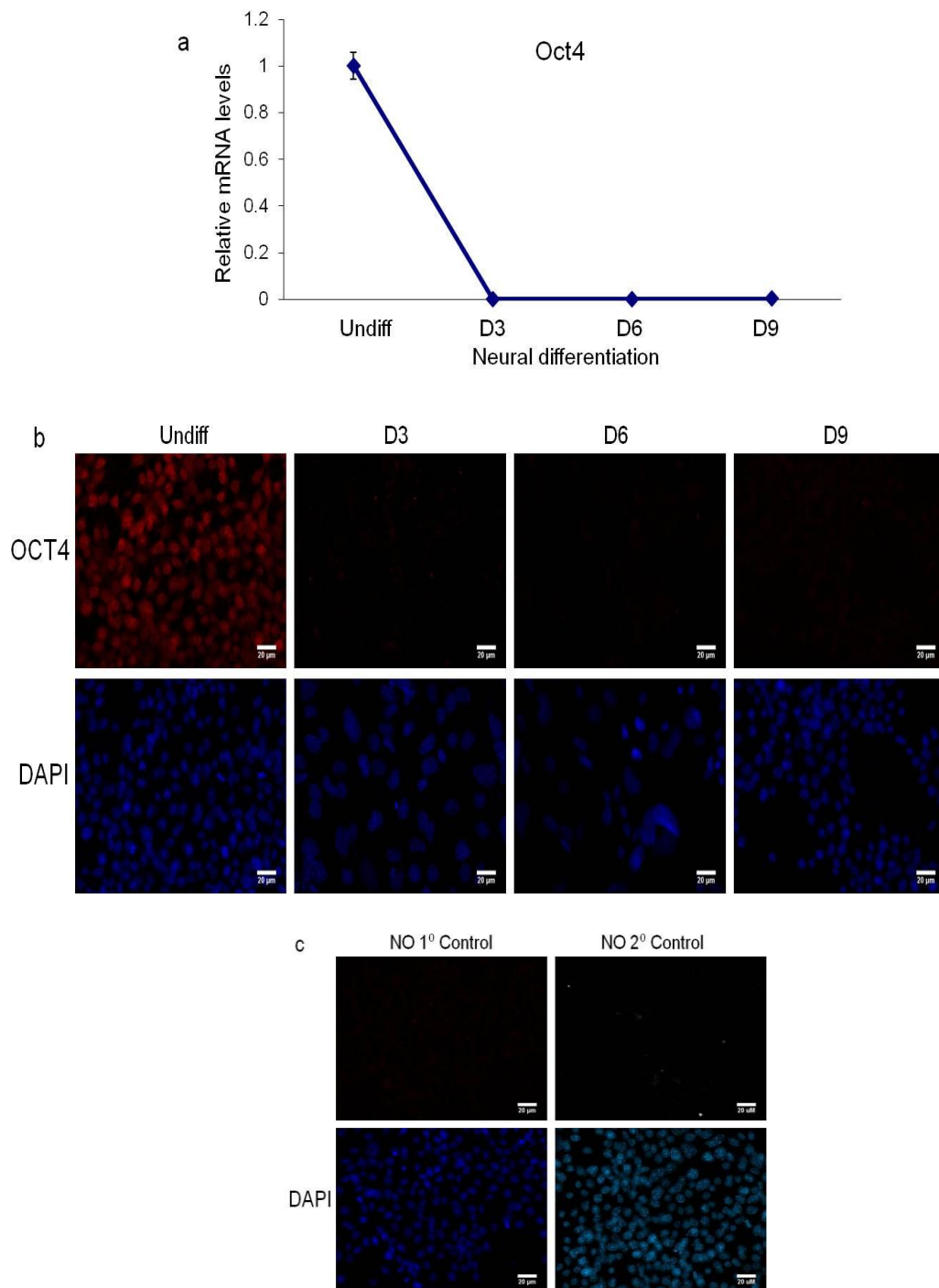


Figure 3.5 Oct4 RNA and protein are highly expressed in undifferentiated cells and are loss upon RA-induced neuronal differentiation.

(a) Oct4 RNA expression during P19 neuronal differentiation. RNA levels are normalised using α -tubulin and shown relative to undifferentiated cells. Error bars reflect standard deviation between three RT-PCR reaction replicates. (b) Immunofluorescence staining of OCT4 during neuronal differentiation. (c) No primary (but Alexa Fluor 596 Goat anti-Rabbit) and secondary (but OCT4) antibodies controls conducted in undifferentiated cells. Scale bar, 20 μ M.

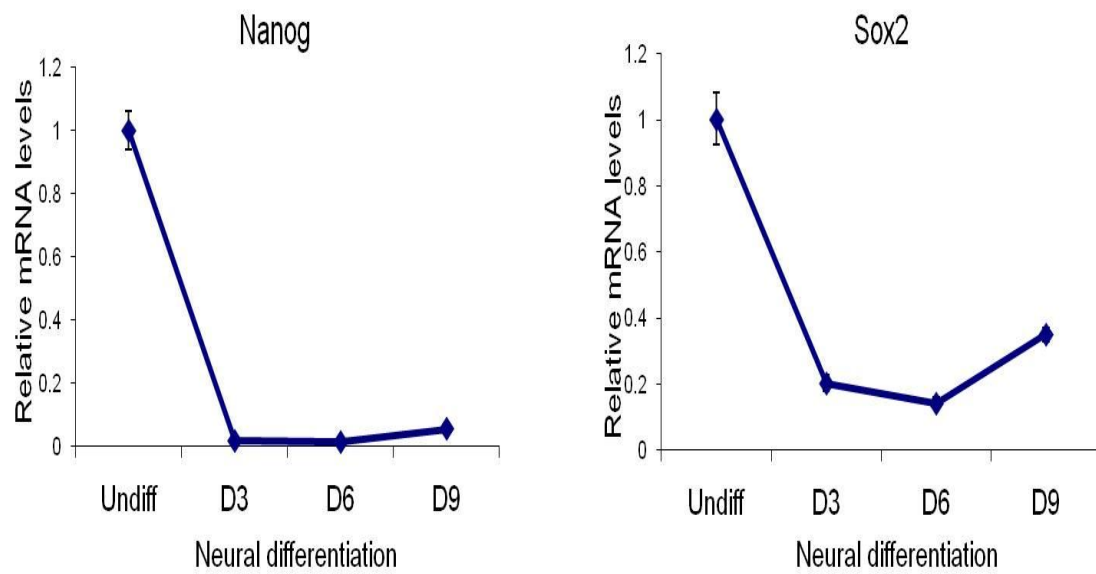


Figure 3.6 Nanog and Sox2 expressions are down-regulated upon RA-induced neuronal differentiation.

Expression levels are normalised using Gapdh as the control housekeeping gene and expressed relative to undifferentiated cells. Error bars reflect standard deviation between three technical RT-PCR reaction replicates.

All three OCT4, SOX2 and NANOG share similar expression profiles in which they are found to be expressed highly in pluripotent cells of embryo and cell lines derived from thereof and are markedly down-regulated upon somatic differentiation into committed lineages. This expression pattern allows them to be used as molecular markers in studying pluripotent versus differentiated cells.

The expression of OCT4, NANOG and SOX2 were analysed in RA-induced P19 neural differentiation. The differentiation protocol was carried out following the similar RA 2+ 2- model with incorporation of the optimised conditions described above. Briefly, P19 EC cells from passage 4-6 was treated with 1.0 μM RA in suspension for 2 days before replacing the media and allowing the formation of neuroectodermal EBs for another 2 days in suspension. EBs were then seeded at 3.5×10^6 in adherent culture and allowed to differentiate for nine days. RNA isolated from day 3, day 6 and day 9 was used to generate cDNA and subjected to qPCR analysis. For qRT-PCR, primers specific to Oct4, Nanog and Sox2 were analysed. Both Gapdh and α -tubulin were individually used as normaliser and both sets of data were comparable. Protein expression of one of the markers was confirmed using immunofluorescence with an antibody specific to OCT4.

Oct4 RNA and protein levels in RA-induced P19 neuronal differentiation are shown in Figure 3.5a. As expected, Oct4 RNA was high in undifferentiated cells and was lost upon RA-induced neuronal differentiation. OCT4 protein expression reflects the mRNA in being highly expressed in undifferentiated cells and undetectable upon neuronal differentiation (Figure 3.5b). Likewise the RNA expression of Nanog and Sox2 was down-regulated upon RA induction (Figure 3.6). The expression of Oct4, Nanog and Sox2 demonstrates the pluripotent state of undifferentiated P19 EC cells. Upon RA-induced neuronal differentiation, the loss of all three pluripotent markers suggests the cells in day 3, day 6 and day 9 have undergone lineage-specific commitment. These results also suggest that the cultures at day 6 and 9, although heterogeneous had eliminated any subset of undifferentiated cells that may interfere in the neuronal differentiation process.

3.6.2 RA- induced P19 EC expressed markers specific to neurons and glia

P19 EC cells treated with RA differentiate into neural progenitors, neuron and glia (Bain et al., 1994; Jones-Villeneuve et al., 1983). Identification of neural subtypes and glia generated in vitro rely on the use of cell specific molecular markers. However, the dependence on the markers has its limitation. For instance, Nestin which is a good marker for neural progenitors is also expressed in differentiated non neural cells. The expression patterns of markers are also shown to be markedly different between RNA and protein. For example, RNA levels of NF-160 kDa (NFM) are detected as early as in EBs and Day 1 after plating but the proteins are only detected in the later stages of neural differentiation (Kaomei Guan et al., 2001). Hence, a cohort of markers (RNA and protein) in combination with morphological indicators is required to determine cell types. Besides that, it is critical to include markers that are known to be absent.

For the characterisation RA-induced P19 neuronal differentiation culture, a set of markers pertaining to neural progenitors, differentiated neuron and glia were analysed. The markers used are categorised based on their function (Table 3.1). The RNA sample used to study the expression these genes was similar to that use for Oct4 analysis (section 3.6.1).

Table 3.1: List of neuronal markers used in the characterisation of RA-induced P19 neuronal differentiation.

Markers	Cellular Function	Cell type
Microtubule-Associated Protein 2 (Map2)	Cytoskeleton	Neuron
Neurofilament-160 kDa (NFM)	Cytoskeleton	Neuron
Nestin	Cytoskeleton	Neuron progenitors
Neuron-specific Enolase (NSE)	Metabolising enzyme	Differentiated Neurons
N-Methyl-D-Aspartic Acid receptor (NR2a)	Neurotransmitter receptor	Differentiated Neurons
Glial-Fibrillary acidic protein (GFAP)	Cytoskeleton	Glia

3.6.2.1 Map2 RNA and protein is expressed in P19 neuronal differentiation

Map2 is member of the MAP/Tau family that possess microtubule stabilising activity along with the role of regulating microtubule networks in the axon and dendrites of neurons (Felgner et al., 1997; Weisshaar et al., 1992). Map2 exists in three isoforms called Map2a, Map2b and Map2c depending on their amino-terminal projection domain. Map2c is the predominant form and has a shorter amino-terminal domain than Map2a and Map2b (Kalcheva et al., 1995). *In vivo*, the expression of MAP2 is mainly neuronal, but MAP2 immunoreactivity is also observed in non-neuronal oligodendrocytes. MAP2 expression is detected in the early stages of neuronal development and in adulthood, concurrent with the expression of neuron-specific α -tubulin (Menezes and Luskin, 1994). MAP2 is known to segregate into nascent dendrites after axonogenesis and as a result it is localised in the cell bodies and dendrites of mature neurons (Matus, 1990). *In vitro* EC neuronal differentiation using RA showed expression of Map2 RNA in the early differentiation stage followed by a lag phase before the presence of the protein (Xu et al., 2011).

To determine whether RA-induced P19 cells differentiate into neurons and express neuron specific markers, qRT-PCR and Immunofluorescence to study Map2 RNA and protein levels were carried out. For qRT-PCR analysis of Map2, primers were design against a target mRNA region that is specific to all three Map2 isoforms. Similarly, immunoreactivity of MAP2 antigen was detected using antibody that recognises all three isoforms. Map2 RNA and protein levels in differentiating P19 cultures are shown relative to undifferentiated cells (Figure 3.7). MAP2 was induced by 30 fold in day 3 neural differentiation compared to undifferentiated cells suggesting that the culture is committed to the neural-lineage.

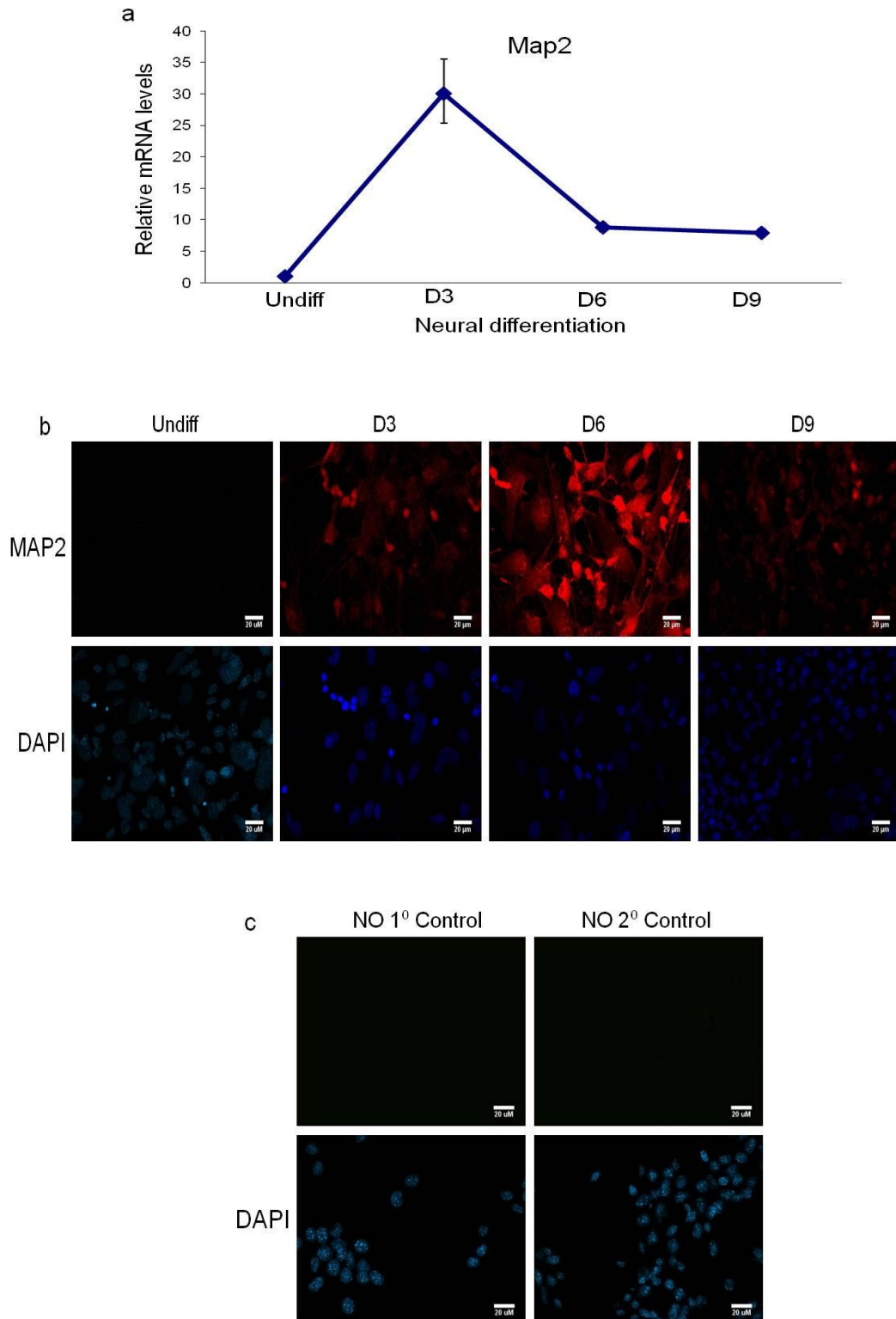


Figure 3.7: Map2 expression is induced to high levels upon neural commitment from undifferentiated P19 EC cells.

(a) Map2 RNA expression during P19 neuronal differentiation. RNA levels are normalised using α -tubulin and shown relative to undifferentiated cells. Error bars reflect standard deviation between three RT-PCR reaction replicates. (b) Immunofluorescence staining of MAP2 during neuronal differentiation. (c) No primary (but Alexa Fluor 596 Goat anti-Rabbit) and secondary (but MAP2) antibodies controls conducted in day 6. Scale bar, 20 μ m.

To analyse MAP2 protein expression, immunofluorescence was conducted in the differentiating P19 cultures (Figure 3.7b). The cells were fixed for MAP2 staining concurrent with RNA isolation used in the qRT-PCR analysis. Controls to determine cross-reactivity absence of antibodies were done on day 6 neural differentiation (Figure 3.7c). MAP2 immunoreactivity was not present in undifferentiated cells and is only detected upon RA induction. MAP2 immunofluorescence staining was found to be strongest in day 6 culture compared to day 3 and day 9. These results although demonstrate inconsistency between RNA and protein expression is in line with the evidence of Map2 expression in differentiating neurons derived from EC cells. Map2 RNA and protein expression in differentiating P19 cultures suggest the cells are undergone neural commitment upon RA induction.

3.6.2.2 NF-160 kDa and Nestin are expressed in P19 neuronal differentiation

NF-160 kDa (NF-M), a member of the neurofilament family, plays a role in the assembly of neuronal filaments and in stabilising of axons, along with other intermediate filament proteins (Walker et al., 2001). NF-160 kDa is concomitantly expressed with the emergence of neurite formation in the central nervous system (Nixon and Shea, 1992). In addition, the expression of NF-160 kDa was previously reported in differentiating neuronal cells derived from ES/EC cells (Kaomei Guan et al., 2001; Bain et al., 1996).

To analyse whether RA- induced P19 differentiating cultures express NF-160 kDa, qRT-PCR using specific primers to NF-160 kDa mRNA was performed. To validate the RNA expression, immunofluorescence using NF-160 kDa specific antibody was carried out. NF-160 kDa RNA is up-regulated upon RA induction in differentiating P19 cells (Figure 3.8a). The RNA levels of NF-160 kDa demonstrated a 1600 fold increase on day 3 neural differentiation compared to undifferentiated cells and decreased at day 6 and day 9. However, the RNA level of NF-160 kDa on day 9 is still 250 fold higher from that seen in undifferentiated cells. The RNA expression pattern of NF-160 kDa mirrors that of Map2. To analyse NF-160 kDa protein expression in P19 neuronal differentiation, immunofluorescence was conducted (Figure 3.8b). NF-160 immunoreactivity was not detected in undifferentiated P19 EC cells (Figure 3.8b). Day 3 and day 6 showed positive staining for NF-160 kDa with the clear appearance of dendrites and axons. The results demonstrate RA-induced P19 EC cells differentiate into neurons with appropriate cytoskeleton morphology.

Another key question that arises from EC/ES/EG derived neuronal differentiation is the identification of neural progenitor type cells. At the early stage the most common NPC marker is Nestin (Wiese et al., 2004; Lee et al., 2000). Most studies classify Nestin as a marker for NSCs (Podgorny, 2006; Savchenko et al., 2005; Wiese, 2004; Fukuda et al., 2003; Lee et al., 2000; Lendahl et al., 1990), whereas some studies claim Nestin is expressed in differentiated cells, particularly astrocytes (Nakamura et al., 2003; Clarke et al., 1994).

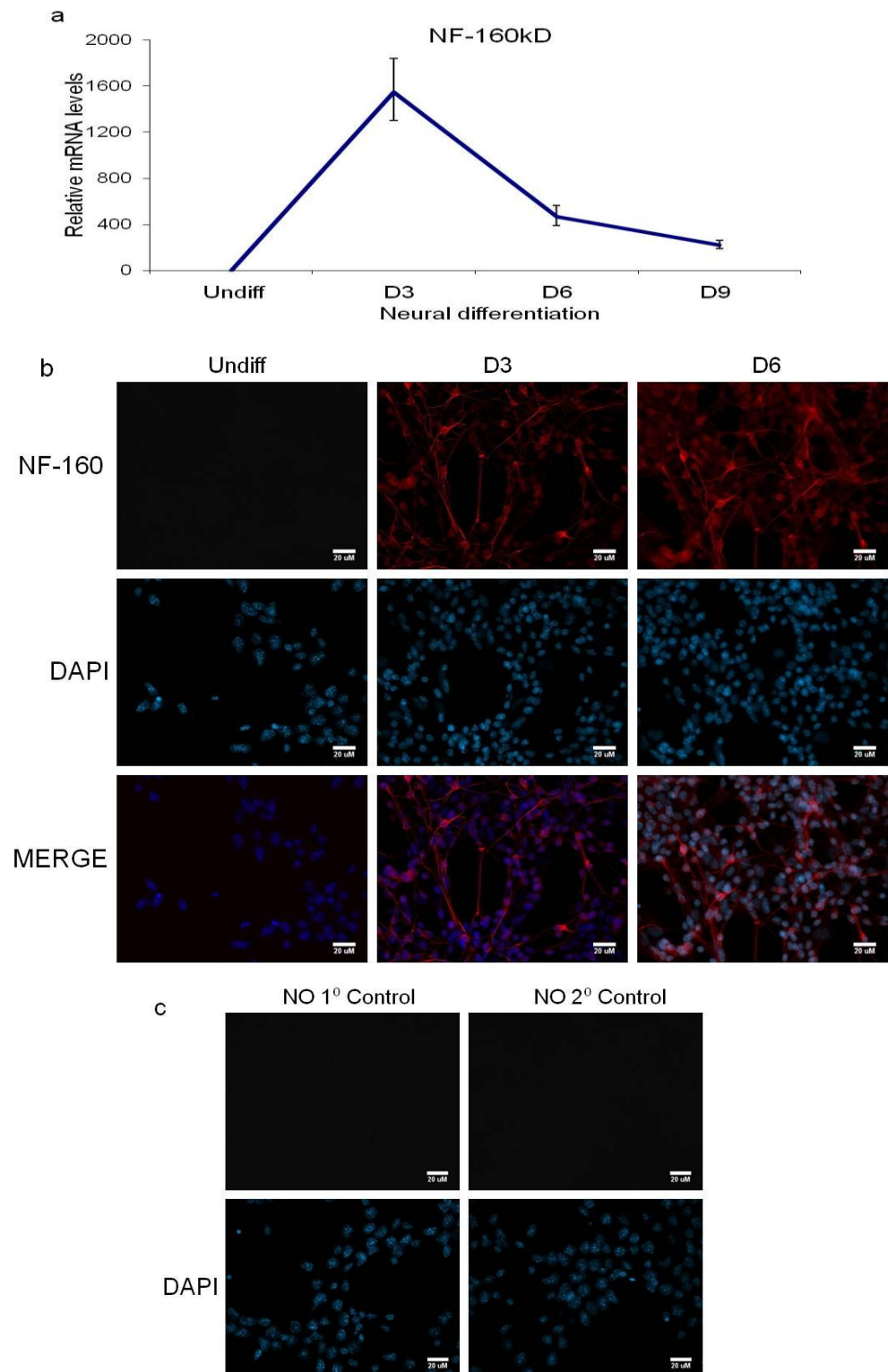


Figure 3.8: NF-160 kDa is highly expressed in day 3 and 6 neural differentiation from undifferentiated P19 EC cell.

(a) NF-160 kDa RNA expression during P19 neuronal differentiation. RNA levels are normalised using α -tubulin and shown relative to undifferentiated cells. Error bars reflect standard deviation between three RT-PCR reaction replicates. (b) Immunofluorescence staining of NF-160 kDa during neuronal differentiation. (c) No primary (but Alexa Fluor 596 Goat anti-Rabbit) and secondary (but NF-160 kDa) antibodies controls conducted in day 3. Scale bar, 20 μ M.

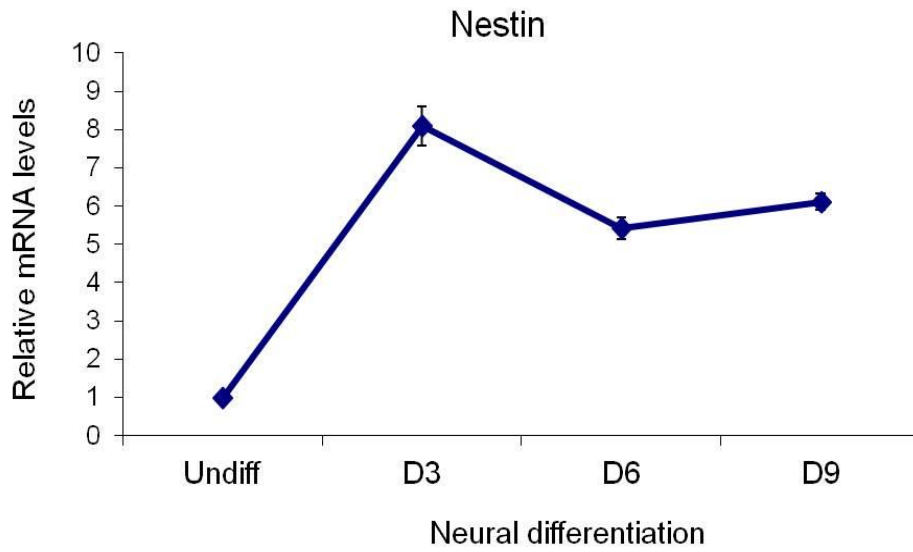


Figure 3.9: Nestin neural progenitor marker is induced upon RA-induced neural differentiation from P19 EC cells

RNA levels are normalised using α -tubulin and shown relative to undifferentiated cells. Error bars reflect standard deviation between three RT-PCR reaction replicates.

Nestin, a type VI intermediate filament protein is expressed in the development of the central nervous system and found mainly in neural progenitor cells (Wiese, 2004; Zimmerman et al., 1994). *In vivo*, Nestin expression is detected in neuronal tissue during embryonic development, and in adult brain is localised to both neurons and glia (Dahlstrand et al., 1995; Hockfield and McKay, 1985). Nestin expression has also been shown to be abundant in damaged brain tissue and various nervous system tumors (Biagiotti et al., 2006; Kambara et al., 2005; Almqvist et al., 2002; Holmin et al., 2001; Kaya et al., 1999).

ES cells initiate Nestin expression upon neural induction and up-regulate it during neuronal differentiation (Smukler et al., 2006). In contrast, P19 EC cells maintain a basal level expression of nestin which is up-regulated immediately upon neural commitment (Jin et al., 2006). The factors that regulate nestin expression are not fully determined, however Tanaka et al demonstrated that group B1/C Sox and class III Pou TFs interact synergistically to activate Nestin expression via its neural enhancer element (Tanaka et al., 2004).

The RNA levels of Nestin is normalised to α -tubulin in P19 neuronal differentiation is presented relative to undifferentiated cells (Figure 3.9). Nestin is induced by 8 folds compared to undifferentiated cells. These results imply that RA-induced P19 EC cells give rise to neural progenitors. Although it has been reported that Nestin is also expressed in non-neural dividing cells in differentiation cultures, high nestin expression on day 3 where the culture is post-mitotic suggest that the cells expressing this marker are most likely neural progenitors (Jin et al., 2006; Lee et al., 2000). The interesting aspect of nestin RNA expression compared to all the other markers analysed, is the fact that the magnitude of RNA induction is the lowest. If the results of day 3 were to be analysed separately, Nestin RNA levels demonstrated a fold increase of 8 whereas the markers such as NF-160 showed an up-regulation of 1600 fold both compared to undifferentiated cells. This is due to the fact that Nestin RNA is present at basal levels in undifferentiated P19 EC cells compared to all the other neuron specific markers.

3.6.2.3 RA-induced P19 cells expressed neuron specific markers NSE and NMDA receptor

Having shown that undifferentiated P19 EC cells upon RA induction, differentiate into neurons based on Map2 and NF-160 kDa expression, the next step was to investigate whether these cells express genes required for normal neuronal function. In order to address neuron functionality, markers specific to NSE and NMDA receptor were assayed. NSE is a major glycolytic enzyme that is found in neurons (Kato et al., 1984). The expression of NSE was previously shown to play a role in synaptic junction processing in neurons (Whitehead et al., 1982).

NMDA receptors play a role in the excitatory transport channel for the influx of Ca²⁺ ions and are crucial regulator of neuronal differentiation (Ghiani et al., 2007; Tozuka et al., 2005). NMDA receptors subunits are classified into NR1, NR2 and NR3. NR2 binds glutamate and consist of 4 different isoforms term NR2a-d. NR2 containing NMDA receptors have been previously reported to be expressed in P19 neuronal differentiation upon RA induction (Georgiev et al., 2008). Together, NSE and NMDA receptor markers provide evidence for neuron functionality in differentiating neuron culture.

The RNA levels of Nse and NR2a are normalised to α -tubulin in P19 neuronal differentiation is presented relative to undifferentiated cells (Figure 3.10). Nse expression is up-regulated upon RA induction with maximum expression on day 6 and day 9. NR2a expression showed sharp increase from day 6 to day 9. The striking difference between Nse and NR2a RNA levels with other markers analysed is the later onset of expression. These results suggest that the neuronal cells derived from P19 EC cells show that cells are undergone appropriate differentiation and has taken up usual neural functionality.

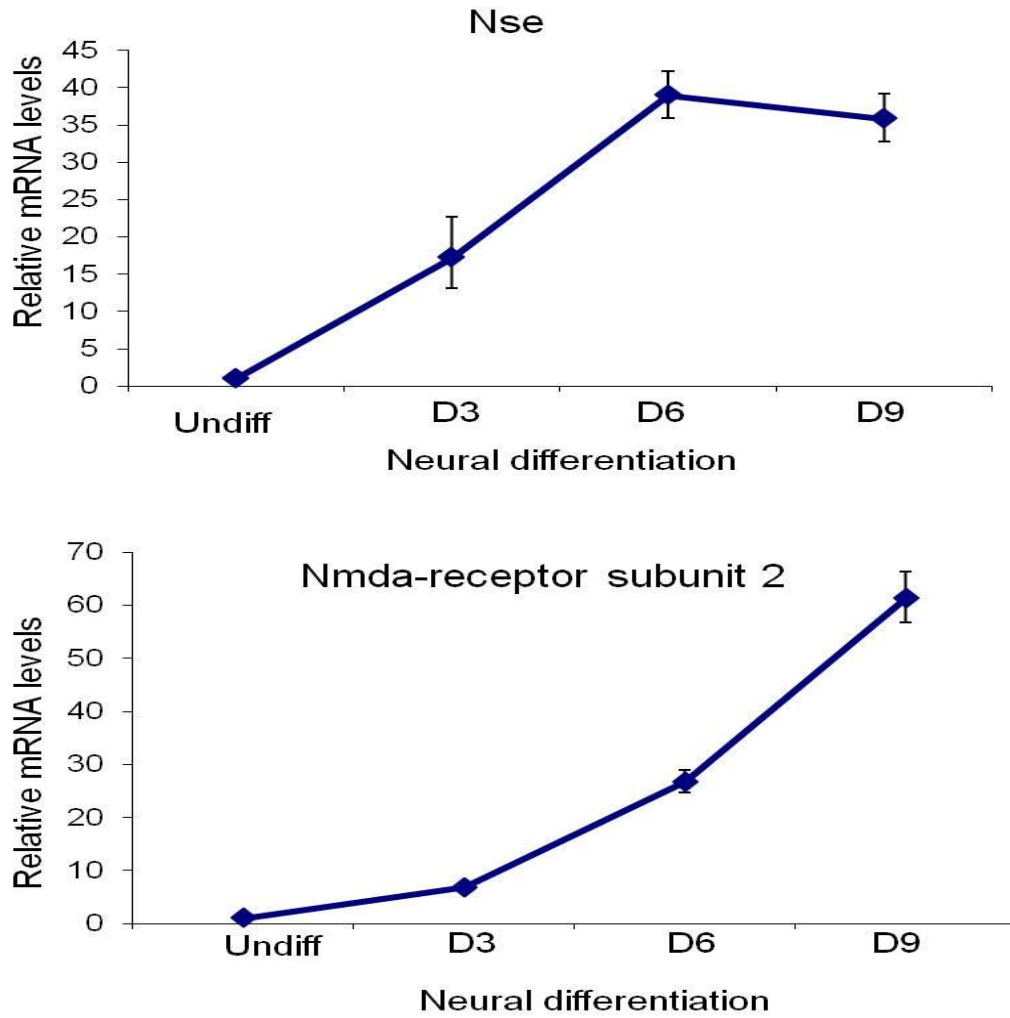


Figure 3.10: Nse and Nmda receptor are expressed in the later stages of neural differentiation derived from P19 EC cells.

RNA levels are normalised using α -tubulin and shown relative to undifferentiated cells. Error bars reflect standard deviation between three RT-PCR reaction replicates.

3.6.2.4 Glia cell marker is expressed in the later stage of RA- induced P19 differentiation

In developing central nervous system, the formation of glia/astrocyte cells is begins after the development of neurons (Sauvageot and Stiles, 2002). Similarly the manifestation of glia/astrocyte cells is delayed in *in vitro* neuronal differentiation of EC cells (Yi Wey et al., 2002). The most common marker used to identify glia/astrocyte cells is GFAP. GFAP is a member of the Class III Intermediate filament proteins that plays a role in maintaining glia/astrocyte cell integrity. There are 8 different GFAP isoforms in which GFAP α is the most predominant form.

To identify the presence of glia/astrocytes in RA- induced P19 neuronal differentiation, Gfap RNA and protein levels were analysed. For RNA detection, primers specific to Gfap α were used for qRT-PCR analysis. The protein expression was detected using immunofluorescence. Gfap RNA and protein levels in RA-induced P19 neuronal differentiation are shown as comparison to undifferentiated cells (Figure 3.11). The RNA levels of Gfap are undetected till day 6 of neural differentiation (Figure 3.11a). From day 6 onward, a dramatic up-regulation is observed with fold increase of 8000 compared to undifferentiated cells. These results suggest that Gfap RNA is only induced in the later stages of P19 neuronal differentiation. In contrast, GFAP is barely detected in any of the neural differentiation time points analysed (Figure 3.11b). Day 9 showed weak staining for GFAP of suggesting probably that glia/astrocyte cells starting to form in the differentiation cultures. This result does not come as a surprise as previous studies in P19 neuronal differentiation although showed the emergence of Gfap RNA, only showed the manifestation of the protein from day 14 neural differentiation onwards (Hádinger et al., 2009).

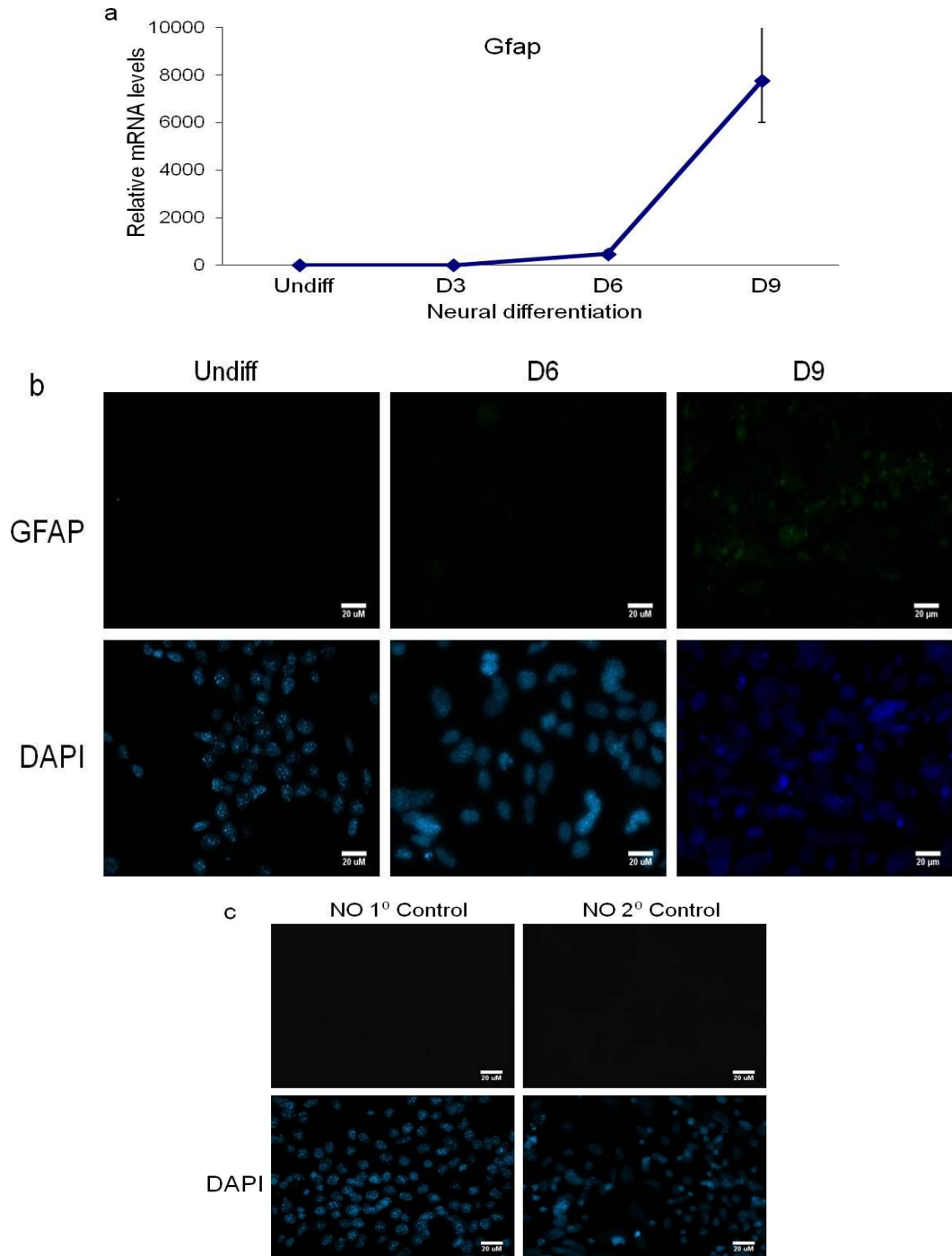


Figure 3.11: Gfap RNA levels are induced to high levels from day 6 whereas the proteins are detected on day 9 of P19 neuronal differentiation.

(a) Gfap RNA expression during P19 neuronal differentiation. RNA levels are normalised using α -tubulin and shown relative to undifferentiated cells. Error bars reflect standard deviation between three RT-PCR reaction replicates. (b) Immunofluorescence staining of GFAP during neuronal differentiation. (c) No primary (but Alexa Fluor 488 Goat) and secondary (but GFAP) antibodies controls conducted in day 9. Scale bar, 20 μ M.

3.7 Discussion

The RA-induced P19 neuronal differentiation provides a model system to study the mechanisms underlying EC cell pluripotency and its ability to differentiate (Runnicki and McBurney, 1987; Jones-Villeneuve et al., 1982). The major advantage of the P19 EC cell line due to their transformed nature, can grow indefinitely in culture without expensive media or growth factors. Previous reports on the characterisation of P19 neuronal differentiation show variability in the concentration of RA used to induced EB formation and the plating density to obtain neuronal differentiation. The studies in this chapter addressed key steps in the existing differentiation protocol, which increased the capacity of neuronal differentiation in culture. The two key steps are RA concentration and EBs seeding density in determining the extent of neuronal differentiation.

When the project started, most of the studies in the literature using P19 neuronal differentiation system used 0.5 μM RA. The increasing RA concentration analysis had managed to induce neuron specific marker Map2. However, 0.5 μM RA showed incomplete neural lineage commitment with the manifestation of a population of cells in the differentiated cultures expressing pluripotent marker Nanog. RA dosage of 1.0 μM but not 1.5 μM was used in all subsequent analysis although the latter showed slightly better efficiency in producing neuronal differentiation cultures. The dosage of 1.0 μM RA compared to 1.5 μM RA was deem optimal and most appropriate as it falls within the optimal range previously reported (Teets et al., 2011; Bain et al., 1995; Edwards and McBurney, 1983). Besides that, a year after this project started, more groups using RA-induced P19 neuronal differentiation reported the use of 1.0 μM RA although none explained the significance (Georgiev et al., 2008; Zhigang Jin et al., 2009).

Thus in order to be able to compare the characteristics of this P19 neuronal differentiation system with previous studies, an RA dosage of 1.0 μM was applied. However, it is clear that 1.5 μM RA can also be used for neural programming. This RA dosage dependence analysis shows that the concentration of RA required for complete neuron lineage commitment is

crucial. Furthermore, it is clear that gene expression should be analysed up to day 6 after plating in order to ensure that Nanog expression is completely suppressed and undifferentiated cells are not present in the neuronal differentiation culture.

The optimal seeding density of EBs in adherent cultures was addressed using Mash1 and Mash2 markers. Mash1 and Mash2 markers provide more sensitive indication of the neuronal differentiation state compared to markers such as Oct4 and Map2. A previous report demonstrated the importance of maintaining cell-to-cell contact during P19 neuronal differentiation (Schmidt et al., 1992). Using molecular markers Mash1 and Mash2 was the key in this experiment. Markers such as Oct4 and Map2 were sharply down-regulated and up-regulated, respectively, upon RA induction and therefore were not sensitive enough. This could be a major reason why the EBs plating step was not previously identified as a crucial step in the differentiation protocol. At seeding densities lower than 2.5×10^6 the differentiation cultures failed to survive whereas at densities higher than 5.5×10^6 the cultures had retained a population of cells expressing the undifferentiated marker Mash2. These results suggest that a cell-to-cell contact-dependent signalling mechanism is important for P19 neuronal differentiation.

RA-induced neuronal cells derived from pluripotent ES/EC cells expressed neuron specific genes in a developmentally controlled manner (Rohwedel et al., 1999). Profiling of molecular markers is the most commonly used method for characterising neuronal differentiation *in vitro*. The expression profiling is based on genes that are known to be expressed upon neural induction and specific to subtypes of neuron and glia cells. In this chapter, a cohort of marker was analysed and the RA-induced P19 differentiation showed programming to the neural lineage. The differentiation cultures expressed the neuron specific markers and the loss of pluripotency markers. A marker for Glia cells was detected in the later stage of differentiation (day 9). The RNA levels of the neuronal markers were detected in the EBs stage onwards but not the proteins. Protein levels of NF-160 and Map2 are detected from day 3 and 6 respectively. Markers such as NMDA-NR2 and NSE are expressed in the later stage of differentiation coinciding with functional neurons. These results

are comparable to previous studies that show neuronal and glia marker expressions in ES/EC cells (Rohwedel et al., 1999; Bain et al., 1995; Fraichard et al., 1995; Strübing et al., 1995, Strübing et al., 1995).

3.8 Conclusion

The characterisation results in this chapter show that RA-induced P19 cells have undergone programming and differentiate into neurons and possibly glia over a period of 9 days. However, the neuronal differentiation carried out here, is over a short length of time and may not be fully functional in inducing neuronal signalling and synaptic transmission as terminal neurons.

Chapter 4

Characterisation of HMGN expression in neural differentiation of P19 EC cells and hippocampal neurons from adult mouse brain

4.1 Introduction

The HMGN proteins are a family of non-histone proteins that bind the nucleosome and alter the organisation of the chromatin structure (Bustin, 2001). The control of embryonic development depends on the precise regulation of tissue specific gene expression. The structure of the chromatin plays a key role in determining gene expression programs. Thus, nucleosome binding proteins such as HMGNs are expected to be important for the regulation of development and cellular differentiation.

HMGN proteins are divided into five members, HMGN1 through HMGN5. HMGN3 is the only member to have splice variants, HMGN3a and HMGN3b. HMGN1 and HMGN2 are the founding members of the family, followed by HMGN3 and HMGN4. HMGN5 has been recently discovered and is unique in terms of its molecular structure when compared to other HMGN members (Shirakawa et al., 2000).

The interest in studying HMGN proteins in embryonic stem cells and neuronal differentiation comes from a previous study conducted by Dr. Katherine L. West (West et al., 2004). In that study, over-expression of HMGN3 in Hepa cells up-regulated a specific gene target, GlyT1. GlyT1 is a gene that encodes Glycine transporter 1 protein that plays a crucial role in neurons. GLYT1 protein is responsible for the re-uptake of extracellular glycine at the synaptic junction of neurons (Zafra et al., 1997; Jursky and Nelson, 1996; Johnson and Asher, 1987). Glycine is an inhibitory neurotransmitter, whose synaptic concentration is regulated by GLYT1 to ensure proper processing of motor and sensory information (Cubelos et al., 2005; Lim et al., 2004). The study conducted by West et al not only showed that HMGN3 binds a target gene and

affects transcription but also suggested that HMGN3 may play a role in the proper functioning of neurons.

Since HMGN genes are regulated in a developmental-stage specific manner during mouse embryogenesis and cellular differentiation (Furusawa et al., 2006; Lehtonen et al., 1998), it is hypothesised that they may play a role in embryonic stem cell-derived neuronal differentiation. The role of HMGN proteins in neuronal differentiation has not yet been studied. In order to study whether HMGNs play a role in embryonic stem cells and neuronal differentiation, RA-induced neuronal differentiation of P19 EC cells was employed. The characterisation and optimisation of RA-induced neuronal differentiation was shown in the previous chapter. The HMGN members that were included in this study are HMGN1, HMGN2, HMGN3a and HMGN3b. HMGN4 and HMGN5 were not studied in this project. The reasons for studying the selected members of HMGN are based on their significance relating to the project. HMGN1 and HMGN2 remain the best characterised members of the family, whereas HMGN3 has been shown to be expressed in glial cells, a cell type associated with neurons (Ito and Bustin, 2002). HMGN4 is closely related to HMGN2 and is thought to have similar functions (Birger et al., 2001), while HMGN5 has a long acidic C terminal domain that is different from all the other members (Rochman et al., 2005). From here onwards whenever HMGNs are referred to in the text, it refers to HMGN1, HMGN2, HMGN3a and HMGN3b. The aims of this chapter are to study the expression of HMGNs during RA-induced P19 neuronal differentiation and in EBs. This chapter also describes the expression of HMGNs in hippocampal neuronal cultures derived from adult mouse brain.

4.2 Objectives

1. To analyse the expression of HMGN RNA and protein levels in neural programmed EBs.
2. To analyse the expression of HMGN RNA and protein levels in neural differentiation of P19 EC cells.

3. To study the cellular localisation of HMGN proteins in undifferentiated and neural differentiated P19 cells.
4. To study the expression of HMGN proteins in hippocampal neuronal culture from adult mouse brain.

4.3 Expression of HMGN in RA-induced EBs derived from P19 EC undifferentiated cells.

P19 EC undifferentiated cells can be induced using RA to form EBs that consists of neuroectodermal cells (Chapter 3). RA triggers an intrinsic transcription program that allows the activation of neuroectodermal-specific genes via the formation of EBs. The expression of HMGNs has not previously studied in the RA-induced EBs. In order to understand whether HMGNs may play a role in the programming of EBs, their expression levels were investigated first of all.

Having extensively validated the RA-induced P19 neuronal differentiation in the previous chapter, the RNA and protein levels of HMGN1, HMGN2, HMGN3a and HMGN3b were analysed in the programmed EBs. The RNA and protein used in these analyses are from the same biological samples used in characterising the cell-specific markers in chapter 3. HMGNs RNA levels were analysed using qRT-PCR as described in chapter 2. To validate the RNA expression, western blots were carried out using antibodies specific to HMGNs.

HMGN1 and HMGN2 RNA levels demonstrated a 8 and 6 fold increases, respectively, in RA-induced EBs compared to undifferentiated cells (Figure 4.1a and 4.1c). HMGN2 protein levels had increased in EBs compared to undifferentiated cells (Figure 4.1d). In contrast, the protein levels of HMGN1 showed a slight decrease in EBs compared to undifferentiated cells (Figure 4.1b).

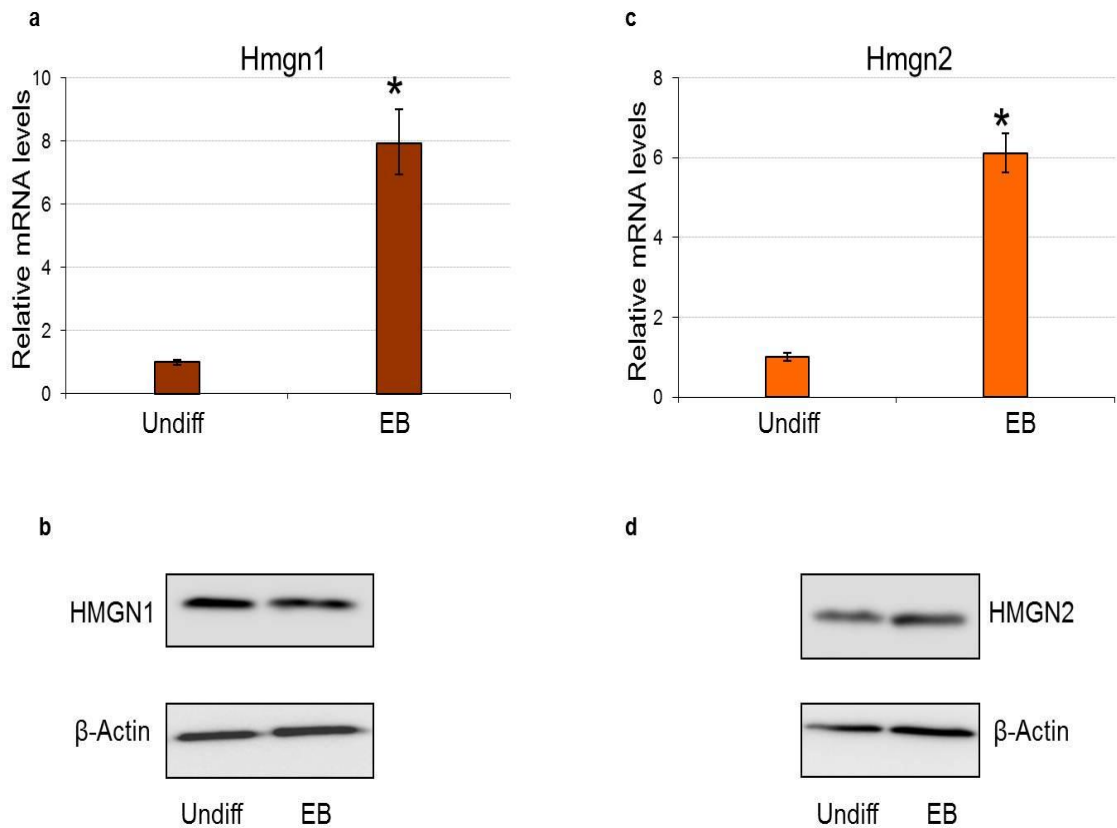


Figure 4.1: HMGN1 expression shows discrepancies between RNA and proteins levels whilst HMGN2 expression is up-regulated in RA-programmed EBs.

(a) & (c) qRT-PCR analysis of HMGN1 and HMGN2 in RA-programmed EBs shown relative to undifferentiated cells. RNA levels are normalised to Gapdh and presented relative to undifferentiated cells. Error bars reflect the standard deviation from RT-PCR triplicates from one biological replicate. * $P < 0.001$, was calculated from Ct average of 3 biological replicates compared to undifferentiated. (b) & (d) Western blots using whole cell extracts showing the expression HMGN1 and HMGN2. The western blotting images correspond to the similar biological replicate in (a). The western blotting images of (HMGN1 & β -Actin, HMGN2 & β -Actin) are from the same gel.

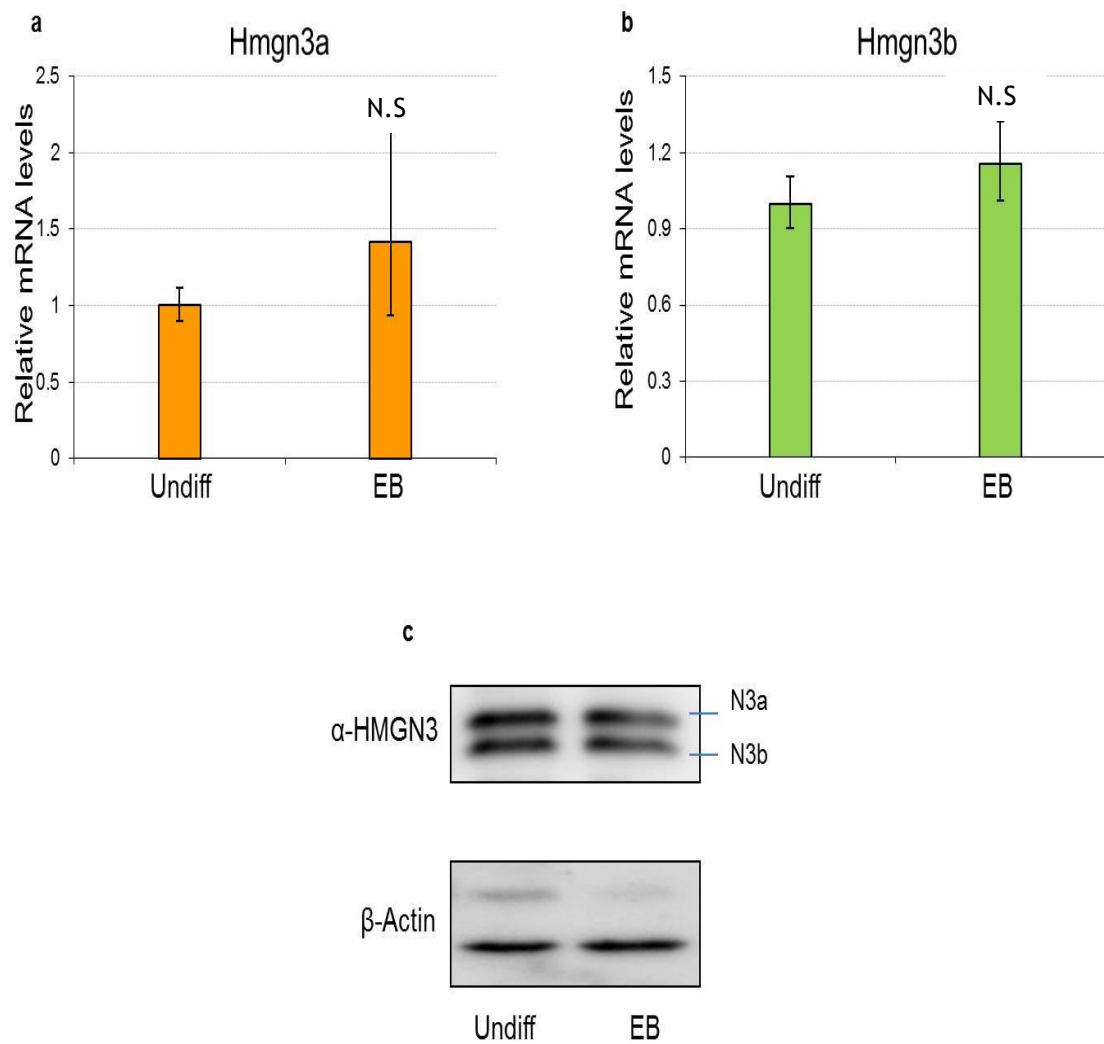


Figure 4.2: The RNA expression of HMGN3a and HMGN3b are up-regulated whilst the protein levels are slightly down-regulated in RA-programmed EBs.

(a) & (b) qRT-PCR analysis of HMGN3a and HMGN3b in RA-programmed EBs shown relative to undifferentiated cells. RNA levels are normalised to Gapdh and presented relative to undifferentiated cells. Error bars reflect the standard deviation from RT-PCR triplicates from one biological replicate. N.S., $p > 0.001$. p values were calculated from Ct average of 3 biological replicates compared to undifferentiated. (c) & (d) Western blots using whole cell extracts showing the expression HMGN3a and HMGN3b. The western blotting images correspond to the similar biological replicate in (a) & (b). The western blotting images are from the same gel.

The changes in HMGN3a and HMGN3b RNA levels were not significant in EBs compared to undifferentiated cells (Figure 4.2a and 4.2b). The protein levels of HMGN3a and HMGN3b decreased in EBs compared to undifferentiated cells (Figure 4.2c). It is interesting to note that even though the levels of HMGN1 and HMGN2 mRNA increased by over 6 fold in EBs, the protein levels were either unchanged (HMGN1) or only slightly increased (HMGN2). These experiments were carried out at least in 3 separate biological replicates and all the results yielded the similar expression profiles. Discrepancies between RNA and protein levels in HMGNs expression in EBs suggest a possible mechanism involving post-transcriptional regulation in turning mRNA to protein.

4.4 Expression of HMGN in P19 neuronal differentiation

The expression of HMGN proteins has been linked to cellular differentiation processes such as erythropoiesis, myogenesis, osteoblast differentiation and kidney organogenesis (Crippa et al., 1991; Begum et al., 1990; Shakoory et al., 1993; Lehtonen and Lehtonen, 2001). Studies using knockout mice, transient depletion and over-expression of these proteins have provided evidence of their role in cellular differentiation during embryonic development (Korner et al., 2003, Mohamed et al., 2001 and Pash et al., 1993). These studies suggest a possible correlation between regulated HMGN expression and cellular differentiation. However, studies on the expression patterns of HMGN during neuronal differentiation *in vitro* have not been performed.

Using the P19 neuronal differentiation system described in chapter 3, HMGN RNA and protein levels were analysed. The RNA and protein obtained were from the same biological replicates used for the characterisation of marker genes in chapter 3. The expression profiling analyses were carried out on 3 different biological replicates to avoid any technical false positives. Gapdh and α -tubulin were used as normalisers, and both sets of results were comparable (data normalised using α -tubulin not shown). Days 3, 6 and 9 were selected to compliment the characterisation data of cell-specific markers in chapter 3. HMGN RNA and protein studies were carried out as described in Chapter 2.

4.4.1 Expression of HMGN1 in the neuronal differentiation of P19 EC cells

Normalised HMGN1 RNA levels were calculated relative to undifferentiated cells and presented as day 3, day 6 and day 9 of neural differentiation cultures (Figure 4.3). Overall, Hmgn1 RNA levels decreased upon neural induction compared to undifferentiated cells. Day 3 neural differentiation showed the major decrease in expression by almost 50%. The RNA levels of HMGN1 in day 6 and day 9 decreased to around 80% compared to undifferentiated cells. However the data point for day 9 was not significant based on the P-values.

To validate the RNA profile of Hmgn1, western blotting was performed to assay protein levels. HMGN1 protein levels were slightly up-regulated during neuronal differentiation compared to undifferentiated cells (Figure 4.3). Comparable western blotting results were obtained in 3 independent biological replicates (data not shown). Similar to the HMGNs expression results found in EB, there were discrepancies between RNA and protein expression data. The P values indicate that the decreased in RNA levels found in day 3 are significant although the protein levels were slightly elevated.

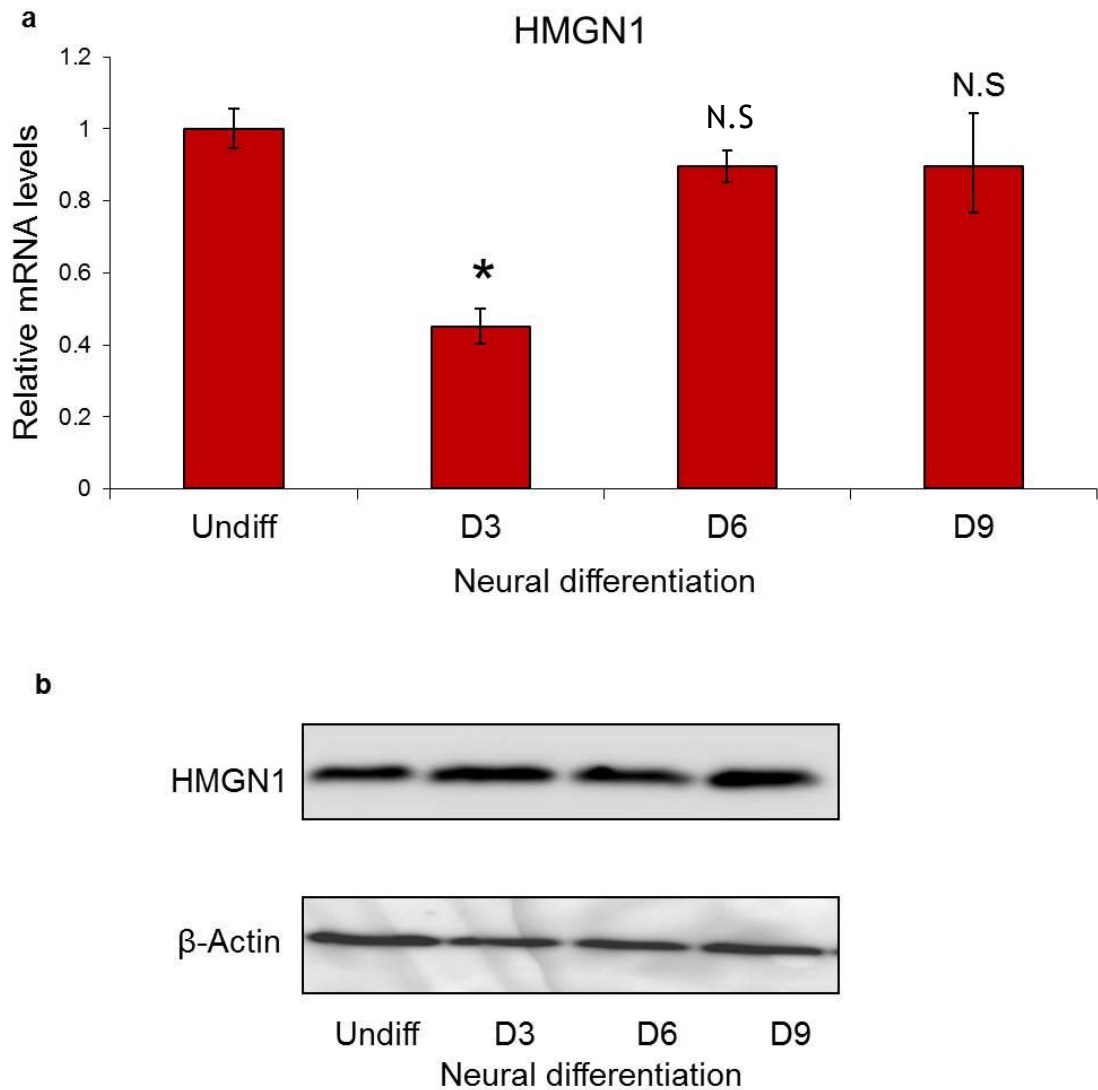


Figure 4.3: HMGN1 RNA and protein expression during neural differentiation of P19 EC cells.

(a) qRT-PCR analysis of HMGN1 RNA levels in RA-induced neural differentiation on days 3, 6 and 9 shown relative to undifferentiated cells. RNA levels are normalised to Gapdh and presented relative to undifferentiated cells. Error bars reflect the standard deviation from RT-PCR triplicates from one biological replicate. * $P < 0.001$ was calculated from Ct average of 3 biological replicates compared to undifferentiated. N.S., $p > 0.001$ compared to undifferentiated. (b) Western blots using whole cell extracts showing the expression HMGN1. The western blotting images correspond to the similar biological replicate in (a). The western blotting images are from the same gel.

4.4.2 Expression of HMGN2 in the neuronal differentiation of P19 EC cells

During neuronal differentiation, Hmgn2 RNA levels demonstrated a gradual increase from days 3 to 9 (Figure 4.4a). The expression of Hmgn2 RNA was highest on day 9, with a 2.3 fold increase compared to undifferentiated cells. Day 3 and day 6 had near similar levels of HMGN2 expression which is approximately 1.5 fold higher compared to undifferentiated. Similarly, the levels of HMGN2 protein were up-regulated during neuronal differentiation compared to undifferentiated cells (Figure 4.4b). These results show that HMGN2 expression profiles are up-regulated upon neural commitment and neuronal differentiation. The regulated expression of HMGN2 suggests a possible role in the differentiation of P19 EC cells.

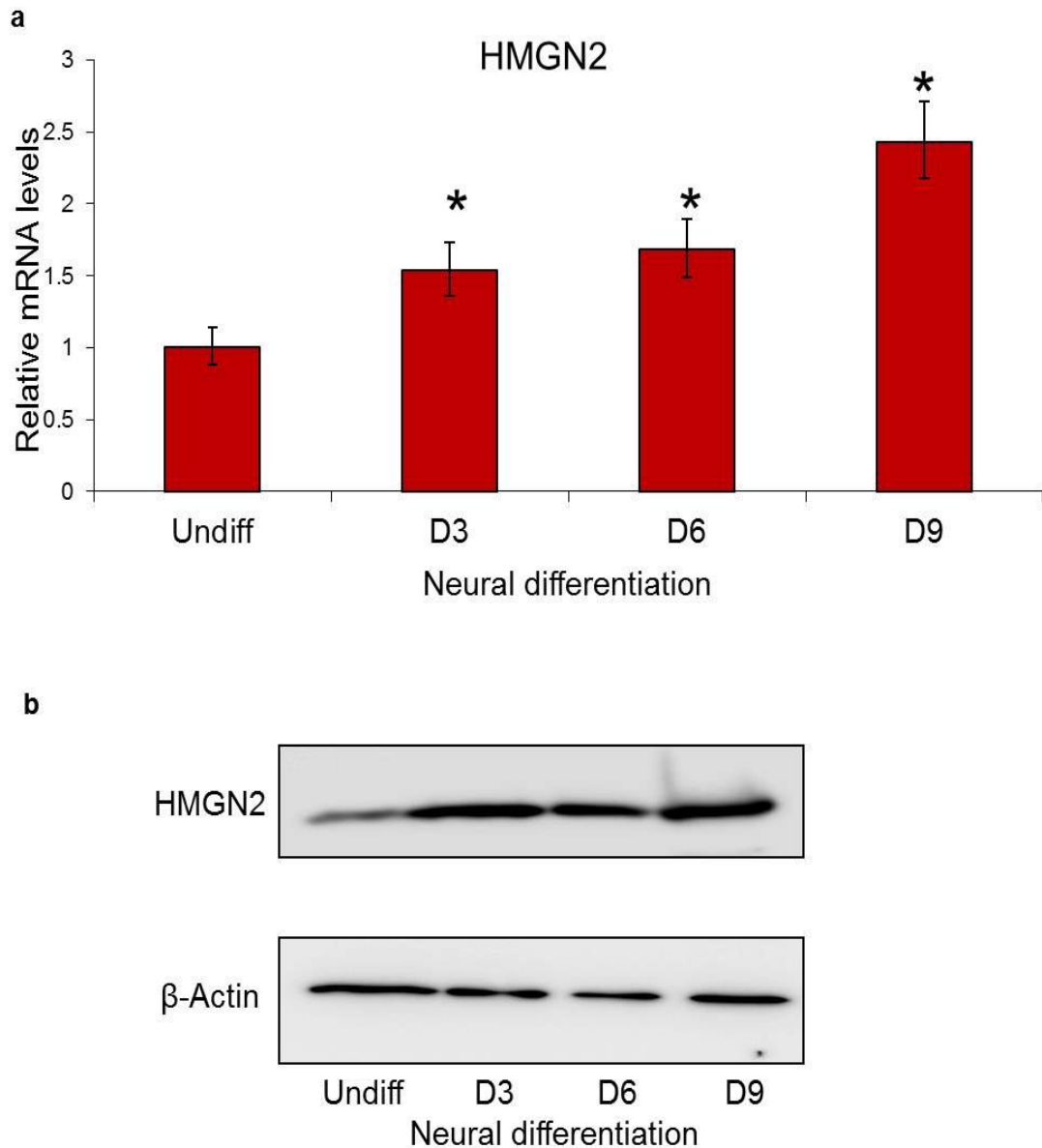


Figure 4.4: Expression of HMGN2 is up-regulated upon neural differentiation of P19 EC cells.

(a) qRT-PCR analysis of HMGN1 RNA levels in RA-induced neural differentiation on days 3, 6 and 9 relative to undifferentiated cells. RNA levels are normalised to Gapdh and presented relative to undifferentiated cells. Error bars reflect the standard deviation from RT-PCR triplicates from one biological replicate. * $P < 0.001$ was calculated from Ct average of 3 biological replicates compared to undifferentiated. (b) Western blots using whole cell extracts showing the expression HMGN2. The western blotting images correspond to the similar biological replicate in (a). The western blotting images are from the same gel.

4.4.3 Expression of HMGN3 in the neuronal differentiation of P19 EC cells

HMGN3a and HMGN3b RNA and proteins were expressed at very low levels in undifferentiated P19 EC cells (Section 4.3). In programmed EBs, the RNA levels of HMGN3a and HMGN3b were found to be increased but the protein levels did not alter significantly. During neuronal differentiation of P19 cells, HMGN3a and HMGN3b demonstrated an up-regulation in their expression (Figure 4.5). Relative to undifferentiated cells, HMGN3a RNA levels increased from 5 fold at day 3 to 15 fold at day 9 (Figure 4.5a and 4.5b). Similarly HMGN3b RNA levels increased between 10 fold at day 3 to approximately 20 fold at day 9. To validate the RNA expression profile of HMGN3a and HMGN3b, western blots were performed using an antibody that detects both isoforms. Overall, the protein levels of HMGN3a and HMGN3b demonstrated an up-regulation during neuronal differentiation of P19 EC cells (Figure 4.5c). These results show that HMGN3a and HMGN3b expression levels are linked to differentiation and these proteins may play a role in the process of neurogenesis.

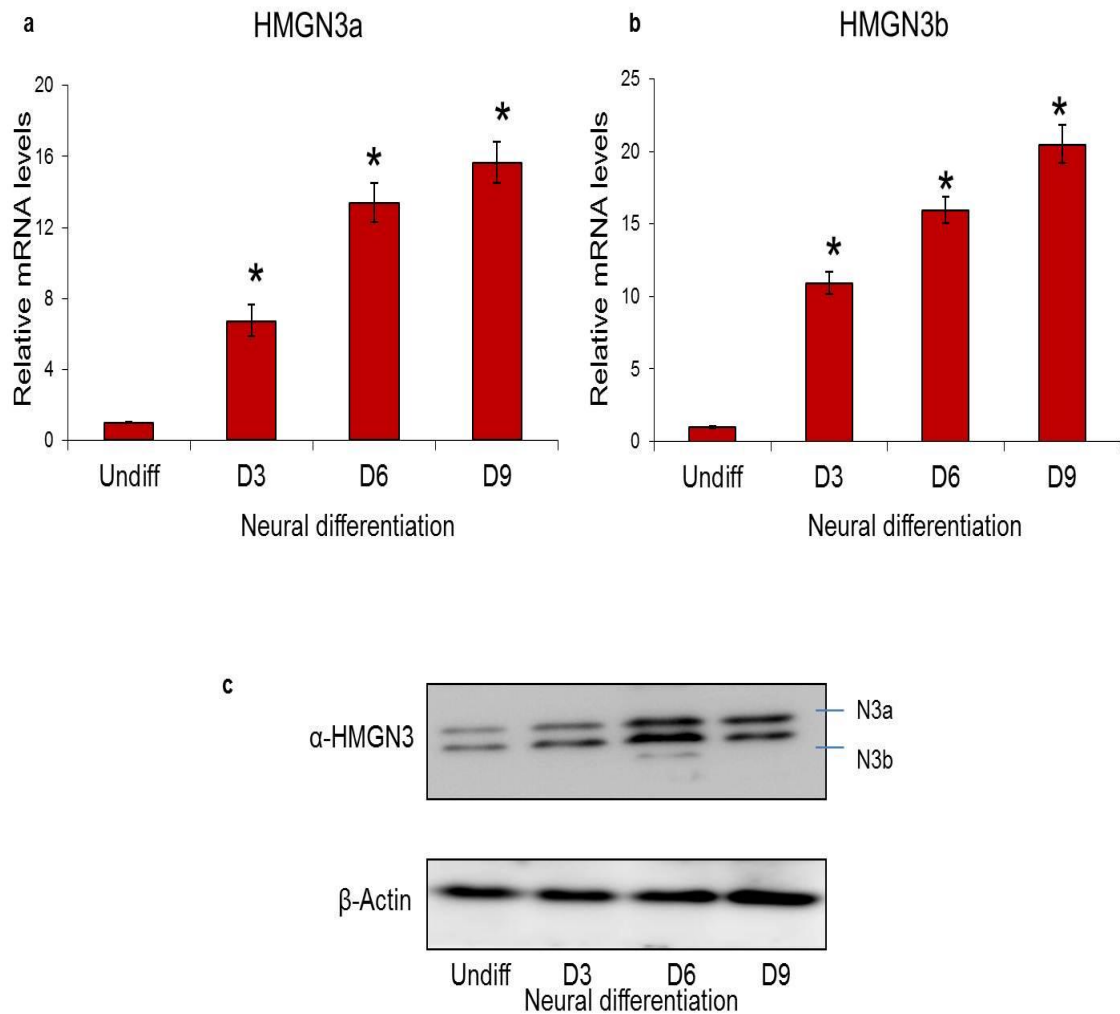


Figure 4.5: Expression of HMGN3a and HMGN3b are up-regulated upon neural differentiation of P19 EC cells.

(a) & (b) qRT-PCR analysis of HMGN3 RNA levels in RA-induced neural differentiation of days 3, 6 and 9 relative to undifferentiated cells. RNA levels are normalised to Gapdh and presented relative to undifferentiated cells. Error bars reflect the standard deviation from RT-PCR triplicates from one biological replicate. * $P < 0.001$ was calculated from Ct average of 3 biological replicates compared to undifferentiated. (c) Western blots using whole cell extracts showing the expression HMGN3. The western blotting images correspond to the similar biological replicate in (a) & (b). The western blotting images are from the same gel.

4.5 Cellular localisation of HMGN in undifferentiated P19 EC cells.

HMGNs are nucleosome binding proteins and are found to be distributed throughout the nucleus (Hock et al., 1998; Postnikov et al., 1997). Previous studies have shown that HMGN1 and HMGN2 are highly dynamic in the nucleus and that their distribution is transcription dependent (Misteli et al., 2000; Hock et al., 1998). Studies on HMGN3 expression in adult mouse brain and retina show that the protein is localised in the nucleus (Lucey et al., 2008; West et al., 2004; Ito and Bustin, 2002). The intra-nuclear organisation of HMGN proteins in P19 EC cells has not been studied.

The RNA and protein expression patterns of HMGNs shown in section 4.3 and 4.4 do not show whether HMGN proteins are ubiquitously expressed in all cells. In order to study whether HMGN proteins are present in all cells or a particular cell type, immunofluorescence using antibodies specific to HMGN1, HMGN2 and HMGN3 was performed using undifferentiated and neural differentiating cultures. Firstly, immunofluorescence studies were conducted in undifferentiated cultures, using the protocol described in chapter 2. These experiments were done in parallel to the immunofluorescence studies of Oct4, Nanog and Sox2 presented in chapter 3. The results showed here are representative of 3 biological replicates tested and at least 30 fields of images taken under 40 X objective.

HMGN1 is ubiquitously expressed in undifferentiated cells (Figure 4.6a). The expression of HMGN1 seems to be evenly distributed in the nuclei of all cells. Single cell images clearly show that HMGN1 is localised within the nucleus and not the cytoplasm (Figure 4.6b). The expression of HMGN2 is similar to that of HMGN1 in undifferentiated P19 EC cells. HMGN2 is ubiquitously expressed in all cells and is localised within the nucleus and not the cytoplasm (Figure 4.7a and 4.7b).

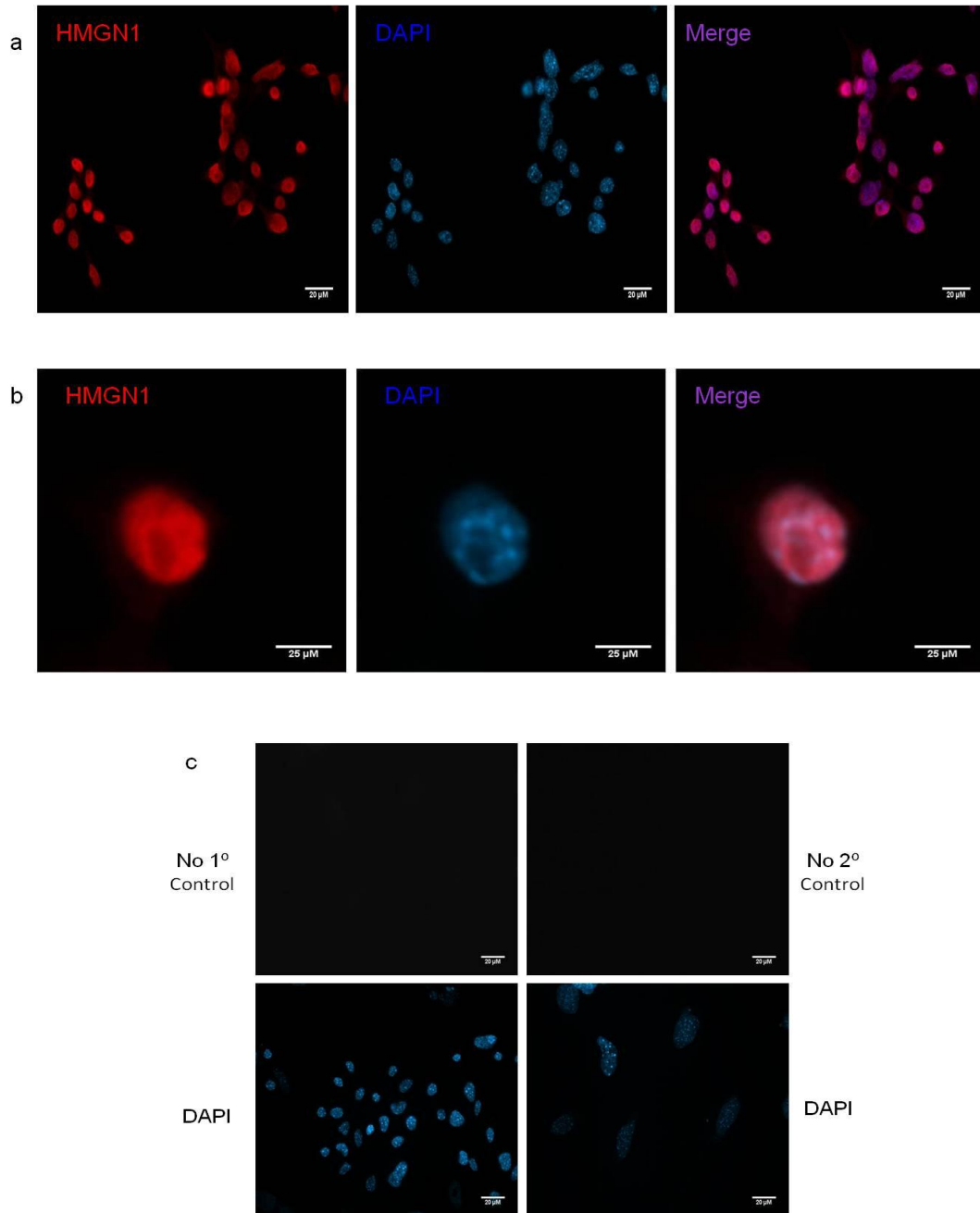


Figure 4.6: Expression of HMGN1 protein is ubiquitous and localises within the nuclei of undifferentiated P19 EC cells.

(a) Detection by immunofluorescence of HMGN1 protein in undifferentiated P19 EC cells. Scale bar = 20 μm . (b) Image digitally re-sized from (a) using image J to show single cell resolution image of HMGN1 protein. Scale bar = 25 μm . (c) Control immunofluorescence experiments conducted without primary (left) or secondary (right) antibodies. Red= HMGN1, Blue= DAPI and Purple= HMGN1 and DAPI merge. Each image is representative of 30 images taken from separate biological replicates. Immunofluorescence images were taken at 40 X objective and analysed using ImageJ software.

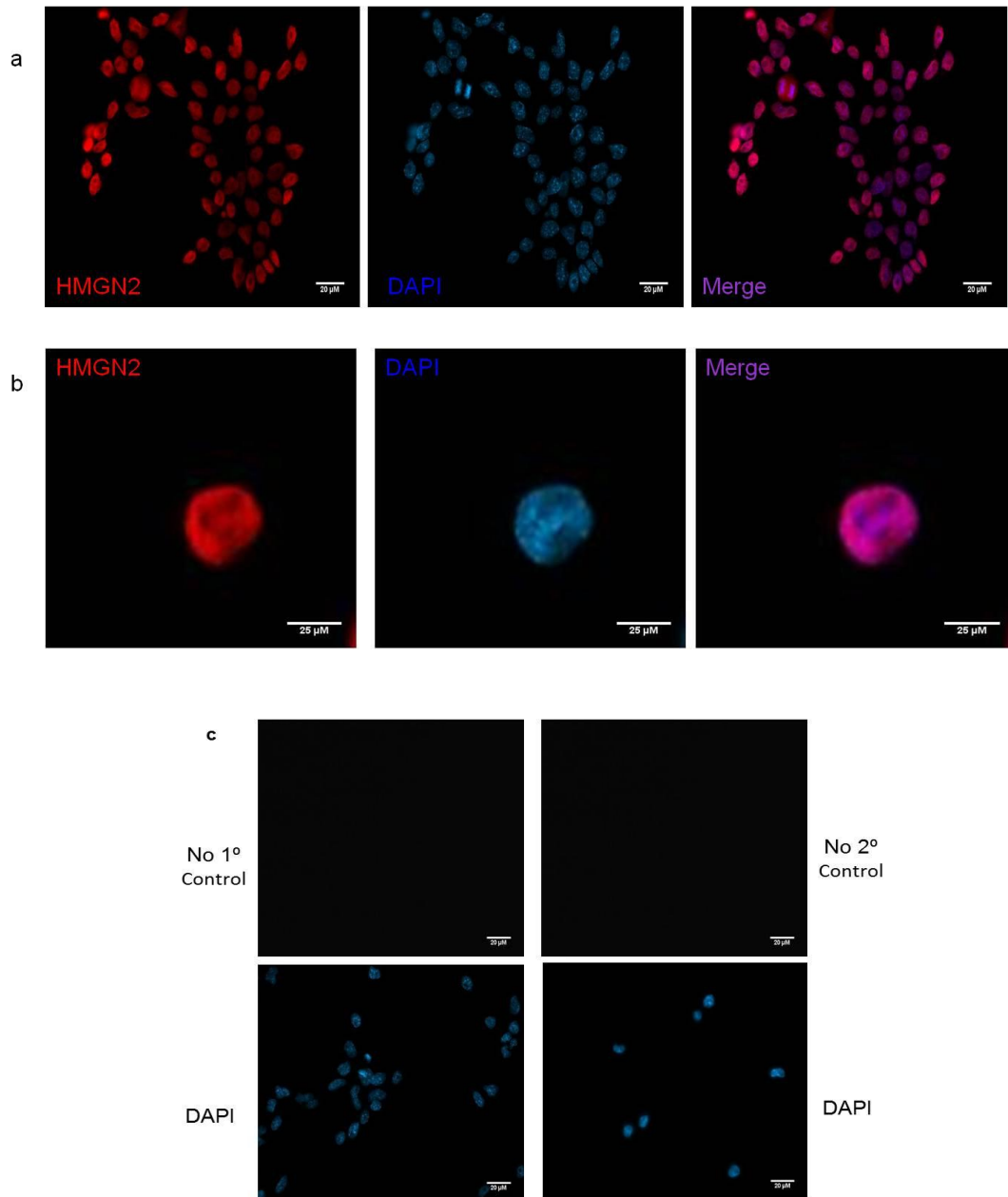


Figure 4.7: Expression of HMGN2 protein is ubiquitous and localises within the nuclei of undifferentiated P19 EC cells.

(a) Detection by immunofluorescence of HMGN2 protein in undifferentiated P19 EC cells. Scale bar = 20 μm . (b) Image digitally re-sized from (a) using image J to show single cell resolution image of HMGN1 protein. Scale bar = 25 μm . (c) Control immunofluorescence experiments conducted without primary (left) or secondary (right) antibodies. Red= HMGN2, Blue= DAPI and Purple= HMGN2 and DAPI merge. Each image is representative of 30 images taken from separate biological replicates. Immunofluorescence images were taken at 40 X objective and analysed using ImageJ software.

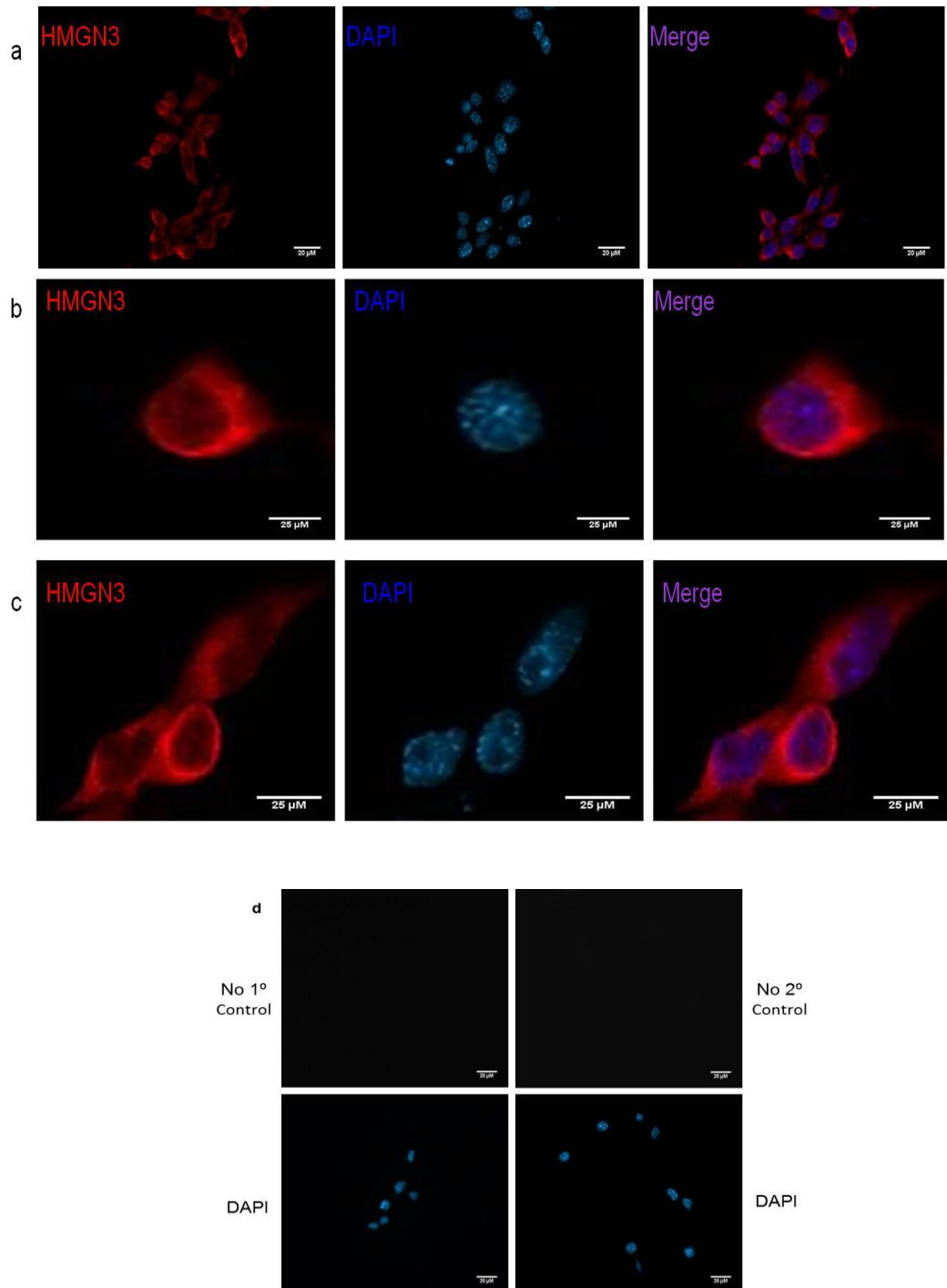


Figure 4.8: HMGN3a and HMGN3b proteins are ubiquitously expressed but predominantly localise with the cytoplasm.

(a) Detection by immunofluorescence of HMGN3a and HMGN3b proteins in undifferentiated P19 EC cells. Scale bar = 20μm. (b) & (c) Image digitally re-sized from (a) using image J to show single cell resolution image of HMGN1 protein. Scale bar = 25 μm. (d) Control immunofluorescence experiments conducted without primary (left) or secondary (right) antibodies. Red= HMGN3, Blue= DAPI and Purple= HMGN3 and DAPI merge. Each image is representative of 30 images taken from separate biological replicates. Immunofluorescence images were taken at 40 X objective and analysed using ImageJ software.

HMGN3 detection via immunofluorescence was conducted using an antibody named HMGN3-2752 that detects both HMGN3a and HMGN3b. This antibody was previously used to detect HMGN3 proteins in different mouse brain regions, and showed HMGN3 localisation within the nuclei (Ito and Bustin, 2002). In undifferentiated P19 EC cells, HMGN3 was found to be ubiquitously expressed in all cells (Figure 4.8a). However, rather surprisingly HMGN3 distribution was predominantly localised to the cytoplasm of undifferentiated cells (Figure 4.8b and 4.8c). These results are representative of at least 7 biological replicates.

Further experiments were carried out to see whether this localisation was an artefact. First, HMGN3-2752 antibody used in the Western Blot experiment detected both HMGN3a and HMGN3b at the correct sizes and no other proteins were detected, ruling out a problem with antibody specificity (refer to figure 4.5). Nevertheless, a different antibody raised against a C-terminal peptide of HMGN3a (named mouse HMGN3a or mHMGN3a) was used in 3 biological replicates to analyse the cellular localisation of the proteins. Similar to the pattern observed using HMGN3-2752 antibody, HMGN3a protein was found to be localised within the cytoplasm of the cells (data not shown).

The analysis of HMGN3 localisation was also performed using methanol as the fixation agent instead of paraformaldehyde to rule out possible artefacts that may arise from the fixation agent. Results obtained from methanol fixed cells showed similar results in which HMGN3 proteins were predominantly cytoplasmic (data not shown). Finally, immunofluorescence studies of HMGN3 were conducted in a range of undifferentiated cells from early passage to late passage, and all experiments showed that HMGN3 is predominantly cytoplasmic (data not shown). Taken together, these results demonstrate that HMGN3, although ubiquitous expressed is predominantly within the cytoplasm. These results raise several questions about the role HMGN3 in P19 EC cells and whether it acts through a different mechanism compared to HMGN1 and HMGN2.

4.6 Cellular localisation of HMGN proteins in neural differentiated cultures of P19 EC cells.

HMGNs were all ubiquitously expressed in undifferentiated cells with HMGN1 and HMGN2 localised to the nucleus while HMGN3 was found to be cytoplasmic. The next question is whether the localisation patterns of HMGNs in undifferentiated cells are similar in neural differentiating cultures. Immunofluorescence analysis using similar conditions were performed on day 3 and day 6 neural differentiation cultures. These cultures were previously validated for neuronal markers (Chapter 3). The results shown here are representative of 2 biological replicates.

HMGN1 and HMGN2 were ubiquitously expressed in day 3 neural differentiated cultures (Figure 4.9a and Figure 4.9b). Similar to the undifferentiated cells, HMGN1 and HMGN2 were found to be localised within the nucleus. HMGN3 was expressed in all neuronal differentiating cells on day 3 and day 6 (Figure 4.9c). Importantly, the distribution pattern of HMGN3 is similar to undifferentiated cells in which the protein is localised within the cytoplasm. Overall, these results suggest that HMGN proteins are ubiquitous in their expression upon neural differentiation. HMGN1 and HMGN2 are localised within the nuclei whereas HMGN3 is predominantly found in the cytoplasm and cell body.

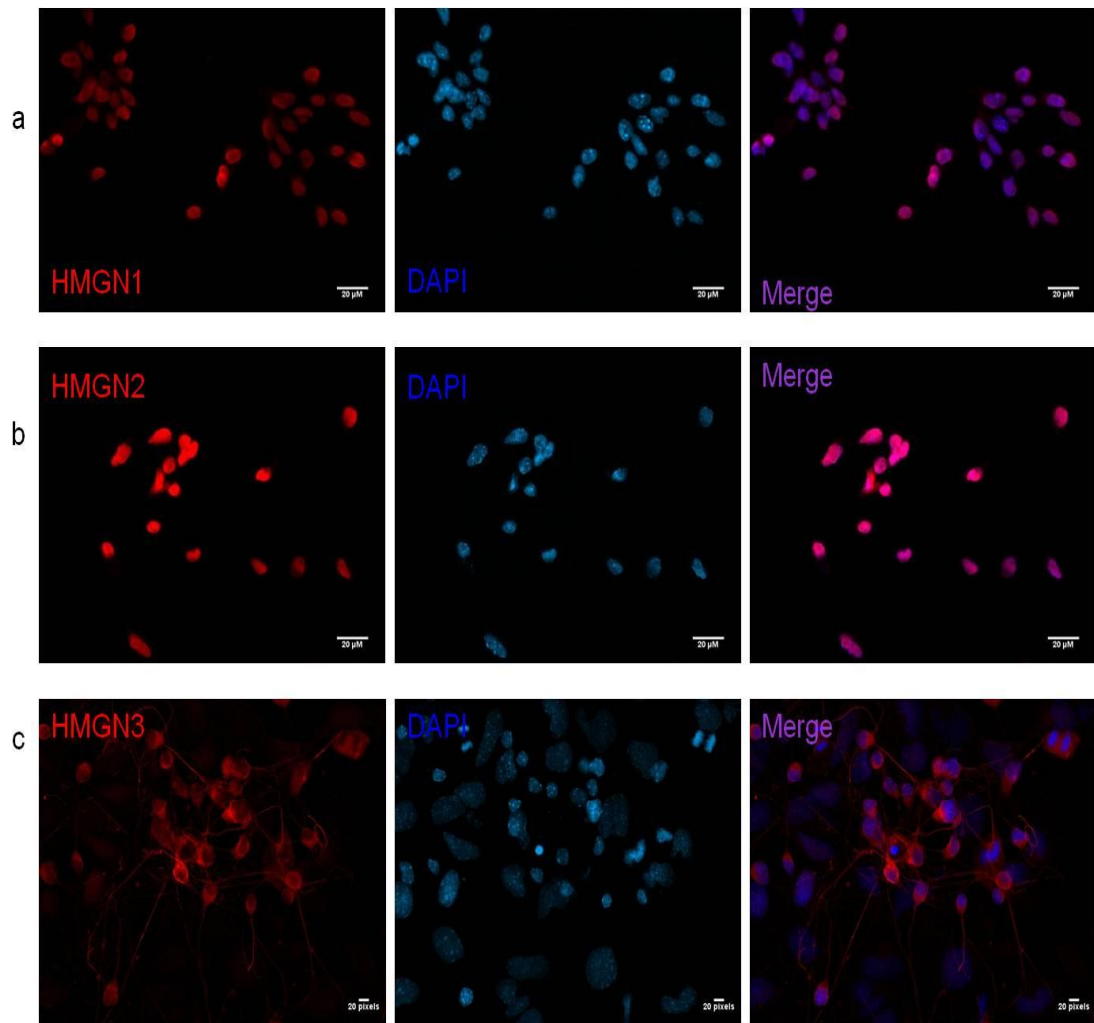


Figure 4.9: Expressions of HMGN proteins in RA-induced neural differentiation of P19 EC cells.

Detection by immunofluorescence of (a) HMGN1 on day 3 neural differentiation, (b) HMGN2 on day 3 neural differentiation and (c) HMGN3a and HMGN3b on day 6 neural differentiation. Scale bar = 20µm. Red= HMGNs, Blue= DAPI and Purple= HMGNs and DAPI merge. Each image is representative of 30 images taken from separate biological replicates. Immunofluorescence images were taken at 40 X objective and analysed using ImageJ software.

4.7 HMGN expression in hippocampal neurons

HMGN proteins are ubiquitously expressed in neuronal differentiating P19 EC cells. HMGN1 and HMGN2 are localised within the nucleus whereas HMGN3 is predominantly cytoplasmic. All previously reported HMGN expression in vivo showed that the proteins were localised within the nucleus (Lucey et al., 2008; West et al., 2004; Ito and Bustin, 2002). To investigate whether the cytoplasmic localisation of HMGN3 is a common feature of neuronal cultures, or whether it is specific to P19 cells, the localisation of HMGNs in primary mouse neuronal cultures was examined.

To obtain primary neuronal cultures, a collaboration with Dr. Stuart Cobb was established (University of Glasgow). Paul Turko (PhD student in Dr. Stuart Cobb's group) had kindly contributed neurons derived from the hippocampus region of the adult mouse brain grown in culture for 18 days. The day 18 hippocampal neuronal cultures had shown to express several neuronal and glia markers such as MAP2 and GFAP (Dr. Stuart Cobb, personal communication). Besides that, these cultures had shown normal neurotransmitter signalling indicating the presence of functional neurons (Dr. Stuart Cobb, personal communication).

Immunofluorescence studies to detect HMGN proteins were conducted on day 18 hippocampal cultures. These experiments were conducted on neurons from 2 separate adult mice and the results presented here are representative of both biological replicates. Overall, HMGN proteins were found to be localised with the nuclei (Figure 4.10). Interestingly, HMGN proteins were not ubiquitously expressed in day 18 neuronal cultures (overlaid images with DAPI). Approximately half the cells in the neuronal culture were not expressing HMGN proteins. These results suggest that HMGN proteins were only expressed in specific neurons or glia from the hippocampal regions and raise the question of their selective roles in these cells. In order to investigate which neurons or glia express HMGN proteins, an experiment using several cell markers could be used.

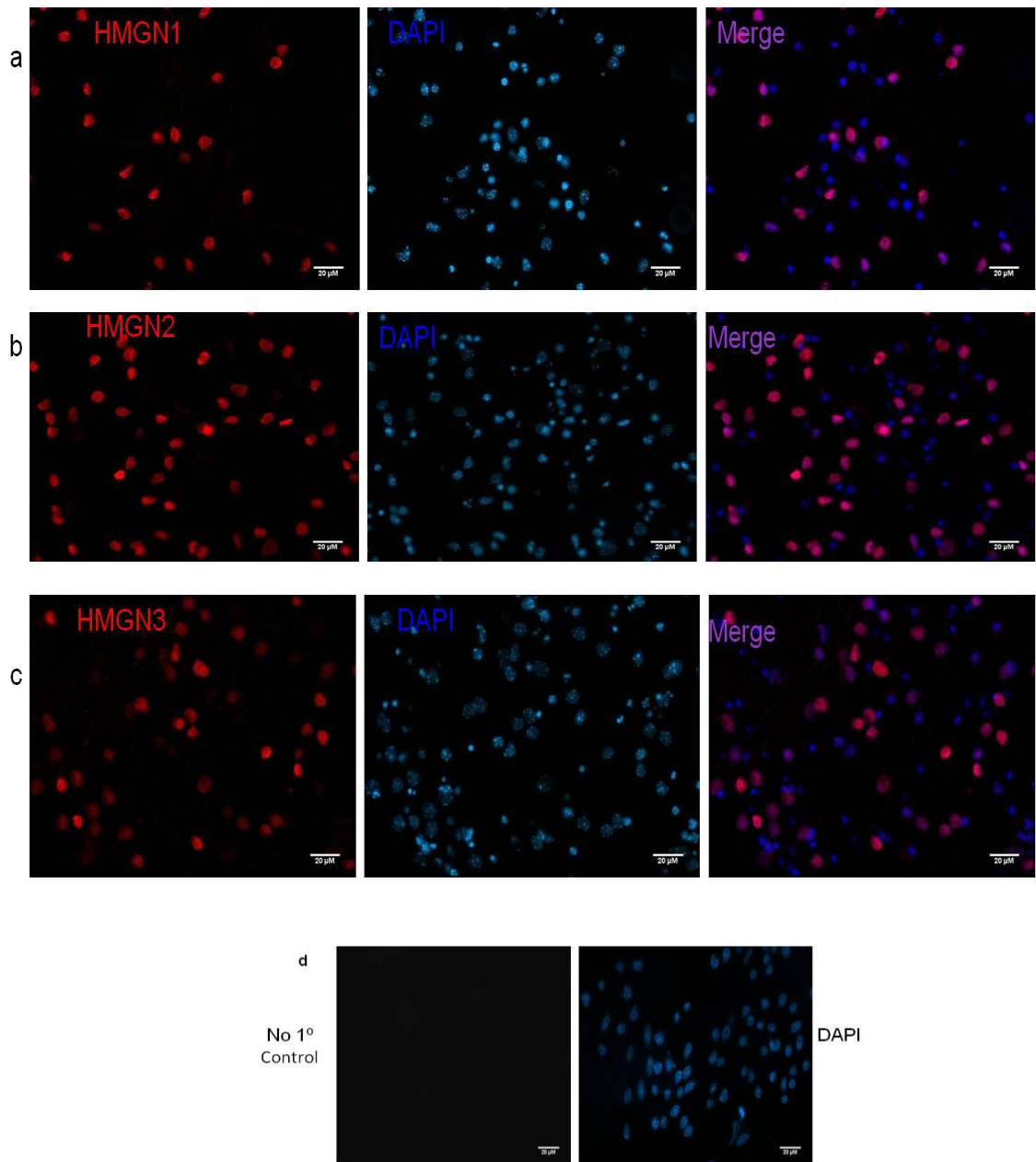


Figure 4.10: Expressions of HMGN proteins are not ubiquitous in day 18 hippocampal neuronal cultures.

Detection by immunofluorescence of (a) HMGN1, (b) HMGN2 and (c) HMGN3a and HMGN3b in day 18 hippocampal neuronal culture. Scale bar = 20 μm. (d) Control immunofluorescence experiments conducted without primary antibody. Red= HMGNs, Blue= DAPI and Purple= HMGNs and DAPI merge. Each image is representative of 10 images taken from separate biological replicates. Immunofluorescence images are taken at 40 X resolution and analysed using ImageJ software.

4.8 Discussion

Previous studies on HMGN proteins in differentiation models have been carried out in chondrocyte, myoblast and erythropoietic cells (Furusawa et al., 2006; Crippa et al., 1991; Begum et al., 1990). Studies from these model systems had one major outcome, with results demonstrating a down-regulation of HMGN1 and HMGN2 proteins upon cellular differentiation. Over-expression of HMGN proteins halted the differentiation process (Begum et al., 1990). In contrast, results shown here demonstrate a clear up-regulation of HMGN2 and HMGN3 expression during neural differentiation of P19 EC cells, whereas HMGN1 protein levels were not significantly changed. One possibility for the contrasting results could be due to the timing of the neuronal differentiation. The cultures shown here are at an early stage and have only undergone a short phase of differentiation (up to day 9). Expression of HMGNs may decrease if the cultures were allowed to differentiate further.

HMGN proteins were found to be ubiquitously expressed in undifferentiated and neural differentiated P19 EC cells. HMGN1 and HMGN2 were localised within the nucleus. Rather interestingly, HMGN3, although ubiquitously expressed in undifferentiated and neural differentiated cells, was found to be predominantly cytoplasmic. Cytoplasmic localisation of HMGN proteins in interphase cells has not been reported before, although it is known that the nuclear localisation of these proteins is regulated by phosphorylation. A study conducted by Prymakowska-Bosak et al in 2002 showed that mitotic phosphorylation of HMGN1 protein inhibited its nuclear import thus the protein were predominantly cytoplasmic following the completion of mitosis (Prymakowska-Bosak et al., 2002). These results demonstrate that there are other possible mechanisms that may cause HMGN3 to be localised in the cytoplasm in P19 EC cells. Further studies on HMGN localisation in other ES/EC/EG cells would determine whether this distribution is a general pattern in all embryonic-derived pluripotent cells or if it is only specific to P19 EC cells.

Studies on day 18 hippocampal neuronal culture showed that HMGN proteins were localised within the nuclei. These results also showed that HMGN proteins were not expressed in all cells. Day 18 hippocampal neuronal cultures have been shown to express both MAP2 and GFAP (Dr. Stuart Cobb, personal communication). Future studies using double immunofluorescence labelling of HMGNs and specific neuronal or glia markers could be performed on these cells to analyse the type of cells that are expressing the proteins. The results may be crucial in understanding the role of HMGN in neurons and glia culture.

This chapter investigates the expression of HMGN RNA and protein in undifferentiated and neural differentiating P19 EC cells. The results suggest that P19 EC cells are a good model system to study the role of HMGNs in pluripotency and neuronal differentiation.

Chapter 5

HMGN1 and HMGN2 knockdown affect the expression of key genes in undifferentiated P19 EC cells and RA-induced neural differentiation

5.1 Introduction

This chapter addresses the question of what is the possible role of HMGN proteins in P19 EC cell-derived neural differentiation? Previous studies show that HMGN1 and HMGN3 can modulate specific gene expression by directly binding directly to their targets, for example Sox9 and GlyT1a, respectively (Furusawa et al., 2006; West et al., 2004). As the results presented here suggest that two of the HMGN proteins are induced upon neural induction, it was hypothesised that HMGN proteins could affect the expression of gene targets that are important for neural commitment or function. In order to address this question, siRNA-based knockdown of HMGN proteins in P19 EC cells was employed. At this stage, the decision was taken to exclude HMGN3 from further experiments due to its unusual cellular localisation in both undifferentiated and neuronal cells. In addition, Hmgn3 RNA expression is around 100-600 fold lower than that of Hmgn1/2 during neural differentiation, and so may have a less crucial role than the more abundant isoforms (Chapter 4- Hmgn RNA ratio). The possible approaches that may be taken to investigate HMGN3 in P19 EC neural differentiation are discussed in Chapter 6 (Conclusions and future perspectives).

The aim of this chapter is to investigate the role of HMGN1 and HMGN2 in pluripotency and neural differentiation of P19 EC cells. It describes the establishment of HMGN1/2 knockdowns in P19 EC cells, followed by experiments to investigate the effect of the knockdowns on the expression of genes specific to pluripotency and neural differentiation.

5.2 Objectives

1. To establish and validate HMGN1/2 knockdowns using specific siRNAs in undifferentiated P19 EC cells.
2. To analyse the effect of HMGN1/2 knockdown on the expression of genes of interest (GOI) in undifferentiated cells.
3. To study the RA neural induction and differentiation ability of undifferentiated P19 EC cells lacking HMGN1/2.
4. To establish and validate HMGN1/2 knockdowns in neural differentiation from P19 EC cells.
5. To analyse the effect of HMGN1/2 knockdown on the expression of genes of interest (GOI) in RA-induced day 3 neural differentiation.

5.3 Establishing an siRNA-based protocol for HMGN1 and HMGN2 knockdown

To establish functional studies on the role of HMGN1/2 in P19 EC cells, knockdown experiments using siRNA-based technology were employed. A siRNA knockdown approach was selected for two main reasons: 1) siRNA-based knockdown, once established, is a rapid and convenient way to obtain functional data. 2) Identification of siRNA sequences that are efficient in knocking down HMGN proteins would enable them to be used in short hairpin RNA (shRNA) vectors for long term knockdown experiments.

The siRNA library for HMGN1 and HMGN2 was purchased from Qiagen's Flexitube GeneSolution system. This system provides 4 pre-selected siRNA sequences for one target that are designed based on their HP OnGuard siRNA design method. Among the key features of this siRNA design method are accurate siRNA design based on the latest NCBI data set and specific improvement to avoid off-target effects (see chapter 2 for details and

sequences). The siRNAs for HMGN1 and HMGN2 is shown in table 5.1. The siRNAs are re-named, for example siRNA N1₀₁, N1=target (HMGN1=N1/HMGN2=N2) whereas the subscripted 01 refers to the siRNA variant.

The siRNA knockdowns were carried out in P19 EC cells according to manufacturer's protocol, except that a different transfection reagent was utilised (Chapter 2). The siRNA initial knockdown screens were conducted using 3 different final siRNA concentrations of 5 nM, 10 nM and 20 nM for 48 hours (data not shown). The western blot results from this experiment showed that N1₀₂ and N1₀₃ knocked down HMGN1 protein levels by slightly more than 60% when used at 20 nM, whereas 5 nM and 10 nM had no or little knockdown of HMGN1 protein when compared to untreated cells and cells transfected with a negative control siRNA. Data from the initial knockdown screen demonstrated that N1₀₂ and N1₀₃ were the most efficient siRNAs when used at 20 nM final concentration. Two siRNAs to target HMGN1 as opposed to just one were used for subsequent experiments to act as a biological validation control.

Next, a time-course analysis of HMGN1 knockdown levels when transfected with N1₀₂ and N1₀₃ siRNAs at a final concentration of 20 nM was performed (Figure 5.1). Briefly, undifferentiated P19 EC cells were transfected with N1₀₂, N1₀₃ and negative control siRNAs for 48 hours before changing the media. The cells were then left to grow and passaged every two days. Whole cell lysates were collected at the indicated time points and assayed for HMGN1 protein levels. Results shown in figure 5.1 indicate that both siRNAs N1₀₂ and N1₀₃ generated more than 90% knockdown of HMGN1 protein levels at 72 hours after transfection. The protein levels were restored close to wild type levels by 6 days after transfection. These results show that N1₀₂ and N1₀₃ siRNAs, when used at a final concentration of 20nM, efficiently knockdown HMGN1 protein levels for almost 4 days (48-120 hours). The negative control siRNA in this experiment was used at 20 nM and the HMGN1 protein levels remained unaltered. Another validation experiment was conducted using an Alexafluor tagged siRNA (provided by Qiagen) to monitor if the siRNA used transfected most of the cells in the culture. Results showed that the siRNAs had transfected more than 80% of the cells in culture (data not shown).

The initial screen for HMGN2 knockdown using the four different siRNAs at 5 nM, 10 nM and 20 nM did not show efficient levels of knockdown (data not shown). A second test was performed using a concentration range of 20-40 nM over 5 days, and western blot results demonstrated that almost 90% of HMGN2 protein was knocked down at 72 hours following the transfection of 40 nM N2₀₁ and N2₀₄ (Figure 5.2). The negative control siRNA in this experiment was used at 40 nM and the protein levels remained unaltered. HMGN2 protein levels were restored to almost wild type levels from day 5 onwards (120 hours). From these results, it is evident that a higher concentration of siRNA is required to knock down HMGN2 compared to HMGN1. This is not surprising as HMGN2 is more abundant than HMGN1 and HMGN3 in P19 EC cells (Chapter 4).

For subsequent functional experiment in P19 EC cells, N1₀₂ and N1₀₃ siRNAs for HMGN1 and N2₀₁ and N2₀₄ for HMGN2 at final concentrations of 20 nM and 40 nM, respectively, were used. The optimal conditions for knocking down HMGN1 and HMGN2 are summarised in table 5.2.

Table 5.1: siRNA library and their designated names for HMGN1 and HMGN2 knockdown.

Target	siRNAs N=target; <i>ox</i> = siRNA variant
HMGN1	N1 ₀₁
	N1 ₀₂
	N1 ₀₃
	N1 ₀₄
HMGN2	N2 ₀₁
	N2 ₀₂
	N2 ₀₃
	N2 ₀₄

Table 5.2: Summary of the knockdown conditions for HMGN1 and HMGN2 in P19 EC cells.

siRNA variant	Optimal concentration (nM)	Knockdown time point (hours)	Knockdown levels (-% compared to wild type)
N1 ₀₂	20	72	90
N1 ₀₃	20	72	90
N2 ₀₁	40	72	85
N2 ₀₄	40	72	90

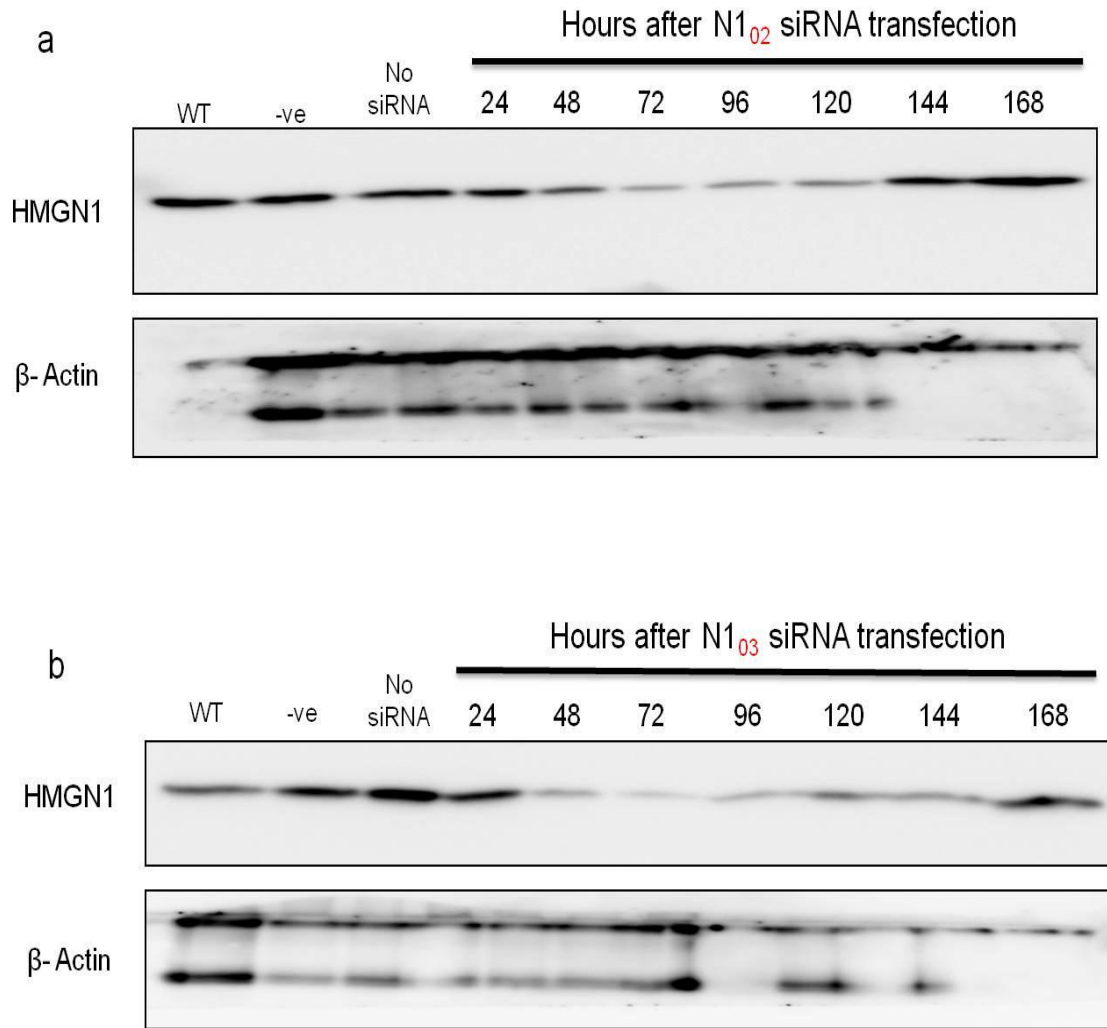


Figure 5.1: siRNA knockdowns reduce levels of HMGN1 protein to approximately 90% after 72 hours post transfection in undifferentiated P19 EC cells.

(a) & (b) Western blot analysis showing time-course expression of HMGN1 after transfection with N1₀₂ and N1₀₃ siRNAs at 20 nM final concentration. siRNAs were removed from media after 48 hours and cells were passaged every two days. WT= wild type, -ve= negative control siRNA, no siRNA= transfection reagent without siRNA. Western blotting images are from separate gels for each panel in (a) & (b).

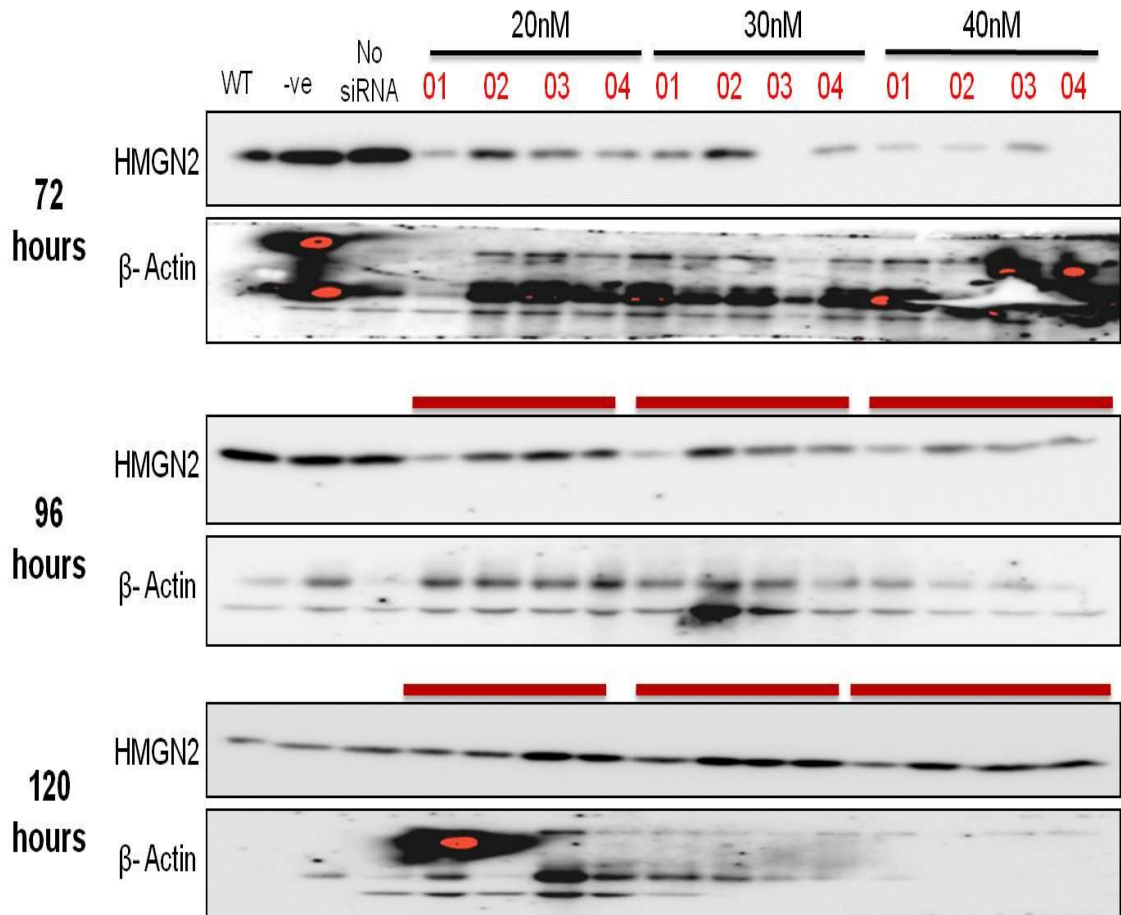


Figure 5.2: HMGN2 knockdown is achieved using siRNA at 40nM final concentration of after 72 hours post-transfection in undifferentiated P19 EC cells.

Time-course and siRNA concentration analysis of HMGN2 knockdown. Western blot analysis from whole cell lysates showing time-course expression of HMGN2 after transfection with increasing amounts of siRNA. siRNAs were removed from media after 48 hours and cells were passaged every two days. WT= wild type, -ve= negative control siRNA, no siRNA= transfection reagent without siRNA. Western blotting images are from separate gels for each panel.

5.4 Validating HMGN1 and HMGN2 knockdowns in P19 EC cells

In order to investigate the role of HMGNs in P19 EC cells, HMGN1 and HMGN2 knockdowns were performed in three independent biological replicates using the conditions summarised in table 5.2. Total RNA and whole cell lysates were collected 72 hours post transfection and qRT-PCR and western blotting was used to confirm HMGN knockdown.

5.4.1 HMGN1 and HMGN2 knockdowns in undifferentiated P19 EC cells

HMGN1 knockdowns were performed using the N1₀₂ and N1₀₃ siRNAs at a final concentration of 20 nM. The negative control siRNA was also transfected at 20 nM to assess for off-target effects of the knockdown system. HMGN1 RNA and protein were dramatically knocked down at 72 hours post transfection using both N1₀₂ and N1₀₃ siRNAs (Figure 5.3). RNA levels dropped by 70% in the knockdown experiments compared to wild type levels (Figure 5.3a & 5.3b). HMGN1 protein levels were knocked down by approximately 90% compared to wild type levels (Figure 5.3c). Both N1₀₂ and N1₀₃ show comparable knockdown efficiency at the RNA and protein levels.

In previous studies, it has not been clear whether reduced expression of one HMGN family member is compensated by the over-expression of another. Furusawa et al showed that compensation of the HMGN1 knockout by HMGN2 does not occur at the protein level, but found higher enrichment of HMGN2 at the Sox9 gene when HMGN1 is depleted (Furusawa et al., 2006). This raises the question of whether knocking down HMGN1 leads to a compensatory increase in HMGN2 expression. However, the data in figure 5.3c show that the expression of HMGN2 is unchanged in P19 EC cells where HMGN1 is knocked down.

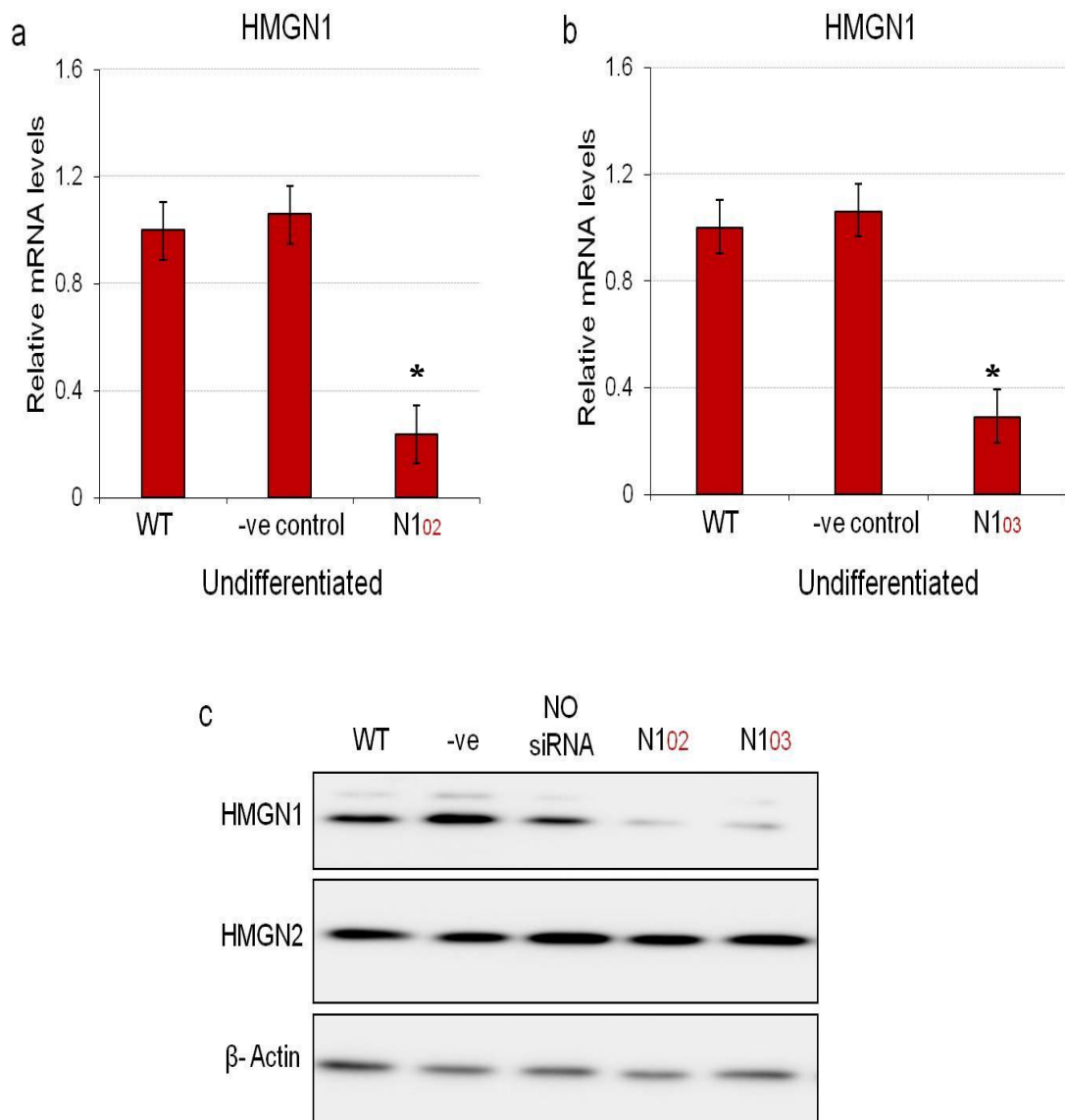


Figure 5.3 HMGN1 protein levels are knockdown by more than 90% in undifferentiated P19 EC cells.

Undifferentiated P19 EC cells were transfected with N1₀₂ and N1₀₃ individually. After 72 hours, total RNA and whole cell lysates were harvested for qRT-PCR analysis and western blotting from independent sample. (a) & (b) show RNA levels of HMGN1 normalised to β -Actin and shown relative to wild type cells (WT). Error bars reflect the standard deviation from RT-PCR triplicates from one biological replicate. * $P < 0.001$ was calculated from Ct average of 2 biological replicates compared to WT. (c) Western blots showing expression of HMGN1 and HMGN2 with β -Actin as the loading control. HMGN2 protein expression is not altered upon HMGN1 knockdown. The western blotting images correspond to the similar biological replicate in (a) & (b). The western blotting images of HMGN1 and β -Actin are from the same gel. WT= wild type, -ve= negative control siRNA, no siRNA= transfection reagent without siRNA.

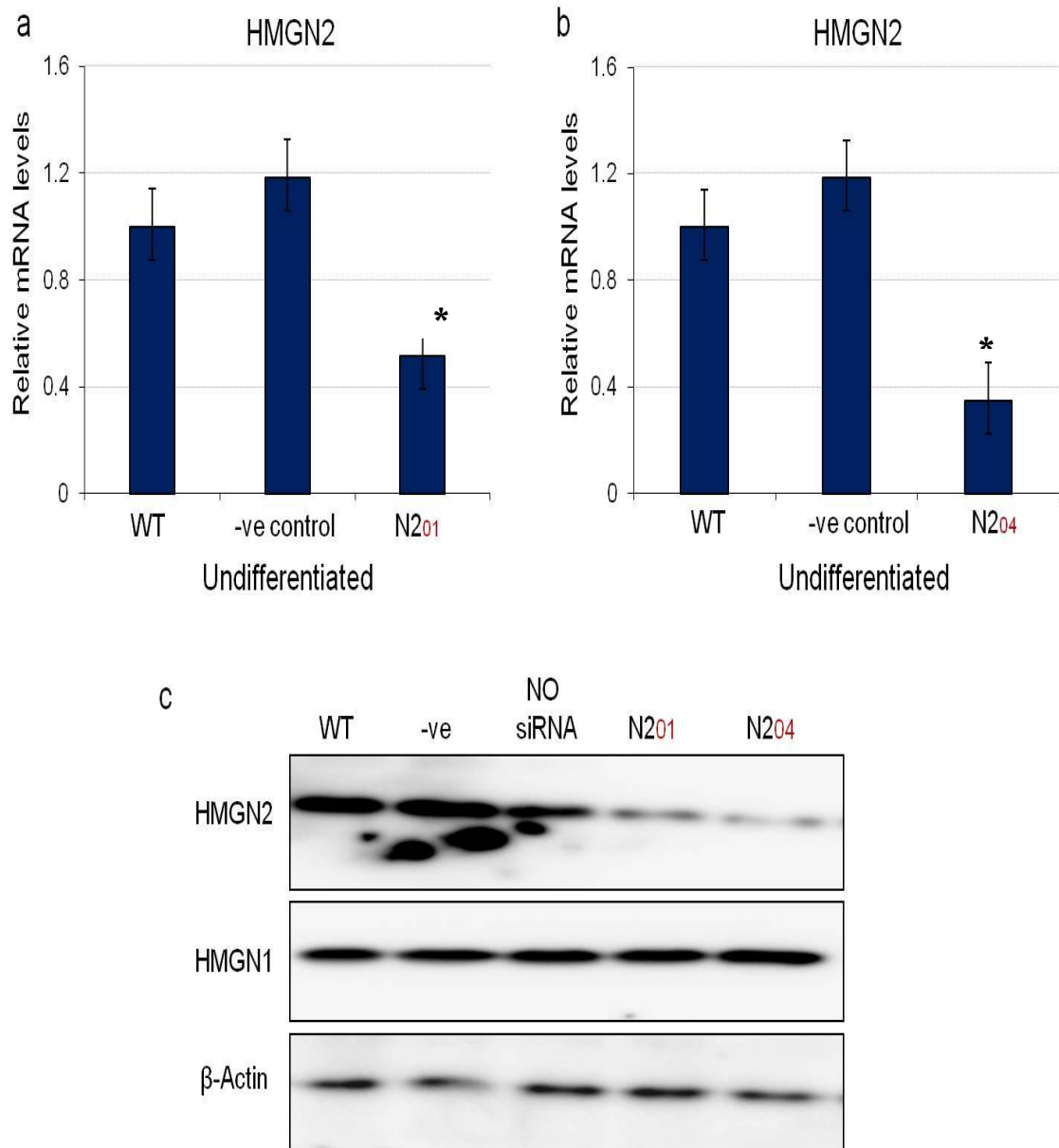


Figure 5.4 HMGN2 protein levels are knockdown by more than 90% in undifferentiated P19 EC cells.

Undifferentiated P19 EC cells were transfected with N2₀₁ and N2₀₄ individually. After 72 hours, total RNA and whole cell lysates were harvested for qRT-PCR analysis and western blotting from independent sample. (a) & (b) show RNA levels of HMGN2 normalised to β -Actin and shown relative to wild type cells (WT). Error bars reflect the standard deviation from RT-PCR triplicates from one biological replicate. * $P < 0.001$ was calculated from Ct average of 2 biological replicates compared to WT. (c) Western blots showing expression of HMGN2 and HMGN1 expression with β -Actin as the loading control. HMGN1 protein expression is not altered upon HMGN2 knockdown. The western blotting images correspond to the similar biological replicate in (a) & (b). The western blotting images of HMGN2 and β -Actin are from the same gel. WT= wild type, -ve= negative control siRNA, no siRNA= transfection reagent without siRNA.

HMGN2 knockdowns were performed using N2₀₁ and N2₀₄ siRNAs at a final concentration of 40 nM. The negative control siRNA was also transfected at 40 nM final concentration. Total RNA and whole cell lysates were harvested at 72 hours after transfection and analysed using qRT-PCR and western blots. RNA levels show HMGN2 knockdown of up to 70% and 65% in N2₀₁ and N2₀₄ siRNA transfections, respectively (Figure 5.4a and 5.4b). HMGN2 protein levels show more than 90% depletion in knockdown experiments compared to wild type. HMGN1 protein levels remain unaltered upon HMGN2 knockdown, again ruling out any compensatory effects at the protein level (Figure 5.4c middle panel).

5.4.2 HMGN1 and HMGN2 double knockdown in undifferentiated P19 EC cells

After establishing robust knockdown systems in undifferentiated P19 EC cells using specific siRNAs towards either HMGN1 or HMGN2, it was considered whether both the siRNAs could be used simultaneously to generate a double HMGN1 and HMGN2 (HMGN1/2) knockdown. There is obvious advantage of having double knockdown as it could be used to address the effects of the loss of the predominant HMGN family members in P19 EC cells. To my knowledge, there have not been reports of double HMGN1 and HMGN2 knockdown in a differentiation model system.

To produce double HMGN1/2 knockdown, N1₀₂ and N2₀₁ siRNAs were selected, and transfected at 20 nM and 40 nM, respectively. The double transfection produced dramatic knockdown for both HMGN1 and HMGN2 at the RNA and protein levels after 72 hours (Figure 5.5). RNA levels of HMGN1 and HMGN2 were reduced by approximately 90% compared to wild type (Figure 5.5a and 5.5b), and HMGN1 and HMGN2 proteins were undetectable (Figure 5.5c). The concentration of negative control was performed at 40 nM. The morphology of the knockdown cells was similar to that of the untransfected cells, although the cells did appear to proliferate more slowly.

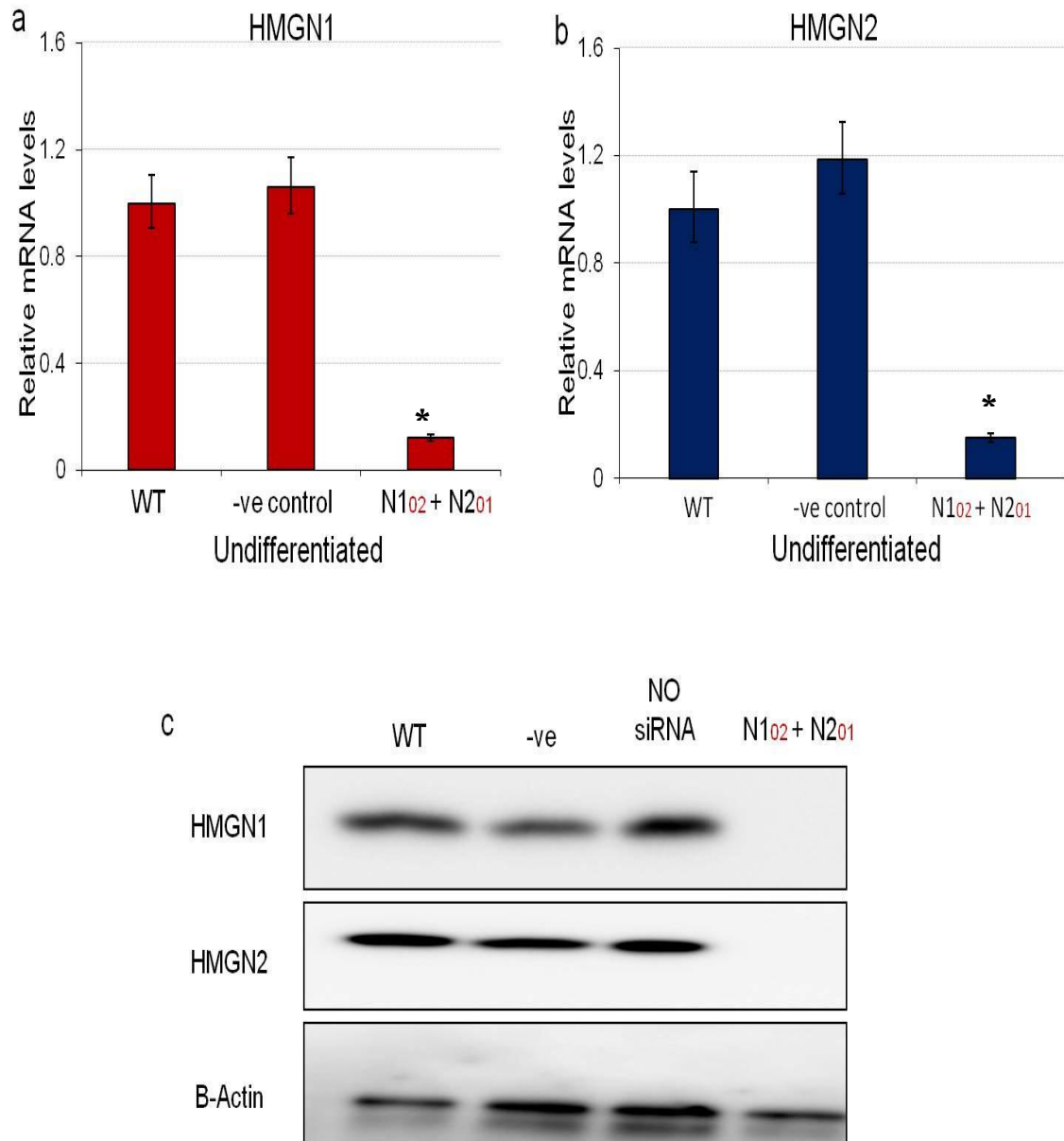


Figure 5.5: HMGN1 and HMGN2 proteins are lost following double knockdown in undifferentiated P19 EC cells

A combination of siRNAs targeting HMGN1 (20 nM) and HMGN2 (40 nM) were transfected simultaneously. After 72 hours, total RNA and whole cell lysates are harvested for qRT-PCR analysis and western blotting from independent sample (a) & (b) HMGN1 and HMGN2 RNA levels normalised to β -Actin and shown relative to wild type cells. Error bars reflect the standard deviation from RT-PCR triplicates from one biological replicate. * $P < 0.001$ was calculated from Ct average of 2 biological replicates compared to WT. (c) Western Blotting demonstrating the expression of HMGN1 (top panel) and HMGN2 (middle panel) with β -Actin as the loading control. The western blotting images correspond to the similar biological replicate in (a) & (b). The western blotting images of HMGN1 and β -Actin are from the same gel. WT = wild type, -ve = negative control siRNA.

5.5 HMGN knockdowns in undifferentiated cells down-regulate the expression of key pluripotency genes

The expression of several genes of interest (GOIs) was analysed in undifferentiated HMGN1/2 knockdown cells in order to investigate whether HMGN1/2 regulate genes that are important for P19 EC identity and pluripotency. The genes analysed were the pluripotency regulators Oct4, Nanog and Sox2, as well as the glycine transporters GlyT1 and Glyt2, and the transcriptional regulator REST. As shown in chapter 3, Oct4, Nanog and Sox2 are highly expressed in undifferentiated P19 EC cells. Their expression is lost upon RA-induced neural induction, and they remain silenced during neural differentiation. In contrast, all neural related genes tested were not expressed in undifferentiated cells, except for a basal level of nestin expression.

To study the differential expression of GOIs, total RNA was isolated from wild type cells and those transfected with negative control siRNA, two siRNAs each for HMGN1 and HMGN2 and double HMGN1/2. Gene expression was assayed by qRT-PCR, normalised to β -actin or Gapdh, and expressed relative to levels in wild type cells. These are the same samples in which HMGN1/2 expression was analysed in figures 5.3, 5.4 and 5.5.

Knockdown of HMGN1, HMGN2 or HMGN1/2 in undifferentiated cells down-regulated the expression of Oct4, Nanog and Sox2 by more than 80% in all 5 knockdown experiments (Figure 5.7). Two different siRNAs for each target act as positive controls to validate the loss of function experiments. The results obtained here are not due to a general loss in mRNA transcription as the total RNA quality from knockdown cells was similar to wild type cells. There were insignificant changes in the Ct values of the GAPDH housekeeping gene, and normalising the GOI to two different housekeeping genes (Gapdh and β -Actin) produces similar results. These data sets are comparable between three independent biological replicates.

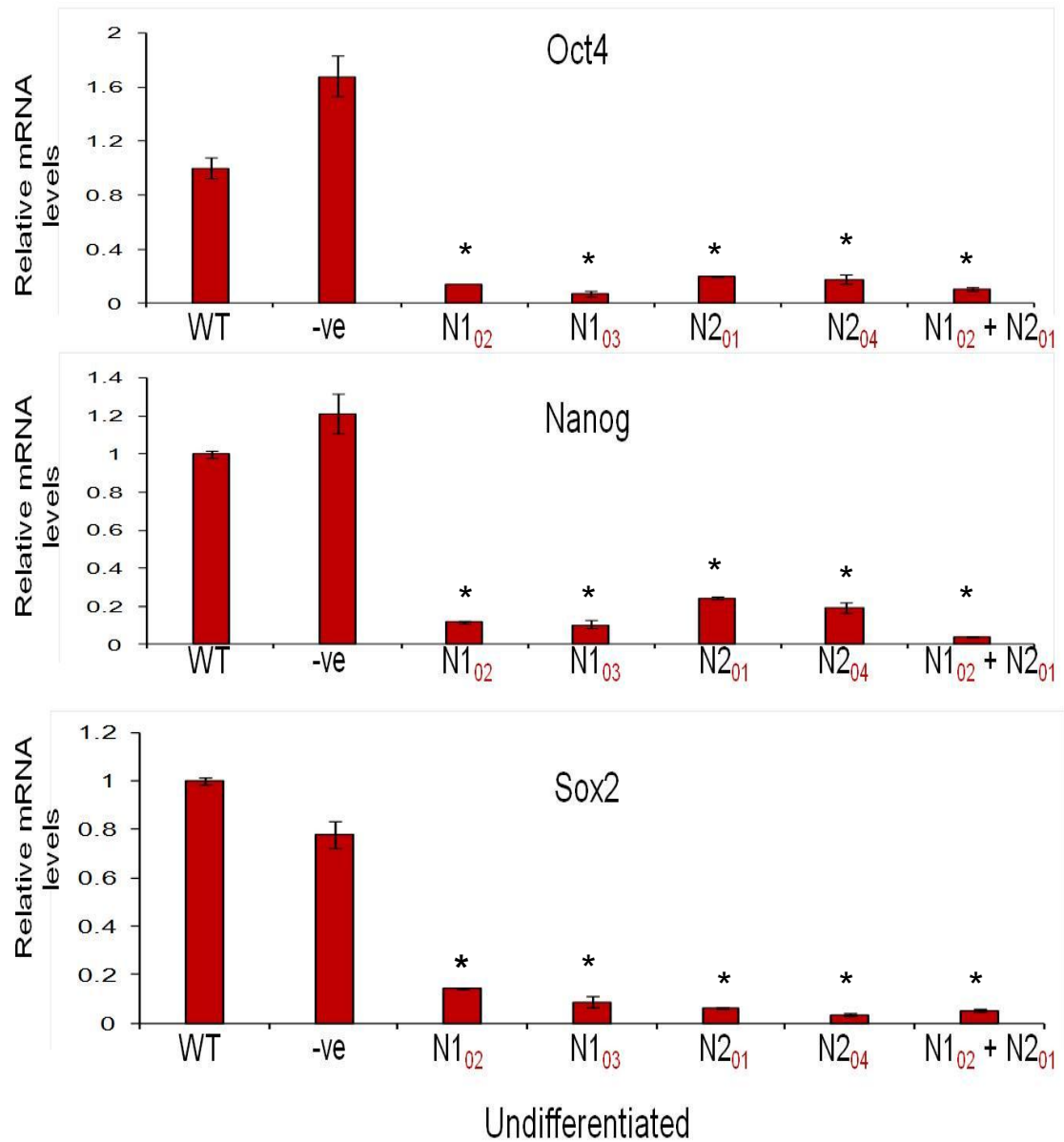


Figure 5.7: HMGN knockdowns in undifferentiated P19 EC cells dramatically down-regulated pluripotency genes Oct4, Nanog and Sox2.

HMGN1, HMGN2 and HMGN1/2 were knocked down using specific siRNAs in undifferentiated cells. Ct values from knockdown cells were normalised to β -actin and shown as relative to wild type levels. Error bars reflect the standard deviation from RT-PCR triplicates from one biological replicate. * $P < 0.001$ was calculated from Ct average of 2 biological replicates compared to WT. WT= wild type, -ve= negative control siRNA.

5.6 HMGN2 knockdown in undifferentiated cells down-regulates GlyT1a gene but does not affect the expression of GlyT2

Previous studies from our lab have shown that HMGN3 binds to and regulates the expression of the glycine transporter GlyT1a in Hepa cells (West et al., 2004). Consequently, we were interested to investigate whether GlyT1a expression is altered following HMGN1/2 knockdown in P19 EC cells.

GlyT1a belongs to the Na⁺/Cl⁻ glycine transporter family that plays a role in the re-uptake of glycine molecules from the synaptic junctions (Zafra et al., 1997; Jursky and Nelson, 1996; Adams et al., 1995; Johnson and Asher, 1987). GlyT1 is predominantly expressed in neurons and glia of the CNS, with additional expression in liver, lung and stomach, while GlyT2 expression is neuron specific (Aragon et al., 2003; Adams et al., 1995; Kim et al., 1994; Liu et al., 1993; Smith et al., 1992).

GlyT1a gene is expressed at basal levels in undifferentiated P19 EC cells and is induced to moderate levels upon neural induction (Figure 5.8). GlyT1b expression is very low in neural differentiated cells and not present in undifferentiated cells (data not shown). GlyT2 is detected at very low levels in undifferentiated cells and is highly expressed upon neural induction (Figure 5.8).

Knockdown of HMGN1 and/or HMGN2 in undifferentiated cells resulted in variable levels of GlyT1a down-regulation (Figure 5.9). Only one of the HMGN1 siRNAs significantly affected GlyT1a expression (N1₀₃), whereas both HMGN2 siRNAs reduced GlyT1a expression by over 50%. The effect of the double HMGN1/HMGN2 knockdown was similar to that of knocking down HMGN2 on its own. Data from two other biological replicates gave similar results. This data suggests that HMGN2 is a positive regulator of GlyT1a expression in undifferentiated P19 EC cells. In contrary, GlyT2 gene expression remains unchanged in the knockdown cells when compared to wild type cells (Figure 5.9).

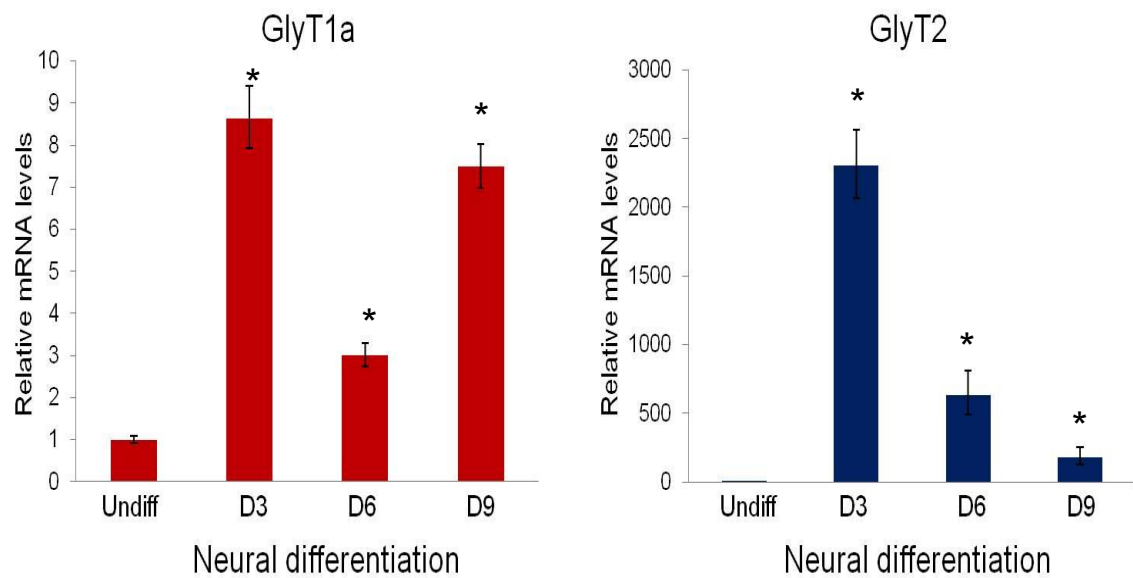


Figure 5.8: GlyT1a and GlyT2 expression during RA-induced P19 EC cell differentiation.

RNA levels are normalised using α -tubulin and shown relative to undifferentiated cells. Error bars reflect the standard deviation from RT-PCR triplicates from one biological replicate. * $P < 0.001$ was calculated from Ct average of 2 biological replicates compared to undifferentiated.

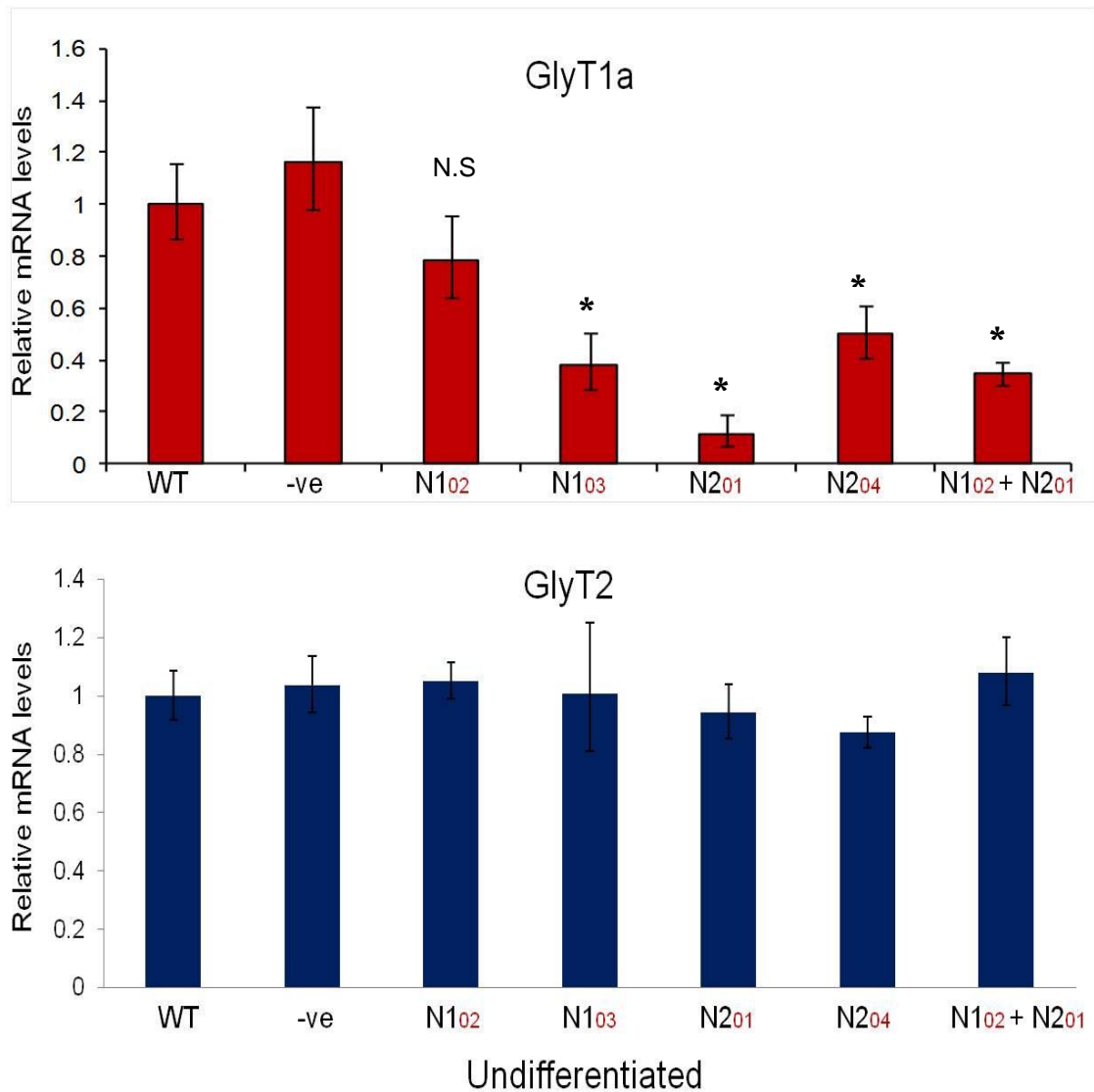


Figure 5.9: GlyT1a is down-regulated whereas GlyT2 is unchanged upon HMGN knockdowns in undifferentiated P19 EC cells.

HMGN1, HMGN2 and HMGN1/2 were knockdown using specific siRNAs in undifferentiated cells. Ct values from knockdown cells were normalised to β -actin and shown relative to wild type levels. Error bars reflect the standard deviation from RT-PCR triplicates from one biological replicate. * $P < 0.001$ was calculated from Ct average of 2 biological replicates compared to WT. N.S, $p > 0.001$, compared to undifferentiated. P values for GlyT2 RNA analyses are above 0.001, $P > 0.001$. WT= wild type, -ve= negative control siRNA.

5.7 Expression of Rest and various neural lineage-specific genes remained unchanged following HMGN knockdowns in undifferentiated cells

Rest, (RE1 silencing transcription factor, also known as NRSF), has been shown to act as a factor that negatively regulates neural lineage-specific gene expression in undifferentiated ES cells (Singh et al., 2008; Ballas et al., 2005). Rest is highly expressed in undifferentiated cells and is dramatically down-regulated upon neural induction (Loh et al., 2006; Ballas et al.; 2005). Similarly, in P19 EC cells, Rest RNA is highly expressed in undifferentiated cells and is down-regulated upon RA-induced neural differentiation (data not shown).

HMGN1, HMGN2 and HMGN1/2 knockdowns did not significantly alter the expression of Rest in undifferentiated P19 EC cells (Figure 5.10). The expression levels of several neural lineage specific genes were also studied and found to be unaltered following HMGN knockdown: Nestin, Zfp521, Map2, NmdaR2, Nse, Nf-160 kDa and Gfap. These genes are expressed at basal (nestin and zfp521) or very low levels in undifferentiated cells, and so it would be difficult to detect any further down-regulation following HMGN1/2 knockdown.

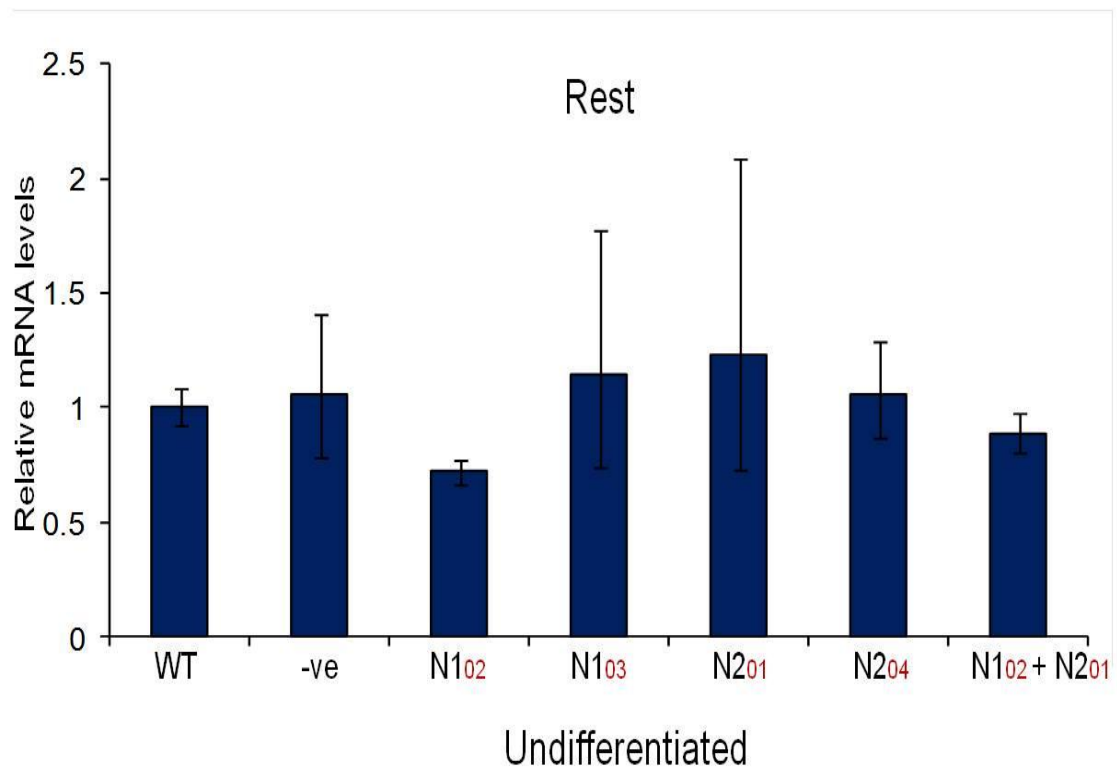


Figure 5.10: Rest expression in undifferentiated P19 EC cells remained unchanged after HMGN knockdowns.

HMGN1, HMGN2 and HMGN1/2 were knockdown using specific siRNAs in undifferentiated cells. Ct values from knockdown cells were normalised to β -actin and shown relative to wild type levels. Error bars reflect the standard deviation from RT-PCR triplicates from one biological replicate. P values for Rest RNA analyses compared to WT are above 0.001, $P > 0.001$. WT= wild type, -ve= negative control siRNA.

5.8 HMGN1/2 depletion in undifferentiated cells does not have a long term effect on neural commitment.

The data in the previous section shows that HMGN knockdowns in undifferentiated P19 EC cells leads to a down-regulation of several pluripotency-related genes. However, HMGN1, HMGN2 and HMGN1/2 depleted cells did not show premature neural lineage commitment, as indicated by the unchanged expression of neural genes. Because of the dramatic loss in pluripotency gene expression, the question arises as to whether HMGN1/2-depleted cells have the same ability as wild type cells to be programmed into neural commitment using RA, and if so, do the cells produce neuronal cell types?

To address these questions, HMGN1/2 depleted cells were treated with RA and then allowed to form EBs. The illustration of the experimental design is shown in Figure 5.11a. Briefly, siRNA-transfected cells were treated with RA after 48 hours and allowed to form EBs using the same neuronal differentiation protocol as described in chapter 3. Total RNA was harvested from EBs and day 3 neural differentiation for qRT-PCR analysis.

Neuronal marker gene expression (Nestin, Map2, NF-160 kDa, Nse) in EBs and day 3 neural cells was not altered in cells derived from HMGN1/2-depleted P19 cells. The expression of Nestin following RA induction in HMGN1/2 depleted cells and control cells is presented as example in Figure 5.11b. However, it is important to note that the transient nature of the siRNA transfection means that the HMGN1/2 expression had returned back to wild type levels by the end of EB formation (see figures 5.1 and 5.2). Thus, this experiment shows that transient knockdown of HMGN1/2 during the initial stages of RA treatment does not have a long term effect on the neural commitment and differentiation of P19 EC cells.

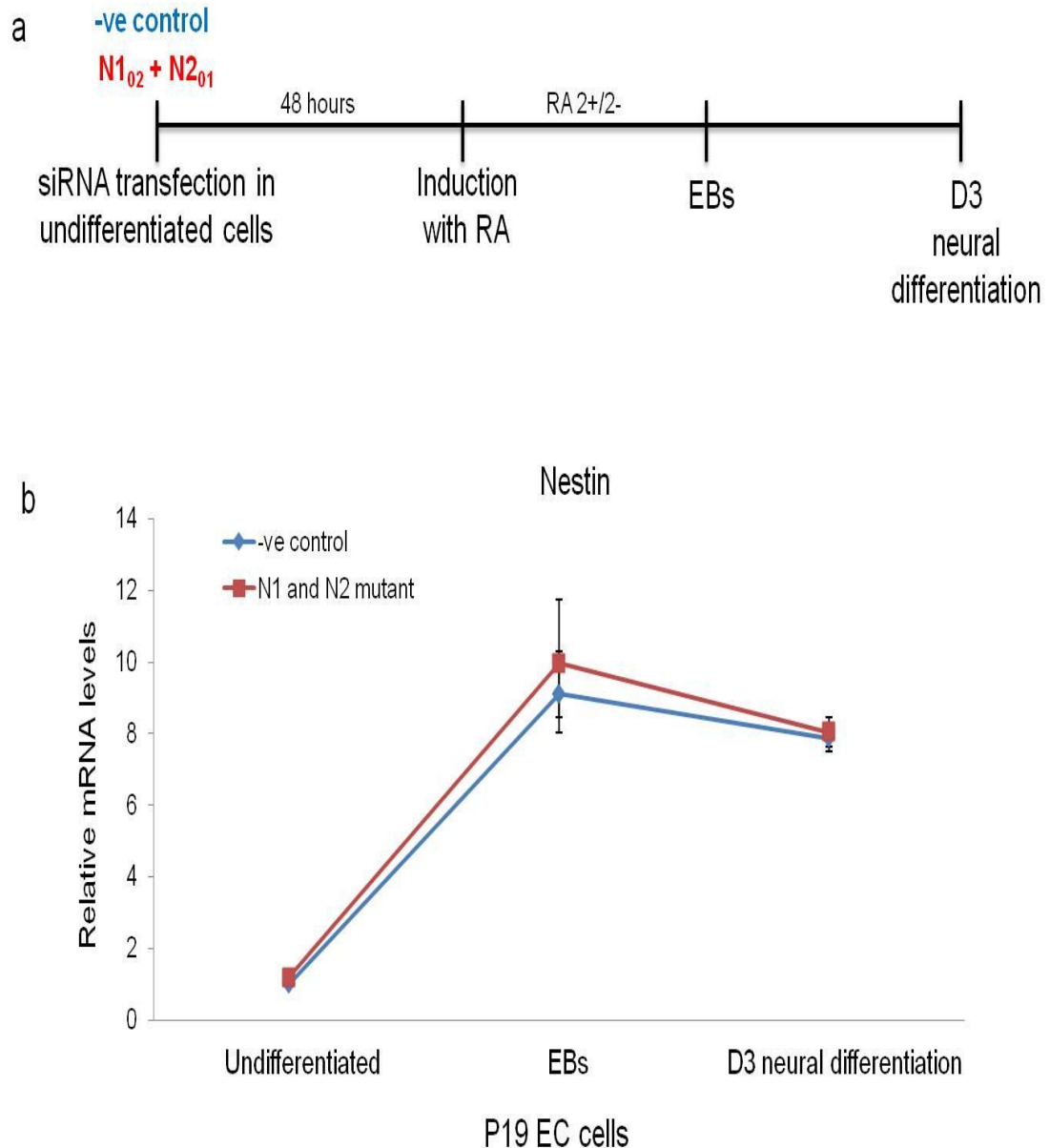


Figure 5.11: HMGN1/2 depletion in undifferentiated cells does not have a long term effect on neural commitment.

(a) Schematic diagram showing the experimental design used to induce HMGN1/2 depleted cells to neural commitment. (b) Expression of Nestin in EBs and day 3 neural cells was similar in HMGN1/2 depleted cells compared to the control. Ct values from knockdown cells and -ve siRNA control transfected cells were normalised to β -actin and shown relative to undifferentiated cells (independent sample). -ve= negative control siRNA. Error bars are representative of three technical replicates.

5.9 HMGN1 and HMGN2 knockdown during neural differentiation of P19 EC cells

The second main objective of this chapter is to investigate the role of HMGN1 and HMGN2 during neural differentiation. The approach taken was to generate knockdowns of HMGN1, HMGN2 and HMGN1/2 at an early stage of neural differentiation, and then to assay the expression of neural markers such Nestin, Map2 and NF-160 kDA at day 3.

In order to maximise the efficiency of HMGN1 and HMGN2 knockdown in the early neuronal differentiation phase, two rounds of siRNA transfection were performed. The protocol for knocking down HMGN proteins is discussed in chapter 2. Undifferentiated P19 EC cells 72 hours prior to RA programming were transfected with siRNAs specific to HMGN1 and HMGN2 (similar to section 5.4). HMGN1, HMGN2 and double HMGN1/2 knockdown cells (undifferentiated), were induced with RA and allowed to form EBs using the system explained in chapter 3. Second siRNA transfections were performed on day -3 (EB) and also precisely 12 hours after seeding, using the same siRNA concentrations described above. Cells transfected earlier than 12 hours after plating did not survive. At day 2 (post seeding), media was carefully replaced without damaging the cells. At this point, morphology of the cells was similar to wild type cells. Total RNA and whole cell lysates were harvested at day 0 and day 3 for qRT-PCR analysis and western blotting.

Four different transfection experiments were conducted using N1₀₂ and N2₀₁ individually, N1₀₂ and N2₀₁ in combination and a negative control siRNA. No significant knockdown of HMGN levels was observed at day 0, suggesting that siRNA transfection of EBs is inefficient (data not shown). However, single and double HMGN knockdowns were observed at day 3 (Figure 5.12). HMGN1 and HMGN2 RNA levels were knocked down by more than 75% in cells transfected with N1₀₂ and N2₀₁ siRNAs respectively (Figure 5.12a, top panel). In the double knockdown experiments, both HMGN1 and HMGN2 RNA levels were knocked down by more than 65% compared to wild type cells (Figure 5.12a, bottom panel).

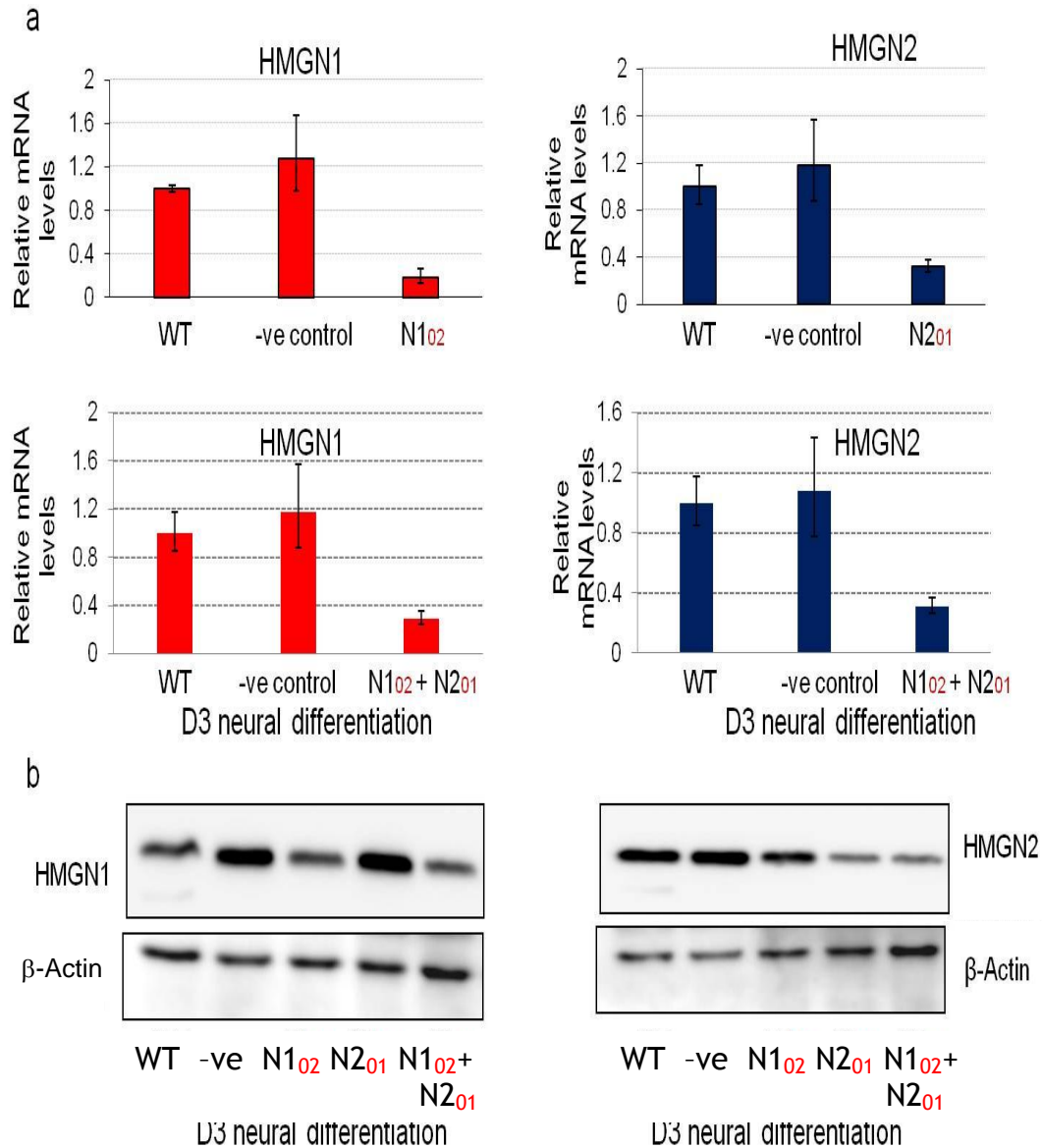


Figure 5.12: HMGN1, HMGN2 and HMGN1/2 knockdowns in day 3 neural differentiation

Day 0 cells, 12 hours after plating out, were transfected with siRNAs N1_{o2}, N2_{o1} and N1_{o2} & N2_{o1} in combination to knockdown the proteins. (a) RNA levels of HMGN1 and HMGN2 on day 3, normalised to wild type cells (WT). Error bars reflect the standard deviation from RT-PCR triplicates from one biological replicate. (b) Western blots showing HMGN1 and HMGN2 protein expression on day 3 with β -Actin as the loading control. The western blotting images correspond to the similar biological replicate in (a). The western blotting images of (HMGN1 & β -Actin, HMGN2 & β -Actin) are from the same gel. WT= wild type, -ve= negative control siRNA.

Although the level of HMGN1 mRNA was reduced by more than 75% in N1₀₂ transfected cells, the level of HMGN1 protein was only reduced by 30% (Figure 5.12b). The level of HMGN2 protein knockdown was greater, with a reduction of more than 70% protein in N2₀₁-transfected cells. Cells transfected with both N1₀₂ and N2₀₁ siRNAs had 50% and 70% reduction in HMGN1 and HMGN2 proteins levels, respectively. HMGN1 protein levels in N2₀₁ transfections were higher compared to wild type levels but similar to the negative control. HMGN2 protein expression remains unchanged in cells transfected with N1₀₂ siRNA. HMGN protein levels in transfected cells recovered to wild type levels by day 6 (data not shown). The RNA data presented here are based on one biological replicate as other attempts at knocking-down HMGN1 and HMGN2 using siRNAs had failed. Statistical analysis could not be carried out due to this reason. However, the data from Ct values for D3 knockdown compared wild type demonstrated changes in the expression of some target genes.

5.10 HMGN2 knockdown during neural differentiation down-regulates Rest expression

HMGN1 and HMGN2 knockdowns in undifferentiated cells do not affect the expression of Rest RNA levels, as shown earlier. As mentioned above, Rest expression is highest in undifferentiated cells and is down-regulated upon neural differentiation. When HMGN2 protein is knocked down by 70% in day 3 neural differentiation, Rest expression is significantly reduced by more than 70% compared to wild type cells (Figure 5.13). The expression of rest is reduced by 40% in cells knocked down for both HMGN1 and HMGN2.

These results suggest that HMGN2 knockdown specifically affected Rest expression in day 3 neural differentiation. A similar pattern of reduced Rest expression is not observed in N1₀₂ transfected cells. This could be because HMGN1 is not a positive regulator of Rest in day 3 cells, or it could be that the weak knockdown of HMGN1 makes it harder to detect changes in target gene expression. These data suggest a possible role for HMGN2 in maintaining Rest expression during neural differentiation.

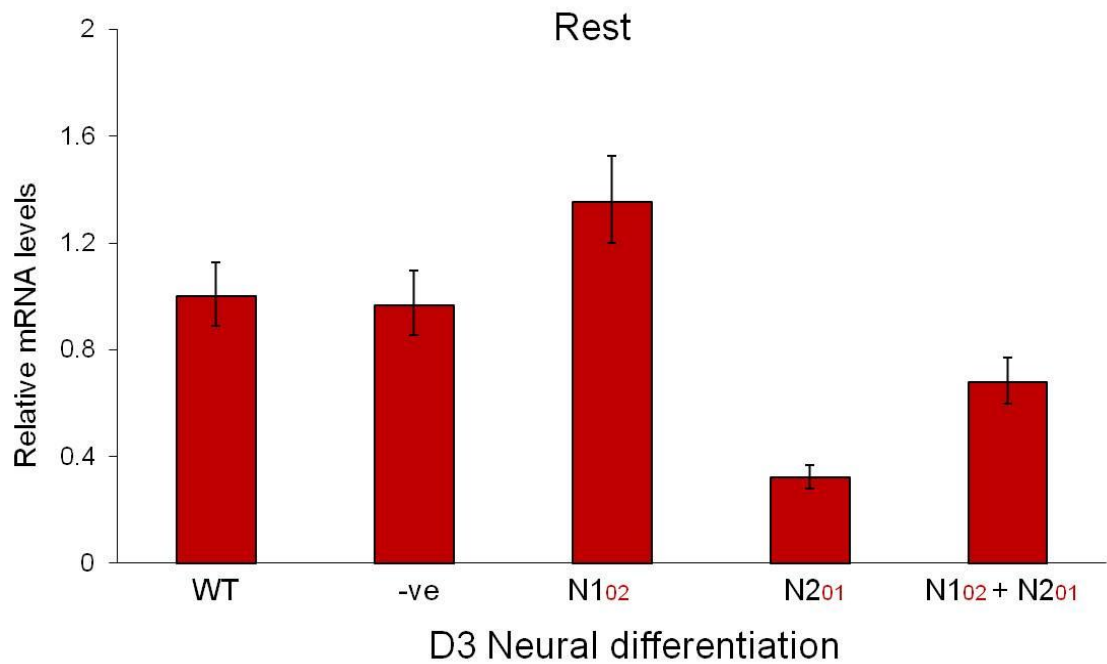


Figure 5.13: HMGN2 knockdown in day 3 neural differentiation cells down-regulates Rest expression.

HMGN1, HMGN2 and HMGN1/2 were knocked down using specific siRNAs, and expression of Rest assayed in day 3 neural cells by qRT=PCR. Ct values from knockdown cells were normalised to β -actin and shown relative to wild type levels. Error bars reflect the standard deviation from RT-PCR triplicates from one biological replicate. WT= wild type, -ve= negative control siRNA.

5.11 HMGN knockdown during neural differentiation affects the expression of early neural induced genes

Nestin is a well known neural stem cell marker (Wiese, 2005). It is expressed at basal levels in undifferentiated P19 EC cells and is induced by about 10 fold upon neural induction (Chapter 3). When HMGN1 is knocked down during neural differentiation, Nestin expression at day 3 is up-regulated by about 80% (Figure 5.14). The increase in nestin expression is less in HMGN2 knockdown cells, and in the double HMGN1/2 knockdown cells it is not significantly different to the control cells. The fact that the double knockdown does not replicate the data for the HMGN1 single knockdown is concerning, and indicates that this experiment needs to be repeated with additional siRNAs before drawing any conclusions.

The role of Zfp521 in ES cell neural differentiation was first shown by Kamiya et al, demonstrating that Zfp521 directly activates early neural genes through the association with p300 (Kamiya et al., 2011). The expression of Zfp521 is not detected in undifferentiated ES cells and is up-regulated by approximately 60 fold upon neural induction (Kamiya et al., 2011). In the P19 system, Zfp521 expression was low in undifferentiated cell and induced to high levels upon RA-induced neural differentiation (data not shown). The highest expression was found in day 3 neural differentiation cells. Interestingly, the expression of Zfp521 is down-regulated upon HMGN1 and/or HMGN2 knockdown (Figure 5.14). The greatest reduction was in the double HMGN1/2 knockdown cells, where Zfp521 expression is down-regulated by 60%. The results shown here suggest a possible role for HMGN proteins in regulating Zfp521 expression.

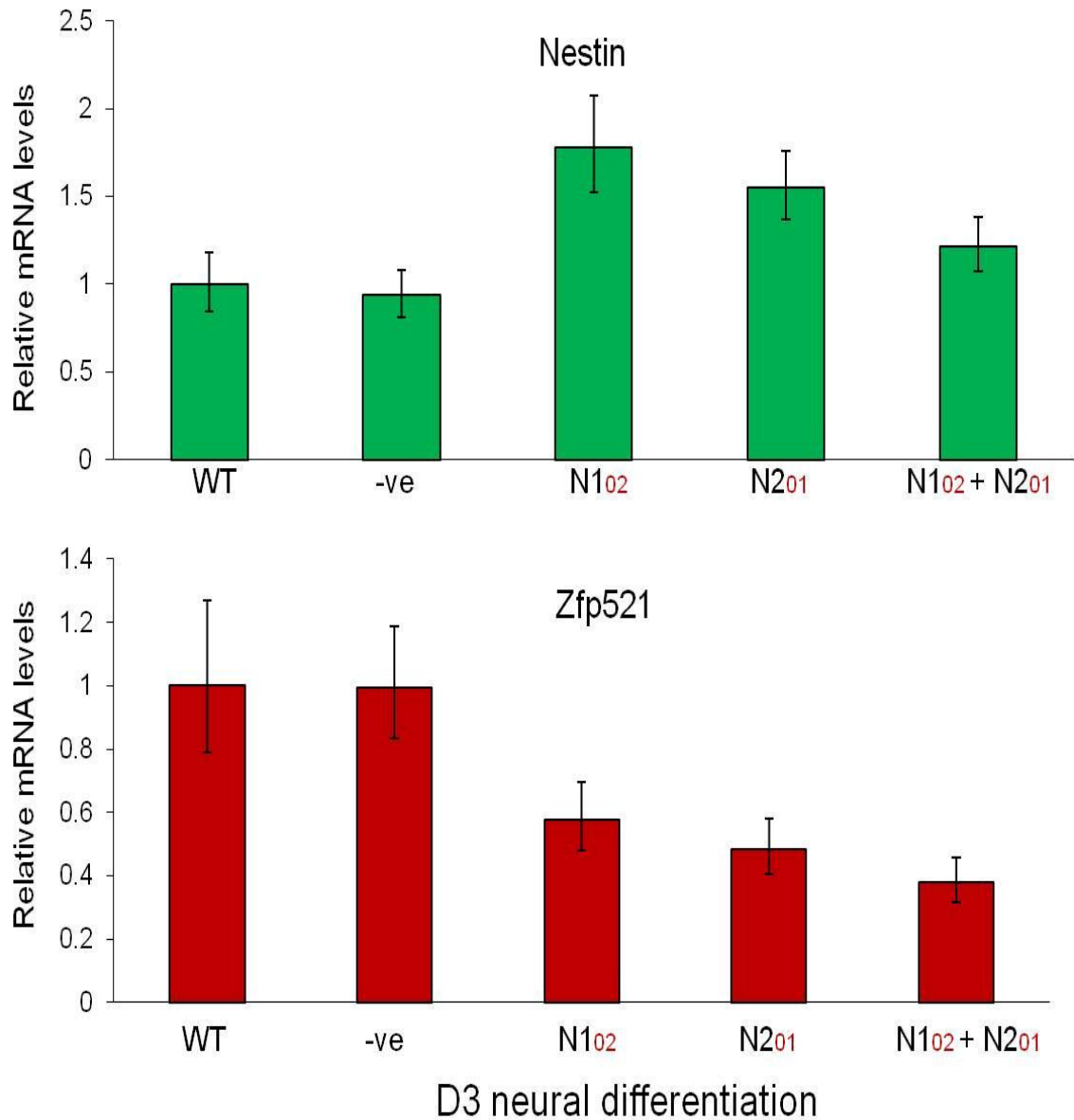


Figure 5.14: HMGN knockdowns in neural differentiating cells affect the expression of Nestin and Zfp521.

HMGN1, HMGN2 and HMGN1/2 were knocked down using specific siRNAs, and Nestin and ZFP521 expression assayed on day 3 of neural differentiation. Ct values from knockdown cells were normalised to β -actin and shown relative to wild type levels. Error bars reflect the standard deviation from RT-PCR triplicates from one biological replicate. WT= wild type, -ve= negative control siRNA.

5.12 HMGN knockdowns during neural differentiation affect the expression of neural specific genes

The genes Map2, NF-160 kDa, Nse and Nmda-receptor subunit 2 (Nmdar2) are not expressed in undifferentiated P19 EC cells, but are induced upon neural differentiation (Chapter 3). Map2 and NF-160 are expressed most highly on day 3 of neural differentiation, and whereas Nse and Nmdar2 expression is highest from day 6 onwards. The expression of these genes following knockdown of HMGN proteins during neural differentiation was assayed on day 3.

Map2 expression was not significantly altered in any of the knockdown cells. NF-160 expression was up-regulated in the HMGN1 single knockdown and the double HMGN1/2 knockdown cells, but was unaffected by the HMGN2 single knockdown (Figure 5.15). This suggests that HMGN1 may have a repressive effect of NF-160 expression during neural differentiation.

The expression of Nse and Nmda-receptor subunit 2 had opposite patterns in HMGN knockdown cells (Figure 5.16). The expression of Nse was down-regulated by approximately 30% in HMGN1, HMGN2 and HMGN1/2 knockdown cells, although the reduction in HMGN1 knockdown cells was not significant due to large error bars. In contrast, Nmdar2 expression was up-regulated by 3-4 fold in HMGN2 and HMGN1/2 double knockdown cells. The effect of the HMGN1 knockdown was much weaker, suggesting that HMGN2 may repress Nmdar2 expression during neural differentiation.

GlyT2 expression is highest on day 3 of neural differentiation (Figure 5.8). HMGN2 knockdown during neural differentiation reduced GlyT2 expression by 75%, whereas the HMGN1 knockdown and the double HMGN1/2 knockdown reduced GlyT2 expression by about 40% compared to wild type cells (Figure 5.17). In contrast, there was a trend towards increased expression of GlyT1a in the HMGN1 and HMGN2 single knockdowns, although the large error bars rendered these changes insignificant.

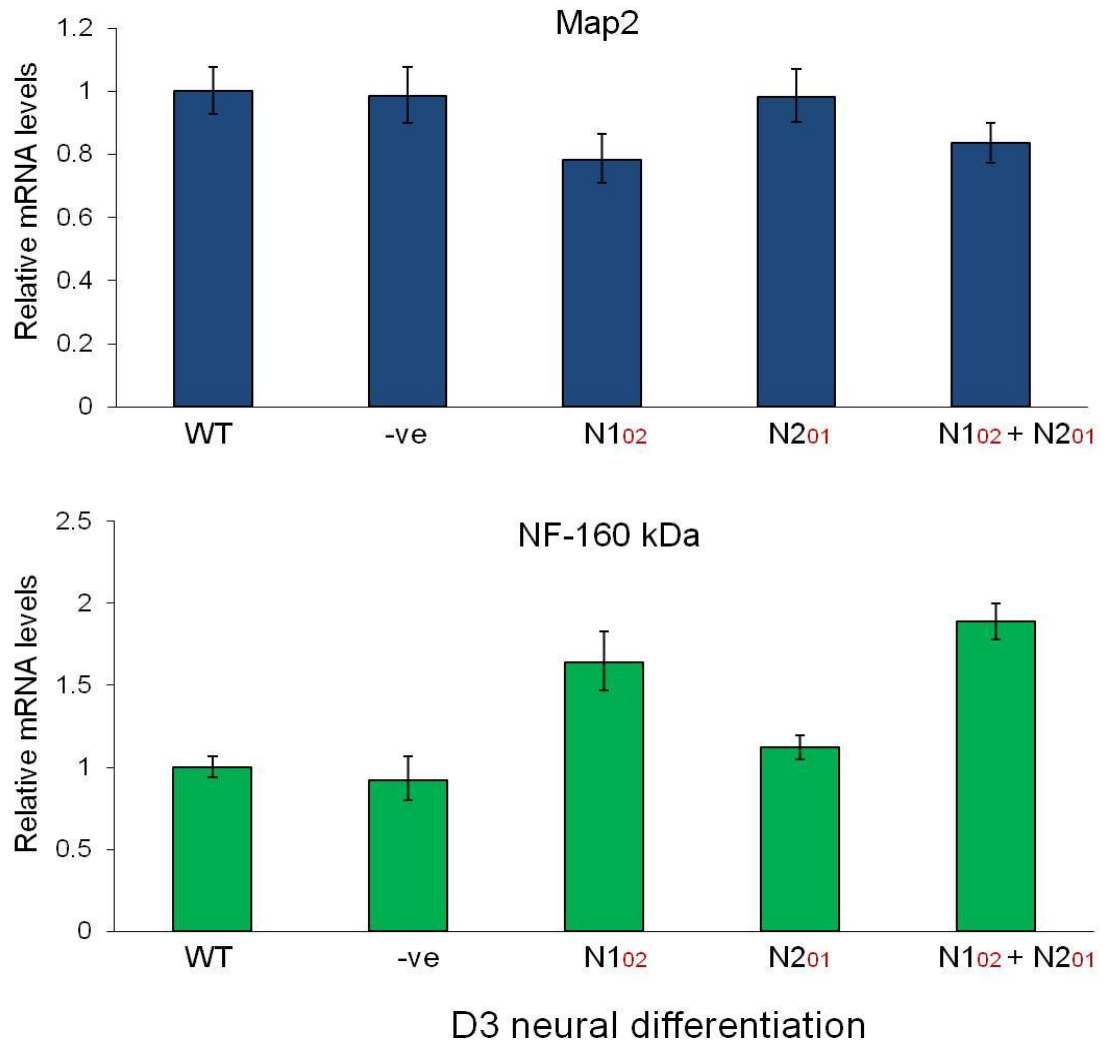


Figure 5.15: Map2 expression remained unchanged but NF-160 kDa is up-regulated following HMGN knockdowns.

HMGN1, HMGN2 and HMGN1/2 were knocked down using specific siRNAs, and MAP2 and NF-160 kDa expression assayed on day 3 of neural differentiation. Ct values from knockdown cells were normalised to β -actin and shown relative to wild type levels. Error bars reflect the standard deviation from RT-PCR triplicates from one biological replicate. WT= wild type, -ve= negative control siRNA.

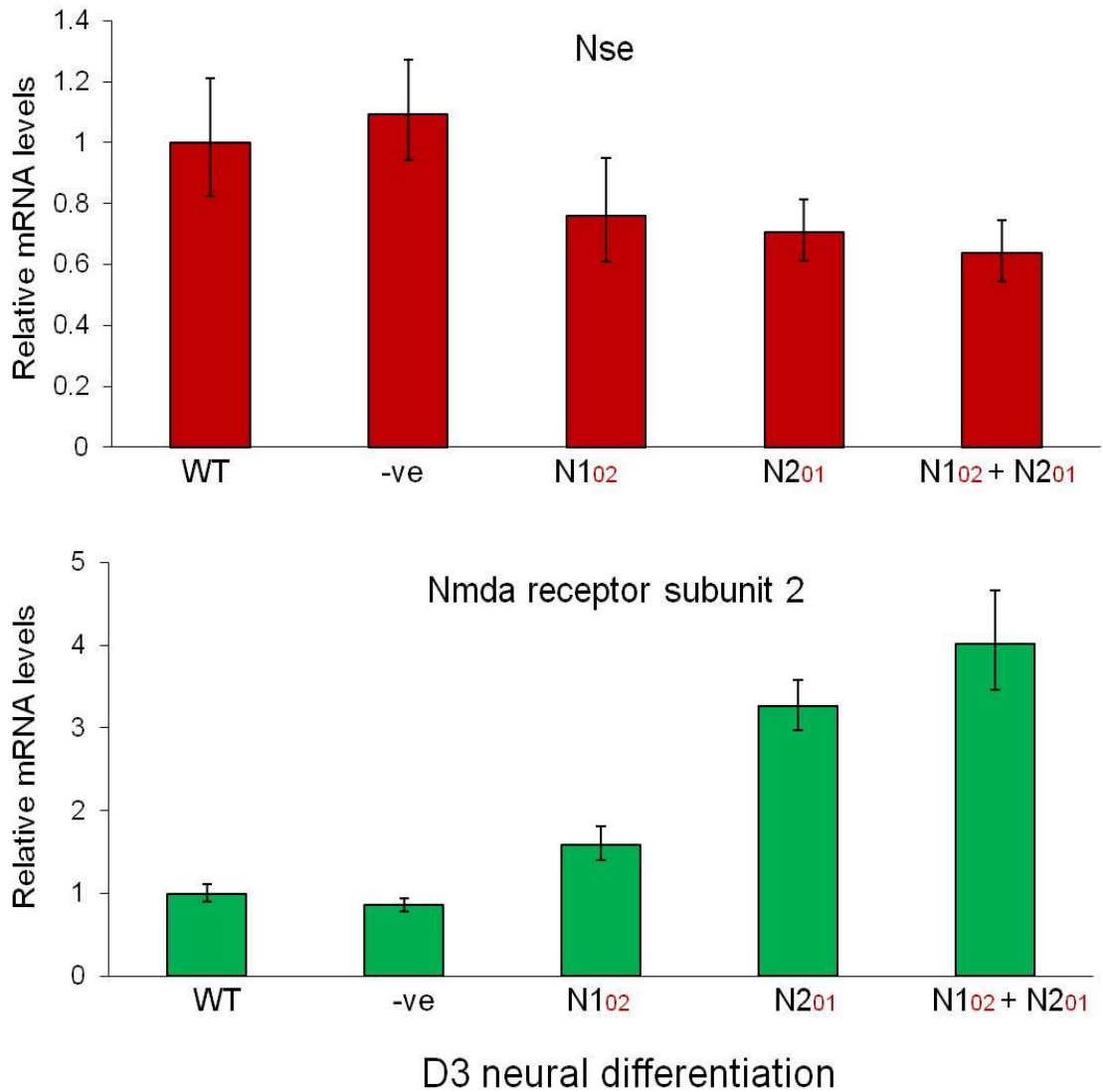


Figure 5.16: Nse and Nmda-receptor subunit 2 demonstrate complimentary expression pattern in HMGN knockdown cells.

HMGN1, HMGN2 and HMGN1/2 were knocked down using specific siRNAs, and NSE and NMDA-NR2a expression assayed on day 3 of neural differentiation. Ct values from knockdown cells were normalised to β -actin and shown relative to wild type levels. Error bars reflect the standard deviation from RT-PCR triplicates from one biological replicate. WT= wild type, -ve= negative control siRNA.

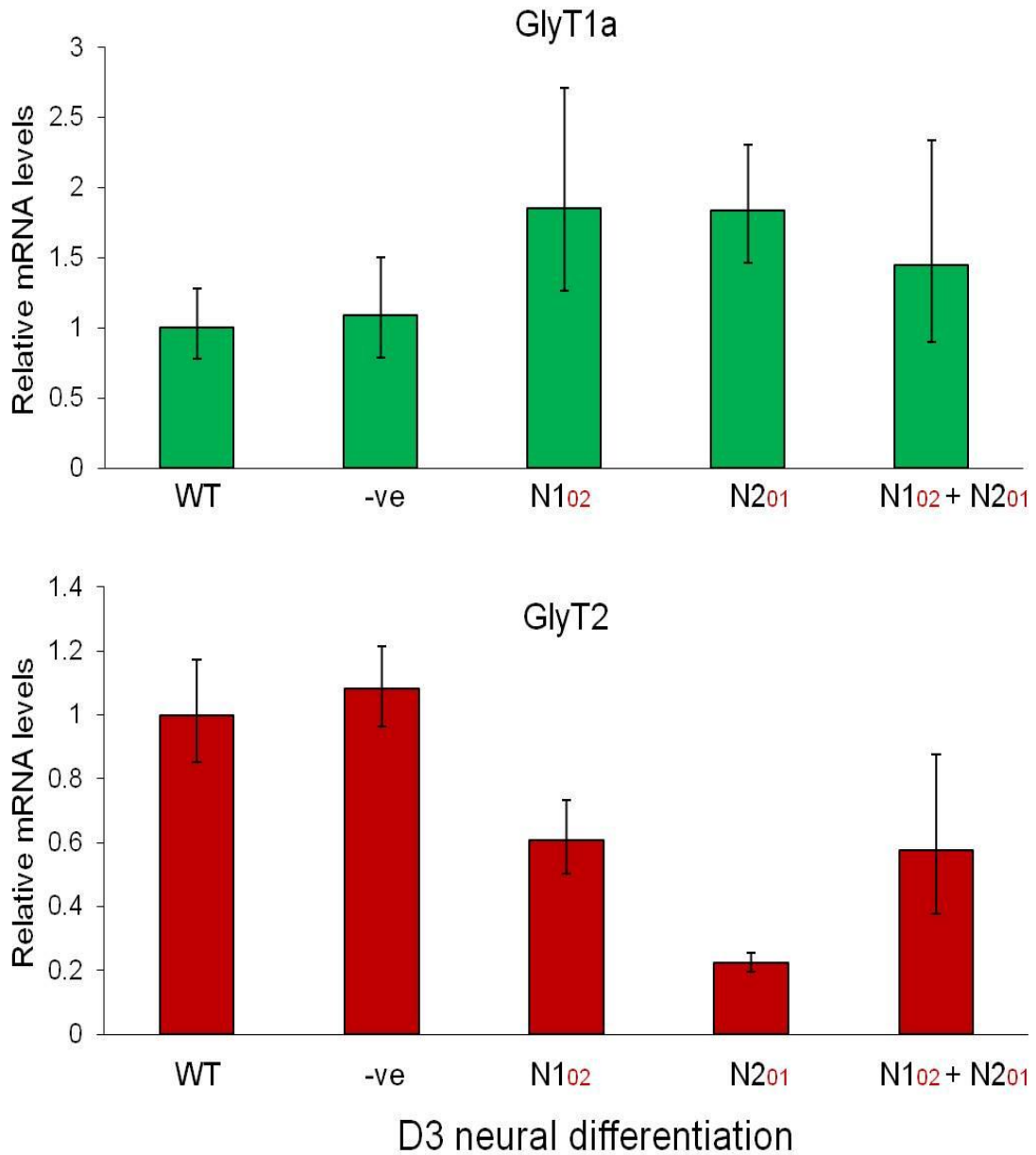


Figure 5.17: GlyT2 expression is significantly down-regulated in HMGN2 knockdown cells.

HMGN1, HMGN2 and HMGN1/2 were knocked down using specific siRNAs, and GlyT1a and GlyT2 expression assayed on day 3 of neural differentiation. Ct values from knockdown cells were normalised to β -actin and shown relative to wild type levels. Error bars reflect the standard deviation from RT-PCR triplicates from one biological replicate. WT= wild type, -ve= negative control siRNA.

5.13 Discussion

5.13.1 HMGN knockdowns in undifferentiated and neuronal differentiating P19 cells

HMGN1 and HMGN2 proteins were transiently knocked down using siRNAs in both undifferentiated and RA-induced neural differentiation of P19 cells. The protocol used to knockdown HMGN1 and HMGN2 during neural differentiation involved two rounds of siRNAs transfections, one during the EB stage and one shortly after plating the cells out on day 0. However, first round of transfection did not knockdown HMGN1 and HMGN2, when the cells were assayed at day 0 (before plating). HMGN1 and HMGN2 knockdowns were only obvious in day 3 neural differentiation. These results suggest that the changes in the expression of GOIs on day 3 are solely due the loss of HMGN1 and HMGN2 during neural differentiation and not the effect of improper RA-induced neural cell programming due to the first round of siRNA transfection.

The knockdowns of HMGN1 or HMGN2 did not affect the expression of other HMGN family members. HMGN1 knockdown did not alter the levels of HMGN2 protein and vice-versa. In addition, neither knockdown of HMGN1 nor HMGN2 changed the expression of HMGN3a and HMGN3b RNA (data not shown). These results suggest that the loss of one HMGN member is not compensated by the increased expression of another member.

It is however important to note that HMGN1 and HMGN2 knockdown results in D3 neural differentiation was from one biological replicate only. Therefore, statistical analysis to measure significance could not be carried out. More biological replicates must be conducted to be able to justify the results presented here.

5.13.2 HMGN knockdowns affect the expression of pluripotency-related genes in undifferentiated cells

In undifferentiated cells, HMGN1 and HMGN2 knockdowns lead to a reduction in the expression of pluripotency-related genes Oct4, Nanog and Sox2,

whereas Rest expression was unaffected. These results suggest that both HMGN1 and HMGN2 may be positive regulators of the key pluripotency genes.

To investigate whether the knockdown cells that have lost 80% of some of their key pluripotency regulators are actually being engaged into cell commitment programmes, the expression of various neural lineage genes was examined: Nestin, Zfp521, Map2, NmdaR2, Nse, Nf-160 kDa, GlyT2 and Gfap. These are all present at very low levels in undifferentiated cells, and no change in their expression was observed following HMGN knockdown. The continued presence of Rest in the HMGN knockdown cells might explain why these neural lineage-specific genes remained silent, even though Oct4, Nanog and Sox2 were down-regulated. In the future, large scale gene expression profiling could be used to investigate whether these knockdown cells express genes that are characteristic of commitment towards the mesodermal, endodermal or ectodermal lineages.

Several studies show that Rest expression is positively regulated by Oct4 and Nanog (Kim et al., 2008; Loh et al., 2006; Boyer et al., 2005). Oct4 and Nanog-dependent regulation of Rest does not fit the results presented here, as Rest levels remained unchanged, even though Oct4 and Nanog are dramatically down-regulated upon HMGN knockdown. Two possible hypotheses can be used to explain this data. Firstly, the already synthesised Oct4 and Nanog proteins may be still present in the cells even though RNA levels are down-regulated, thus maintaining Rest expression. Secondly, HMGN1 and HMGN2 proteins may play a dual role by acting as positive regulators of Oct4 and Nanog (hence the down-regulation of these genes in the HMGN knockout cells), while also inhibiting Rest expression, with the net result that Rest expression is not significantly altered in the HMGN knockdown cells.

5.13.3 HMGN knockdowns affected the expression of neural-related genes in day 3 cells

In day 3 of neural differentiation, knockdown of HMGN1 and/or HMGN2 affected the expression of 7 out of 9 neural lineage genes tested. Rest, Zfp521, Nse and GlyT2 were down-regulated following HMGN knockdown,

whereas Nestin, Nf-160 kDa Nmdar2 were up-regulated. Map2 and Glyt1a were unaffected. Large scale gene expression profiling is required to investigate whether HMGNs affect the majority of neural lineage genes in a similar way, but the implication from this small scale study is that HMGNs may play a key role in regulating the identity and function of neuronal cells. Whether HMGN1 and HMGN2 affect the expression of these genes by directly binding to them or through other indirect mechanisms remained to be studied. One mechanism that could be used to explain how HMGN1-2 are affecting the expression of GOIs are through histone acetylation. In study conducted by Lim et al, HMGN1 were previously shown to affect the expression of a subset of immediate early (IE) genes through promoting H3K14ac and inhibiting phosphorylation of histone 3 (H3S10) (Lim et al., 2005).

In the undifferentiated cells, all the genes affected by the knockdowns were affected by both HMGN1 and HMGN2. In the day 3 cells, some genes were altered by knocking down either HMGN1 or HMGN2 (Zfp521, Nestin, Nse and GlyT2), whereas others were affected only by the specific knockdown of HMGN1 (NF-160 kDa) or HMGN2 (Nmdar2 and Rest). Thus, HMGN1 and HMGN2 appear to have some redundant functions, particularly in the regulation of pluripotency-related genes, but they also have isoform-specific roles in the regulation of some neuronal lineage genes.

It is interesting to note that the loss of HMGN1 and HMGN2 led to a reduction in GlyT1a expression in undifferentiated P19 EC cells, but not in the day 3 cells. Previously, HMGN3 over-expression was shown to increase GlyT1a transcription in Hepa cells by binding directly to the gene (West et al., 2004). It would have been interesting to examine the role of HMGN3 in regulating GlyT1a expression in the P19 EC system, but this knockdown was not performed due to the unexpected cytoplasmic localisation of HMGN3 in these cells. It is clear that the GlyT1a gene is responsive to HMGN levels, and further studies are required to investigate the roles that the three different HMGN isoforms play in regulating its expression.

5.13.4 Cell-type specific effects of HMGN1 and HMGN2

HMGN1 and/or HMGN2 knockdowns altered the expression of many of the neural lineage genes in day 3 of neural differentiation but not in undifferentiated cells. Similarly, knockdown of HMGN2 reduced Rest expression in day 3 cells but not in undifferentiated cells. In contrast, Glyt1a expression was altered by HMGN1/2 knockdown in undifferentiated cells but not in day 3 cells. Some of these apparent discrepancies could be due to detection limits of the qPCR technology, meaning that it is not possible to accurately measure small changes in expression of a gene that is expressed at a very low level in the first place. However, this cannot explain the Rest and Glyt1a data, and so it seems HMGN1 and HMGN2 may have a different set of target genes in undifferentiated compared to neuronal differentiated cells in the P19 EC system. Therefore, the role of HMGN1 and HMGN2 in regulating the expression of specific genes appears to be linked to the differentiation status of the cells.

5.14 Summary

The results of this chapter show that HMGN1 and HMGN2 may play specific roles in pluripotency and neural differentiation of P19 cells. HMGN1 and HMGN2 specifically affect the expression of key pluripotency and neural-related genes. Further experiments to validate the changes in GOIs seen here must be carried out before any conclusion can be derived from these results.

Chapter 6

Summary and Future work

6.1 Summary

Investigating the mechanisms of ES/EC cell pluripotency and neuronal differentiation are critical to understanding the early differentiation processes that occur *in vivo*. The role of HMGN proteins in ES/EC cells and neuronal differentiation remains largely unknown. This thesis presents the characterisation of HMGN1, HMGN2 and HMGN3 expression in undifferentiated and neural differentiating P19 EC cells. RNA interference was used to knockdown HMGN1 and HMGN2 in order to investigate the roles that they play in this system.

6.1.1 Characterisation of RA-induced neuronal differentiation of P19 cells (Chapter 3)

P19 EC cells are a commonly used system for studying the mechanisms underlying stem cell-derived neuronal differentiation. In this study, a retinoic acid protocol was used to promote neuronal differentiation from P19 EC cells. Studies in chapter 3 characterised the neuronal differentiation system based on the expression of specific molecular markers. Two main steps in the RA protocol were shown to be crucial in inducing neural differentiation: the concentration of retinoic acid used, and the density of EB-derived neuroectodermal cells plated out for further differentiation. Specifically, an RA concentration of 1.0 μM and 1.5 μM showed higher capacity for neural induction compared to 0.5 μM , and a density of 3.5×10^6 cells per 10 cm dish were shown to be optimal for subsequent neuronal differentiation.

Using the optimised protocol, P19-derived neuronal differentiation was characterised using specific molecular markers. The differentiating cultures showed the expression of neuron and glia specific markers. In addition, core pluripotent markers were lost upon neural induction. The expression of these

specific markers demonstrates that P19 EC cells can be used to study the early events involved in neuronal differentiation.

6.1.2 HMGN expression during neuronal differentiation (chapter 4)

Chapter 4 presents the characterisation of HMGN1-3 expression and cellular localisation in undifferentiated and neural differentiating P19 cells. The major finding of this chapter is that the expression of HMGN2 and HMGN3 is up-regulated upon neural differentiation (while HMGN1 remained unchanged), contrary to other findings in differentiation models where HMGNs were shown to be down-regulated (Furusawa et al., 2006; Crippa et al., 1991; Begum et al., 1990).

The other finding from this chapter is that HMGN3 is predominantly localised to the cytoplasm of undifferentiated and neural differentiating P19 cells, whereas all previous studies show HMGN proteins to be localised in the nucleus. It is possible that the HMGN3 gene in P19 cells has a mutation in the nuclear localisation signal, or that a component of the nuclear import apparatus is mutated, thus preventing the import of HMGN3 into the nucleus. To address this question, HMGN3 from P19 cells could be cloned and sequenced to identify any possible mutations in the gene, and a GFP-tagged version of HMGN3 could be transfected into P19 cells to study whether it is localised to the nucleus or the cytoplasm. It would also be informative to investigate the localisation of HMGN3 in mouse ES cells. If the cytoplasmic localisation of HMGN3 in P19 cells does not appear to result from a mutation, it may be that the nuclear import of HMGN3 is regulated differently to that of HMGN1 and HMGN2, with the implication that HMGN3 plays a specific role in P19 EC cells that is different to those of HMGN1 and HMGN2.

6.1.3 HMGN1 and HMGN2 knockdowns in undifferentiated and neural differentiating P19 cells

Chapter 5 initially describes the establishment of HMGN1 and HMGN2 knockdowns using siRNA in undifferentiated P19 EC cells. Four siRNAs (2 specific to each HMGN family member) generated knockdown of HMGN1 or HMGN2 proteins by approximately 90%. Using these knockdown cells, the expression of key genes were studied. HMGN1 and HMGN2 knockdown cells dramatically down-regulated key pluripotency regulators Oct4, Nanog and Sox2. GlyT1a was also down-regulated by HMGN1 and HMGN2 knockdowns, but other neural lineage genes were unaffected. These results indicate that HMGN1 and HMGN2 may play roles in regulating the pluripotency state and the consequent differentiation process from P19 EC cells. In day 3 neural differentiating cells, the expression of neuron-specific genes were affected following HMGN1 and HMGN2 knockdown. Expression of key genes like Nmdar2, Nestin, Zfp521, NF-160 kDa, GlyT2, Nse and Rest were differentially expressed following HMGN1 and/or HMGN2 knockdowns. However it is not known whether the HMGN proteins directly or indirectly affect the expression of these genes. It can be speculated that HMGN1/2 bind these genes and trigger changes in histone modifications that lead to either transcriptional activation or repression. However the role, HMGN1 and HMGN2 in neuronal differentiation of P19 EC cells needs to be further investigated.

6.2 Future work

Results from this work showed that HMGN proteins may play an important role in stem cells and neuronal differentiation. One of the major accomplishments of this project is that it opened up several new aspects for further research, particularly in elucidating the role of HMGN proteins in stem cells and cellular differentiation. Some of the ongoing and future directions are briefly outlined below.

The changes in GOIs expression following HMGN1/2 knockdown in this project were shown using a transient system. Ongoing work is being performed to establish an inducible knockdown system for HMGN1 and HMGN2 using the

miRNA lentiviral platform described by Shin et al (Shin et al., 2006). This lentiviral system can be used to stably knockdown HMGN1/2 and study the relevant GOs. This is an important experiment as it should validate the results shown in this project.

Following the establishment of the stable knockdown system, several questions could be addressed. The first is to study whether HMGN knockdowns affect the expression of other pluripotency genes, and/or those associated with lineage commitment, by conducting genome-wide gene expression analyses. Changes in gene expression could be validated using western blotting analysis.

The next question that could be addressed is whether HMGN proteins directly bind the GOs that show changes in expression. This could be performed using Chromatin Immunoprecipitation (ChIP) studies. Further analysis could be conducted to study whether the binding profiles of HMGNs overlap with those of any specific histone modifications. The HMGN binding profile could be compared with histone modifications such as the H3K4me3 active mark or the H3K27me3 repressive mark, particularly on bivalent genes. It would then be interesting to investigate whether these marks change following HMGN knockdown. This study could elucidate a mechanism for the role of HMGNs in regulating specific genes in undifferentiated EC cells and neural differentiating cells.

The results from the studies outlined above could be validated using ES cells. Cells like mouse E14 ES cells could be used to study whether the roles of HMGNs are specific to EC cells or they have a global function in all embryonic-like stem cells. For the neural differentiation, other protocols besides RA could be employed.

6.3 Concluding remarks

The findings presented in this thesis have revealed a possible role for HMGN1 and HMGN2 in undifferentiated and neural differentiating P19 EC cells. The expression of HMGN2 and HMGN3 was shown to be up-regulated in early differentiating neurons derived from P19 EC cells. HMGN3 proteins were shown to be exclusively localised in the cytoplasm of these cells. HMGN1 and HMGN2 knockdowns affected the expression of key pluripotency regulator genes in undifferentiated cells and neuron-specific genes in neural differentiating cells.

Appendix

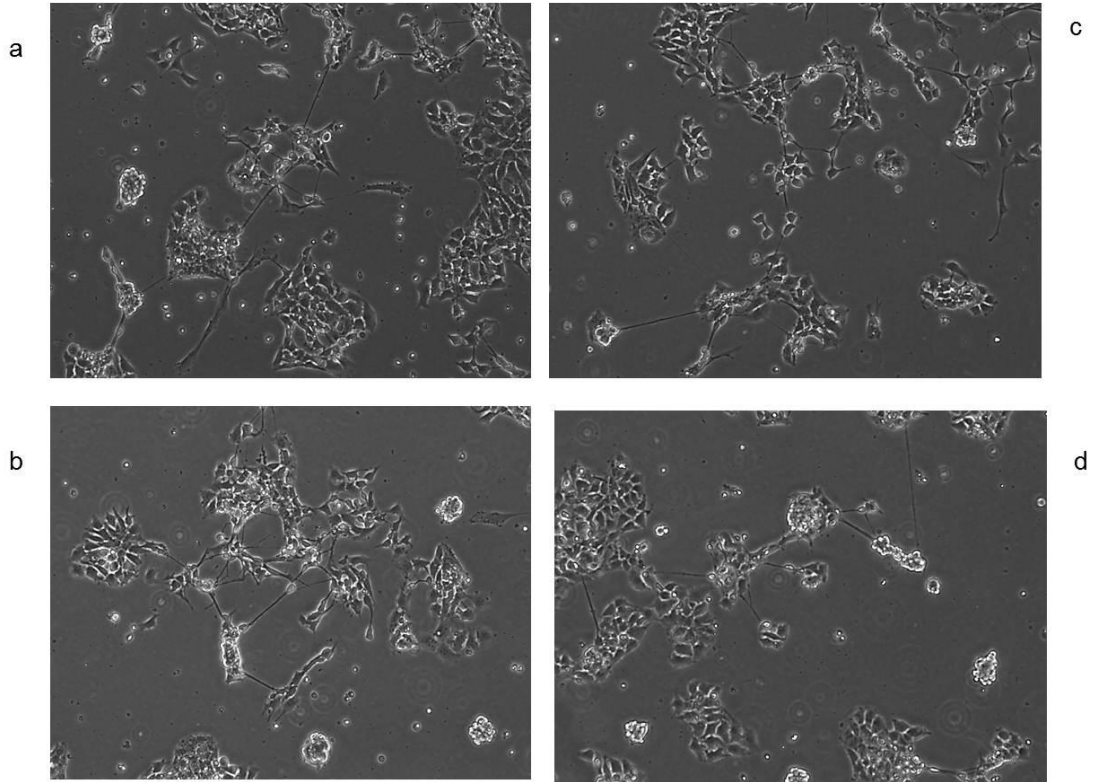


Figure A.1: Cell images showing RA-induced neuronal differentiation from P19 EC cells at day 2 from different EB plating densities. (a) A seeding density of 7.5×10^6 . (b) A seeding density of 5.5×10^6 . (c) & (d) A seeding density of 3.5×10^6 . Images were taken under 20 X objective using Olympus (IX51) microscope.

List of references

- Abdelalim, E.M. and Tooyama, I. (2009) BNP signaling is crucial for embryonic stem cell proliferation. *PLoS One*, **4**, 5341.
- Adams, R.H., Sato, K., Shimada, S., Tohyama, M., Püschel, A.W. and Betz, H. (1995) Gene structure and glial expression of the glycine transporter GlyT1 in embryonic and adult rodents. *J Neurosci*, **3**, 524-532.
- Agalioti, T., Chen, G. and Thanos, D. (2002) Deciphering the transcriptional histone acetylation code for a human gene. *Cell*, **3**, 381-392.
- Akai, J., Halley, P.A. and Storey, K.G. (2005) FGF-dependent Notch signaling maintains the spinal cord stem zone. *Genes Dev*, **23**, 2877-2887.
- Alfonso, P.J., Crippa, M.P., Hayes, J.J. and Bustin, M. (1994) The footprint of chromosomal proteins HMG-14 and HMG-17 on chromatin subunits. *Mol Biol*, **1**, 189-198.
- Almqvist, P.M., Mah, R. and Lendahl, U., Jacobsson, B. and Hendson, G. (2002) Immunohistochemical detection of nestin in pediatric brain tumors. *J Histochem Cytochem*, **50**, 147-158.
- Alonso, A., Breuer, B., Steuer, B. and Fischer, J. (1991) The F9-EC cell line as a model for the analysis of differentiation. *Int J Dev Biol*, **4**, 389-397.
- Ambrosetti, D.C., Basilico, C., and Dailey, L. (1997) Synergistic activation of the fibroblast growth factor 4 enhancer by Sox2 and Oct-3 depends on protein-protein interactions facilitated by a specific spatial arrangement of factor binding sites. *Mol Cell Biol*, **17**, 6321-6329.
- Ambrosetti, D.C., Schöler, H.R., Dailey, L. and Basilico, C. (2000) Modulation of the activity of multiple transcriptional activation domains by the DNA binding domains mediates the synergistic action of Sox2 and Oct-3 on the fibroblast growth factor-4 enhancer. *J Biol Chem*, **30**, 23387-23397.
- Andrés, M.E., Burger, C., Peral-Rubio, M.J., Battaglioli, E., Anderson, M.E., Grimes, J., Dallman, J., Ballas, N. and Mandel, G. (1999) CoREST: a functional corepressor required for regulation of neural-specific gene expression. *Proc Natl Acad Sci U S A*, **17**, 9873-9878.
- Andrews, P. W., Casper, J., Damjanov, I., Duggan-Keen, M., Giwerzman, A., Hata, J., von Keitz, A., Looijenga, L. H., Millan, J. L., Oosterhuis, J. W., Pera, M., Sawada, M., Schmoll, H.J., Skakkebaek, N.E., van Putten, W. and Stern, P. (1996) Comparative-analysis of cell-surface antigens expressed by cell-lines derived from human germ-cell tumors. *Int. J. Cancer*, **66**, 806-816.

- Andrews, P.W., Matin, M.M., Bahrami, A.R., Damjanov, I., Gokhale, P. and Draper, J.S. (2005) Embryonic stem (ES) cells and embryonal carcinoma (EC) cells: opposite sides of the same coin. *Biochem Soc Trans*, **33**, 1526-1530.
- Aragón, C. and López-Corcuera, B. (2003) Structure, function and regulation of glycine neurotransmitters. *Eur J Pharmacol*, **1-3**, 249-262.
- Aubert, J., Dunstan, H., Chambers, I. and Smith, A. (2002) Functional gene screening in embryonic stem cells implicates Wnt antagonism in neural differentiation. *Nat Biotechnol*, **12**, 1240-1245.
- Avilion, A. A., Nicolis, S. K., Pevny, L. H., Perez, L., Vivian, N., and Lovell-Badge, R. (2003) Multipotent cell lineages in early mouse development depend on SOX2 function. *Genes Dev*. **17**, 126-140.
- Azuara, V., Perry, P., Sauer, S., Spivakov, M., Jørgensen, H.F., John, R.M., Gouti, M., Casanova, M., Warnes, G., Merckenschlager, M. and Fisher, A.G. (2006) Chromatin signatures of pluripotent cell lines. *Nat Cell Biol*, **5**, 532-538.
- Bain, G., and Gottlieb, D.I. (1994) Expression of retinoid X receptors in P19 embryonal carcinoma cells and embryonic stem cells. *Biochem. Biophys. Res. Commun.* **200**, 1252-1256.
- Bain, G., Kitchens, D., Yao, M., Huettner, J.E. and Gottlieb, D.I. (1995) Embryonic stem cells express neuronal properties in vitro. *Develop Biol*, **168**. 342-357.
- Bain, G., Ray, W.J., Yao, M. and Gottlieb, D.I. (1996) Retinoic acid promotes neural and represses mesodermal gene expression in mouse embryonic stem cells in culture. *Biochem Biophys Res Commun.* **3**. 691-694.
- Baker, J.C., Beddington, R.S. and Harland, R.M. (1999) Wnt signaling in *Xenopus* embryos inhibits bmp4 expression and activates neural development. *Genes Dev*, **23**, 3149-3159.
- Ballas, N., Battaglioli, E., Atouf, F., Andres, M.E., Chenoweth, J., Anderson, M.E., Burger, C., Moniwa, M., Davie, J.R., Bowers, W.J., Federoff, H.J., Rose, D.W., Rosenfeld, M.G., Brehm, P. and Mandel, G. (2001) Regulation of neuronal traits by a novel transcriptional complex. *Neuron*, **3**, 353-365.
- Ballas, N., Grunseich, C., Lu, D.D., Spohr, J.C. and Mandel, G. (2005) REST and its corepressors mediate plasticity of neuronal gene chromatin throughout neurogenesis. *Cell*, **4**, 645-57.
- Bao, Y. and Shen, X. (2007) SnapShot: chromatin remodeling complexes. *Cell*, **3**, 632.

- Barberi, T., Klivenyi, P., Calingasan, N.Y., Lee, H., Kawamata, H., Loonam, K., Perrier, A.L., Bruses, J., Rubio, M.E., Topf, N., Tabar, V., Harrison, N.L., Beal, M.F., Moore, M.A. and Studer, L. (2003) Neural subtype specification of fertilization and nuclear transfer embryonic stem cells and application in parkinsonian mice. *Nat Biotechnol*, **10**, 1200-1207.
- Barski, A., Cuddapah, S., Cui, K., Roh, T.Y., Schones, D.E., Wang, Z., Wei, G., Chepelev, I. and Zhao, K. (2007) High-resolution profiling of histone methylations in the human genome. *Cell*, **4**, 823-837.
- Bastos, G.M., Gonçalves, P.B. and Bordignon, V. (2008) Immunolocalization of the high-mobility group N2 protein and acetylated histone H3K14 in early developing parthenogenetic bovine embryos derived from oocytes of high and low developmental competence. *Mol Reprod Dev*, **2**, 282-290.
- Begum, N., Pash, J.M., Bhorjee, J.S. (1990) Expression and synthesis of high mobility group chromosomal proteins in different rat skeletal cell lines during myogenesis. *J Biol Chem*. **20**.11936-11941.
- Belova, G.I., Postnikov, Y.V., Furusawa, T., Birger, Y. and Bustin, M. (2008) Chromosomal protein HMGN1 enhances the heat shock-induced remodeling of Hsp70 chromatin. *J Biol Chem*, **13**, 8080-8088.
- Berg, R.W. and McBurney, M.W. (1990) Cell density and cell cycle effects on retinoic acid-induced embryonal carcinoma cell differentiation. *Dev Biol*, **1**, 123-135.
- Bernstein, B.E., Mikkelsen, T.S., Xie, X., Kamal, M., Huebert, D.J., Cuff, J., Fry, B., Meissner, A., Wernig, M., Plath, K., Jaenisch, R., Wagschal, A., Feil, R., Schreiber, S.L. and Lander, E.S. (2006) A bivalent chromatin structure marks key developmental genes in embryonic stem cells. *Cell*, **2**, 315-326.
- Biagiotti, T., D'Amico, M., Marzi, I., Di Gennaro, P., Arcangeli, A., Wanke, E. and Olivotto, M. (2006) Cell renewing in neuroblastoma: electrophysiological and immunocytochemical characterization of stem cells and derivatives. *Stem Cells*, **2**, 443-453.
- Birger, Y., Ito, Y., West, K.L., Landsman, D. and Bustin, M. (2001) HMGN4, a newly discovered nucleosome-binding protein encoded by an intronless gene, **5**, 257-264.
- Birger, Y., West, K.L., Postnikov, Y.V., Lim, J.H., Furusawa, T., Wagner, J..P, Laufer, C.S., Kraemer, K.H. and Bustin, M. (2003) Chromosomal protein HMGN1 enhances the rate of DNA repair in chromatin. *EMBO J*, **7**, 1665-1675.

- Birger, Y., Catez, F., Furusawa, T., Lim, J.H., Prymakowska-Bosak, M., West, K.L., Postnikov, Y.V., Haines, D.C. and Bustin, M. (2005) Increased tumorigenicity and sensitivity to ionizing radiation upon loss of chromosomal protein HMGN1. *EMBO J*, **5**, 6711-6718.
- Birger, Y., Davis, J., Furusawa, T., Rand, E., Piatigorsky, J. And Bustin, M. (2006) A role for chromosomal protein HMGN1 in corneal maturation. *Differentiation*, **1**, 19-29.
- Boyer, L.A., Lee, T.I., Cole, M.F., Johnstone, S.E., Levine, S.S., Zucker, J.P., Guenther, M.G., Kumar, R.M., Murray, H.L., Jenner, R.G., Gifford, D.K., Melton, D.A., Jaenisch, R. and Young, R.A. (2005) Core transcriptional regulatory circuitry in human embryonic stem cells. *Cell*, **6**, 947-956.
- Boyer, L.A., Plath, K., Zeitlinger, J., Brambrink, T., Medeiros, L.A., Lee, T.I., Levine, S.S., Wernig, M., Tajonar, A., Ray, M.K., Bell, G.W., Otte, A.P., Vidal, M., Gifford, D.K., Young, R.A. and Jaenisch, R. (2006) Polycomb complexes repress developmental regulators in murine embryonic stem cells. *Nature*, **7091**, 349-353.
- Brook, F.A. and Gardner, R.L. (1997) The origin and efficient derivation of embryonic stem cells in the mouse. *Proc Natl Acad Sci U S A*, **11**, 5709-5712.
- Burdon, T., Smith, A. and Savatier, P. (2002) Signalling, cell cycle and pluripotency in embryonic stem cells. *Trends Cell Biol*, **9**, 432-438.
- Burdon, T., Stracev, C., Chambers, I., Nichols, J. and Smith, A. (1999) Suppression of SHP-2 and ERK signalling promotes self-renewal of mouse embryonic stem cells. *Dev Biol*, **1**, 210(1), 30-43.
- Bustin, M., Catez, F. and Lim, J.H. (2005) The dynamics of histone H1 function in chromatin. *Mol Cell*, **5**, 617-620.
- Bustin, M. and Reeves, R. (1996) High-mobility-group chromosomal proteins: architectural components that facilitate chromatin function. *Prog Nucleic Acid Res Mol Biol*, **54**, 35-100.
- Bustin, M. (1999) Regulation of DNA-dependent activities by the functional motifs of the high-mobility-group chromosomal proteins. *Mol Cell Biol*, **8**, 5237-5246.
- Bustin, M. (2001) Chromatin unfolding and activation by HMGN(*) chromosomal proteins. *Trends Biochem. Sci.*, **26**, 431-437.
- Cao, R. and Zhang, Y. (2004) SUZ12 is required for both the histone methyltransferase activity and the silencing function of the EED-EZH2 complex. *Mol Cell*, **1**, 57-67.
- Cartwright, P., McLean, C., Sheppard, A., Rivett, D., Jones, K. and Dalton, S. (2005) LIF/STAT3 controls ES cell self-renewal and pluripotency by a Myc-dependent mechanism. *Development*, **5**, 885-896.

- Catez, F., Ueda, T. and Bustin, M. (2006) Determinants of histone H1 mobility and chromatin binding in living cells. *Nat Struct Mol Biol*, **4**, 305-10.
- Chambers, I., Colby, D., Robertson, M., Nichols, J., Lee, S., Tweedie, S. and Smith, A. (2003) Functional expression cloning of Nanog, a pluripotency sustaining factor in embryonic stem cells. *Cell*, **5**, 643-655.
- Chambers, I., Silva, J., Colby, D., Nichols, J., Nijmeijer, B., Robertson, M., Vrana, J., Jones, K., Grotewold, L. and Smith, A. (2007) Nanog safeguards pluripotency and mediates germline development. *Nature*, **7173**, 1230-1234.
- Chen, Z.F., Paquette, A.J. and Anderson, D.J. (1998) NRSF/REST is required in vivo for repression of multiple neuronal target genes during embryogenesis. *Nat Genet*, **2**, 136-142.
- Cheung, P., Allis, C.D. and Sassone-Corsi, P. (2000) Signaling to chromatin through histone modifications. *Cell*, **2**, 263-271.
- Chew, J.L., Loh, Y.H., Zhang, W., Chen, X., Tam, W.L., Yeap, L.S., Li, P., Ang, Y.S., Lim, B., Robson, P. and Ng, H.H. (2005) Reciprocal transcriptional regulation of Pou5f1 and Sox2 via the Oct4/Sox2 complex in embryonic stem cells. *Mol Cell Biol*, **14**, 6031-6046.
- Clagett-Dame, M. and DeLuca, H.F. (2002) The role of vitamin A in mammalian reproduction and embryonic development. *Annu Rev Nutr*, **22**, 347-381.
- Clarke, S.R., Shetty, A.K., Bradley, J.L. and Turner, D.A. (1994) Reactive astrocytes express the embryonic intermediate neurofilament nestin. *Neuroreport*, **15**, 1885-1888.
- Cole, M.F., Johnstone, S.E., Newman, J.J., Kagey, M.H. and Young, R.A. (2008) Tcf3 is an integral component of the core regulatory circuitry of embryonic stem cells. *Genes Dev*, **6**, 746-755.
- Colombo, E., Giannelli, S.G., Galli, R., Tagliafico, E., Foroni, C., Tenedini, E., Ferrari, S., Ferrari, S., Corte, G., Vescovi, A., Cossu, G. and Broccoli, V. (2006) Embryonic stem-derived versus somatic neural stem cells: a comparative analysis of their developmental potential and molecular phenotype. *Stem Cells*, **4**, 825-34.
- Coucovanis, E. and Martin, G.R. (1995) Signals for death and survival: a two-step mechanism for cavitation in the vertebrate embryo. *Cell*, **2**, 279-287.
- Crippa, M.P., Nickol, J.M. and Bustin, M. (1991) Developmental changes in the expression of high mobility group chromosomal proteins. *J Biol Chem*, **5**, 2712-2714.

- Crippa, M.P., Trieschmann, L., Alfonso, P.J., Wolffe, A.P. and Bustin, M. (1993) Deposition of chromosomal protein HMG-17 during replication affects the nucleosomal ladder and transcriptional potential of nascent chromatin. *EMBO J*, **10**, 3855-6384.
- Cross, S.H., Meehan, R.R., Nan, X. and Bird, A. (1997) A component of the transcriptional repressor MeCP1 shares a motif with DNA methyltransferase and HRX proteins. *Nat Genet*, **3**, 256-259.
- Cubelos, B., Giménez, C. and Zafra, F. (2005) Localization of the GLYT1 glycine transporter at glutamatergic synapses in the rat brain. *Cereb Cortex*, **4**, 448-459.
- Cuddapah, S., Schones, D.E., Cui, K., Roh, T.Y., Barski, A., Wei, G., Rochman, M., Bustin, M. and Zhao, K (2011) Genomic profiling of HMGN1 reveals an association with chromatin at regulatory regions. *Mol Cell Biol*, **4**, 700-709.
- Dahlstrand, J., Lardelli, M. and Lendahl, U. (1995) Nestin mRNA expression correlates with the central nervous system progenitor cell state in many, but not all, regions of developing central nervous system. *Brain Res Dev Brain Res*, **1**, 109-129.
- Dejosez, M., Levine, S.S., Frampton, G.M., Whyte, W.A., Stratton, S.A., Barton, M.C., Gunaratne, P.H., Young, R.A. and Zwaka, T.P. (2010) Ronin/Hcf-1 binds to a hyperconserved enhancer element and regulates genes involved in the growth of embryonic stem cells. *Genes Dev*, **14**, 1479-1484.
- Denslow, S.A. and Wade, P.A. (2007) The human Mi-2/NuRD complex and gene regulation. *Oncogene*, **37**, 5433-5438.
- Ding, H.F., Rimsky, S., Batson, S.C., Bustin, M. And Hansen, U. (1994) Stimulation of RNA polymerase II elongation by chromosomal protein HMG-14. *Science*, **5173**, 796-799.
- Ding, H.F., Bustin, M. and Hansen, U. (1997) Alleviation of histone H1-mediated transcriptional repression and chromatin compaction by the acidic activation region in chromosomal protein HMG-14. *Mol Cell Biol*, **10**, 5843-55.
- Doetsch, F. (2003) The glial identity of neural stem cells. *Nat Neurosci*, **11**, 127-134.
- Edwards, M. K. S. and McBurney, M. W. (1983) The concentration of retinoic acid determines the differentiated cell types formed by a teratocarcinoma cell line. *Dev. Bio*, **98**, 187-191.

- Efroni, S., Duttagupta, R., Cheng, J., Dehghani, H., Hoepfner, D.J., Dash, C., Bazett-Jones, D.P., Le Grice, S., McKay, R.D., Buetow, K.H., Gingeras, T.R., Misteli, T. and Meshorer, E. (2008) Global transcription in pluripotent embryonic stem cells. *Cell Stem Cell*, **5**, 437-447.
- Ema, M., Mori, D., Niwa, H., Hasegawa, Y., Yamanaka, Y., Hitoshi, S., Mimura, J., Kawabe, Y., Hosoya, T., Morita, M., Shimosato, D., Uchida, K., Suzuki, N., Yanagisawa, J., Sogawa, K., Rossant, J., Yamamoto, M., Takahashi, S. and Fujii-Kuriyama, Y. (2008) Krüppel-like factor 5 is essential for blastocyst development and the normal self-renewal of mouse ESCs. *Cell Stem Cell*, **5**, 555-567.
- Evans, M.J. and Kaufman, M.H. (1981) Establishment in culture of pluripotential cells from mouse embryos. *Nature*, **5819**, 154-156.
- Fainsod, A., Dibler, K., Yelin, R., Marom, K., Epstein, M., Pillemer, G., Steinbeisser, H. and Blum, M. (1997). The dorsalizing and neural inducing gene follistatin is an antagonist of BMP-4. *Mech. Dev.* **63**, 39-50.
- Fazio, T.G., Huff, J.T. and Panning, B. (2008) An RNAi screen of chromatin proteins identifies Tip60-p400 as a regulator of embryonic stem cell identity. *Cell*, **1**, 162-174.
- Felgner, H., Frank, R., Biernat, J., Mandelkow, E.M., Mandelkow, E., Ludin, B., Matus, A. and Schliwa, M. (1997) Domains of neuronal microtubule-associated proteins and flexural rigidity of microtubules. *J Cell Biol.* **5**, 1067-1075.
- Felsenfeld, G. and Groudine, M. (2003) Controlling the double helix. *Nature*, **6921**, 448-453.
- Feng, B., Jiang, J., Kraus, P., Ng, J.H., Heng, J.C., Chan, Y.S., Yaw, L.P., Zhang, W., Loh, Y.H., Han, J., Vega, V.B., Cacheux-Rataboul, V., Lim, B., Lufkin, T. and Ng, H.H. (2009) Reprogramming of fibroblasts into induced pluripotent stem cells with orphan nuclear receptor Esrrb. *Nat Cell Biol.* **2**, 197-203.
- Finch, B.W. and Ephrussi, B. (1967) Retention of Multiple Developmental Potentialities by cells of a mouse testicular teratocarcinoma during prolonged culture in vitro and their extinction upon hybridization with cells of permanent lines. *Proc Natl Acad Sci U S A*, **3**, 615-621.
- Finley, M.F., Kulkarni, N. and Huettnner, J.E. (1996) Synapse formation and establishment of neuronal polarity by P19 embryonic carcinoma cells and embryonic stem cells. *J Neurosci*, **3**, 1056-1065.

- Fousteri, M., Vermeulen, W., van Zeeland, A.A. and Mullenders, L.H. (2006) Cockayne syndrome A and B proteins differentially regulate recruitment of chromatin remodeling and repair factors to stalled RNA polymerase II in vivo. *Mol Cell*, **4**, 471-482.
- Fraichard, A., Chassande, O., Bilbaut, G., Dehay, C., Savatier, P. and Samarut, J. (1995) In vitro differentiation of embryonic stem cells into glial cells and functional neurons. *J Cell Sci*, **108**, 3181-3188.
- Fukuda, S., Kato, F., Tozuka, Y., Yamaguchi, M., Miyamoto, Y. and Hisatsune, T. (2003) Two distinct subpopulations of nestin-positive cells in adult mouse dentate gyrus. *J Neurosci*, **28**, 9357-9366.
- Furusawa, T., Lim, J.H., Catez, F., Birger, Y., Mackem, S. and Bustin, M. (2006) Down-regulation of nucleosomal binding protein HMGN1 expression during embryogenesis modulates Sox9 expression in chondrocytes. *Mol. Cell. Biol*, **26**, 592-604.
- Furusawa, T., Ko, J.H., Birger, Y. and Bustin, M. (2009) Expression of nucleosomal protein HMGN1 in the cycling mouse hair follicle. *Gene Expr Patterns*, **5**, 289-295.
- Gaiano, N. and Fishell, G. (2002) The role of notch in promoting glial and neural stem cell fates. *Annu Rev Neurosci*, **25**, 471-490.
- Gazit, B., Panet, A. and Cedar, H. (1980) Reconstitution of a deoxyribonuclease I-sensitive structure on active genes. *Proc Natl Acad Sci U S A*, **4**, 1787-1790.
- Georgiev, D., Taniura, H., Kambe, Y., Takarada, T. and Yoneda, Y. (2008) A critical importance of polyamine site in NMDA receptors for neurite outgrowth and fasciculation at early stages of P19 neuronal differentiation. *Exp Cell Res*, **14**, 2603-2617.
- Ghiani, C.A., Beltran-Parrasal, L., Sforza, D.M., Malvar, J.S., Seksenyan, A., Cole, R., Smith, D.J., Charles, A., Ferchmin, P.A. and de Vellis, J. (2007) Genetic program of neuronal differentiation and growth induced by specific activation of NMDA receptors. *Neurochem Res*, **2**, 363-376.
- Ghysen, A. and Dambly-Chaudiere, C. (1988) From DNA to form: The *achaete-scute* complex. *Genes & Dev*, **2**, 495-501.
- Glazer, R.I., Wang, X., Yuan, H. and Yin, Y. (2007) Mammary stem and progenitor cell regulation. *Cancer Biomark*, **4-5**, 171-181.
- Glover, J.C., Renaud, J.S. and Rijli, F.M. (2006) Retinoic acid and hindbrain patterning. *J Neurobiol*, **66**, 705-725.
- Goodwin, G.H., Mathew, C.G., Wright, C.A., Venkov, C.D. and Johns, E.W. (1979) Analysis of the high mobility group proteins associated with salt-soluble nucleosomes. *Nucleic Acids Res*, **7**, 1815-1835.

- Gotlieb, A.I., Rosenthal, A. and Kazemian, P. (2002) Fibroblast growth factor 2 regulation of mitral valve interstitial cell repair in vitro. *J Thorac Cardiovasc Surg*, **3**, 591-597.
- Guan, K., Chang, H., Rolletschek, A. and Wobus, A.M. (2001) Embryonic stem cell-derived neurogenesis. Retinoic acid induction and lineage selection of neuronal cells. *Cell Tissue Res*, **2**, 171-176.
- Hádinger, N., Varga, B.V., Berzsenyi, S., Környei, Z., Madarász, E. and Herberth, B. (2009) Astroglia genesis in vitro: distinct effects of retinoic acid in different phases of neural stem cell differentiation. *Int J Dev Neurosci*, **4**, 365-375.
- Hao, J., Li, T.G., Qi, X., Zhao, D.F. and Zhao, G.Q. (2006) WNT/beta-catenin pathway up-regulates Stat3 and converges on LIF to prevent differentiation of mouse embryonic stem cells. *Dev Biol*, **1**, 81-91.
- Hassan, A.H., Prochasson, P., Neely, K.E., Galasinski, S.C., Chandy, M., Carrozza, M.J. and Workman, J.L. (2002) Function and selectivity of bromodomains in anchoring chromatin-modifying complexes to promoter nucleosomes. *Cell*, **3**, 369-379.
- Heng, J.C., Feng, B., Han, J., Jiang, J., Kraus, P., Ng, J.H., Orlov, Y.L., Huss, M., Yang, L., Lufkin, T., Lim, B. and Ng, H.H. (2010) The nuclear receptor Nr5a2 can replace Oct4 in the reprogramming of murine somatic cells to pluripotent cells. *Cell Stem Cell*, **2**, 167-174.
- Hemmati-Brivanlou, A. and Melton, D. A. (1994). Inhibition of activin receptor signaling promotes neuralization in *Xenopus*. *Cell* **77**, 273-281.
- Hemmati-Brivanlou, A. and Melton, D. (1997). Vertebrate embryonic cells will become nerve cells unless told otherwise. *Cell* **88**, 13-17.
- Hill, D.A., Peterson, C.L. and Imbalzano, A.N. (2005) Effects of HMGN1 on chromatin structure and SWI/SNF-mediated chromatin remodeling. *J Biol Chem*, **50**, 41777-41783.
- Ho, L., Ronan, J.L., Wu, J., Staahl, B.T., Chen, L., Kuo, A., Lessard, J., Nesvizhskii, A.I., Ranish, J. and Crabtree, G.R. (2009) An embryonic stem cell chromatin remodeling complex, esBAF, is essential for embryonic stem cell self-renewal and pluripotency. *Proc Natl Acad Sci U S A*, **13**, 5181-5186.
- Hock, R., Wilde, F., Scheer, U. and Bustin, M. (1998) Dynamic relocation of chromosomal protein HMG-17 in the nucleus is dependent on transcriptional activity. *EMBO J*, **23**, 6992-7001.
- Hockfield, S. and McKay, R.D. (1985) Identification of major cell classes in the developing mammalian nervous system. *J Neurosci*, **12**, 3310-3328.

- Holmin, S., von Gertten, C., Sandberg-Nordqvist, A.C., Lendahl, U. and Mathiesen, T. (2001) Induction of astrocytic nestin expression by depolarization in rats. *Neurosci Lett*, **3**, 151-155.
- Horn, P.J. and Peterson, C.L. (2002) Molecular biology. Chromatin higher order folding--wrapping up transcription. *Science*, **5588**, 1824-1827.
- Horn, P.J. and Peterson, C.L. (2006) Heterochromatin assembly: a new twist on an old model. *Chromosome Res*, **1**, 83-94.
- Hsieh, J. and Gage, F.H. (2004) Epigenetic control of neural stem cell fate. *Curr Opin Genet Dev*, **5**, 461-469.
- Hsieh, J., Nakashima, K., Kuwabara, T., Mejia, E. and Gage, F.H. (2004) Histone deacetylase inhibition-mediated neuronal differentiation of multipotent adult neural progenitor cells. *Proc Natl Acad Sci U S A*, **47**, 16659-16664.
- Humphrey, G.W., Wang, Y.H., Hirai, T., Padmanabhan, R., Panchision, D.M., Newell, L.F., McKay, R.D. and Howard, B.H. (2008) Complementary roles for histone deacetylases 1, 2, and 3 in differentiation of pluripotent stem cells. *Differentiation*, **4**, 348-356.
- Hwang, C.K., Song, K.Y., Kim, C.S., Choi, H.S., Guo, X.H., Law, P.Y., Wei, L.N. and Loh, H.H. (2007) Evidence of endogenous mu opioid receptor regulation by epigenetic control of the promoters. *Mol Cell Biol*, **13**, 4720-4736.
- Hwang, C.K., Song, K.Y., Kim, C.S., Choi, H.S., Guo, X.H., Law, P.Y., Wei, L.N. and Loh, H.H. (2009) Epigenetic programming of mu-opioid receptor gene in mouse brain is regulated by MeCP2 and Brg1 chromatin remodelling factor. *J Cell Mol Med*, **9B**, 3591-3615.
- Hwang, C.K., Kim, C.S., Kim do, K., Law, P.Y., Wei, L.N. and Loh, H.H. (2010) Up-regulation of the mu-opioid receptor gene is mediated through chromatin remodeling and transcriptional factors in differentiated neuronal cells. *Mol Pharmacol*, **1**, 58-68.
- Ito, Y. and Bustin, M. (2002) Immunohistochemical localization of the nucleosome-binding protein HMGN3 in mouse brain. *J Histochem Cytochem*, **9**, 1273-1275.
- Ivanova, N., Dobrin, R., Lu, R., Kotenko, I., Levorse, J., DeCoste, C., Schafer, X., Lun, Y. and Lemischka, I.R. (2006) Dissecting self-renewal in stem cells with RNA interference. *Nature*, **7102**, 533-538.

- Jackson, J.P., Johnson, L., Jasencakova, Z., Zhang, X., PerezBurgos, L., Singh, P.B., Cheng, X., Schubert, I., Jenuwein, T. and Jacobsen, S.E. (2004) Dimethylation of histone H3 lysine 9 is a critical mark for DNA methylation and gene silencing in *Arabidopsis thaliana*. *Chromosoma*, **6**, 308-315.
- Jacobs, S., Lie, D.C., DeCicco, K.L., Shi, Y., DeLuca, L.M., Gage, F.H. and Evans, R.M. (2006) Retinoic acid is required early during adult neurogenesis in the dentate gyrus. *Proc Natl Acad Sci U S A*, **10**, 3902-3907.
- Jiang, J., Chan, Y.S., Loh, Y.H., Cai, J., Tong, G.Q., Lim, C.A., Robson, P., Zhong, S. and Ng, H.H. (2008) A core Klf circuitry regulates self-renewal of embryonic stem cells. *Nat Cell Biol*, **3**, 353-360.
- Jin, Z.G., Liu, L., Zhong, H., Zhang, K.J., Chen, Y.F., Bian, W., Cheng, L.P. and Jing, N.H. (2006) Second intron of mouse nestin gene directs its expression in pluripotent embryonic carcinoma cells through POU factor binding site. *Acta Biochim Biophys Sin (Shanghai)*, **3**, 207-212.
- Johnson, J.W. and Ascher, P. (1987) Glycine potentiates the NMDA response in cultured mouse brain neurons. *Nature*, **325**, 529-531.
- Johnson, J.E., Birren, S.J. and Anderson, D.J. (1990) Two rat homologues of *Drosophila* achaete-scute specifically expressed in neuronal precursors. *Nature*, **6287**, 858-861.
- Johnson, J.E., Zimmerman, K., Saito, T. and Anderson, D.J. (1992) Induction and repression of mammalian achaete-scute homologue (MASH) gene expression during neuronal differentiation of P19 embryonal carcinoma cells. *Development*, **1**, 75-87.
- Jones-Villeneuve, E.M., McBurney, M.W., Rogers, K.A. and Kalnins, V.I. (1982) Retinoic acid induces embryonal carcinoma cells to differentiate into neurons and glial cells. *J Cell Biol*, **2**, 253-62.
- Jones-Villeneuve, E.M., Rudnicki, M.A., Harris, J.F. and McBurney, M.W. (1983) Retinoic acid-induced neural differentiation of embryonal carcinoma cells. *Mol Cell Biol*, **12**, 2271-2279.
- Jung, S., Park, R.H., Kim, S., Jeon, Y.J., Ham, D.S., Jung, M.Y., Kim, S.S., Lee, Y.D., Park, C.H. and Suh-Kim, H. (2010) Id proteins facilitate self-renewal and proliferation of neural stem cells. *Stem Cells Dev*, **6**, 831-841.
- Jursky, F. and Nelson, N. (1996) Developmental expression of the glycine transporters GLYT1 and GLYT2 in mouse brain. *J Neurochem*, **1**, 336-344.
- Kaji, K., Caballero, I.M., MacLeod, R., Nichols, J., Wilson, V.A. and Hendrich, B. (2006) The NuRD component Mbd3 is required for pluripotency of embryonic stem cells. *Nat Cell Biol*, **3**, 285-292.

- Kalcheva, N., Albala, J., O'Guin, K., Rubino, H., Garner, C. and Shafit-Zagardo, B. (1995) Genomic structure of human microtubule-associated protein 2 (MAP-2) and characterization of additional MAP-2 isoforms. *Proc Natl Acad Sci, USA*, **92**, 10894-10898
- Kambara, H., Okano, H., Chiocca, E.A. and Saeki, Y. (2005) An oncolytic HSV-1 mutant expressing ICP34.5 under control of a nestin promoter increases survival of animals even when symptomatic from a brain tumor. *Cancer Res*, **7**, 2832-2839.
- Kamiya, D., Banno, S., Sasai, N., Ohgushi, M., Inomata, H., Watanabe, K., Kawada, M., Yakura, R., Kiyonari, H., Nakao, K. and Jakt, L.M., Nishikawa, S. and Sasai, Y. (2011) Intrinsic transition of embryonic stem-cell differentiation into neural progenitors. *Nature*, **7335**, 503-509.
- Kato, K., Suzuki, F., Watanabe, T., Semba, R. and Keino, H. (1984) Developmental profile of three enolase isozymes in rat brain determination from one-cell embryo to adult brain. *Neurochem Int*, **1**, 51-54.
- Kaushansky, K. (2006) Lineage-specific hematopoietic growth factors. *N Engl J Med*, **19**, 2034-2045.
- Kawasaki, H., Mizuseki, K., Nishikawa, S., Kaneko, S., Kuwana, Y., Nakanishi, S., Nishikawa, S.I. and Sasai, Y. (2000) Induction of midbrain dopaminergic neurons from ES cells by stromal cell-derived inducing activity. *Neuron*, **1**, 31-40.
- Keenen, B. and de la Serna, I.L. (2009) Chromatin remodeling in embryonic stem cells: regulating the balance between pluripotency and differentiation. *J Cell Physiol*, **1**, 1-7.
- Kerppola, T.K. (2009) Polycomb group complexes--many combinations, many functions. *Trends Cell Biol*, **12**, 692-704.
- Kieffer, M., Stern, Y., Cook, H., Clerici, E., Maulbetsch, C., Laux, T. and Davies, B. (2006) Analysis of the transcription factor WUSCHEL and its functional homologue in *Antirrhinum* reveals a potential mechanism for their roles in meristem maintenance. *Plant Cell*, **3**, 560-573.
- Kielman, M.F., Rindapää, M., Gaspar, C., van Poppel, N., Breukel, C., van Leeuwen, S., Taketo, M.M., Roberts, S., Smits, R. and Fodde, R. (2002) Apc modulates embryonic stem-cell differentiation by controlling the dosage of beta-catenin signaling. *Nat Genet*, **4**, 594-605.

- Kim, J., Chu, J., Shen, X., Wang, J. and Orkin, S.H. (2008) An extended transcriptional network for pluripotency of embryonic stem cells. *Cell*, **6**, 1049-1061.
- Kim, K.M., Kingsmore, S.F., Han, H., Yang-Feng, T.L., Godinot, N., Seldin, M.F., Caron, M.G. and Giros, B. (1994) Cloning of the human glycine transporter type 1: molecular and pharmacological characterization of novel isoform variants and chromosomal localization of the gene in the human and mouse genomes. *Mol Pharmacol*, **4**, 608-617.
- Kleinsmith, L.J. and Pierce, G.B.Jr. (1964) Multipotentiality of single embryonal carcinoma cells. *Cancer Res*, **24**, 1544-1551.
- Kondo, T. (2006) Epigenetic alchemy for cell fate conversion. *Curr Opin Genet Dev*, **5**, 502-507.
- Körner, U., Bustin, M., Scheer, U. and Hock, R. (2003) Developmental role of HMGN proteins in *Xenopus laevis*. *Mech Dev*, **10**, 1177-1192.
- Kouzarides, T. (2007) Chromatin modifications and their function. *Cell*, **4**, 693-705.
- Kunath, T., Saba-El-Leil, M.K., Almousailleakh, M., Wray, J., Meloche, S. and Smith, A. (2007) FGF stimulation of the Erk1/2 signalling cascade triggers transition of pluripotent embryonic stem cells from self-renewal to lineage commitment. *Development*, **16**, 2895-2902.
- Kuroda, T., Tada, M., Kubota, H., Kimura, H., Hatano, S.Y., Suemori, H., Nakatsuji, N. and Tada, T. (2005) Octamer and Sox elements are required for transcriptional cis regulation of Nanog gene expression. *Mol Cell Biol*, **6**, 2475-2485.
- Ku, M., Koche, R.P., Rheinbay, E., Mendenhall, E.M., Endoh, M., Mikkelsen, T.S., Presser, A., Nusbaum, C., Xie, X., Chi, A.S., Adli, M., Kasif, S., Ptaszek, L.M., Cowan, C.A., Lander, E.S., Koseki, H. and Bernstein, B.E. (2008) Genomewide analysis of PRC1 and PRC2 occupancy identifies two classes of bivalent domains. *PLoS Genet*, **10**, e1000242.
- Labosky, P.A., Barlow, D.P. and Hogan, B.L. (1994) Mouse embryonic germ (EG) cell lines: transmission through the germline and differences in the methylation imprint of insulin-like growth factor 2 receptor (Igf2r) gene compared with embryonic stem (ES) cell lines. *Development*, **11**, 3197-3204.
- Lamba, D.A., Hayes, S., Karl, M.O. and Reh, T. (2008) Baf60c is a component of the neural progenitor-specific BAF complex in developing retina. *Dev Dyn*, **10**, 3016-3023.

- Lebkowski, J.S., Gold, J., Xu, C., Funk, W., Chiu, C.P. and Carpenter, M.K. (2001) Human embryonic stem cells: culture, differentiation, and genetic modification for regenerative medicine applications. *Cancer J*, **2**, S83-S93.
- Lee, D.Y., Hayes, J.J., Pruss, D. and Wolffe, A.P. (1993) A positive role for histone acetylation in transcription factor access to nucleosomal DNA. *Cell*, **1**, 73-84.
- Lee, T.I., Jenner, R.G., Boyer, L.A., Guenther, M.G., Levine, S.S., Kumar, R.M., Chevalier, B., Johnstone, S.E., Cole, M.F., Isono, K., Koseki, H., Fuchikami, T., Abe, K., Murray, H.L., Zucker, J.P., Yuan, B., Bell, G.W., Herbolsheimer, E., Hannett, N.M., Sun, K., Odom, D.T., Otte, A.P., Volkert, T.L., Bartel, D.P., Melton, D.A., Gifford, D.K., Jaenisch, R. and Young RA. (2006) Control of developmental regulators by Polycomb in human embryonic stem cells. *Cell*, **2**, 301-313.
- Lehtonen, S., Olkkonen, V.M., Stapleton, M., Zerial, M. and Lehtonen, E. (1998) HMG-17, a chromosomal non-histone protein, shows developmental regulation during organogenesis. *Int J Dev Biol*, **6**, 775-782.
- Lehtonen, S. and Lehtonen, E. (2001) HMG-17 is an early marker of inductive interactions in the developing mouse kidney. *Differentiation*, **4-5**, 154-163.
- Lendahl, U., Zimmerman, L.B. and McKay, R.D. (1990) CNS stem cells express a new class of intermediate filament protein. *Cell*, **4**, 585-595.
- Lessard, J., Wu, J.I., Ranish, J.A., Wan, M., Winslow, M.M., Staahl, B.T., Wu, H., Aebersold, R., Graef, I.A. and Crabtree, G.R. (2007) An essential switch in subunit composition of a chromatin remodeling complex during neural development. *Neuron*, **2**, 201-215.
- Levine, S.S., King, I.F. and Kingston, R.E. (2004) Division of labor in polycomb group repression. *Trends Biochem Sci*, **9**, 478-485.
- Li, X.J., Du, Z.W., Zarnowska, E.D., Pankratz, M., Hansen, L.O., Pearce, R.A. and Zhang, S.C. (2005) Specification of motoneurons from human embryonic stem cells. *Nat Biotechnol*, **2**, 215-221.
- Liang, J., Wan, M., Zhang, Y., Gu, P., Xin, H., Jung, S.Y., Qin, J., Wong, J., Cooney, A.J., Liu, D. and Songyang, Z. (2008) Nanog and Oct4 associate with unique transcriptional repression complexes in embryonic stem cells. *Nat Cell Biol*, **6**, 731-739.
- Lim, R., Hoang, P. and Berger, A.J. (2004) Blockade of glycine transporter-1 (GLYT-1) potentiates NMDA receptor-mediated synaptic transmission in hypoglossal motoneurons. *J Neurophysiol*, **4**, 2530-2537.

- Lim, J.H., West, K.L., Rubinstein, Y., Bergel, M., Postnikov, Y.V. and Bustin, M. (2005) Chromosomal protein HMGN1 enhances the acetylation of lysine 14 in histone H3. *EMBO J*, **17**, 3038-3048.
- Lim, C.Y., Tam, W.L., Zhang, J., Ang, H.S., Jia, H., Lipovich, L., Ng, H.H., Wei, C.L., Sung, W.K., Robson, P., Yang, H. and Lim, B. (2008) Sall4 regulates distinct transcription circuitries in different blastocyst-derived stem cell lineages. *Cell Stem Cell*, **3**, 543-554.
- Lin, P., Kusano, K., Zhang, Q., Felder, C.C., Geiger, P.M. and Mahan, L.C. (1996) GABAA receptors modulate early spontaneous excitatory activity in differentiating P19 neurons. *J Neurochem*, **1**, 233-242.
- Liour, S.S. and Yu, R.K. (2003) Differentiation of radial glia-like cells from embryonic stem cells. *Glia*, **2**, 109-117.
- Liour, S.S., Kraemer, S.A., Dinkins, M.B., Su, C.Y., Yanagisawa, M. and Yu, R.K. (2006) Further characterization of embryonic stem cell-derived radial glial cells. *Glia*, **1**, 43-56.
- Liu, Q.R., López-Corcuera, B., Mandiyan, S., Nelson, H. and Nelson, N. (1993) Cloning and expression of a spinal cord- and brain-specific glycine transporter with novel structural features. *J Biol Chem*, **30**, 22802-22808.
- Liu, Q., Babb, S.G., Novince, Z.M, Doedens, A.L., Marrs, J. and Raymond, P.A. (2001) Differential expression of cadherin-2 and cadherin-4 in the developing and adult zebrafish visual system. *Vis Neurosci*, **6**, 923-933.
- Lo, L.C., Johnson, J.E., Wuenschell, C.W., Saito, T. and Anderson, D.J. (1991) Mammalian achaete-scute homolog 1 is transiently expressed by spatially restricted subsets of early neuroepithelial and neural crest cells. *Genes Dev*, **9**, 1524-1537.
- Loh, Y.H., Wu, Q., Chew, J.L., Vega, V.B., Zhang, W., Chen, X., Bourque, G., George, J., Leong, B., Liu, J., Wong, K.Y., Sung, K.W., Lee, C.W., Zhao, X.D., Chiu, K.P., Lipovich, L., Kuznetsov, V.A., Robson, P., Stanton, L.W., Wei, C.L., Ruan, Y., Lim, B. and Ng, H.H. (2006) The Oct4 and Nanog transcription network regulates pluripotency in mouse embryonic stem cells. *Nat Genet*, **4**, 431-440.
- Lowell, S., Benchoua, A., Heavey, B. and Smith, A.G. (2006) Notch promotes neural lineage entry by pluripotent embryonic stem cells. *PLoS Biol*, **5**, e121.
- Lucey, M.M., Wang Y., Bustin, M. and Duncan, M.K. (2008) Differential expression of the HMGN family of chromatin proteins during ocular development. *Gene Expr Patterns*, **6**, 433-437.
- Lunyak, V.V. and Rosenfeld, M.G. (2005) No rest for REST: REST/NRSF regulation of neurogenesis. *Cell*, **4**, 499-501.

- Lunyak, V.V., Burgess, R., Prefontaine, G.G., Nelson, C., Sze, S.H., Chenoweth, J., Schwartz, P., Pevzner, P.A., Glass, C., Mandel, G. and Rosenfeld, M.G. (2002) Corepressor-dependent silencing of chromosomal regions encoding neuronal genes. *Science*, **5599**, 1747-1752.
- MacDonald, J.L. and Roskams, A.J. (2008) Histone deacetylases 1 and 2 are expressed at distinct stages of neuro-glial development. *Dev Dyn*, **8**, 2256-2267.
- MacPherson, P.A., Jones, S., Pawson, P.A., Marshall, K.C. and McBurney, M.W. (1997) P19 cells differentiate into glutamatergic and glutamate-responsive neurons in vitro. *Neuroscience*, **2**, 487-499.
- Maden, M. (2007) Retinoic acid in the development, regeneration and maintenance of the nervous system. *Nat Rev Neurosci*, **10**, 755-765.
- Mansergh, F.C., Daly, C.S., Hurley, A.L., Wride, M.A., Hunter, S.M. and Evans, M.J. (2009) Gene expression profiles during early differentiation of mouse embryonic stem cells. *BMC Dev Biol*, **9**, 9:5.
- Martin, G.R., Wiley, L.M. and Damjanov, I. (1977) The development of cystic embryoid bodies in vitro from clonal teratocarcinoma stem cells. *Dev Biol*, **2**, 230-244.
- Martin, A.O. (1980) Characteristics of amniotic fluid cells in vitro and attempts to improve culture techniques. *Clin Obstet Gynaecol*, **1**, 143-173.
- Martin, G.R. (1981) Isolation of a pluripotent cell line from early mouse embryos cultured in medium conditioned by teratocarcinoma stem cells. *Proc Natl Acad Sci U S A*, **12**, 7634-7638.
- Masui, S., Nakatake, Y., Toyooka, Y., Shimosato, D., Yagi, R., Takahashi, K., Okochi, H., Okuda, A., Matoba, R., Sharov, A.A., Ko, M.S. and Niwa, H. (2007) Pluripotency governed by Sox2 via regulation of Oct3/4 expression in mouse embryonic stem cells. *Nat Cell Biol*, **6**, 625-635.
- Matise, M.P., Auerbach, W. and Joyner, A.L. (2000) Production of targeted embryonic stem cell clones. In *Gene Targeting - A Practical Approach.*, 2nd edn (Joyner AL, ed.), pp. 101-132, Oxford University Press, New York.
- Matsuda, T., Nakamura, T., Nakao, K., Arai, T., Katsuki, M., Heike, T. and Yokota, T. (1999) STAT3 activation is sufficient to maintain an undifferentiated state of mouse embryonic stem cells. *EMBO J*, **15**, 4261-4269.

- Matsui, Y., Zsebo, K. and Hogan, B.L. (1992) Derivation of pluripotential embryonic stem cells from murine primordial germ cells in culture. *Cell*, **5**, 841-847.
- Matus, A. (1990) Microtubule-associated proteins and the determination of neuronal form. *J Physiol (Paris)*, **84**, 134-137.
- Maye, P., Becker, S., Siemen, H., Thorne, J., Byrd, N., Carpentino, J., Grabel, L. (2004) Hedgehog signaling is required for the differentiation of ES cells into neurectoderm. *Dev Biol*, **1**, 276-290.
- McBurney, M.W. and Rogers, B.J. (1982) Isolation of male embryonal carcinoma cells and their chromosome replication patterns. *Dev Biol*, **2**, 503-508.
- McBurney, M.W. (1993) P19 embryonal carcinoma cells. *Int J Dev Biol*, **1**, 135-140.
- McLaren, A. and Durcova-Hills, G. (2001) Germ cells and pluripotent stem cells in the mouse. *Reprod Fertil Dev*, **7-8**, 661-664.
- Meissner, A., Mikkelsen, T.S., Gu, H., Wernig, M., Hanna, J., Sivachenko, A., Zhang, X., Bernstein, B.E., Nusbaum, C., Jaffe, D.B., Gnirke, A., Jaenisch, R. and Lander, E.S. (2008) Genome-scale DNA methylation maps of pluripotent and differentiated cells. *Nature*, **7205**, 766-770.
- Menezes, J.R. and Luskin, M.B. (1994) Expression of neuron-specific tubulin defines a novel population in the proliferative layers of the developing telencephalon. *J Neurosci*, **9**, 5399-5416.
- Misteli, T., Gunjan, A., Hock, R., Bustin, M. and Brown, D.T. (2000) Dynamic binding of histone H1 to chromatin in living cells. *Nature*, **6814**, 877-81.
- Mitsui, K., Tokuzawa, Y., Itoh, H., Segawa, K., Murakami, M., Takahashi, K., Maruyama, M., Maeda, M. and Yamanaka, S. (2003) The homeoprotein Nanog is required for maintenance of pluripotency in mouse epiblast and ES cells. *Cell*, **5**, 631-642.
- Mikkelsen, T.S., Ku, M., Jaffe, D.B., Issac, B., Lieberman, E., Giannoukos, G., Alvarez, P., Brockman, W., Kim, T.K., Koche, R.P., Lee, W., Mendenhall, E., O'Donovan, A., Presser, A., Russ, C., Xie, X., Meissner, A., Wernig, M., Jaenisch, R., Nusbaum, C., Lander, E.S. and Bernstein, B.E. (2007) Genome-wide maps of chromatin state in pluripotent and lineage-committed cells. *Nature*, **7153**, 553-560.

- Mohamed, O.A., Bustin, M. and Clarke, H.J. (2001) High-mobility group proteins 14 and 17 maintain the timing of early embryonic development in the mouse. *Dev Biol*, **1**, 237-249.
- Mohn, F., Weber, M., Rebhan, M., Roloff, T.C., Richter, J., Stadler, M.B., Bibel, M. and Schübeler, D. (2008) Lineage-specific polycomb targets and de novo DNA methylation define restriction and potential of neuronal progenitors. *Mol Cell*, **6**, 755-766.
- Morassutti, D.J., Staines, W.A., Magnuson, D.S., Marshall, K.C. and McBurney, M.W. (1994) Murine embryonal carcinoma-derived neurons survive and mature following transplantation into adult rat striatum. *Neuroscience*, **4**, 753-763.
- Müller, J. and Verrijzer, P. (2009) Biochemical mechanisms of gene regulation by polycomb group protein complexes. *Curr Opin Genet Dev*, **2**, 150-158.
- Nan, X., Campoy, F.J. and Bird, A. (1997) MeCP2 is a transcriptional repressor with abundant binding sites in genomic chromatin. *Cell*, **4**, 471-481.
- Nat, R., Nilbratt, M., Narkilahti, S., Winblad, B., Hovatta, O. and Nordberg, A. (2007) Neurogenic neuroepithelial and radial glial cells generated from six human embryonic stem cell lines in serum-free suspension and adherent cultures. *Glia*, **4**, 385-399.
- Nakamura, T., Xi, G., Hua, Y., Hoff, J.T. and Keep, R.F. (2003) Nestin expression after experimental intracerebral hemorrhage. *Brain Res*, **1-2**, 108-117.
- Nichols, J., Zevnik, B., Anastassiadis, K., Niwa, H., Klewe-Nebenius, D., Chambers, I., Schöler, H. and Smith, A. (1998) Formation of pluripotent stem cells in the mammalian embryo depends on the POU transcription factor Oct4. *Cell*, **3**, 379-391.
- Nishimoto, M., Fukushima, A., Okuda, A. and Muramatsu, M. (1999) The gene for the embryonic stem cell coactivator UTF1 carries a regulatory element which selectively interacts with a complex composed of Oct-3/4 and Sox-2. *Mol Cell Biol*, **8**, 5453-5465.
- Niwa, H., Burdon, T., Chambers, I. and Smith, A. (1998) Self-renewal of pluripotent embryonic stem cells is mediated via activation of STAT3. *Genes Dev*, **13**, 2048-2060.
- Niwa, H., Toyooka, Y., Shimosato, D., Strumpf, D., Takahashi, K., Yagi, R., Rossant, J. (2005) Interaction between Oct3/4 and Cdx2 determines trophectoderm differentiation. *Cell*, **5**, 917-929.

- Niwa, H., Ogawa, K., Shimosato, D. and Adachi, K. (2009) A parallel circuit of LIF signalling pathways maintains pluripotency of mouse ES cells. *Nature*, **7251**, 118-122.
- Niwa, H., Miyazaki, J. and Smith, A.G. (2000) Quantitative expression of Oct-3/4 defines differentiation, dedifferentiation or self-renewal of ES cells. *Nat Genet*, **4**, 372-376.
- Niwa, H. (2001) Molecular mechanism to maintain stem cell renewal of ES cells. *Cell Struct Funct*, **3**, 137-148.
- Nixon, R.A. and Shea, T.B. (1992) Dynamics of neuronal intermediate filaments: a developmental perspective. *Cell Motil Cytoskeleton*, **2**, 81-91.
- Ogawa, K., Matsui, H., Ohtsuka, S. and Niwa, H. (2004) A novel mechanism for regulating clonal propagation of mouse ES cells. *Genes Cells*, **5**, 471-477.
- Ogawa, K., Nishinakamura, R., Iwamatsu, Y., Shimosato, D. and Niwa, H. (2006) Synergistic action of Wnt and LIF in maintaining pluripotency of mouse ES cells. *Biochem Biophys Res Commun*, **1**, 159-166.
- Okabe, S., Forsberg-Nilsson, K., Cyril Spiro, A., Segal, M. and McKay, R.D. (1996) Development of neuronal precursor cells and functional postmitotic neurons from embryonic stem cells in vitro. *Mech Dev*, **59**, 89- 102.
- Okamoto, K., Okazawa, H., Okuda, A., Sakai, M., Muramatsu, M. and Hamada, H. (1990) A novel octamer binding transcription factor is differentially expressed in mouse embryonic cells. *Cell*, **3**, 461-472.
- Okano, M., Bell, D.W., Haber, D.A. and Li, E. (1999) DNA methyltransferases Dnmt3a and Dnmt3b are essential for de novo methylation and mammalian development. *Cell*, **3**, 247-257.
- Ooi, L., Belyaev, N.D., Miyake, K., Wood, I.C. and Buckley, N.J. (2006) BRG1 chromatin remodeling activity is required for efficient chromatin binding by repressor element 1-silencing transcription factor (REST) and facilitates REST-mediated repression. *J Biol Chem*, **51**, 38974-38980.
- Otto, S.J., McCorkle, S.R., Hover, J., Conaco, C., Han, J.J., Impey, S., Yochum, G.S., Dunn, J.J., Goodman, R.H. and Mandel, G. (2007) A new binding motif for the transcriptional repressor REST uncovers large gene networks devoted to neuronal functions. *J Neurosci*, **25**, 6729-6739.
- Packer, A.N., Xing, Y., Harper, S.Q., Jones, L. and Davidson, B.L. (2008) The bifunctional microRNA miR-9/miR-9* regulates REST and CoREST and is downregulated in Huntington's disease. *J Neurosci*, **53**, 14341-14346.

- Palacios, D. and Puri, P.L. (2006) The epigenetic network regulating muscle development and regeneration. *J. Cell Physiol*, **207**, 1-11.
- Paling, N.R., Wheadon, H., Bone, H.K. and Welham, M.J. (2004) Regulation of embryonic stem cell self-renewal by phosphoinositide 3-kinase-dependent signaling. *J Biol Chem*, **46**, 48063-48070.
- Palmieri, S.L., Peter, W., Hess, H. and Schöler, H.R. (1994) Oct-4 transcription factor is differentially expressed in the mouse embryo during establishment of the first two extraembryonic cell lineages involved in implantation. *Dev Biol*, **1**, 259-267.
- Pan, G.J. and Pei, D.Q. (2003) Identification of two distinct transactivation domains in the pluripotency sustaining factor nanog. *Cell Res*, **6**, 499-502.
- Paranjape, S.M., Krumm, A. and Kadonaga, J.T. (1995) HMG17 is a chromatin-specific transcriptional coactivator that increases the efficiency of transcription initiation. *Genes Dev*, **16**, 1978-1991.
- Parnas D. and Linial, M. (1995) Cholinergic properties of neurons differentiated from an embryonal carcinoma cell-line (P19). *Int J Dev Neurosci*, **7**, 767-781.
- Pash, J.M., Alfonso, P.J. and Bustin, M. (1993) Aberrant expression of high mobility group chromosomal protein 14 affects cellular differentiation. *J Biol Chem*, **18**, 13632-13638.
- Pash, J.M., Bhorjee, J.S., Patterson, B.M. and Bustin, M. (1990) Persistence of chromosomal proteins HMG-14/-17 in myotubes following differentiation-dependent reduction of HMG mRNA. *J Biol Chem*, **8**, 4197-4199.
- Piccolo, S., Sasai, Y., Lu, B. and de Robertis, E. M. (1996). Dorsoventral Patterning in Xenopus: Inhibition of ventral signals by direct binding of chordin to BMP-4. *Cell* **86**, 589-598.
- Pierce G.B. and Dixon, F.J. Jr. (1959) Testicular teratomas. I. Demonstration of teratogenesis by metamorphosis of multipotential cells. *Cancer*, **3**, 573-583.
- Plachta, N., Bibel, M., Tucker, K.L. and Barde, Y.A. (2004) Developmental potential of defined neural progenitors derived from mouse embryonic stem cells. *Development*, **21**, 5449-5456.
- Podgorny, O.V., Poltavtseva, R.A., Marei, M.V., Sukhikh, G.T. and Aleksandrova, M.A. (2005) Formation of neuroepithelial structures in culture of neural stem cells from human brain. *Bull Exp Biol Med*, **1**, 113-117.

- Postnikov, Y. and Bustin, M. (2010) Regulation of chromatin structure and function by HMGN proteins. *Biochim Biophys Acta*, **1-2**, 62-68.
- Postnikov, Y.V., Shick, V.V., Belyavsky, A.V., Khrapko, K.R., Brodolin, K.L., Nikolskaya, T.A. and Mirzabekov, A.D. (1991) Distribution of high mobility group proteins 1/2, E and 14/17 and linker histones H1 and H5 on transcribed and non-transcribed regions of chicken erythrocyte chromatin. *Nucleic Acids Res*, **4**, 717-725.
- Postnikov, Y.V., Belova, G.I., Lim, J.H. and Bustin, M. (2006) Chromosomal protein HMGN1 modulates the phosphorylation of serine 1 in histone H2A. *Biochemistry*, **50**, 15092-15099.
- Postnikov, Y.V., Herrera, J.E., Hock, R., Scheer, U. and Bustin, M. (1997) Clusters of nucleosomes containing chromosomal protein HMG-17 in chromatin. *J Mol Biol*, **4**, 454-465.
- Prymakowska-Bosak, M., Hock, R., Catez, F., Lim, J.H., Birger, Y., Shirakawa, H., Lee, K. and Bustin, M. (2002) Mitotic phosphorylation of chromosomal protein HMGN1 inhibits nuclear import and promotes interaction with 14.3.3 proteins. *Mol Cell Biol*, **19**, 6809-6819.
- Rathjen, J., Lake, J.A., Bettess, M.D., Washington, J.M., Chapman, G., Rathjen, P.D. (1999) Formation of a primitive ectoderm like cell population, EPL cells, from ES cells in response to biologically derived factors. *J Cell Sci*, **112**, 601-612.
- Rathjen, J., Haines, B.P., Hudson, K.M., Nesci, A., Dunn, S. and Rathjen, P.D. (2002) Directed differentiation of pluripotent cells to neural lineages: homogeneous formation and differentiation of a neurectoderm population. *Development*, **11**, 262649-61.
- Rattner, B.P., Yusufzai, T. and Kadonaga, J.T. (2009) HMGN proteins act in opposition to ATP-dependent chromatin remodeling factors to restrict nucleosome mobility. *Mol Cell*, **5**, 620-626.
- Reid, J.L., Iyer, V.R., Brown, P.O. and Struhl K. (2000) Coordinate regulation of yeast ribosomal protein genes is associated with targeted recruitment of Esa1 histone acetylase. *Mol Cell*, **6**, 1297-1307.
- Reik, W. (2007) Stability and flexibility of epigenetic gene regulation in mammalian development. *Nature*, **7143**, 425-342.
- Reynolds, B.A. and Weiss, S. (1996) Clonal and population analyses demonstrate that an EGF-responsive mammalian embryonic CNS precursor is a stem cell. *Dev Biol*, **1**, 1-13.
- Rice, J.C. and Allis, C.D. (2001) Histone methylation versus histone acetylation: new insights into epigenetic regulation. *Curr Opin Cell Biol*, **3**, 263-273.

- Rochman, M., Postnikov, Y., Correll, S., Malicet, C., Wincovitch, S., Karpova, T.S., McNally, J.G., Wu, X., Bubunenko, N.A., Grigoryev, S. and Bustin, M. (2009) The interaction of NSBP1/HMGN5 with nucleosomes in euchromatin counteracts linker histone-mediated chromatin compaction and modulates transcription. *Mol Cell*, **5**, 642-656.
- Rochman, M., Malicet, C. and Bustin, M. (2010) HMGN5/NSBP1: a new member of the HMGN protein family that affects chromatin structure and function. *Biochim Biophys Acta*, **1-2**, 86-92.
- Rochman, M., Taher, L., Kurahashi, T., Cherukuri, S., Uversky, V.N., Landsman, D., Ovcharenko, I. and Bustin, M. (2011) Effects of HMGN variants on the cellular transcription profile. *Nucleic Acids Res*, **10**, 4076-4087.
- Rodda, D.J., Chew, J.L., Lim, L.H., Loh, Y.H., Wang, B., Ng, H.H. and Robson, P. (2005) Transcriptional regulation of nanog by OCT4 and SOX2. *J Biol Chem*, **26**, 24731-24737.
- Rossant, J. and McBurney, M.W. (1982) The developmental potential of a euploid male teratocarcinoma cell line after blastocyst injection. *J Embryol Exp Morphol*, **70**, 99-112.
- Rohwedel, J., Kleppisch, T., Pich, U., Guan, K., Jin, S., Zuschratter, W., Hopf, C., Hoch, W., Hescheler, J., Witzemann, V. and Wobus, A.M. (1998) Formation of postsynaptic-like membranes during differentiation of embryonic stem cells in vitro. *Exp Cell Res*, **2**, 214-225.
- Rohwedel, J., Guan, K. and Wobus, A.M. (1999) Induction of cellular differentiation by retinoic acid in vitro. *Cells Tissues Organs*, **3-4**, 190-202.
- Rolletschek, A., Chang, H., Guan, K., Czyz, J., Meyer, M. and Wobus, A.M. (2001) Differentiation of embryonic stem cell-derived dopaminergic neurons is enhanced by survival-promoting factors. *Mech Dev*, **1-2**, 93-104.
- Rosner, M.H., Vigano, M.A., Ozato, K., Timmons, P.M., Poirier, F., Rigby, P.W. and Staudt, L.M. (1990) A POU-domain transcription factor in early stem cells and germ cells of the mammalian embryo. *Nature*, **6277**, 686-692.
- Ross, S.A., McCaffery, P.J., Drager, U.C. and De Luca, L.M. (2000) Retinoids in embryonal development. *Physiol*, **80**, 1021-1054.
- Rubinstein, Y.R., Furusawa, T., Lim, J.H., Postnikov, Y.V., West, K.L., Birger, Y., Lee, S., Nguyen, P., Trepel, J.B. and Bustin, M. (2005) Chromosomal protein HMGN1 modulates the expression of N-cadherin. *FEBS J*, **22**, 5853-5863.

- Rudnicki, M. A. and McBurney, M. W. (1987) Cell culture methods and induction of differentiation of embryonal carcinoma cell lines. In: Robertson, E. J., ed. *Teratocarcinomas and embryonic stem cells. A practical approach*, 19-49.
- Sanalkumar, R., Vidyanand, S., Lalitha, Indulekha. C. and James, J. (2010) Neuronal vs. glial fate of embryonic stem cell-derived neural progenitors (ES-NPs) is determined by FGF2/EGF during proliferation. *J Mol Neurosci*, **1**, 17-27.
- Santiago, M.F., Liour, S.S., Mendez-Otero, R. and Yu, R.K. (2005) Glial-guided neuronal migration in P19 embryonal carcinoma stem cell aggregates. *J Neurosci Res*, **1**, 9-20.
- Sasai, Y., Lu, B., Steinbeisser, H. and De Robertis, E.M. (1995) Regulation of neural induction by the Chd and Bmp-4 antagonistic patterning signals in *Xenopus*. *Nature*, **6551**, 757.
- Sauvageot, C.M. and Stiles, C.D. (2002) Molecular mechanisms controlling cortical gliogenesis. *Curr Opin Neurobiol*, **3**, 244-249.
- Savchenko, E.A., Andreeva, N.A., Dmitrieva, T.B., Viktorov, I.V. and Chekhonin, V.P. (2005) Culturing of specialized glial cells (olfactory ensheathing cells) of human olfactory epithelium. *Bull Exp Biol Med*, **4**, 510-513.
- Schmidt, J.W., Brugge, J.S. and Nelson, W.J. (1992) pp60src tyrosine kinase modulates P19 embryonal carcinoma cell fate by inhibiting neuronal but not epithelial differentiation. *J Cell Biol*, **4**, 1019-1033.
- Schmidt, M.M., Guan, K. and Wobus, A.M. (2001) Lithium influences differentiation and tissue-specific gene expression of mouse embryonic stem (ES) cells in vitro. *Int J Dev Biol*, **2**, 421-429.
- Schöler, H.R., Ruppert, S., Suzuki, N., Chowdhury, K. and Gruss, P. (1990) New type of POU domain in germ line-specific protein Oct-4. *Nature*, **6265**, 435-439.
- Schuettengruber, B., Chourrout, D., Vervoort, M., Leblanc, B. and Cavalli, G. (2007) Genome regulation by polycomb and trithorax proteins. *Cell*, **4**, 735-745.
- Shakoori, A.R., Owen, T.A., Shalhoub, V., Stein, J.L., Bustin, M., Stein, G.S. and Lian, J.B. (1993) Differential expression of the chromosomal high mobility group proteins 14 and 17 during the onset of differentiation in mammalian osteoblasts and promyelocytic leukemia cells. *J Cell Biochem*, **4**, 479-487.
- Shirakawa, H., Herrera, J.E., Bustin, M. and Postnikov, Y. (2000) Targeting of high mobility group-14/-17 proteins in chromatin is independent of DNA sequence. *J Biol Chem*, **48**, 37937-37944.

- Shirakawa, H., Rochman, M., Furusawa, T., Kuehn, M.R., Horigome, S., Haketa, K., Sugita, Y., Inada, T., Komai, M. and Bustin, M. (2009) The nucleosomal binding protein NSBP1 is highly expressed in the placenta and modulates the expression of differentiation markers in placental Rcho-1 cells. *J Cell Biochem*, **4**, 651-658.
- Singh, U., Bongcam-Rudloff, E. and Westermarck, B. (2009) A DNA sequence directed mutual transcription regulation of HSF1 and NF1X involves novel heat sensitive protein interactions. *PLoS One*, **4**, e5050.
- Singh, S.K., Kagalwala, M.N., Parker-Thornburg, J., Adams, H. and Majumder, S. (2008) REST maintains self-renewal and pluripotency of embryonic stem cells. *Nature*, **7192**, 223-227.
- Smith, C.L. and Peterson, C.L. (2005) ATP-dependent chromatin remodeling. *Curr Top Dev Biol*, **65**, 115-148.
- Smukler, S.R., Runciman, S.B., Xu, S. and van der Kooy, D. (2006) Embryonic stem cells assume a primitive neural stem cell fate in the absence of extrinsic influences. *J Cell Biol*, **1**, 79-90.
- Solter, D. (2006) From teratocarcinomas to embryonic stem cells and beyond: a history of embryonic stem cell research. *Nat Rev Genet*, **4**, 319-327.
- Solter, D., Skreb, N. and Damjanov, I. (1970) Extrauterine growth of mouse egg-cylinders results in malignant teratoma. *Nature*, **1**;227(5257):503-4.
- Soprano, D.R., Teets, B.W. and Soprano, K.J. (2007) Role of retinoic acid in the differentiation of embryonal carcinoma and embryonic stem cells. *Vitam Horm*, **75**, 69-95.
- Sparmann, A. and van Lohuizen, M. (2006) Polycomb silencers control cell fate, development and cancer. *Nat Rev Cancer*, **11**, 846-856.
- Staines, W.A., Morassutti, D.J., Reuhl, K.R., Ally, A.I. and McBurney, M.W. (1994) Neurons derived from P19 embryonal carcinoma cells have varied morphologies and neurotransmitters. *Neuroscience*, **4**, 735-751.
- Stern, C.D. (2005) Neural induction: old problem, new findings, yet more questions. *Development*, **9**, 2007-2021.
- Stern, C.D. (2006) Neural induction: 10 years on since the 'default model'. *Curr Opin Cell Biol*, **6**, 692-697.
- Sterner, D.E. and Berger, S.L. (2000) Acetylation of histones and transcription-related factors. *Microbiol Mol Biol Rev*, **2**, 435-459.
- Stevens, L. C. (1959) Embryology of testicular teratomas in strain 129 mice. *J Natl Cancer Inst.* **23**, 1249-1295.

- Strahl, B.D. and Allis, C.D. (2000) The language of covalent histone modifications. *Nature*, **6765**, 41-5.
- Strübing, C., Ahnert-Hilger, G., Shan, J., Wiedenmann, B., Hescheler, J. and Wobus, A.M. (1995) Differentiation of pluripotent embryonic stem cells into the neuronal lineage in vitro gives rise to mature inhibitory and excitatory neurons. *Mech Dev*, **2**, 275-287.
- Strübing, C., Wobus, A.M. and Hescheler, J. (1995) Establishment of an in vitro model system for the differentiation of synaptically coupled neurons from mouse embryonic stem cells. *ALTEX*, **3**, 129-137.
- Subramanian, M., Gonzalez, R.W., Patil, H., Ueda, T., Lim, J.H., Kraemer, K.H., Bustin, M. and Bergel, M. (2009) The nucleosome-binding protein HMG2 modulates global genome repair. *FEBS J*, **22**, 6646-6657.
- Suzuki, A., Raya A, Kawakami, Y., Morita, M., Matsui, T., Nakashima, K., Gage, F.H., Rodríguez-Esteban, C. and Izpisua Belmonte, J.C. (2006) Nanog binds to Smad1 and blocks bone morphogenetic protein-induced differentiation of embryonic stem cells. *Proc Natl Acad Sci U S A*, **27**, 10294-10299.
- Tanaka, S., Kamachi, Y., Tanouchi, A., Hamada, H., Jing, N. and Kondoh, H. (2004) Interplay of SOX and POU factors in regulation of the Nestin gene in neural primordial cells. *Mol Cell Biol*, **20**, 8834-8846.
- Tanaka, S.S., Togooka, Y., Sato, H., Seiki, M., Tojo, H. and Tachi, C. (1998) Expression and localization of membrane type matrix metalloproteinase-1 (MT1-MMP) in trophoblast cells of cultured mouse blastocysts and ectoplacental cones. *Placenta*, **1**, 41-8.
- Takizawa, T., Nakashima, K., Namihira, M., Ochiai, W., Uemura, A., Yanagisawa, M., Fujita, N, Nakao M, Taga T. (2001), DNA methylation is a critical cell-intrinsic determinant of astrocyte differentiation in the fetal brain. *Dev Cell*, **6**, 749-758.
- Teets, B.W., Soprano, K.J. and Soprano, D.R. (2011) Role of SF-1 and DAX-1 during differentiation of P19 cells by retinoic acid. *J Cell Physiol*. [Epub ahead of print]
- Tokuzawa, Y., Kaiho, E., Maruyama, M., Takahashi, K., Mitsui, K., Maeda, M., Niwa, H. and Yamanaka, S. (2003) Fbx15 is a novel target of Oct3/4 but is dispensable for embryonic stem cell self-renewal and mouse development. *Mol Cell Biol*, **8**, 2699-2708.
- Tomioka, M., Nishimoto, M., Miyagi, S., Katayanagi, T., Fukui, N., Niwa, H., Muramatsu, M. and Okuda A. (2002) Identification of Sox-2 regulatory region which is under the control of Oct-3/4-Sox-2 complex. *Nucleic Acids Res*, **14**, 3202-3213.

- Tompers, D.M. and Labosky, P.A. (2004) Electroporation of murine embryonic stem cells: a step-by-step guide. *Stem Cells*, **3**, 243-249.
- Tozuka, Y., Fukuda, S., Namba, T., Seki, T. and Hisatsune, T. (2005) GABAergic excitation promotes neuronal differentiation in adult hippocampal progenitor cells. *Neuron*, **6**, 803-815.
- Tremethick, D.J. and Hyman, L. (1996) High mobility group protein 14 and 17 can prevent the close packing of nucleosomes by increasing the strength of protein contacts in the linker DNA. *J Biol Chem*, **20**, 12009-12016.
- Trieschmann, L., Postnikov, Y.V., Rickers, A. and Bustin, M. (1995) Modular structure of chromosomal proteins HMG-14 and HMG-17: definition of a transcriptional enhancement domain distinct from the nucleosomal binding domain. *Mol Cell Biol*, **12**, 6663-6669.
- Trieschmann, L., Alfonso, P.J., Crippa, M.P., Wolffe, A.P. and Bustin, M. (1995) Incorporation of chromosomal proteins HMG-14/HMG-17 into nascent nucleosomes induces an extended chromatin conformation and enhances the utilization of active transcription complexes. *EMBO J*, **7**, 1478-1489.
- Trojer, P. and Reinberg, D. (2007) Facultative heterochromatin: is there a distinctive molecular signature? *Mol Cell*, **1**, 1-13.
- Tropepe, V., Hitoshi, S., Sirard, C., Mak, T.W., Rossant, J. and van der Kooy, D. (2001) Direct neural fate specification from embryonic stem cells: a primitive mammalian neural stem cell stage acquired through a default mechanism. *Neuron*, **1**, 65-78.
- Tse, C., Sera, T., Wolffe, A.P. and Hansen, J.C. (1998) Disruption of higher-order folding by core histone acetylation dramatically enhances transcription of nucleosomal arrays by RNA polymerase III. *Mol Cell Biol*, **8**, 4629-3468.
- Umesono, K., Giguere, V., Glass, C.K., Rosenfeld, M.G. and Evans, R.M. (1988) Retinoic acid and thyroid hormone induce gene expression through a common responsive element. *Nature*, **6196**, 262-265.
- Ueda, T., Furusawa, T., Kurahashi, T., Tessarollo, L. and Bustin, M. (2009) The nucleosome binding protein HMGN3 modulates the transcription profile of pancreatic beta cells and affects insulin secretion. *Mol Cell Biol*, **19**, 5264-5276.
- Ueda, T., Catez, F., Gerlitz, G. and Bustin, M. (2008) Delineation of the protein module that anchors HMGN proteins to nucleosomes in the chromatin of living cells. *Mol Cell Biol*, **9**, 2872-2883.

- van den Berg, D.L., Snoek, T., Mullin, N.P., Yates, A., Bezstarosti, K., Demmers, J., Chambers, I. and Poot, R.A. (2010) An Oct4-centered protein interaction network in embryonic stem cells. *Cell Stem Cell*, **4**, 369-381.
- Vandesompele, J., De Preter, K., Pattyn, F., Poppe, B., Van Roy, N., De Paepe, A. and Speleman, F. (2002) Accurate normalization of real-time quantitative RT-PCR data by geometric averaging of multiple internal control genes. *Genome Biol*, **3** (7)
- Verheijen, M.H., Wolthuis, R.M., Bos, J.L. and Defize, L.H. (1999) The Ras/Erk pathway induces primitive endoderm but prevents parietal endoderm differentiation of F9 embryonal carcinoma cells. *J Biol Chem*, **3**, 1487-94.
- Verheijen, M.H., Wolthuis, R.M., Defize, L.H., den Hertog, J. And Bos, J.L. (1999) Interdependent action of RalGEF and Erk in Ras-induced primitive endoderm differentiation of F9 embryonal carcinoma cells. *Oncogene*, **31**, 4435-4439.
- Vigneault, C., McGraw, S., Massicotte, L. and Sirard, M.A. (2004) Transcription factor expression patterns in bovine in vitro-derived embryos prior to maternal-zygotic transition. *Biol Reprod*, **6**, 1701-9.
- Waddington, W. C. (1936) Organizers in mammalian development. *Nature*, **138**, 125.
- Walker, K.L., Yoo, H.K., Undamatla, J. and Szaro, B.G. (2001) Loss of neurofilaments alters axonal growth dynamics. *J Neurosci*, **21**, 9655-9666.
- Wang, J., Trowbridge, J.J., Rao, S. and Orkin, S.H. (2008) Proteomic studies of stem cells. *StemBook* [Internet]. Cambridge (MA): Harvard Stem Cell Institute.
- Weigmann, N., Trieschmann, L. and Bustin, M. (1997) Enhancement of the transcription potential of nascent chromatin by chromosomal proteins HMG-14/-17 is coupled to nucleosome assembly and not DNA synthesis. *DNA Cell Biol*, **10**, 1207-1216.
- Weisbrod, S., Groudine, M. and Weintraub, H. (1980) Interaction of HMG 14 and 17 with actively transcribed genes. *Cell*, **1**, 289-301.
- Weisbrod, S. and Weintraub, H. (1981) Isolation of actively transcribed nucleosomes using immobilized HMG 14 and 17 and an analysis of alpha-globin chromatin. *Cell*, **2**, 391-400.
- Weisbrod, S. and Weintraub, H. (1979) Isolation of a subclass of nuclear proteins responsible for conferring a DNase I-sensitive structure on globin chromatin. *Proc Natl Acad Sci U S A*, **2**, 630-634.

- Weisbrod, S.T. (1982) Properties of active nucleosomes as revealed by HMG 14 and 17 chromatography. *Nucleic Acids Res*, **6**, 2017-2142.
- Weisshaar, B., Doll, T. and Matus, A. (1992) Reorganisation of the microtubular cytoskeleton by embryonic microtubule-associated protein 2 (MAP2c). *Development*, **4**, 1151-1161.
- West, K.L., Ito, Y., Birger, Y., Postnikov, Y., Shirakawa, H. and Bustin, M. (2001) HMGN3a and HMGN3b, two protein isoforms with a tissue-specific expression pattern, expand the cellular repertoire of nucleosome-binding proteins. *J Biol Chem*, **28**, 25959-25969.
- West, K.L. (2004) HMGN proteins play roles in DNA repair and gene expression in mammalian cells. *Biochem Soc Trans*, **6**, 918-919.
- Whitehead, M.C., Marangos, P.J., Connolly, S.M. and Morest, D.K. (1982) Synapse formation is related to the onset of neuron-specific enolase immunoreactivity in the avian auditory and vestibular systems. *Dev Neurosci*, **4**, 298-307.
- Whitcomb, E.A. and Taylor, A. (2009) Ubiquitin control of S phase: a new role for the ubiquitin conjugating enzyme, Ubch7. *Cell Div*, **4**, 17.
- Wiese, C., Rolletschek, A., Kania, G., Blyszczuk, P., Tarasov, K.V., Tarasova, Y., Wersto, R.P., Boheler, K.R. and Wobus AM. (2004) Nestin expression--a property of multi-lineage progenitor cells? *Cell Mol Life Sci*, **19-20**, 2510-222.
- Reynolds, B.A., and Weiss, S. (1996). Clonal and population analyses demonstrate that an EGF-responsive mammalian embryonic CNS precursor is a stem cell. *Dev. Biol.* **175**, 1-13.
- Willert, K. and Jones, K.A. (2006) Wnt signaling: is the party in the nucleus? *Genes Dev*, **1**, 1394-1404.
- Wilson, S.I. and Edlund, T. (2001) Neural induction: toward a unifying mechanism. *Nat Neurosci*, **4**, 1161-1168.
- Wilson, S.I., Rydström, A., Trimborn, T., Willert, K., Nusse, R., Jessell, T.M., and Edlund, T. (2001) The status of Wnt signalling regulates neural and epidermal fates in the chick embryo. *Nature*, **6835**, 325-330
- Wilson, M.E., Yang, K.Y., Kalousova, A., Lau, J., Kosaka, Y., Lynn, F.C., Wang, J., Mrejen, C., Episkopou, V., Clevers, H.C. and German, M.S. (2005) The HMG box transcription factor Sox4 contributes to the development of the endocrine pancreas. *Diabetes*, **12**, 3402-9.
- Wobus, A.M., Kleppisch, T., Maltsev, V. and Hescheler, J. (1994) Cardiomyocyte-like cells differentiated in vitro from embryonic carcinoma cells P19 are characterized by functional expression of

- adrenoceptors and Ca²⁺ channels. *In Vitro Cell Dev Biol Anim*, **7**, 425-434.
- Wobus, A.M. and Boheler, K.R. (1999) Embryonic Stem Cells as Developmental Model in vitro. Preface. *Cells Tissues Organs*, **3-4**, 129-130.
- Wobus, A.M. and Guan, K. (1998) Embryonic Stem Cell-Derived Cardiac Differentiation: Modulation of Differentiation and "Loss-of-Function" Analysis In Vitro. *Trends Cardiovasc Med*, **2**, 64-74.
- Wobus, A.M., Guan, K. and Pich, U. (2001) In vitro differentiation of embryonic stem cells and analysis of cellular phenotypes. *Methods Mol Biol*, **158**, 263-286.
- Wray, J., Kalkan, T., Gomez-Lopez, S., Eckardt, D., Cook, A., Kemler, R. and Smith, A. (2011) Inhibition of glycogen synthase kinase-3 alleviates Tcf3 repression of the pluripotency network and increases embryonic stem cell resistance to differentiation. *Nat Cell Biol*, **19**;13(7):838-45.
- Xu, J., Wang, H., Liang, T., Cai, X., Rao, X., Huang, Z. and Sheng, G. (2011) Retinoic acid promotes neural conversion of mouse embryonic stem cells in adherent monoculture. *Mol Biol Rep*. [Epub ahead of print]
- Yan, J., Tanaka, S., Oda, M., Makino, T., Ohgane, J. and Shiota, K. (2001) Retinoic acid promotes differentiation of trophoblast stem cells to a giant cell fate. *Dev Biol*, **2**, 422-432.
- Ying, Q.L., Nichols, J., Chambers, I. and Smith, A. (2003) BMP induction of Id proteins suppresses differentiation and sustains embryonic stem cell self-renewal in collaboration with STAT3. *Cell*, **3**, 281-292.
- Yuan, H., Corbi, N., Basilico, C. and Dailey, L. (1995) Developmental-specific activity of the FGF-4 enhancer requires the synergistic action of Sox2 and Oct-3. *Genes Dev*, **21**, 2635-2645.
- Yi, W., Thomas, H. And Geoffery, C. (2002) Global gene expression patterns during neural differentiation of P19 embryonic carcinoma cells. *Differentiation*, **70**, 204-219.
- Zafra, F., Poyatos, I. and Gimenez, C. (1997) Neuronal dependency of the glycine transporter GLYT1 expression in glial cells. *Glia*, **2**, 155-162.
- Zhang, S.C.(2006) Neural subtype specification from embryonic stem cells. *Brain Pathol*, **2**, 132-142.
- Zhigang, J., Liu, L., Bian, W., Chen, Y., Xu,G., Cheng, L. and Jing, N. (2009) Different transcription factors regulate nestin gene expression during P19 cell neural differentiation and central nervous system development. *J Biol Chem*, **12**, 8160-8173. *J Biol Chem*.

- Zhong ,X. and Jin, Y. (2009) Critical roles of coactivator p300 in mouse embryonic stem cell differentiation and Nanog expression. *J Biol Chem*, **14**, 9168-9175.
- Zhu, N. and Hansen, U. (2007) HMGN1 modulates estrogen-mediated transcriptional activation through interactions with specific DNA-binding transcription factors. *Mol Cell Biol*, **24**, 8859-8873.
- Zimmerman, L., Parr, B., Lendahl, U., Cunningham, M., McKay, R., Gavin, B., Mann, J., Vassileva, G. and McMahon, A. (1994) Independent regulatory elements in the nestin gene direct transgene expression to neural stem cells or muscle precursors. *Neuron*, **1**, 11-24.